

The American Mineralogist

Journal of the Mineralogical
Society of America

VOL. 46

JANUARY-FEBRUARY, 1961

Nos. 1 and 2

Contents

CHICAGO

Differential thermal analysis of galena and clausthalite.....	J. A. Dunne and P. F. Kerr	1
New data on boltwoodite, an alkali uranyl silicate.....	Russell M. Honea	12
Nomograms for determining 2θ from precession photographs.....	F. D. Bloss and G. V. Gibbs	26
Isomorphous substitution and infra-red spectra of the layer lattice silicates....	V. Stubičan and R. Roy	32
Mineralogy and petrology of the system Al_2O_3 - SiO_2 - H_2O in some pyrophyllite deposits of North Carolina.....	E-an Zen	52
Differential thermal analysis of shattuckite.....	Ming-Shan Sun	67
Lattice expansion of kaolin minerals by treatment with potassium acetate....	Koji Wada	78
Some observations on "iddingsite".....	P. Gay and R. W. LeMaitre	92
Synthesis and origin of chalcedony.....	J. F. White and J. F. Corwin	112
Fluorescent x-ray spectrographic analyses of amphibolite rocks.....	A. A. Chodos and C. G. Engel	120
Titanomagemite in igneous rocks.....	T. Katsura and I. Kushiro	134
Vernadskite discredited: pseudomorphs of antlerite after dolerophanite.....	Mary E. Mrose	146
Helium in limestone and marble.....	F. Fanale and J. L. Kulp	155
New data on deweylite.....	Davis M. Lapham	168
Celestite and calciostrontianite from Virginia.....	R. S. Mitchell and R. F. Pharr	189
Phase transformations in silica as examined by continuous x-ray diffraction..	F. M. Wahl, R. E. Grim and R. B. Graf	196

(Continued on Cover 2)



EDITOR: LEWIS S. RAMSDELL

CO-EDITOR: E. WM. HEINRICH

BOARD OF ASSOCIATE EDITORS:

GEORGE W. BRINDLEY

ADOLF PABST (1959-61)

RICHARD H. JAHNS

EDWIN W. ROEDDER (1960-62)

CARL W. CORRENS

HERBERT INSLEY (1961-63)

Published bi-monthly by the Society

Mineralogy of the bauxite deposits near Weipa, Queensland	F. C. Loughnan and P. Bayliss	209
Radiation coloration of silica minerals	H. W. Kohn and B. M. Benjamin	218
Optical crystallography of orientite from Oriente Province, Cuba	Charles B. Sclar	226
Notes and News		233
Book Reviews		235
New Mineral Names		241

Mineralogical Society of America

ASSOCIATED WITH THE GEOLOGICAL SOCIETY OF AMERICA

President: **E. F. Osborne**, Pennsylvania State University, University Park, Pennsylvania.

Past-President: **Joseph Murdoch**, University of California at Los Angeles, Los Angeles 24, California

Vice-President: **Ian Campbell**, State Division of Mines, San Francisco 11, Calif.

Secretary: **George Switzer**, U. S. National Museum, Washington 25, D. C.

Treasurer: **Marjorie Hooker**, U. S. Geological Survey, Washington 25, D. C.

Editor: **Lewis S. Ramsdell**, University of Michigan, Ann Arbor, Michigan.

Co-Editor: **E. Wm. Heinrich**, University of Michigan, Ann Arbor, Michigan.

Councilors:

(1959-61) **Wilfrid R. Foster**, Ohio State University, Columbus 10, Ohio.

(1959-61) **Edward W. Nuffield**, University of Toronto, Toronto 5, Ontario, Canada.

(1960-62) **Julian R. Goldsmith**, University of Chicago, Chicago 37, Illinois.

(1960-62) **Horace Winchell**, Yale University, New Haven, Connecticut.

(1961-63) **Robert M. Garrels**, Harvard University, Cambridge 38, Massachusetts.

(1961-63) **O. F. Tuttle**, Pennsylvania State University, University Park, Pennsylvania.

Advertising Manager: **Martin L. Ehrmann**, 369 South Robertson Blvd., Beverly Hills, California.

The enlarged issues of this journal for 1961 are made possible by a grant from the Penrose Fund of the Geological Society of America.

The American Mineralogist—Journal of the Mineralogical Society of America

The journal, containing articles on mineralogy, crystallography, and allied sciences, is issued every two months. Contributions are invited.

The general conduct of the journal is in the hands of the editor, Lewis S. Ramsdell, Department of Mineralogy, University of Michigan, to whom all manuscripts should be submitted.

Authors are requested to submit two copies of each manuscript typewritten on standard size paper, 8½ by 11 inches. Photographs submitted for cuts should be glossy prints. Tables, figures and cuts should be planned for the page size of the American Mineralogist, approximately 4 by 7 inches. If possible, tracings and large tables should be photographed and submitted as glossy prints.

Authors are entitled to 50 free reprints, without covers, of each article published. Sent to all members and fellows of the Mineralogical Society of America. Annual dues are \$8.00 (\$4.00 for students). Membership includes receipt of the American Mineralogist and GeoTimes, which is published by the American Geological Institute. Subscriptions for libraries, colleges, institutions, companies and similar organizations \$10.00 annually.

Entered as second class matter at the post office at Menasha, Wis., under Act of March 3, 1879. Acceptance for mailing at the special rate of postage provided for in section 1103, Act of Oct 3, 1917, paragraph 4 section 429 P. L. & R. authorized March 13, 1922.

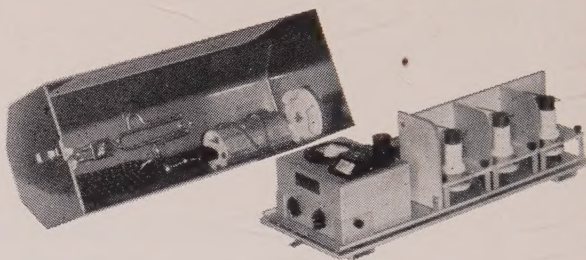
Notice of change of address, orders, and remittances should be sent to Marjorie Hooker, c/o U. S. Geological Survey, Washington 25, D. C.

Printed by George Banta Company, Inc., Menasha, Wisconsin
Printed in the United States of America

*"... one experiment is worth ten thousand
expert opinions ..."*

Well! perhaps more than one, but if you want it done at
high temperatures and/or high pressures we can do it for you
or help you significantly with the proper research equipment.

TEM-PRES RESEARCH INC.
STATE COLLEGE, PENNSYLVANIA



PORTABLE

DIFFERENTIAL THERMAL ANALYSIS APPARATUS

Eberbach
CORPORATION

P. O. Box 1024 Ann Arbor, Michigan

Certain mineralogical analyses can be performed on the apparatus which involves measuring and graphing the difference in temperature between the sample being examined and an inert substance as the two are heated rapidly. The temperature of the sample during a test is influenced by the reactions taking place. This portable apparatus operates from 115 volt A.C. or D.C. Request Bulletin 320 for complete information.

MINERAL SPECIMENS

Large variety of crystals, crystal groups, rare minerals, and ore minerals for collectors, universities and museums.

Mineral Catalog 25¢, or sent free when requested on official letterhead.

Filer's are interested in buying or exchanging for good quality minerals, especially from foreign countries. Correspondence is invited.

F I L E R ' S

P. O. Box 372, Redlands, California

Our Specialty is

SELECTED MINERAL SPECIMENS

FROM WORLD-WIDE LOCALITIES FOR COLLECTORS AND MUSEUMS

we also carry a complete line of
MINERALIGHTS, DETECTOR GEIGER COUNTERS, ESTWING
PROSPECTOR PICKS, MINERALOGICAL BOOKS, ETC.

Send for free current bulletin

SCHORTMANN'S MINERALS

6 McKinley Avenue

Easthampton, Massachusetts

For Mineralogists:

Index of Refraction Liquids

Range: 1.35 to 2.11 index; available in sets of limited range, or in sets with various intervals, or in any selection. Note that liquids 2.01 to 2.11 are now available.

Write for Price List Nd-AM

Allen Reference Sets for Microscopical Studies in Mineralogy and Petrology

Six sets of Authentic materials for use as standards for refractive index, for standard materials mounted in balsam to be compared with unknowns, and for demonstration of typical optical characteristics under microscopical study.

Write for descriptive material A-AM

Text: Practical Refractometry by Means of the Microscope

By ROY M. ALLEN, D.SC.

Describes the technique of the immersion method of microscopy, with particular reference to the identification of minerals. Written primarily for elementary instruction, but this text will be very useful also to advanced workers. Price \$1.00. Copy will be sent on approval.

Heavy Liquids

Formulated especially for determination of specific gravity of minerals, but special formulations are being made to order for various procedures. If you have any special problem in this field of separation of minerals or other materials by differences in specific gravity, please write us about your problem. Or, just write for leaflet HL-AM.

Gems, Testing For Identity and For Defects

The CARGILLE-ALLEN GEM TESTING SET is the title of our new book describing the properties of gems and also the equipment for certain identification of gems by a new simple procedure. Price \$1.00; this amount applicable to purchase price of any of the items listed in the book.

**R. P. Cargille Laboratories, Inc.
117 Liberty St., New York 6, N.Y.**

MINERAL SPECIMENS *For Sale or Exchange*
MICROSCOPES BOOKS • GEOLOGICAL SUPPLIES

Catalog on request

SCOTT J. WILLIAMS
Mineralogist

440 N. SCOTTSDALE ROAD • SCOTTSDALE, ARIZONA, U.S.A.

The
Lapidary Journal

SUBSCRIBE NOW

THE ORIGINAL GEM MAGAZINE

for gem cutters, gem collectors
and jewelry craftsmen

A non-technical craft publication, not a gemological or mineralogical magazine. Most quoted publication in its field. Bimonthly. Now in its 14th year.

RATES: \$3.00 in U.S., North and South America
\$3.50 in other foreign countries

Address: P.O. Box 518G, Del Mar, California

SHALE'S

9226 W. Pico Blvd., Los Angeles 35, California

FINE MINERAL SPECIMENS FOR MUSEUMS AND COLLECTORS

Minerals for study

We buy mineral collections. Inquiries invited.

d. m. organist

*petrographic
laboratory*

BOX 176, NEWARK, DELAWARE

THIN SECTIONS OF

ROCKS, MINERALS, ORES, CERAMICS

PREPARED ROCK SECTIONS FOR

STUDENT USE

PHOTOMICROGRAPHS

PETROGRAPHIC ANALYSIS

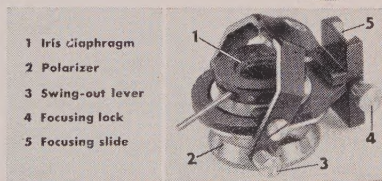
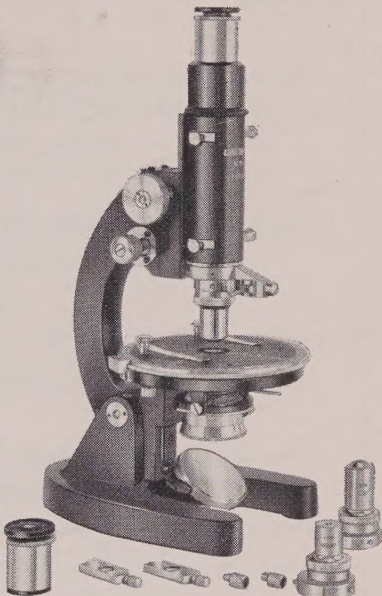
FIRST: LOOK AT UNITRON'S NEW POLARIZING MICROSCOPE

Here is a precision measuring instrument for both orthoscopic and conoscopic observations, designed to meet the exacting requirements of science, education, and industry. Its many features make it ideal for work in chemistry, crystallography, mineralogy and biology as well as in the technology of paper, glass, textiles and petroleum.

CHECK THESE OPTICAL & MECHANICAL FEATURES

Note that UNITRON'S new Model MPS comes complete with optics and accessories and includes features usually associated only with much more costly models.

- **EYEPIECES:** Micro 5X providing measurements to 0.0025mm. and cross-hair 10X. The eye lenses focus to produce sharp reticle images and are keyed to prevent rotation.
- **OBJECTIVES:** 4X(N.A.0.1), 10X(N.A.0.25), 40X(N.A.0.65), achromatic, strain-free, each with centerable mount.
- **NOSEPIECE:** quick-change type for critical centering.
- **CONDENSER and POLARIZER:** three-lens condenser with upper elements on a swing-out mounting, provides either parallel or convergent light. A dovetail-slide focusing mount and iris diaphragm insure optimum illumination and resolution.
- **POLAROID POLARIZER:** rotatable through 360° and graduated every 45°. Plano-concave mirror.
- **ANALYZER:** Polaroid, in sliding metal mount.
- **BERTRAND LENS:** for the study of interference figures, fixed-focus lens is centerable and mounted in a slideway.
- **STAGE:** diameter 115mm., revolves through 360°, graduated in degrees and reads to 6' with vernier. The top is calibrated in mms. in two directions and is drilled and tapped for an accessory mechanical stage. Stage clips.
- **COMPENSATORS:** two compensators are included; a quarter-wave plate and first order red plate. These fit into a slot above the objective lens.
- **FOCUSING:** coarse and micrometric fine adjustments.
- **STAND:** heavy stand, arm inclines to horizontal position.



Condenser and Polarizer

THEN: LOOK AT THE PRICE!

Model MPS complete as described,
in fitted cabinet.
Quantity prices on three or more.
Accessory mechanical stage.

\$269
FOB BOSTON
\$1475

UNITRON

Instrument Company, Microscope Sales Division
66 Needham St., Newton Highlands 61, Mass.

Please rush UNITRON Catalog on Microscopes.

Name _____
Company _____
Address _____
City _____ State _____

AVAILABLE ON FREE 10 DAY TRIAL
Send for complete catalog on UNITRON Microscopes.

THE TREND IS TO UNITRON



Important McGraw-Hill Books

MINERALOGY: An Introduction to the Study of Minerals and Crystals

By EDWARD H. KRAUS, WALTER F. HUNT, and L. S. RAMSDELL, University of Michigan. New Fifth Edition. 686 pages, \$9.00.

FIELD GEOLOGY, Sixth Edition

By FREDRIC H. LAHEE, Consulting Geologist, Dallas, Texas. Ready in October 1961.

PHOTOGEOLOGY

By VICTOR C. MILLER, Miller & Associates, Inc., Denver, Colorado. Ready in Spring.

McGRAW-HILL BOOK COMPANY, INC.

330 WEST 42ND STREET, NEW YORK 18, N.Y.

TOURMALINE

WORLD FAMOUS in the early 1900's! The HIMALAYA MINING COMPANY, of Mesa Grande, California, is again producing the rich pinks, greens and bi-colors for which it was so noted, in single crystals and crystal groups.

CORRESPONDENCE INVITED

Will consider trades for rare, or exceptional crystals or crystal groups.

Dr. Delmar B. Cosby
Owners Personal Representative
Himalaya Mining Company
11055 Puebla Drive
La Mesa, California

RARE AND UNUSUAL MINERALS

We specialize in uncommon forms and associations, and in choice collectors items in all sizes. We have crystals of childrenite, purple apatite and rose quartz; endellite-halloysite, chalcoalumite, damourite, and others. We can furnish bulk material for class study.

List available—Will exchange

MINERALS WHOLESALE
Box 174, La Jolla, California
Tel. Gl-4-6086 for appointment

The Leitz logo, featuring the word "Leitz" in a stylized, cursive font with a registered trademark symbol (®) to its right.

SATISFIES THE MOST EXACTING REQUIREMENTS

RESEARCH POLARIZING MICROSCOPE

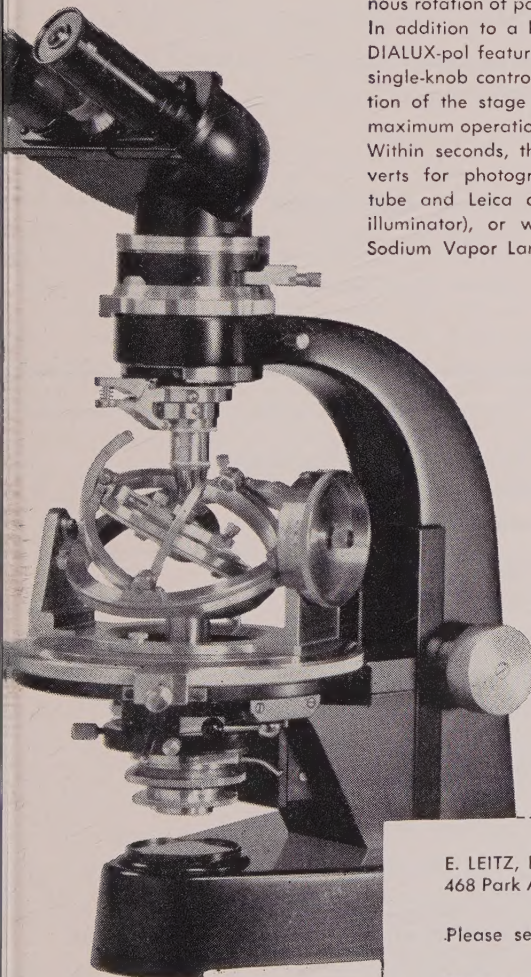
DIALUX-POL

The new LEITZ DIALUX-pol is the most advanced, universal polarizing research microscope ever manufactured. It was designed for the geologist, mineralogist, petrographer, paleontologist, and the industrial research microscopist.

The DIALUX-pol maintains the principle of interchangeability, famous with all LEITZ precision instruments, so that it is readily used for transmitted light as well as for reflected-polarized light. With the simple addition of a connecting bar, it provides synchronous rotation of polarizer and analyzer.

In addition to a built-in light source and condenser system, the DIALUX-pol features many other operational advantages: unique single-knob control of both coarse and fine adjustment by alteration of the stage height (and not the tube), thus focusing with maximum operational ease.

Within seconds, the DIALUX-pol, through LEITZ accessories, converts for photography (through combined monocular-binocular tube and Leica camera), for ore microscopy (through vertical illuminator), or will accommodate the LEITZ Universal Stage, Sodium Vapor Lamp, and other facilities.



- monocular or binocular vision
- combination tube FS for photography
- synchronous polarizer-analyzer rotation upon request
- dual coarse and fine focusing
- built-in light source; 6-volt, 2.5-amp, variable intensity
- vertical illumination for ore microscopy
- polarizing filters or calcite prisms
- adaptable to all universal stage methods

Send for the DIALUX-pol information bulletin—then see and examine this fine instrument for yourself.

E. LEITZ, INC.
468 Park Avenue South, New York 16, N. Y.

Please send me the LEITZ DIALUX-pol brochure.

Name _____

Street _____

City _____ Zone _____ State _____

E. LEITZ, INC., 468 PARK AVENUE SOUTH, NEW YORK 16, N. Y.
Distributors of the world-famous products of
Ernst Leitz G. m. b. H., Wetzlar, Germany—Ernst Leitz Canada Ltd.
LEICA CAMERAS · LENSES · PROJECTORS · MICROSCOPES · BINOCULARS

BARIUM FELDSPAR (HYALOPHANE)

Found during the last stages of mining at Franklin, N.J. before the mine was closed permanently. Material analyzed at Harvard University shows from 5 to 10 per cent barium oxide. Some specimens showed up to 30 per cent BaO. This hyalophane also shows lead as an impurity. The lead, if not derived from lead silicates peculiar to the Parker Shaft zone of minerals, makes this hyalophane scientifically important. Study specimens from 2 x 2 to 5 x 6, priced at \$2.00 to \$20.00. A suite of six specimens, 2 x 2 to 3 x 3, priced at \$25.00. Parcel post charges extra.

JOHN S. ALBANESE

P.O. Box 221

Union, New Jersey

Articles to appear in early issues of THE AMERICAN MINERALOGIST

Nature and origin of glauconite

John Hower

Vulcanite, a new copper telluride from Colorado

E. N. Cameron and I. M. Threadgold

Dielectric behavior of rocks and minerals

B. F. Howell, Jr., and P. H. Licastro

Imbibometry, a new method for the investigation of clays

J. Konta

Abnormal effect in D.T.A. of clay minerals

W. F. Cole and N. M. Rowland

Calciferous amphiboles oxyhornblende, kaersutite and barkevikite

J. F. G. Wilkinson

Stability relations of iron and manganese minerals

A. Muan and S. Somiya

Poorly crystallized, low barium, psilomelane-type mineral

A. A. Levinson

Estimation of the chemical composition of rocks

K. S. Heier

Phase equilibria in system iron oxide-titanium oxide

J. B. MacChesney and A. Muan

Manganooan cummingtonite from Nsuta, Ghana

H. W. Jaffe, W. O. J. Groeneveld Meijer and D. H. Selchow

Neighborite, NaMgF_3 , a new mineral from the Green River formation, Utah

E. C. T. Chao, H. T. Evans, Jr., B. J. Skinner and C. Milton

Ludwigite from Crestmore, California

W. T. Schaller and A. C. Vlisidis

Norsethite, $\text{BaMg}(\text{CO}_3)_2$, a new mineral from Wyoming

M. E. Mrose, E. C. T. Chao, J. J. Fahey and C. Milton

Urano-organic mineral association

A. M. Abdel-Gawad and P. F. Kerr

THE AMERICAN MINERALOGIST

JOURNAL OF THE MINERALOGICAL SOCIETY OF AMERICA

Vol. 46

JANUARY-FEBRUARY, 1961

Nos. 1 and 2

DIFFERENTIAL THERMAL ANALYSIS OF GALENA AND CLAUSTHALITE

JAMES A. DUNNE, AND PAUL F. KERR, *Columbia University,
New York, N. Y.*

ABSTRACT

Differential thermal analyses have been conducted on both natural and artificial lead-sulfur-selenium compounds. Thermal curves of twelve natural galenas exhibit a striking consistency regardless of the genetic associations of the minerals studied. In certain instances, limited (5–10° C.) variations from the overall average peak temperature of $783 \pm 2^\circ$ appear, which seem to be related to lattice parameter differences.

A range of synthetic compounds at ten molecular per cent solid solution intervals from PbS to PbSe has been formed by pyrosynthesis. X-ray measurements of the series showing three-dimensional lattice variation in relation to composition plot as a straight line. Thermal data, on the other hand, produce a more complex plot which may be interpreted in terms of both lattice energies and the nature of the observed reactions. DTA reaction temperatures are systematically related to cell dimensions in the range $\text{PbSe} - \text{PbS}_{0.7}\text{Se}_{0.3}$. DTA data taken from samples in the compositional range $\text{PbS}_{0.7}\text{Se}_{0.3} - \text{PbS}$ are believed to be affected by incongruent anion behavior and surface oxidation effects. Data on pyrosynthesis reaction (formation) temperatures exhibit a fundamental and systematic relation to molar composition throughout the entire compositional range.

INTRODUCTION

Differential thermal analysis has long been utilized in the study of minerals, beginning with the pioneer experiments of Le Chatelier (1887) and Roberts-Austin (1899). The method has found valuable application in the study of clay minerals, carbonates, sulfates and zeolites. Because of their destructive effects on thermocouples and metal heads, sulfides, selenides and related minerals have until recently received little attention in DTA studies. The difficulties encountered in the study of these materials are discussed by McLaughlin (1957, p. 365), who presents several sulfide curves obtained with conventional DTA apparatus. Hiller and Probsthain (1955, 1956) subjected sulfide minerals to DTA in an inert atmosphere and also in air. The technique employed, however, failed to yield complete oxidation as shown by the resulting curves. At about the same time Kopp and Kerr (1957a) introduced a specially designed apparatus which, by means of alundum shielding for the thermocouples and head metal, allowed DTA of corrosive materials in air. The

thermal head used in the present work is a modification of this unit, and is described elsewhere (Dunne and Kerr, 1960). Sabatier (1956) and Levy (1958), using dilution techniques, have obtained DTA curves for sulfides with unshielded thermocouples. Their work is, however, not directly comparable to that of Kopp and Kerr because of the use of greatly different grain size and heating rates.

TECHNIQUE

The sample weight has been fixed at 50 mg., and grain size maintained in the range 100–120 mesh (149–125 microns), both being selected for convenience in handling and measurement. The weights and dimensions conform to those used by Kopp and Kerr (1957a). The sample is mixed with approximately 300 mg. of pure quartz sand which has been ground to a diameter which ranges from 50–100 mesh (149–297 microns). Quartz provides both an internal temperature standard and a loosely packed framework with interstices large enough to assure adequate sample combustion. Uniform mixing of the sample and the quartz is allowed by the flat alundum bottom of the modified sample well (Dunne and Kerr, 1960). Consistent packing is assured by tamping each charge with a specially constructed brass tamping tool. Reproducibility has been found to be a function of chart reading error. The 6" chart of the Leeds and Northrup Speedomax H recorder can be read to an accuracy of $\pm 5^\circ \text{C}$. The 12" chart of the Leeds and Northrup Speedomax G recorder can be read to an accuracy of $\pm 2^\circ \text{C}$. The latter instrument, part of the multiple point arrangement used by Kulp and Kerr (1948) and Kopp and Kerr (1957a), has been used in the galena study, while the Speedomax H, contained in a new, more rapid single point recording system, has been used in the study of the synthetic PbS-PbSe series. All samples were heated at a rate of $12\frac{1}{2}^\circ \text{C}$. per minute.

DIFFERENTIAL THERMAL ANALYSIS OF GALENA

Twelve galena samples from widely separated localities were analyzed, as tabulated in Table 1. Five representative DTA curves derived from these specimens have been selected as shown in Fig. 1. Sabatier (1956) and Levy (1958) present similar curves for galena with somewhat higher peak temperatures (850 – 860°C .). The temperature difference results from the use of different experimental procedures, particularly in the choice of grain size and heating rates. Temperatures are corrected by internal standard calibration to coincide with a quartz inversion temperature of 580°C ., which corresponds to the value for this phenomenon given by the equipment used (Kopp and Kerr, 1957a). All samples exhibit a well defined exothermic deflection beginning around 740°C . and

eaching a peak value between 780 and 790° C. The reaction represented by this deflection is one of oxidation. X-ray diffraction diagrams of the reaction products exhibit a complex array of lines indicative of a mixture of sulfates, oxysulfates and oxides of lead.

The uniformity which marks the five representative curves shown in fig. 1 is found to characterize all of the specimens examined, regardless of their widely varied genetic associations. There are, however, certain constant variations from the overall average corrected peak temperature

TABLE 1. D.T.A. PEAK TEMPERATURES FOR GALENA

Sample No.	Locality	DTA peak temperature ($\pm 2^\circ$ C.)	Lattice constant (\AA)
P-1	Joplin, Missouri	783	5.935
P-2	Vinegar Hill—Barr mine, Tristate District	782	
P-3	Bonnetterre, Missouri	782	
P-4	Potosi, Wisconsin	782	
P-5	Leadville, Colorado	784	
P-6	Silver King mine, Park City, Utah	785	5.935
P-8	Cornwall, England	783	
P-9	Ana mine, Przibram, Bohemia	788	
P-10	Freiberg, Saxony	783	5.934
P-11	Los Lamentos, Chihuahua, Mexico	784	
P-12	Oruro, Bolivia	794	5.933
P-14	Sidney mine, Coeur d'Alene District, Idaho	786	

$783 \pm 2^\circ$ C., notably in the case of the sample from Oruro, Bolivia ($794 \pm 2^\circ$ C.) and the sample from Przibram, Bohemia ($788 \pm 2^\circ$ C.). Lattice constant determinations were made on these and two average temperature samples, using standard x-ray diffractometer equipment with reference to tables prepared by Parrish, *et al.* (1953). The results of these four measurements are tabulated along with peak temperature values in Table 1. The small inverse relationship here indicated is considered a possibility, assuming cation substitution to be the controlling factor for both anomalies. Kopp and Kerr (1957a) showed a similar relationship between peak temperatures and lattice dimensions in ferrian chalerites. As lattice constants increased in response to increasing iron substitution, peak temperatures decreased. It must be recognized, however, that DTA data are frequently not subject to interpretation in terms of lattice dimensions, as it may be shown that anion substitution in certain proportions can produce results that are entirely different from those indicated above.

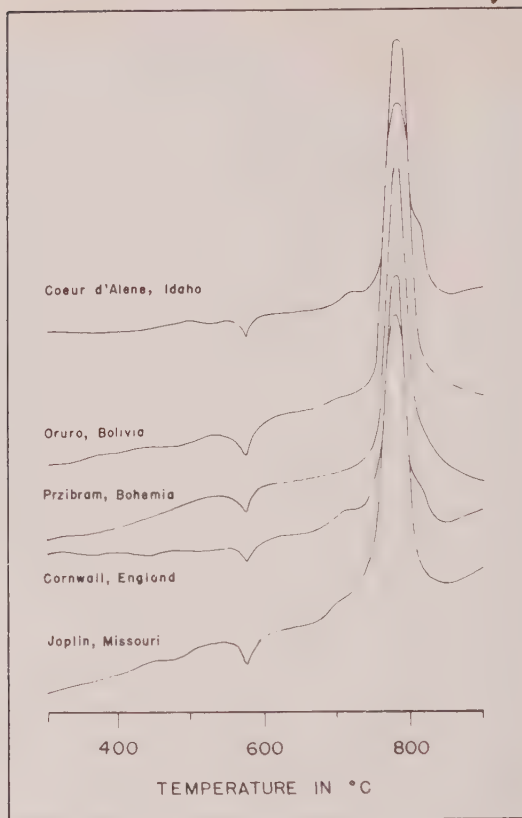


Fig. 1. Representative D.T.A. curves of galena. The endothermic peaks at 580° C represent the inversion of quartz, which is used as an internal temperature standard.

THE GALENA—CLAUSTHALITE SOLID SOLUTION SERIES

Earley (1950) in a comprehensive study of the selenide minerals, described a synthetic solid solution series between galena (PbS) and clausthalite (PbSe). More recently, Coleman (1959) demonstrated the existence of the series in nature associated with the vanadium-uranium mineralization of the Colorado Plateau. The samples discussed below have been formed by a dynamic method of pyrosynthesis, similar to the static pyrosynthesis described by Earley. The procedure followed is given below.

The weights of the constituent elements are calculated on the basis of their respective mole fractions in the desired mineral. After homogenization in a Wig-L-Bug mixer, a 0.5 gm. charge is extracted from the sample

mixture and introduced into a Pyrex tube which has been previously closed at one end. The tube is evacuated and sealed, then placed in a resistance furnace and heated at a uniform rate to approximately 450° C. After heating, the sample is removed from the furnace and allowed to cool to room temperature. A temperature record is furnished by a thermocouple inserted into a preformed recess in the bottom of the sample tube. This thermocouple and one similarly placed in a reference tube function as a differential pair, and a strip chart record of the reactions occurring during pyrosynthesis is obtained. This method for the differential thermal study of pyrosynthesis reactions is described elsewhere (Bollin, Dunne and Kerr, 1960).

LATTICE PARAMETER MEASUREMENTS

Lattice parameter measurements were made on all samples, using standard x-ray diffractometer equipment. As the measurements were made in an effort to secure data on the relative variation in lattice dimension with molar composition, they are not to be interpreted in terms of absolute lattice constants. Hence, the data are given as measured d -spacings, and have not been converted to a_0 values. The measurements were made at a goniometer speed of $\frac{1}{2}^\circ 2\theta$ per minute, and the standard chart speed of 30" per hour. Thus, the charts can be read to an accuracy of $\pm 0.05^\circ 2\theta$, which in the range of the d -values measured represents a maximum reading error of one part in twenty-five hundred. Since sets of determinations were taken consecutively over a small range in 2θ values (98.10–102.44° 2θ), relative errors arising from goniometer alignment may be considered negligible. Similarly, sample mount derivations were found to produce no measurable error. Hence, the maximum error inherent in the measurements is essentially the maximum chart reading error, *i.e.*, one part in twenty-five hundred, or approximately 0.004 Å in relative values.

Measured values for the (600) line of samples representing a ten molar per cent series between PbS and PbSe are shown plotted against molar composition in Fig. 2. The linear relationship between cell dimension and composition here indicated agrees with the conclusions of Earley (1950) and Coleman (1959). In terms of Zen's (1956) analytical treatment of Vegard's Law, these data indicate that the difference in the end member cell volumes in this series is so small that no measurable distortion results from the fact that cell edge data are plotted against composition, although it may be cell volume that varies linearly with molar composition.

On the basis of cell dimension measurements such as are shown in Fig. 2 it was discovered that a systematic compositional error exists in the

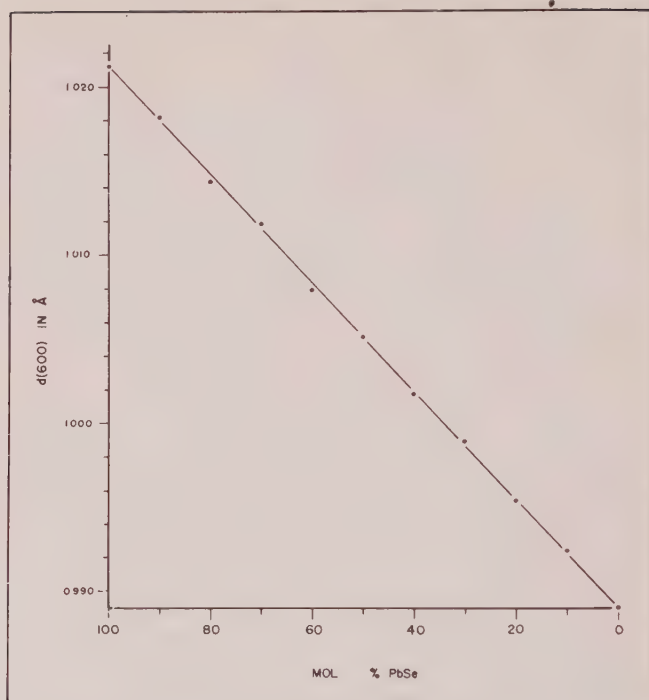


FIG. 2. Measured (600) d spacing vs. molar composition of samples comprising the synthetic PbS-PbSe series at intervals of ten mol per cent.

samples used in differential thermal analyses. This error is believed to have resulted from the use of oxidized Pb in the preparation of certain specimens, and appears in the unequal compositional intervals between samples described in the DTA discussion. The samples represented in Fig. 2 were prepared using unoxidized Pb.

REACTION TEMPERATURE DATA

Strip chart records of the reactions involved in the formation of certain of the synthetic samples were obtained, utilizing the method outlined in the discussion of synthesis. In order to obtain reproducible temperatures, it was considered desirable to control the volume of the sample mixture run. To this end, a scratch was made 16 mm. above the closed end of a 2 mm. (I.D.) glass capillary tube, and the volume thereby defined (0.05 cm.³) was used as the volume of all sample charges.

Strip chart records of the pyrosynthesis reactions of samples comprising a twenty mol per cent series between PbS and PbSe are shown in Fig.

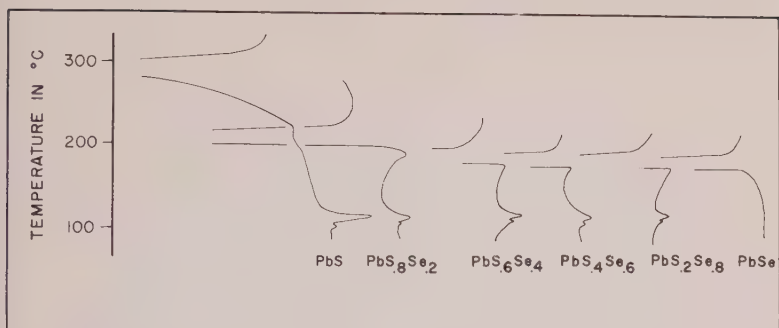


FIG. 3. Differential thermal pyrosynthesis (DTP) curves. The samples comprise a twenty mol per cent synthetic PbS-PbSe series.

3. For the sake of brevity, such records will be referred to henceforth as DTP curves. A small endothermic deflection at about 110° records the melting of sulfur and characterizes all curves, except the one obtained from PbSe. The large, well defined exothermic peaks are representative of the formation of the compounds corresponding to the molar composition of the respective sample mixtures. Additional reactions were not observed below 1000° C. The $d(600)$ measurements of these samples have been found to correspond closely to those of the samples whose measurements are given in Fig. 2. In Fig. 4 initial temperatures of the exothermic formation reactions on the DTP curves are plotted against molar composition. Note that the peak areas (Fig. 3) exhibit a corresponding increase with increasing mol per cent PbS. This relationship is to be

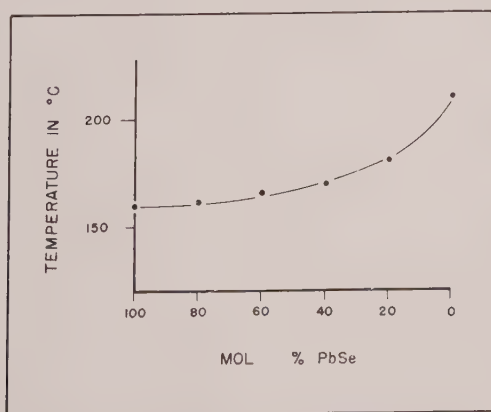


FIG. 4. Pyrosynthesis reaction (formation) temperature vs. molar composition. The samples listed are those whose DTP curves are given in Fig. 3.

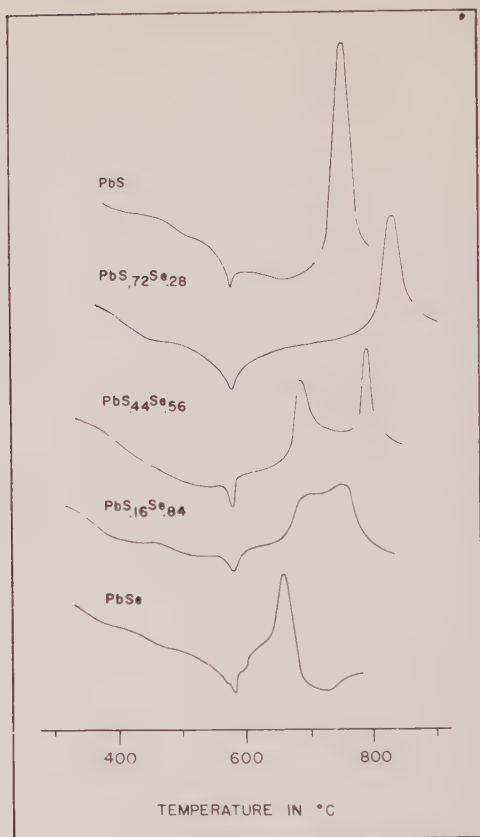


FIG. 5. D.T.A. curves of synthesized compounds. The samples comprise a twenty five mol per cent synthetic series. The uneven compositional spacing of the samples indicated here results from the use of oxidized lead in their preparation. This compositional error was found on the basis of x ray measurements to characterize all of the synthetic specimens used for D.T.A. studies.

expected in light of the dynamic nature of the DTP technique. The observed initial temperatures do not represent equilibrium temperatures, being to a large extent a function of reaction kinetics and therefore closely related to ΔH , of which peak area is a direct function.

DTA ON THE GALENA—CLAUSTHALITE SERIES

DTA records were obtained from the synthetic samples comprising the PbS-PbSe series. The curves of a 25 mol per cent series are shown in Fig. 5. These curves are representative of over forty DTA curves covering the synthetic series. An exothermic peak representing sample

oxidation begins at the clausthalite end of the series as a multiple deflection which splits into two distinct peaks near the midpoint of the series. These, in turn, merge to form a single sharp deflection which then characterizes the remainder of the suite. The development of two peaks in the vicinity of the series midpoint and their subsequent merging may result from a combination of factors. A comparison of the end member curves shows the clausthalite oxidation peak to be distinctly broader than the galena deflection. This relationship is believed to be indicative of the lower partial pressures of Se reaction products, which result in a higher order of reaction retardation caused by surface oxidation effects. As the sulfur content of the samples rises, more thermal energy is required to cause sample oxidation, and the reaction temperatures rise accordingly. The energy required to effect complete sample destruction rises at a faster rate than does the specific heat of the oxidation reaction. This effect combines with surface coating and interstitial clogging by reaction products to produce two peaks. These merge when low Se content and high reaction temperatures reduce the retardation effect of the early reaction products to a vanishing point.

From the foregoing discussion, it appears that the most significant temperature on these DTA curves is that of the initial deflection accompanying sample oxidation, since other peak characteristics result in part from factors which have no relationship to the fundamental properties of the minerals under consideration. The effect of grain size, for example, is demonstrated by the fact that a finely ground sample of composition $\text{PbS}_{0.5}\text{Se}_{0.5}$ was found to be characterized by a single exothermic peak.

As is evident from an examination of Fig. 5, initial reaction temperature has been found to increase with mol per cent PbSe throughout most of the synthetic series. The reversal of this relationship, evident in the range $\text{PbS}_{.72}\text{Se}_{.28}$ -PbS (Fig. 5) is believed to be caused by the decrease in the Se content of the samples, which in turn results in a decrease in the amount of surface coating by high stability Se rich reaction products. Oxidation products have been detected in Se-bearing samples which have been heated in air to temperatures as low as 200° C. Since surface area is held effectively constant by the control of both sample weight and grain size, it appears likely that all samples whose Se content exceeds a certain threshold value will suffer complete surface coating by reaction products rich in Se at temperatures below the DTA initiation temperature. Thus the effect of surface reaction on the initial deflection temperatures of these samples may be negligible in a relative sense. Within the experimental conditions under which the DTA data described herein were obtained, it appears that this threshold value lies near the composition

$\text{PbS}_{0.7}\text{Se}_{0.3}$. The conclusion that the reversal in the relationship between initiation temperatures and molar composition is not related to fundamental mineral properties is supported by the x-ray and DTP data given earlier.

The interpretation of the DTA data is based on the assumption that the recorded temperature of reaction is a function of the lattice energy of the material under analysis. That is to say, although reaction temperature is in no way an actual measure of lattice energy, it is fundamentally and linearly related to it. According to the Born-Landé expression for the lattice energy of binary ionic compounds, the relation between lattice energy and interionic distance is reciprocal in the first degree. Thus, if one assumes reaction temperature to be directly related to lattice energy, the reciprocal of this temperature should plot linearly with a measure of interionic distance. Figure 6 shows a plot of the reciprocal of DTA

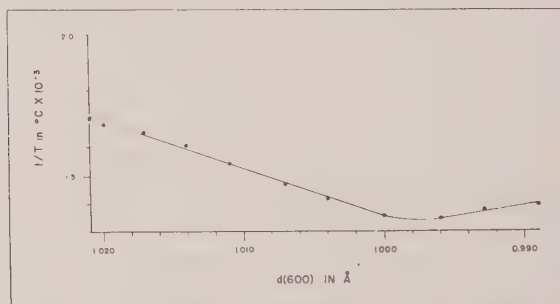


FIG. 6. Plot of the reciprocal of D.T.A. initial reaction temperature vs. measured $d(600)$.

initiation temperatures against measured $d(600)$ values for the series PbS-PbSe. The data apparently conform to the theoretical considerations just discussed through the compositional range PbSe-PbS_{0.7}Se_{0.3}. However, for those samples with compositions in the range PbS_{0.7}Se_{0.3}-PbS, this relationship does not obtain.

CONCLUSIONS

X-ray, DTA and DTP data show that a definite solid solution series exists between galena (PbS) and clausthalite (PbSe). A linear increase in cell dimensions corresponds to the increase in mol per cent PbSe. This relationship is also reflected through part of the series in the DTA data, but not through the entire series. However, measurements made on both natural galena and the synthetic specimens indicate that lattice parameter variations are systematically reflected in DTA reaction temperatures. Although data of this type must be interpreted with caution

in the case of systems characterized by anion substitution, the agreement between several lines of experimental evidence in the interval $\text{PbSe-PbS}_{0.7}\text{Se}_{0.3}$ is significant.

ACKNOWLEDGMENTS

This study has been made possible by a grant from the National Science Foundation. The cooperation of Dr. Richards Rowland of the Shell Development Corporation and Prof. Otto C. Kopp of the University of Tennessee in reading and commenting on this paper is greatly appreciated. Material assistance in equipment design and maintenance has been provided by Mr. E. M. Bollin, Technical Assistant on the project. The writers also express their appreciation to Messers. S. Kamhi, R. Giese, and J. Barrington of the mineralogy group at Columbia University for useful discussion.

REFERENCES

- BOLLIN, EDGAR M., DUNNE, JAMES A., AND KERR, PAUL F., (1960), Differential Thermal Study of Pyrosynthesis: *Science*, **131**, No. 3401, 661-662.
- COLEMAN, R. G. (1959), The natural occurrence of galena-clausthalite solid solution series: *Am. Mineral.*, **44**, 166-175.
- DUNNE, JAMES A., AND KERR, PAUL F. (1960), An improved thermal head for D.T.A. of corrosive materials: *Am. Mineral.*, 881-883.
- FARLEY, J. W. (1950), Description and synthesis of the selenide minerals: *Am. Mineral.*, **35**, 337-364.
- HILLER, J. E., AND PROBSTHAIN, K. (1955), Eine Apparatus für die differentialthermoanalyse von Sulfiden: *Erzmetall*, **VIII**, 257-304.
- HILLER, J. E., AND PROBSTHAIN, K. (1956), Differentialthermoanalyse von Sulfidemineralen: *Geologie (Berlin)* **5**, 607-616.
- KERR, P. F., AND KULP, J. L. (1948), Multiple differential thermal analysis: *Am. Mineral.*, **33**, 387-419.
- KOPP, O. C., AND KERR, P. F. (1957a), Differential thermal analysis of sulfides and arsenides: *Am. Mineral.*, **42**, 445-454.
- KOPP, O. C., AND KERR, P. F. (1957b), Differential thermal analysis of sphalerite: *Am. Mineral.*, **43**, 732-747.
- LE CHATELIER, H. (1887), De l'action de la chaleur sur les argiles: *Bull. Soc. Français Mineral.*, **10**, 204-211.
- LEVY, C. (1958), Analyse thermique différentielle des minerais sulfures: *Bull. Soc. française Minér. Crist.*, **81**, 29-34.
- McLAUGHLIN, J. W. (1957), "Other Minerals." The Differential thermal investigation of clays: *The Mineralogical Society (Clay Minerals Group) London*, 364-367.
- PARRISH, W., EKSTEIN, M. G., AND IRWIN, B. W. (1953), Data for x-ray analysis, Vol. 11: Philips Laboratories, Inc., Irvington-on-Hudson, N. Y., 81 pp.
- ROBERTS-AUSTIN, W. C. (1899), Fifth report to alloys research committee: *Proc. Instn. mech. Engrs.*, 35-102.
- CHATIER, G. (1956), Analyse thermique différentielle de quelques sulfures: *Bull. Soc. française Minér. Crist.*, **79**, 172-174.
- WEN, E.-an (1956), Validity of "Vegard's Law": *Am. Mineral.*, **41**, 523.

NEW DATA ON BOLTWOODITE, AN ALKALI URANYL SILICATE

RUSSELL M. HONEA, *Department of Geology, University of Colorado, Boulder, Colorado.*

ABSTRACT

Boltwoodite is an alkali uranyl silicate with the composition $K(H_2O)UO_2(SiO_4) \cdot nH_2O$ where n is zero to one. Chemical analysis, recalculated after deducting impurities, gives SiO_2 -14.8, UO_3 -68.5, K_2O -9.4, Na_2O -0.4, H_2O -6.9, total 100.0 per cent. The proposed formula is supported by infra red data, and the formula and other lines of evidence are shown to indicate a relationship to kasolite. Strongest lines of the x ray powder pattern are 6.81 (10), 3.40 (9), 2.95 (8), 3.54 (7), and 2.91 (7). Optically biaxial negative with $nX = 1.668$ -1.670, $nY = 1.695$ -1.696, $nZ = 1.698$ -1.703; 2V large, anomalous blue interference color, parallel extinction. Color pale yellow. Habit: radiating acicular to fibrous, and dense micro-crystalline pseudomorphic aggregates. Hardness $3\frac{1}{2}$ to 4. Perfect (010) and imperfect (001) cleavage. Symmetry orthorhombic on basis of optical study, but may be monoclinic with b -axis elongation. Boltwoodite occurs as a secondary mineral coating fractures and cavities, and as pseudomorphs after uraninite. Twenty one localities representing a variety of geological environments are listed. Data are presented on the hydrothermal synthesis of the potassium, potassium plus sodium, sodium, and ammonium analogues of the mineral.

INTRODUCTION

Boltwoodite was described from the Delta mine, Emery County, Utah, by Frondel and Ito (1956). It was the first of the alkali uranyl silicates to be noted, and with gastunite (Honea, 1959) is one of two such minerals now known. Since the original description, many additional widely scattered localities with different geological environments have been noted. The new material available has allowed the compiling of additional data concerning properties and occurrence, and has permitted infra-red analysis to determine the structural relationship of boltwoodite to other members of the uranyl silicate group. This new information concerning the natural mineral is presented herein, along with data on the hydrothermal synthesis of the potassium, potassium plus sodium, sodium, and ammonium analogues.

PHYSICAL PROPERTIES

In general aspect, boltwoodite is very similar to both sklodowskite and uranophane, but is somewhat paler in color than the latter. At the Delta mine, Utah, and the Lookout No. 22 mine, Colorado, the mineral occurs as yellow wartlike aggregates of fibers. Specimens from Myponga South Australia, and Quebrada del Tigre, Argentina, are pale yellow in color and contain boltwoodite in flattened radial aggregates between grains and along cleavage surfaces. Pseudomorphic aggregates from Alto Boqueirao, Brazil, and the Little Indian mine, Colorado, are dense mi-

microcrystalline and pale straw yellow in color. Specific gravity about 3.6 (Fron del and Ito, 1956). Hardness $3\frac{1}{2}$ to 4. Perfect (010) and imperfect (001) cleavage. Luster of crystals pearly on cleavage surfaces, of radial aggregates vitreous to silky, depending on crystal size. Dull to earthy in microcrystalline pseudomorphs. The mineral fluoresces dull green under both long- and shortwave ultraviolet excitation.

CHEMICAL ANALYSIS

The only available chemical analysis of boltwoodite is listed below in Table 1. As indicated in column E of the table, the analysis is in good agreement with the originally proposed formula $K_2(UO_2)_2(SiO_3)_2(OH)_2 \cdot 5H_2O$ except for the low water content. However, more recent data

TABLE 1. CHEMICAL ANALYSIS OF BOLTWOODITE

	A	B	C	D	E	F
SiO ₂	12.74	14.8	0.246	2	13.44	14.29
UO ₃	58.68	68.5	0.243	2	63.96	68.07
K ₂ O	8.03	9.4	0.100	1	10.52	11.21
Na ₂ O	0.33	0.4	0.006		—	—
CuO	9.61	—	—	—	—	—
SO ₃	2.12	—	—	—	—	—
H ₂ O	7.33	6.9	0.373	3	12.08	6.43
Insol.	0.19	—	—	—	—	—
Rem.	0.34	—	—	—	—	—
Total	99.37	100.0			100.00	100.00

A. Boltwoodite, Delta mine, Emery County, Utah. Remainder includes Al₂O₃, CaO, MgO, PbO, and V₂O₅. Analyst Jun Ito in Fron del and Ito, 1956.

B. Analysis recalculated after deducting brochantite, Cu₄SO₄(OH)₆, insoluble, and undetermined portions.

C. Molecular amounts calculated from B.

D. Molecular proportions from B.

E. Ideal composition of $K_2(UO_2)_2(SiO_3)_2(OH)_2 \cdot 5H_2O$.

F. Ideal composition of $K_2O \cdot 2UO_3 \cdot 2SiO_2 \cdot 3H_2O$ or $K(H_3O)UO_2(SiO_4) \cdot nH_2O$ where $n=0$.

from infra-red analysis indicates that the water as determined is correct and that the mineral has a nesosilicate structure. The formula proposed on the basis of this new data is $K(H_3O)(UO_2)(SiO_4) \cdot nH_2O$, in which n designates zeolitic water which on the basis of limited analytical data varies from zero through one. The ideal composition for the newly proposed formula is listed in column F, and is seen to be in even closer agreement than the above. The formula here proposed is close to that of

kasolite, a relationship discussed more fully in a following section of this paper. The analysis sample of Frondel and Ito contained brochantite and small amounts of unidentified materials, which are deducted in the recalculated analysis in column B.

OPTICAL DATA

As shown in Table 2 there is close agreement between optical constants for boltwoodite from the several natural occurrences. It is worthy

TABLE 2. OPTICAL DATA FOR NATURAL AND SYNTHETIC BOLTWOODITE

	1	2	3	4	5	Pleochroism	
nX	1.668	1.669	1.670	1.670	1.661-1.671	Colorless	Biaxial neg.
nY	1.696 (?)	1.695	1.695		1.682-1.694	Pale ylw	Anomalous blue
nZ	1.703	1.698	1.702	1.70	1.689-1.702	Pale ylw	Parallel extinction Z=elongation
1. Boltwoodite, Delta mine, Emery County, Utah (Fron­del and Ito, 1956).							
2. Boltwoodite, La Chiquita mine, Quebrada del Tigre, Cordoba Province, Argentina.							
3. Boltwoodite, Myponga, South Australia.							
4. Unknown type 1b, Bad Gastein, Salzburg (Haberlandt and Schiener, 1951).							
5. Beta-uranophane, <i>n</i> for yellow light, (Steinöcher and Novacek, 1939).							
	6	7	8	9	10		
Average <i>n</i>	1.695	1.61	1.61	1.62	1.642		
6. Boltwoodite, Alto Boqueirao, Brazil. Dense, microcrystalline aggregate.							
7. Synthetic potassium boltwoodite containing amorphous silica.							
8. Synthetic potassium plus sodium boltwoodite containing amorphous silica.							
9. Synthetic sodium boltwoodite containing amorphous silica.							
10. Synthetic ammonium boltwoodite containing amorphous silica in lesser amount than above, and coarser grained.							

of note that the indices of refraction of boltwoodite are in close agreement with those of the upper range for beta-uranophane as determined by Steinöcher and Nováček (1939). Because of this similarity, it is believed that x-ray examination of specimens labelled beta-uranophane will add to the number of occurrences listed in this paper. Two of the localities herein noted have previously had beta-uranophane identified on the basis of optical data. Indices of refraction for beta-uranophane are presented for comparison in Table 2.

Haberlandt and Schiener (1951) list an unknown uranyl silicate from Bad Gastein, Salzburg, with optics identical to those determined by the writer. Since the x-ray powder pattern of this unknown did not check with that of beta-uranophane, which is present in the same suite, the unknown mineral is here tentatively identified as boltwoodite.

The synthetic products, and dense pseudomorphs after uraninite from

natural occurrences, were too fine-grained to yield complete optical data. In such instances only an average index of refraction is reported. It is immediately obvious that the values obtained for most of the fine-grained synthetic products are lower than expected. This is the result of the presence of both adsorbed water and excess amorphous silica in the submicroscopically crystallized aggregates. Although too fine-grained for optical data, these products give good x -ray powder diffraction patterns in which the only effect of grain size is a very slight broadening of lines.

X-RAY AND CRYSTALLOGRAPHIC DATA

The small size of available crystals precluded the use of morphologic or single crystal x -ray methods. Optical study indicates orthorhombic symmetry, but like most of the other acicular uranyl silicates, boltwoodite may be monoclinic with b -axis elongation. Measured d -spacings

TABLE 3. X-RAY POWDER DIFFRACTION DATA FOR BOLTWOODITE FROM THE DELTA MINE, EMERY COUNTY, UTAH. COPPER RADIATION, NICKEL FILTER, WAVELENGTH 1.5418A

d	I	d	I	d	I
7.53	2	1.994	2	1.335	2
6.81	10	1.983	2	1.311	2
6.40	5	1.950	3	1.297	4b
5.45	5	1.935	1	1.270	$\frac{1}{2}$
4.74	4	1.900	6b	1.242	2b
4.32	4	1.874	1	1.211	1
4.11	2	1.820	2	1.196	1
3.91	1	1.780	1	1.174	2
3.75	1	1.764	6	1.149	2b
3.54	7	1.700	3	1.122	1b
3.40	9	1.658	3	1.112	2
3.13	5	1.627	2	1.087	1b
3.07	1	1.602	2b	1.072	1
2.95	8	1.580	2	1.053	2
2.91	7	1.566	1	1.041	1
2.69	1b*	1.550	1	1.023	1b
2.53	3	1.530	2	1.000	1
2.45	5	1.515	3b	0.980	1b
2.34	4	1.502	3b	0.971	1
2.26	5	1.487	1b	0.963	2b
2.21	4	1.455	1	0.928	1b
2.16	2	1.438	1	0.915	1b
2.13	3	1.411	3	0.884	1b
2.11	2	1.393	1	0.876	1
2.08	1	1.378	2	0.845	$\frac{1}{2}$
2.05	3	1.356	1b		

* b=broad.

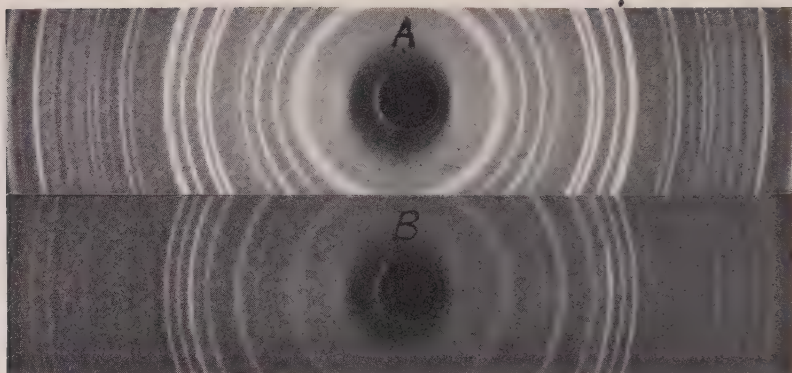


FIG. 1. X-ray powder diffraction patterns of: A. Boltwoodite, Delta mine, Emery County, Utah, and B. Kasolite, Shinkolobwe, Belgian Congo. Copper radiation, nickel filter. Contact print.

from an x-ray powder diffraction pattern corrected for film shrinkage are listed in Table 3. These spacings are in close agreement with the spacings for the first ten lines given in the preliminary description of Frondel and Ito (1956).

Figure 1 shows powder patterns for both boltwoodite and kasolite. Similarities in the general configuration of the patterns are seen to be present, and coupled with other lines of evidence, to be discussed later, are taken to indicate a structural relationship between the two phases.

INFRA-RED ABSORPTION SPECTRUM

Infra-red absorption spectra were made of both the natural and synthetic mineral, the curves for which are reproduced below as Fig. 2A and B. Analyses were made on a Perkin-Elmer instrument with sodium chloride analyzing prism. Samples were prepared for analysis by mixing two mg. of the very finely ground mineral (minus 325 mesh) with 0.5 grams of specially dried potassium bromide, and pressing the mixture into a thin wafer. Since not enough material was available from the type specimen, the absorption curve for the natural mineral was prepared with material from the locality in Cordoba Province, Argentina.

Absorption maxima appearing on all curves near 3.0 and 6.2 microns correspond to the stretching and bending vibrations respectively of the hydroxyl (or HOH) bond (Randall, *et al.*, 1949). The additional low wavelength maxima at 3.2 and 7.15 microns on curve B mark the stretching and bending vibrations of the ammonium bond. Stronger absorption peaks in the region from 10.1 to 11.7 microns result from silicate bonding, and are within the region from 9.7 to 12.2 microns shown by

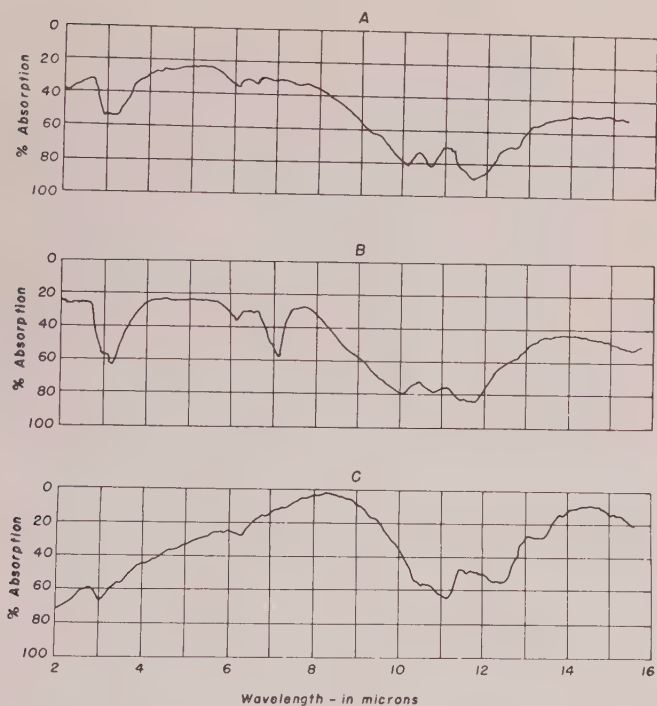


FIG. 2. Infra-red absorption spectra of natural and synthetic boltwoodite, and kasolite. A. Boltwoodite, La Chiquita mine, Quebrada del Tigre, Cordoba Province, Argentina, B. synthetic ammonium boltwoodite, C. kasolite, Shinkolobwe, Belgian Congo.

Launer (1952) to be typical of minerals having nesosilicate structures. On the basis of this evidence it is proposed that boltwoodite, like uranophane (Smith, Gruner, and Lipscomb, 1957), contains independent silicate tetrahedra as basic structural units.

The infra-red spectral curve for kasolite is included as Figure 2C for purposes of comparison. It is shown in the following discussion that boltwoodite most closely approaches the kasolite nesosilicate formula early proposed by Billiet and de Jong (1936), and since supported by Gorman (1957) on the basis of single crystal *x*-ray study. It is noted that the strong absorption maxima of kasolite are also present in the range typical of minerals with the nesosilicate structure, and thus that both minerals are comprised of the same basic silicate structural units.

COMPARISON WITH KASOLITE

Boltwoodite is found to be quite similar to kasolite on the basis of molecular ratios from chemical analyses, a conclusion supported by

x-ray powder diffraction patterns, infra-red data, and optical data. Both minerals show a much lower water content than the other uranyl silicates, containing respectively one (kasolite— $\text{PbO} \cdot \text{UO}_3 \cdot \text{SiO}_2 \cdot \text{H}_2\text{O}$) and three (boltwoodite— $\text{K}_2\text{O} \cdot 2\text{UO}_3 \cdot 2\text{SiO}_2 \cdot 3\text{H}_2\text{O}$) molecules of water in the oxide formulas derived from analyses. Further, the three water molecules in the boltwoodite formula are required to occupy cation positions as hydronium ions to balance the electrostatic charge demanded by the nesosilicate structure indicated by infra-red analysis. A lower water content for boltwoodite is also suggested by the significantly higher indices of refraction as compared to gastunite— $(\text{K}, \text{Na})_2(\text{UO}_2)_3(\text{Si}_2\text{O}_5)_4 \cdot 8\text{H}_2\text{O}$, which is also a potassium uranyl silicate.

The ionic radii of the principal cations ($\text{K}^+—1.33\text{\AA}$, $\text{H}_3\text{O}^+—1.33\text{\AA}(?)$, $\text{Pb}^{++}—1.20\text{\AA}$) indicates that these cations are well within the size range that would allow the formation of similarly coordinated structures. The similarities in line configuration and d -spacings of x-ray powder diffraction patterns of the two minerals, previously pointed out in Fig. 1, suggests this similarity in structure. It is not suggested that the minerals are isostructural, but rather that their structures are similar and closely related. The mechanism of positioning the monovalent potassium and hydronium ions for divalent lead ions is not known.

It is felt that though there is a superficial resemblance of the x-ray powder pattern to that of sklodowskite, as suggested in the original description, there is more similarity of boltwoodite to kasolite. This similarity is indicated in the above discussion, and is strongly favored over resemblances to other uranyl silicates by the low water content.

THERMAL BEHAVIOR

A study of the thermal behavior of boltwoodite was carried out on material pseudomorphic after uraninite from Quebrada del Tigre, Cordoba Province, Argentina. The material used contains about two per cent impurities and is extremely fine-grained, but was the only material available in sufficient amount for such a study. The differential thermal analysis curve for boltwoodite is reproduced as Fig. 3, and a weight loss curve is shown as Fig. 4. Distinct endothermic peaks are present at 170° , 708° , and $906^\circ \text{C}.$, and a single exothermic reaction at $1010^\circ \text{C}.$ The low temperature peak results from expulsion of capillary and adsorbed water, and possibly from the loss of small amounts of zeolitic water. The most rapid water loss is seen in Fig. 4 to take place below $100^\circ \text{C}.$, and optical and x-ray powder studies of material heated to $100^\circ \text{C}.$ shows no change in optical constants or d -spacings. Material heated to $200^\circ \text{C}.$ shows an increase in indices of refraction, and a very slight change in line intensities on x-ray patterns. When the heated sample is placed over

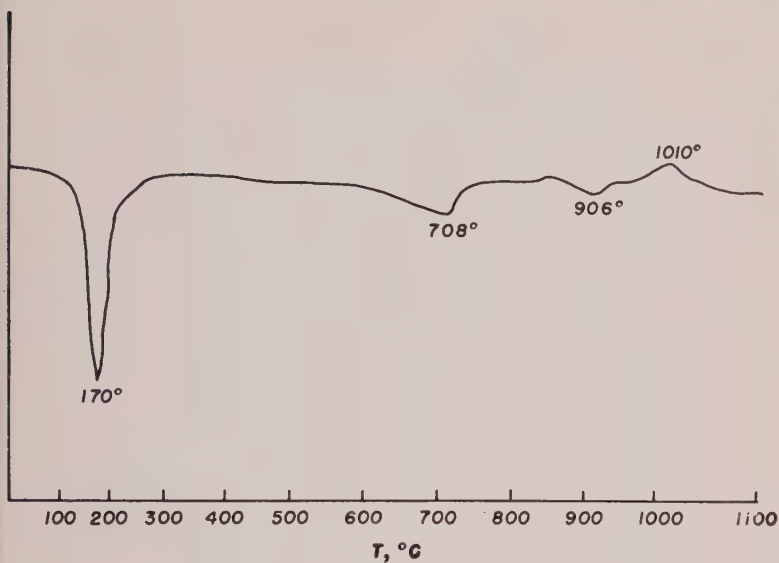


FIG. 3. Differential thermal analysis curve for boltwoodite from the La Chiquita mine, Quebrada del Tigre, Cordoba Province, Argentina.

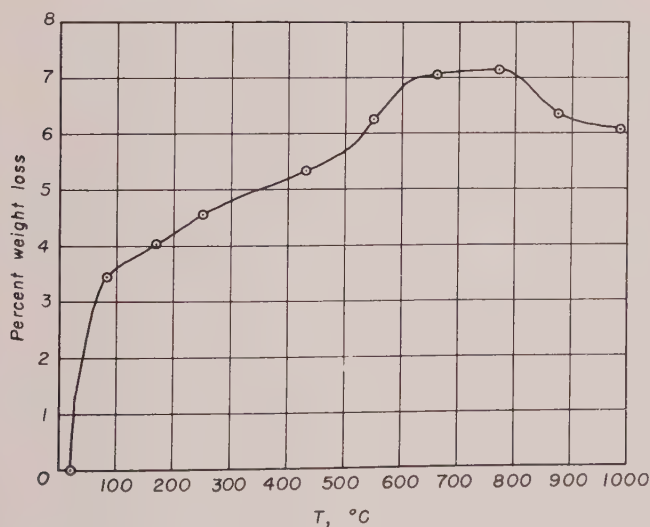


FIG. 4. Weight loss curve for boltwoodite from the La Chiquita mine, Quebrada del Tigre, Cordoba Province, Argentina.

water in a sealed container it regains normal optical constants in 48 hours. Above 100° C. weight loss continues at a lesser rate to approximately 500° C., at which temperature the curve steepens to slightly above 600° C. This final loss of weight corresponds to the broad exothermic reaction beginning at 600° C. and culminating at 708° C., and marks the final loss of water bonded as hydronium ions. *X*-ray patterns of material heated between 200° and 750° C. show a gradual collapse of the boltwoodite structure, and the appearance of small amounts of uraninite and U_3O_8 above 550° C. Total collapse of the boltwoodite structure has occurred at 750° C., and very broad and diffuse lines of a new phase appear. The gain of weight above 800° C. results from oxidation of the partially reduced uranium, and is expressed on the differential thermal analysis curve as an endothermic trough near 906° C. *X*-ray study indicates the appearance of a new phase at 875° C., the powder pattern of which resembles the *x*-ray pattern of clarkeite. This phase is stable to the highest temperature attained in the study (1100° C.), and at temperatures above 1000° C. is accompanied by an additional phase. The exothermic reaction at 1010° C. marks the appearance of this new phase, which could not be identified in the present study.

HYDROTHERMAL SYNTHESIS

Boltwoodite is readily synthesized by hydrothermal techniques in both low temperature runs and in higher temperature bomb runs. The method of synthesis used consists of coprecipitation of the essential ions in a gel from the soluble acetates. In all cases a 0.01 molar solution containing the essential ions was precipitated by raising the pH with a strong base. Bomb runs were made by heating the product of the low temperature precipitation in distilled water in a teflon-lined steel bomb. The potassium, potassium plus sodium, sodium, and ammonium analogues of boltwoodite were prepared. Results of the various syntheses are summarized in Table 4.

Although no attempt was made to systematically test complete solid solution between the several cations, the similarity in ionic radii and the isostructural character indicated by powder diffraction photographs indicate the probability that such is the case. The *x*-ray patterns of all synthetic products are essentially identical in both *d*-spacings and line intensities with each other and with the natural mineral (see Table 5). Slight broadening of the lines is evident in most of the synthetic products, and results from the microcrystalline nature of the precipitates. This is further shown on optical examination by the appearance as masses of extremely small, intergrown fibers which yield only an average index of refraction.

TABLE 4. SYNTHESIS OF BOLTWOODITE

Reagents	pH	Temp.	Product	Bomb Run	pH	Product
potassium acetate ammonium silicofluoride uranyl sulfate ammonium hydroxide	8½	90°	Ammonium boltwoodite	48 hrs. @ 246°	8	Boltwoodite
potassium silicofluoride uranyl acetate potassium hydroxide	8	95	Boltwoodite	46 hrs. @ 235	7	Boltwoodite gastunite
potassium silicofluoride uranyl acetate sodium hydroxide	7½	85	(K, Na) boltwoodite	46 hrs. @ 243	6½	(K, Na) boltwoodite
sodium metasilicate uranyl acetate sodium hydroxide	10½	85	Na bolt- woodite	42 hrs. @ 242	8	Na bolt- woodite
ammonium silicofluoride uranyl acetate ammonium hydroxide	7	95	Ammonium boltwoodite	48 hrs. @ 152	6	Ammonium boltwoodite soddyite

TABLE 5. COMPARISON OF X-RAY POWDER SPACINGS OF SYNTHETIC BOLTWOODITE WITH THOSE FOR THE NATURAL MINERAL

Natural (K, Na) boltwoodite		Synthetic K boltwoodite		Synthetic (K, Na) boltwoodite		Synthetic Na boltwoodite		Synthetic NH ₃ boltwoodite	
d	I	d	I	d	I	d	I	d	I
7.53	2								
6.81	10	6.84	10	7.03	10	6.81	10	6.89	10
6.40	5	6.35	5	6.51	4			6.42	5
5.45	5	5.47	4	5.54	4			5.43	1
4.74	4	4.74	3	4.71	1	4.75	5	4.74	6
4.32	4	4.35	2	4.35	1			4.33	3
4.11	2	4.11	1	4.11	1			4.11	1
3.91	1	3.88	2	3.91	1			3.93	1
3.75	1	3.75	1	3.79	2			3.75	1
3.54	7	3.55	8	3.53	9			3.55	9
3.40	9	3.41	6	3.38	3	3.45	7	3.44	5
3.13	5	3.16	8	3.16	8			3.15	6
3.07	1	3.09	1	3.08	1			3.09	3
2.95	8	2.96	7	2.98	6	2.97	6	2.96	7
2.91	7	2.91	6	2.91	7	2.93	8	2.91	6

Ammonium boltwoodite appears in the low temperature product in the synthesis of all the other uranyl silicates. With ammonium gastunite, it is the stable phase in the presence of high concentrations of ammonium ion. In all instances where there is no other monovalent cation of similar radius, the ammonium boltwoodite is destroyed in bomb runs above 200° C. and either a hydrated uranyl oxide or other uranyl silicate formed. The formation of soddyite as shown in Table 4 is an example of this breakdown. The presence of ammonium ion in the low temperature precipitates is shown by characteristic absorption maxima for the ammonium ion on infra-red spectra, by the ammonia odor emitted on heating in an open tube, and by the high pH of water condensing on the walls of closed tubes.

Boltwoodite is relatively unstable in bomb runs above 200° C. This is indicated by more diffuse lines on x-ray patterns of the bomb products, and by conversion of boltwoodite from low temperature runs to soddyite and uranyl oxides in bomb runs. Stability relations between boltwoodite and gastunite are indicated in Table 4. Boltwoodite is consistently the stable phase at higher pH values, and is in some instances broken down in higher temperature runs to gastunite. Synthesis of boltwoodite has been reported in a brief note by Pommer and Chandler (1958), and Pommer (1958, personal communication) by the action of uranyl carbonate solutions on glass.

OCCURRENCE

Boltwoodite is a moderately common secondary uranium mineral, and has been recognized from twenty one localities representing a variety of geological associations. Of the localities noted since the description of the mineral, one is described in the literature, six were noted by the writer, seven are listed by J. W. Gruner (personal communication, 1958), five have been noted by the U. S. Geological Survey (Daphne Ross, personal communication, 1959), and one is proposed on the basis of optical constants of an unknown uranium silicate from the literature (Haberlandt and Schiener, 1951).

The mineral occurs in the outer silicate zone of alteration surrounding the zone of hydrated uranyl oxides, which encrust primary uraninite. Boltwoodite is also found filling fractures and interstitial openings some distance from primary uraninite. Frondel and Ito (1956) describe boltwoodite from the type locality at the Delta mine, Emery County, Utah, as occurring in yellow wartlike aggregates of radial fibers coating fractures in sandstone. Other specimens from the same locality show small radial aggregates associated with uranyl sulfates which surround bec-

berelite and fourmarierite altering from uraninite. Other minerals present include brochantite, gypsum, and an unidentified uranyl silicate. Boltwoodite is present in the outer alteration rims of "gummite" pseudomorphs after uraninite from pegmatite occurrences at the La Chiquitane, Quebrada del Tigre, Cordoba Province, Argentina; and Alto Boqueirao, Brazil. In both instances boltwoodite appears as dense microcrystalline aggregates with a pale straw-yellow color. In the La Chiquitane, boltwoodite is also present as radial aggregates along cleavage planes and fractures in microcline and muscovite several inches from the pods of altered uraninite. Phosphuranylite is present as fracture coatings at both localities.

Montgomery (1957) mentions boltwoodite as pseudomorphs after thorian uraninite in serpentine at the Williams quarry, near Easton, Pennsylvania. The mineral is present in pseudomorphic aggregates with dull luster, rough granular appearance, and pale translucent-yellow color. As in the other localities listed, boltwoodite also occurs as finely fibrous material and as thin coatings on fracture surfaces. Uranophane is closely associated, and other minerals present include thorogummite and "Mineral C" of Frondel (1956). Montgomery proposes late-stage hydrothermal metamorphism of the thorian uraninite as an origin for the pseudomorphous material, and supergene alteration for the origin of the fracture coatings and efflorescences on exposed surfaces.

At the Little Indian No. 36 mine and the Lookout No. 22 mine of the Marshall Pass area, Gunnison County, Colorado, boltwoodite is present as small wartlike aggregates on becquerelite and as dense earthy aggregates pseudomorphic after uraninite. Occurrences at the Little Indian mine are restricted to a shear zone near the fault contact between the Proterozoic Harding quartzite and Precambrian gneiss, schist, and migmatite (R. Malan, U. S. Atomic Energy Commission, oral communication). The boltwoodite is secondary in origin, and is present in the oxidized zone along with uranophane, goethite, schoepite, ianthinite, and individual cores of uraninite. Uraninite is the only ore mineral, and sulfides are only sparsely present. Surface ore from the nearby Lookout No. 22 mine also contains soddyite, metazeunerite, and becquerelite.

Alteration of zirconian uraninite from the Sonia mine, near Guandac, La Rioja Province, Argentina, has produced boltwoodite as small euhedral aggregates of fibrous crystals intimately associated with brookite, and as interstitial filling in sandstone country rock surrounding lenticular pods of uraninite. Becquerelite is also present as a secondary mineral, and veins and encrusts uraninite.

Highly argillized granitic gneiss from Myponga, South Australia, con-

tains boltwoodite as coatings and interstitial fillings in the friable rock. The mineral here has an earthy luster, is very pale yellow in color, and is intimately intermixed with clay minerals. Under the microscope the coatings are seen to consist of minute radial fibrous aggregates. Boltwoodite is present with "gummite," uranophane, kasolite, and uranospinite, as a secondary alteration product of uraninite; and has been transported short distances from its primary source before deposition in the argillized gneiss. According to W. C. Woodmansee of the U. S. Atomic Energy Commission (oral communication), the Myponga deposit was a small but rich concentration of uranium minerals in the faulted crest of a small, tightly folded anticlinal structure. The oxidized uranium minerals of the surface zone do not persist with depth, and as ore is followed down the plunge of the fold relatively unaltered uraninite becomes the dominant mineral. Brannerite has also been identified from the mine.

Gruner (personal communication, 1958) has noted several additional localities in the Colorado Plateau and adjoining areas. These include: the Happy Jack mine, White Canyon district, San Juan County, Utah; the Pay Day mine, San Rafael Swell, Emery County, Utah; the Jerry group, Red Canyon, Utah; Seven Mile Canyon, Grand County, Utah; in the Todilto formation, Grants, New Mexico; the Moore claim, Niobrara County, Wyoming; and the Big Hill claim, Big Horn County, Wyoming.

Daphne Ross of the U. S. Geological Survey (personal communication, 1959) lists other localities in the Colorado Plateau at: the Pete No. 6 claim, San Juan County, Utah; Julia claims, San Juan County, Utah; Blue Jay mine, San Juan County, Utah; and the Huskon Nos. 17 and 20 mines, Cameron, Coconino County, Arizona. Mrs. Ross points out that these samples show variation both in chemical composition and x-ray pattern, and thus do not yield patterns that are identical in all respects with that of material from the Delta mine, which is used here as a standard for the natural mineral.

Optical data for an unknown uranium silicate mineral (Unknown, type 1b) listed by Haberlandt and Schiener (1951) are identical with those of boltwoodite, and indicate a probable occurrence with associated gastunite, uranophane, beta-uranophane, and other secondary uranium minerals at Bad Gastein, Salzburg.

NAME

The mineral was named after Bertram B. Boltwood (1870-1927), radiochemist of Yale University, who provided evidence that lead was the first disintegration product of uranium and devised the very fruitful

method of measuring geologic time on the basis of lead content of uranium minerals.

ACKNOWLEDGMENTS

I wish to express my deepest appreciation to Professor Clifford Frondel for his aid in all stages of this research, particularly for many helpful suggestions on the methods of synthesis, and for reading the manuscript. Acknowledgment is also made of financial assistance and aid in purchase of laboratory supplies by the U. S. Atomic Energy Commission research contract AT (301-1)-1403 at the Department of Mineralogy and Petrography, Harvard University. W. S. Keys, W. C. Woodmansee, and R. Malan, all of the U. S. Atomic Energy Commission, kindly donated specimens for some of the described localities.

REFERENCES

- FRONDEL, CLIFFORD (1956), Mineral composition of gummite: *Am. Mineral.*, **41**, 539-568.
- FRONDEL, CLIFFORD AND ITO, JUN (1956), Boltwoodite, a new uranium silicate mineral: *Science*, **124**, 931.
- GRIMAN, D. H. (1957), The uranium silicate minerals: Unpublished Ph.D. dissertation, University of Toronto.
- LABERLANDT, HERBERT AND SCHIENER, ALFRED (1951), Die Mineral- und Elementvergesellschaftung des Zentralgneissgebietes von Badgastein (Hohe Tauern): *Tschermaks Min. Pet. Mitt.*, Band 2, Heft 3, 307-313.
- ONEA, R. M. (1959), New data on gastunite, an alkali uranyl silicate: *Am. Mineral.*, **44**, 1047-1056.
- RAUNER, P. J. (1952), Regularities in the infra-red absorption spectra of silicate minerals: *Am. Mineral.*, **37**, 764-784.
- MONTGOMERY, ARTHUR (1957), Three occurrences of high thorian uraninite near Easton, Pennsylvania: *Am. Mineral.*, **42**, 804-820.
- OMMER, A. M. AND CHANDLER, J. C. (1958), Mineral synthesis, in Semiannual Report (12/1/57-5/31/57): U. S. Geol. Survey, Trace Elements Invest. Rept. 740, 295.
- DANDALL, H. M., FOWLER, R. G., FUSON, NELSON, AND DANGL, J. R. (1949), *Infrared Determination of Organic Structures*: D. Van Nostrand Co., New York.

Manuscript received March 11, 1960.

NOMOGRAMS FOR DETERMINING 2θ FROM PRECESSION PHOTOGRAPHS¹F. DONALD BLOSS² AND GERALD V. GIBBS³

ABSTRACT

Two nomograms are presented which permit 2θ to be evaluated from diffraction spot locations on precession photographs. By means of the first nomogram, 2θ for the wavelength used to produce the precession photograph is obtained. The second permits 2θ ($\text{CuK}\alpha$) to be determined from precession spots produced by molybdenum ($\text{K}\alpha$) radiation. The accuracy is usually sufficient to allow, in conjunction with observed intensities, unequivocal indexing of the more intense powder diffraction lines of crystalline materials.

INTRODUCTION

The writers have occasionally used indexed precession photographs of single crystals to index in turn the more intense lines of the corresponding powder diffraction pattern. In the course of this work, two nomograms were developed to permit evaluation of 2θ ($\pm 0.3^\circ$) for any reflecting plane whose diffraction spot is recorded on a precession photograph. Since they may similarly save others time in indexing powder diffraction patterns, these nomograms and their use are herein described.

DEVELOPMENT OF NOMOGRAMS

Figure 1 illustrates the relationship between dimensions in reciprocal lattice space (CO , OP , etc.) and those (CO' , $\text{O}'\text{P}'$, etc.) in what may be called "precession lattice" space. By similar triangles

$$\frac{\text{PO}}{\text{CO}} = \frac{\text{P}'\text{O}'}{\text{CO}'} \quad \text{Eq. (1)}$$

However, CO equals $1/\lambda$, the radius of the sphere of reflection; PO equals $1/d_{hkl}$ for the diffracting plane; and CO' equals F , the crystal-to-film distance (6 cm.). Substituting these values, Eq. (1) becomes

$$\frac{\lambda}{d_{hkl}} = \frac{\text{P}'\text{O}'}{6 \text{ cm.}} \quad \text{Eq. (2)}$$

From the Bragg equation for reflection, however,

$$\frac{\lambda}{d_{hkl}} = 2 \sin \theta.$$

¹ Contribution from Bureau of Mines, U. S. Department of the Interior, Electrotechnical Experiment Station, Norris, Tenn.

² Academic address: Department of Geology, Southern Illinois University, Carbondale, Ill.

³ Academic Address: Department of Mineralogy, Pennsylvania State University, University Park, Pa.

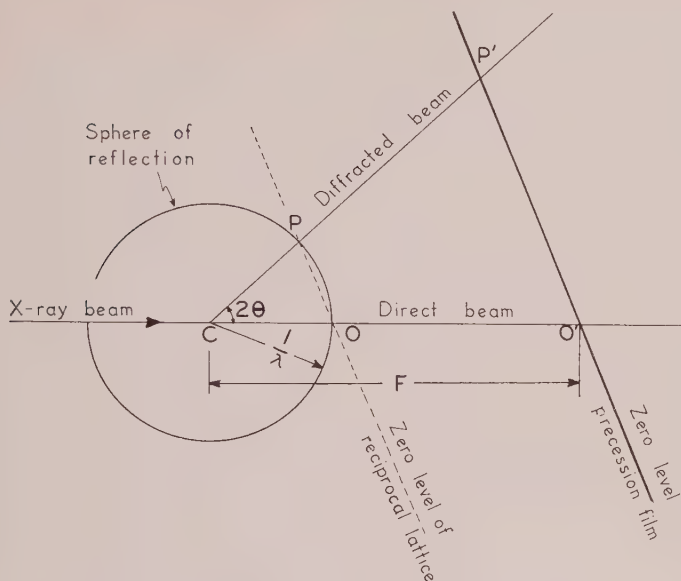


FIG. 1. Relationship between distances in the reciprocal lattice (origin at O) and precession film lattice (origin at O') for a crystal located at C. CO' is the crystal-to-film-distance, and P is the reciprocal lattice projection of a crystal plane satisfying the Bragg equation.

consequently Eq. (2) may be rewritten

$$\sin \theta = \frac{P'O'}{12 \text{ cm}} \quad \text{Eq. (3)}$$

where P'O' represents the distance of the precession spot (in cm.) from the center of the film.

For n -level precession photographs similar reasoning may be applied to develop the relation

$$\sin \theta = \frac{\sqrt{(Fd^*)^2 + (P'O')^2}}{12 \text{ cm}} \quad \text{Eq. (4)}$$

where P'O' now represents the distance of the precession spot (in cm.) from the center of the n -level photograph and Fd^* is the film displacement used in making this photograph.

The nomogram permits rapid solution of Eq. (3) or Eq. (4). On the scale reproduced here, Fig. 2 converts $2P'O'$, where P'O' represents the distance of a precession spot from the film center, into the value of 2θ for the reflecting plane responsible for the spot. Its use is best described by an example.⁴

⁴ The original Figs. 2 and 3 were exactly 14 cm. and 9 cm. wide, respectively. Glossy prints of the originals are available by request from the U. S. Bureau of Mines, Electrochemical Experiment Station, Norris, Tenn.

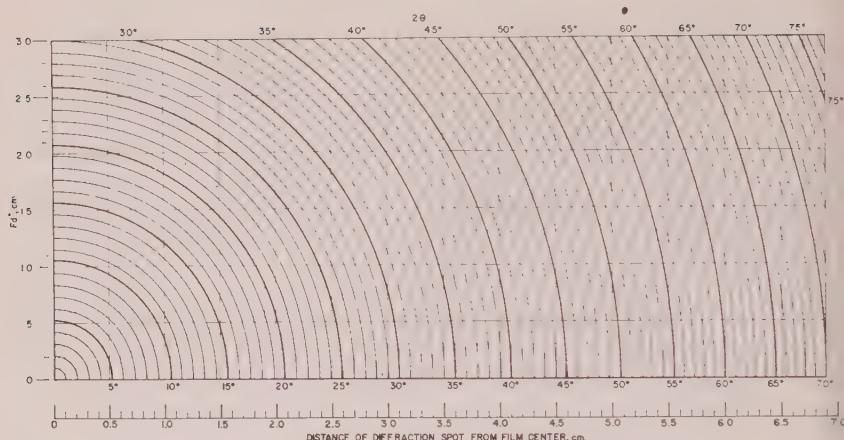


FIG. 2. Nomogram for converting precession spot distances to the corresponding 2θ values.

USE OF NOMOGRAMS

The first three columns of Table 1 represent data taken, with one exception, from two precession photographs, ($hk0$) and ($hk1$), of synthetic proto-amphibole, an orthorhombic amphibole recently described by Gibbs, Bloss, and Shell.⁵ From indexed photographs, twice the distance from the film center (i.e. $2\text{ O}'\text{P}'$) was measured for each precession spot of moderate intensity or greater. This measurement, as well as the precession spot's index and estimated intensity, was then recorded in Table 1 (but not necessarily in the present order). The value of $2\text{ O}'\text{P}'$ was, for each point, translated into its 2θ equivalent by means of Fig. 2, about 15 minutes being required for the entire conversion. Column 5, Table 1, contains 2θ values from powder diffraction data. These angles have an accuracy of ± 0.01 . Comparison of 2θ values in Columns 4 and 5 shows that the angles agree closely.

The conversion of the distances $2\text{ O}'\text{P}'$ into 2θ by means of Fig. 2 is particularly simple for the precession spots of a O-level photograph. The Friedel law indicates that, except in the neighborhood of a wave crystal resonance level, a precession spot ($hk0$) will be accompanied by a companion spot ($\bar{h}\bar{k}0$) collinear with it and the film center. Both are at an equal distance from the film center, and, therefore, the distance between the centers of these two spots represents $2\text{ O}'\text{P}'$ for either.

In actual practice the distance $2\text{ O}'\text{P}'$ need not be measured. Prefer-

⁵ *Am. Mineral.*, **45**, 974-989, 1960.

TABLE 1. SINGLE CRYSTAL AND POWDER DATA FOR PROTO-AMPHIBOLE

Precession data (CuK α)				Powder diffraction data	
Index	2 O'P' (cm.) ¹	I est.	2 θ from nomogram	2 $\theta_{(obs)}$ ²	I/I ₁
1)	(2)	(3)	(4)	(5)	(6)
020	2.07	S	10.0°	9.85(α)	5
110	2.24	S	10.9	10.69(α)	67
130	3.79	M	18.25	17.67(α)	4
200	3.98	S	19.3	19.02(α)	14
040	4.14	VS	20.1	19.87(α)	28
131	4.65 ³	S	24.5	24.428(α)	16
150	5.56	M	26.7	26.697(α)	6
				27.36(α)	13
240	5.74	VS	27.7	27.63	33
310	6.07	VS	29.3	29.13	100
231	5.07	S	29.7	29.58(α)	7
151	5.55	VS	31.7	31.71(α)	22
330	6.72	VS	32.7	32.42	25
				35.25	
161	6.53	M	36.1	35.90	21
251	6.53	S	36.1		
170	7.52	M	36.7		
350	7.90	M	38.5	38.33(α)	4
400	7.96	S	38.7	38.58(α)	4
261	7.37	M	39.7	39.71	7
080	8.30	M	40.3		
171	7.52	S	40.5	40.36	8
421	8.20	M	43.8	43.54	4
280	9.21	M	45.0		
361	8.59	S	45.5	45.48	7
370	9.39	S	46.0		
190	9.55	M	47.0		
510	9.98	VS	49.3	49.04	8
460	10.10	M	49.9		
451	9.48	W	50.0		
191	9.52	M	50.1		
				51.26	4
461	10.07	M	52.9	52.73	8
				57.05	3
				57.56	5
561	11.69	S	61.2°	61.10	14
				62.30	10
				70.55	11
				73.68	6

¹ Except where indicated, all precession spots were measured from either an ($hk0$) or (hkl) precession photograph. Fd* for (hkl) equaled 1.75 cm.

² For CuK α_1 except where noted as CuK α .

³ From ($1kl$) film; Fd*=0.99 cm.

ably it may be "picked off" the photograph with a pair of dividers and then set off along the abscissa of Fig. 2. The position of the divider point with respect to the circular 2θ scale then permits 2θ to be estimated to the nearest tenth of a degree. The accuracy, generally within $\pm 0.2^\circ$, increases as the size of the precession spots decreases.

For an n -level photograph, the process is precisely similar to that above except that the scale used to convert $2\text{ O}'\text{P}'$ to 2θ is not the abscissa line of Fig. 2. Instead, it is a line parallel to the abscissa but above it by the amount Fd^* , the film displacement utilized in photographing this particular n -level. In the example of Table 1, the value of Fd^* for the ($hk1$) photograph was 1.75 cm. A transparent straight edge was therefore so placed over Fig. 2 that it (1) passed through this point on the Fd^* scale and (2) was parallel to the abscissa. The precession spot distances for ($hk1$) planes were then set off along the line marked by the straight-edge to obtain 2θ from the circular scales as before.

In this manner 2θ was estimated to the nearest tenth of a degree for all the indexed spots of moderate intensity (or stronger) on the ($hk0$) and ($hk1$) precession photographs. These spots were listed in order of increasing 2θ value so as to facilitate comparison with the more accurately determined 2θ peaks and intensities of a powder pattern of proto-amphibole (Table 1, cols. 5 and 6). As may be seen, the precession indexing may now be carried over to index unequivocally over 50 per cent of the powder peaks. Index (171) rather than index (080) was assigned to the 40.36° powder peak, partly on the basis of its being represented by a more intense precession spot and partly from the observation that, in general, 2θ determined from the nomogram usually exceeded the 2θ value of the powder peak even in the unambiguous cases. Using the 2θ values of the newly indexed powder peaks, the lattice parameters could now be calculated for proto-amphibole with the accuracy characteristic of the powder method.

The method works particularly well for all O-level photographs as well as for n -level photographs of orthogonal crystals and monoclinic crystals in the first setting. For n -level photographs of non-orthogonal crystals, it is necessary to (a) locate the film center and (b) measure the distance $\text{O}'\text{P}'$ of points from this center (rather than $2\text{ O}'\text{P}'$ as was done heretofore to reduce the measuring error). In this case, since Fig. 2 represents a scale twice that of the normal precession photograph (in which $F=6$ cm.), it is necessary to set off twice the distance $\text{O}'\text{P}'$ along the appropriate abscissa-parallel line in Fig. 2 to obtain 2θ .

The method developed around Fig. 2 applies to precession photographs made with any wavelengths. Precession spot distances are converted into 2θ values for the wavelength used in making the precession photograph.

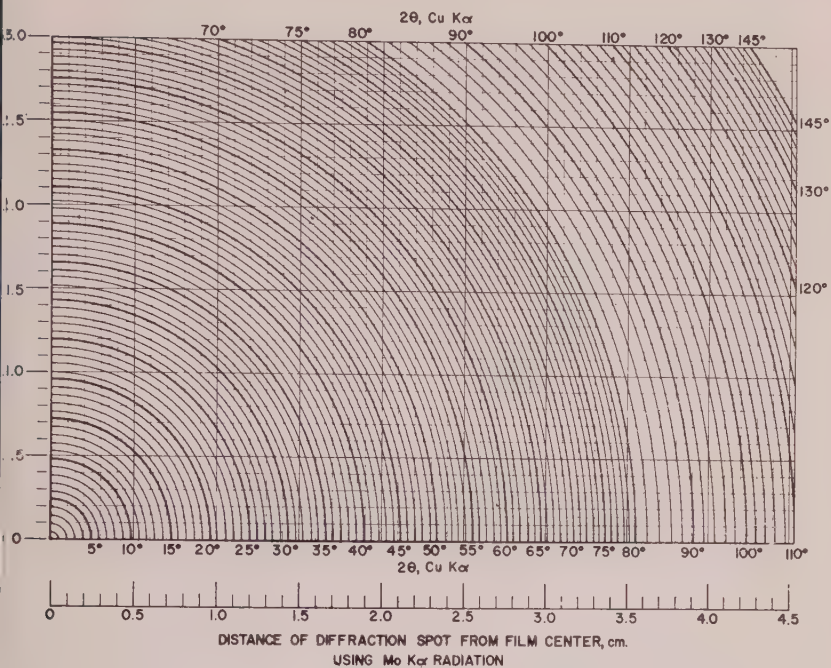


FIG. 3. Nomogram for converting precession spot distances on a precession film made with $\text{MoK}\alpha$ into 2θ $\text{CuK}\alpha$ values.

Thus, for proto-amphibole $\text{CuK}\alpha$ precession spot distances were converted to 2θ $\text{CuK}\alpha$. If $\text{FeK}\alpha$ had been used to produce the precession photograph, 2θ $\text{FeK}\alpha$ values would have resulted.

Most powder diffraction measurements are carried out with copper radiation, whereas certain advantages accrue in using $\text{MoK}\alpha$ in the photography of the reciprocal lattice. Consequently a second nomogram has been developed (Fig. 3) which is used precisely like Fig. 2. Its use is confined, however, to precession photographs made with $\text{MoK}\alpha$. By means of it, precession spot distances for $\text{MoK}\alpha$ may be converted to 2θ ($\text{CuK}\alpha$) values.

Manuscript received March 19, 1960.

ISOMORPHOUS SUBSTITUTION AND INFRA-RED SPECTRA OF THE LAYER LATTICE SILICATES*

V. STUBIČAN AND RUSTUM ROY, *The Pennsylvania State
University, University Park, Pennsylvania.*

ABSTRACT

Infra-red spectra of series of dioctahedral and trioctahedral synthetic clays in the region 400-5000 cm^{-1} have been obtained. Characteristic changes in the IR spectra with ionic substitution have been observed with both types. From these results some general conclusions concerning the variations of IR spectra with ionic substitution in both groups of clay minerals can be drawn. In many cases quantitative relationships between frequencies or intensities of the characteristic absorption bands and the extent of ionic substitutions could be established. The same parameters can also be used for the location of substituent ions.

INTRODUCTION

The investigation of solids by the absorption of infra-red rays has attracted considerable interest in recent years. The same technique has also been applied to the study of minerals. Among them the infra-red spectra of the clays have been reported by several workers. For example, Hunt *et al.* (1950, 1951, 1953), Adler (1951), and Keller and Pickett (1949, 1950) surveyed the infra-red spectra of the principal natural clay minerals between 650-5000 cm^{-1} . In the paper of Nahin (1955) the differences between infra-red spectra of some clay minerals as well as the unresolved problems have been pointed out. Further progress in this field was made when Beutelspacher (1956) extended the spectral range of study to 400 cm^{-1} , obtaining well resolved spectra of many clay minerals. An analysis of the literature concerning this subject shows that much remains to be done before the infra-red absorption technique can be successfully applied not only for analytical purposes but also for the study of the crystal chemistry and the structure of clay minerals. To attain this aim it is naturally of the greatest importance to study well defined "pure" specimens, which can rarely be found in nature. On the other hand, synthetic specimens can be prepared in very pure form, and only with such authenticated specimens can one hope to approach more directly the complex relationship between structure or composition and the infra-red spectra of clay minerals. Whereas the first part of our research (Stubičan and Roy, 1959) was concerned with an attempted assignment of the absorption bands to the proper metal-oxygen bonds, in the present investigation an attempt has been made to correlate the nature and extent of ionic substitutions with the changes caused in IR

* Contribution No. 59-74 College of Mineral Industries, The Pennsylvania State University, University Park, Pennsylvania.

spectra. As a matter of fact the results of the latter approach were very helpful in the attempted assignments.

EXPERIMENTAL PROCEDURES

Preparation of the synthetic minerals

The synthetic clays and micas were prepared from mixtures of gels. The gels were obtained as previously described by Roy (1956), by starting with "Ludox" silica sol or ethyl orthosilicate, and solutions of nitrates (Al, Mg). In some cases, to obtain the composition required by the mineral formula, an addition of sodium or potassium hydroxide solution was necessary. The mixtures were evaporated to dryness and then heated to about 500° C. until the nitrates were completely decomposed. The syntheses were carried out in small sealed gold or platinum tubes. A small amount of distilled water was added before the tubes were sealed. The usual equipment (Roy and Tuttle, 1956) was used for the hydrothermal syntheses. The conditions for the syntheses (temperature, pressure) have in general been the same as previously reported from this laboratory, except that in some cases the time of hydrothermal runs was prolonged to obtain better crystallinity of specimens. The crystallinity and the purity of each synthesized specimen were checked by x-rays before infra-red spectra were run. A few natural specimens were used, when analyses were available. The specimens investigated are listed in Table I.

Infra-red Spectra

Measurements were made with a Perkin-Elmer model 21 double beam spectrometer in the spectral region between 400–5000 cm^{-1} using NaCl and KBr prisms. The previously dried specimens (110° C.) were intimately mixed with KBr powder and pressed under vacuum. Usually 8–15 mg. of the specimens were mixed with 300 mg. KBr. The pressure applied was 75,000 lb/sq. in. Spectra were obtained with scanning speed 1000 and with the gain 5–6. It was very convenient to obtain the spectra using different gear combinations which correspond to various scale factors. Generally spectra were obtained with the NaCl prism with the scale factor 2 cm/μ and with the KBr prism with the scale factor 1 cm/μ . For quantitative work scale factors of 4 cm/μ or 2 cm/μ were used. Apparently the faster speed did not adversely affect the resolution for our purposes but much better defined absorption bands were obtained.

RESULTS

In Figs. 1 and 2 are shown the spectra for the end-member minerals presenting the dioctahedral and trioctahedral analogues of the 1:1 and 1:2 clays.

TABLE I. SPECIMENS USED IN THIS INVESTIGATION

I. Trioctahedral 2:1 family

1. Talc $\text{Mg}_3(\text{Si}_4\text{O}_{10})(\text{OH})_2$
2. Ni-Mg-Talc $\text{NiMg}_2(\text{Si}_4\text{O}_{10})(\text{OH})_2$

Saponites

3. $\text{Mg}_3(\text{Al}_{0.17}\text{Si}_{3.83})\text{O}_{10}(\text{OH})_2 \cdot \text{Na}_{0.17}^+$
4. $\text{Mg}_3(\text{Al}_{0.33}\text{Si}_{3.67})\text{O}_{10}(\text{OH})_2 \cdot \text{Na}_{0.33}^+$
5. $\text{Mg}_3(\text{Al}_{0.50}\text{Si}_{3.50})\text{O}_{10}(\text{OH})_2 \cdot \text{Na}_{0.50}^+$
6. $\text{Mg}_3(\text{Al}_{0.67}\text{Si}_{3.33})\text{O}_{10}(\text{OH})_2 \cdot \text{Na}_{0.67}^+$

The Phlogopite-Biotite Series

7. Phlogopite $\text{KMg}_3(\text{AlSi}_3)\text{O}_{10}(\text{OH})_2$
8. Ni-Mg-Phlogopite $\text{KNiMg}_2(\text{AlSi}_3)\text{O}_{10}(\text{OH})_2$
9. Al—Phlogopite $\text{K}(\text{Mg}_{2.5}\text{Al}_{0.5})(\text{Al}_{1.5}\text{Si}_{2.5})\text{O}_{10}(\text{OH})_2$
10. Al—Biotite I $\text{K}(\text{Mg}_{2.0}\text{Al})(\text{Al}_{2.0}\text{Si}_2)\text{O}_{10}(\text{OH})_2$

II. Dioctahedral 2:1 family

11. Pyrophyllite $\text{Al}_2(\text{Si}_4\text{O}_{10})(\text{OH})_2$

Beidellites

12. $\text{Al}_2(\text{Al}_{0.17}\text{Si}_{3.83})\text{O}_{10}(\text{OH})_2 \cdot \text{Na}_{0.17}^+$
13. $\text{Al}_2(\text{Al}_{0.33}\text{Si}_{3.67})\text{O}_{10}(\text{OH})_2 \cdot \text{Na}_{0.33}^+$
14. $\text{Al}_2(\text{Al}_{0.50}\text{Si}_{3.50})\text{O}_{10}(\text{OH})_2 \cdot \text{Na}_{0.50}^+$
15. $\text{Al}_2(\text{Al}_{0.67}\text{Si}_{3.33})\text{O}_{10}(\text{OH})_2 \cdot \text{Na}_{0.67}^+$

Montmorillonites

16. $(\text{Al}_{1.83}\text{Mg}_{0.17})\text{Si}_4\text{O}_{10}(\text{OH})_2 \cdot \text{Na}_{0.17}^+$
17. $(\text{Al}_{1.67}\text{Mg}_{0.33})\text{Si}_4\text{O}_{10}(\text{OH})_2 \cdot \text{Na}_{0.33}^+$
18. $(\text{Al}_{1.33}\text{Mg}_{0.67})\text{Si}_4\text{O}_{10}(\text{OH})_2 \cdot \text{Na}_{0.67}^+$

The Muscovite-Phengite Series

19. Muscovite $\text{KAl}_2(\text{AlSi}_3)\text{O}_{10}(\text{OH})_2$
20. $\frac{1}{2}$ Muscovite and $\frac{1}{2}$ Phengite $\text{K}(\text{Al}_{1.75}\text{Mg}_{0.75})(\text{Al}_{0.75}\text{Si}_{3.25})\text{O}_{10}(\text{OH})_2$
21. Phengite $\text{K}(\text{Al}_{1.80}\text{Mg}_{0.50})(\text{Al}_{0.50}\text{Si}_{3.50})\text{O}_{10}(\text{OH})_2$

III. Trioctahedral 1:1 family

22. Antigorite $\text{Mg}_3(\text{Si}_2\text{O}_5)(\text{OH})_4^*$
23. Chrysotile $\text{Mg}_3(\text{Si}_2\text{O}_5)(\text{OH})_4$

Chlorites

24. $(\text{Mg}_{2.88}\text{Al}_{0.12})(\text{Al}_{0.12}\text{Si}_{1.88})\text{O}_5(\text{OH})_4$
25. $(\text{Mg}_{2.76}\text{Al}_{0.24})(\text{Al}_{0.24}\text{Si}_{1.76})\text{O}_5(\text{OH})_4$
26. $(\text{Mg}_{2.50}\text{Al}_{0.50})(\text{Al}_{0.50}\text{Si}_{1.50})\text{O}_5(\text{OH})_4^\dagger$
27. $(\text{Mg}_{2.36}\text{Al}_{0.64})(\text{Al}_{0.64}\text{Si}_{1.36})\text{O}_5(\text{OH})_4$
28. $(\text{Mg}_{2.26}\text{Al}_{0.74})(\text{Al}_{0.74}\text{Si}_{1.26})\text{O}_5(\text{OH})_4^\dagger$
29. $(\text{Mg}_{2.12}\text{Al}_{0.88})(\text{Al}_{0.88}\text{Si}_{1.12})\text{O}_5(\text{OH})_4$
30. $(\text{Mg}_{2.00}\text{Al}_{1.00})(\text{Al}_{1.00}\text{Si}_{1.00})\text{O}_5(\text{OH})_4^\dagger$

IV. Dioctahedral 1:1 family

31. Kaolinite $\text{Al}_2(\text{Si}_2\text{O}_5)(\text{OH})_4$
32. Halloysite (Meta-) $\text{Al}_2(\text{Si}_2\text{O}_5)(\text{OH})_4$

* The natural platy antigorite from Vermlands Taberg, Western Sweden.

† These specimens were investigated both, as the 7 Å and 14 Å polymorphs.

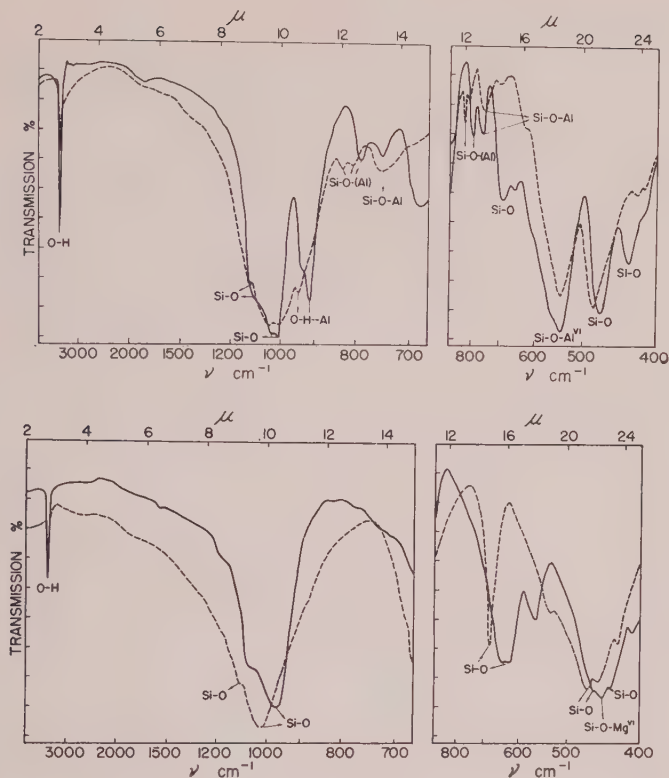


FIG. 1 (above). Infra-red spectra of kaolinite (full line) and pyrophyllite (dashed line).

FIG. 2 (below). Infra-red spectra of antigorite (full line) and talc (dashed line).

Assignments for the main bands are shown on the diagrams themselves and have been discussed by use elsewhere (Stubičan and Roy, 1959).^{*} Starting with each of these end-member spectra one can follow the various types of substitutions common in clays:

Trioctahedral 2:1 family

Two types of substitution may be distinguished in this as in most other mineral families. The first involves a simple ion for ion substitution of Ni^{2+} for Mg^{2+} . Ni^{2+} is used here as a model for the Fe^{2+} common in nature yet relatively difficult to handle in the laboratory. Talc,

^{*} Assignments for the main absorption bands have been accomplished by studying layer lattice silicates where complete replacement of an ion e.g. Mg^{2+} by Ni^{2+} and Fe^{2+} , Al^{3+} by Ga^{3+} or Fe^{3+} , Ge^{4+} for Si^{4+} . The bands involving various OH-vibrations were located by complete replacement of OH^- by OD^- .

$3\text{MgO} \cdot 4\text{SiO}_2 \cdot 2\text{H}_2\text{O}$ may be regarded as the end-member structure here. In this case one can see a distinct shift as follows: the band which appears in talc at 668 cm^{-1} moves slightly towards higher frequencies (with $\frac{1}{3}\text{Ni}$ and $\frac{2}{3}\text{Mg}$ it is at 675 cm^{-1}), and the new poorly resolved band appears at 710 cm^{-1} . (Fig. 3.)

The second type of substitution involves a balanced charge dual substitution. In talc itself experiments in this laboratory have demonstrated that the 2Al^{3+} for $(\text{Mg}^{2+} + \text{Si}^4)$ substitution is very limited. However, it is of course well known that the replacement of Si^{4+} by $(\text{Al}^{3+} + \text{Na}^+ \text{ in exchange positions})$ gives rise to the saponite family of the

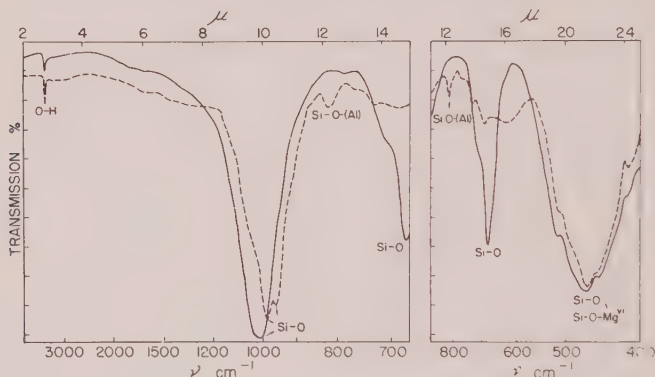


FIG. 3. Infra-red spectra of Ni-Mg-talc No. 2 (full line) and Ni-Mg-phlogopite No. 8 (dashed line).

montmorillonoid; and the extent of substitution is very substantial (see Koisumi and Roy, 1959).

Saponites

Infra-red spectra of four synthetic specimens (Table I) with increasing amounts of aluminum ions in the tetrahedral sites were obtained. In this case 1 mg. of each specimen was mixed and pressed with 300 mg. KBr.

The spectra obtained (Fig. 4) are comparable to the spectrum of talc. Some differences become more pronounced as the number of aluminum ions in the tetrahedral sites increases. For example, with increasing alumina content there is an increasing intensity of the weak absorption band at 877 cm^{-1} as well as the gradual appearance of the weak bands between $800\text{--}850\text{ cm}^{-1}$. At the same time the absorption bands at 527 , 467 , and 427 cm^{-1} are becoming more diffuse with slight changes in their

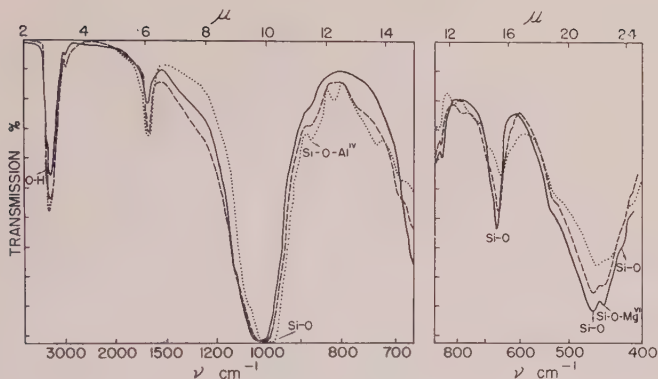


FIG. 4. Infra-red spectra of saponites: No. 3 (full line), No. 4 (dashed line), No. 6 (dotted line).

position. The most radical change can be observed with the Si-O band of talc with the frequency center at 668 cm^{-1} which decreases in intensity and moves towards lower frequencies. To determine more accurately the position and the intensity of this band for every synthetic saponite, the absorption spectra in the frequency region between $600\text{--}740\text{ cm}^{-1}$ were run using a scale factor of $4\text{ cm}/\mu$ (Fig. 5). In Fig. 6 one can see that

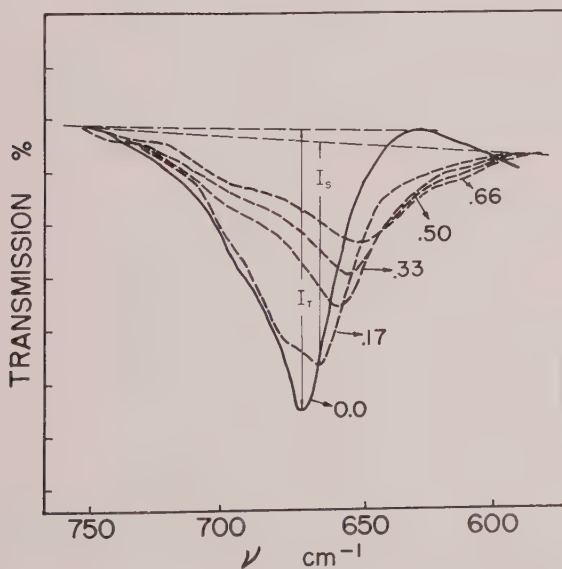


FIG. 5. The Si-O band with talc and saponites. Numbers on the curves refer to the amount of aluminum ions in the tetrahedral coordination.

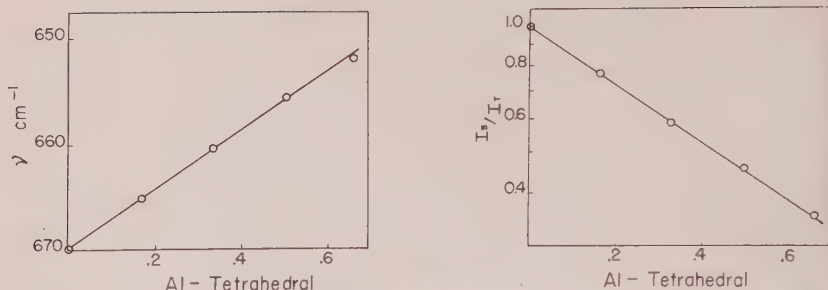


FIG. 6 (left). The relationship between the frequency of the Si-O band in the region 600–750 cm^{-1} with saponites and the amount of aluminum ions in tetrahedral coordination.

FIG. 7 (right). The ratio of the intensities of the Si-O band with saponites (I_s) to that with talc (I_t) as a function of the amount of aluminum ions in the tetrahedral sites.

there is a simple relationship between the content of aluminum ions in the tetrahedral sites and the frequency at the center of the Si-O vibration, and in Fig. 7 the relative intensities of this band are correlated to the amount of aluminum ions present.

The Phlogopite-Biotite Series

A comparison of the saponite with a phlogopite absorption pattern (Fig. 4 and Fig. 8) shows what one would expect; as the substitution of Al for Si is carried further the changes proceed in the same direction as in the saponite series with increasing exchange capacity. Thus a new band appears at about 830 cm^{-1} and a series of weak maxima between 600 and 780 cm^{-1} replaces the very sharp band at 668 cm^{-1} . The former is due presumably to a new Si-O-Al^{IV} stretching absorption and the lat-

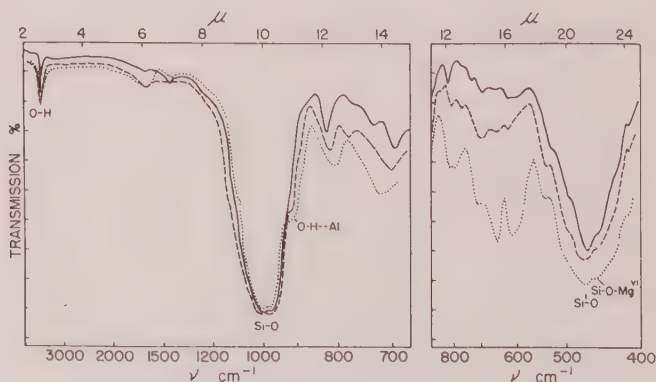


FIG. 8. Infra-red spectra of the members of the phlogopite-Al biotite series: No. 7 (full line), No. 9 (dashed line), No. 10 (dotted line).

er due to the different Si-O-Si and Si-O-Al combinations made possible. The substitution of Ni^{2+} for Mg^{2+} in phlogopite again shows (Figs. 3 and 8) as in talc, that the substitution of ions with the same charge influences the infra-red spectra much less than the substitution of ions with different charges. This is generally true if the substitution does not exceed a certain value where new bands appear.

Turning to the balanced substitutions one finds that the influence of introducing *octahedral* as well as tetrahedral substitution is most clearly noticed in the increased absorption at about 730 cm^{-1} which may correspond to the Si-O-Al stretching frequency, and the new sharp bands in the Si-Al, Si-Si, stretching region near $610, 675\text{ cm}^{-1}$. In addition the pronounced shift in the absorption peak at 830 in pure phlogopite towards 810 in the "Al-biotite" composition may be used as an index of the extent of the balanced substitution in phlogopite.

7. Dioctahedral 2:1 Family

Just as in talc natural pyrophyllite itself shows very little variability in composition. However, when some of the Si^{4+} ions are replaced by Al^{3+} ions and the charge balanced by large cations between the sheets we generate a series of montmorillonoids—the beidellites.

Beidellites

Infra-red spectra of four synthetic beidellites (Table I) were run using 55 mg. of each specimen with 300 mg. of KBr. The spectra obtained of these specimens are shown in Fig. 9. If we compare these spectra with the spectrum of pyrophyllite, some differences can be observed. It is possible to find in the spectra of beidellites all major Si-O bands as well as

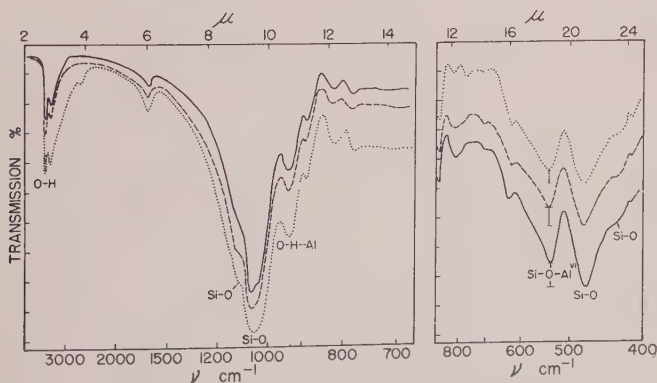


FIG. 9. Infra-red spectra of beidellites: No. 12 (full line), No. 13 (dashed line), No. 15 (dotted line).

the O-H stretching and H-O--Al bands in approximately the same position as in the spectrum of pyrophyllite. Some differences can be observed with the weak bands in the region 700-900 cm^{-1} . With the beidellite of highest alumina content the broad absorption band at 806-^{-1} is replaced by two weak bands at 753 and 820-^{-1} .

The quantitative relationship between the amount of aluminum ions in the tetrahedral sites and the infra-red spectra can be seen if we consider the intensities of the two strong absorption bands at 535 and 474-^{-1} . One can hope to find differences in the intensities of these bands with specimens having the same structures but different relative amounts of octahedral alumina and tetrahedral alumina and tetrahedral silica. With decreasing amount of silica in the tetrahedral sites as the result of

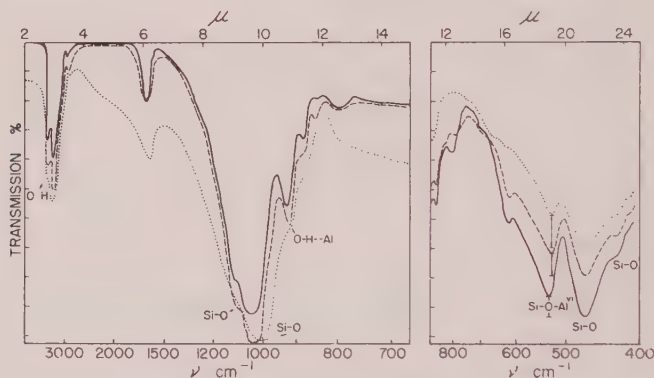


FIG. 10. Infra-red spectra of montmorillonites: No. 16 (full line), No. 17 (dashed line), No. 18 (dotted line).

replacement with aluminum ions in beidellites, the difference in the intensities of the bands at 473 and 535-^{-1} decreases. These changes in the intensities can be correlated with the amount of aluminum ions in the tetrahedral sites, but the precision here is low.

Another family of montmorillonoids can be generated when Mg^{2+} replaces Al^{3+} in the octahedral layer: this is the montmorillonite family.

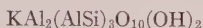
Montmorillonites

Infra-red spectra of only three synthetic montmorillonites (Table I) were obtained (Fig. 10). In this case 1.5 mg. of each specimen were pressed with 300 mg. of KBr. The infra-red spectrum of specimen No. 16 which contains only a small amount of magnesia in the octahedral site is essentially identical with the spectra of beidellites. The influence of the

increasing amount of magnesia can be observed in two spectral regions which are sensitive to the ionic substitution in the octahedral sites. The absorption band assigned to the H-O-Al at 935 cm^{-1} becomes more poorly resolved from the main Si-O band and the absorption band at 1333 cm^{-1} shows a small shift towards higher frequencies. The latter band decreases in intensity as the amount of aluminum ions in the octahedral sites decreases, and presumably could be generated by Si-O-AL^{VI} vibrations.

Muscovite-Phengite Series

The type dioctahedral mica is muscovite: this mineral



represents in reality only an end-member of the phengite family in which Mg^{2+} replaces Al^{3+} in the octahedral layer while some of the Al^{3+} of the tetrahedral layer is replaced by Si^{4+} .

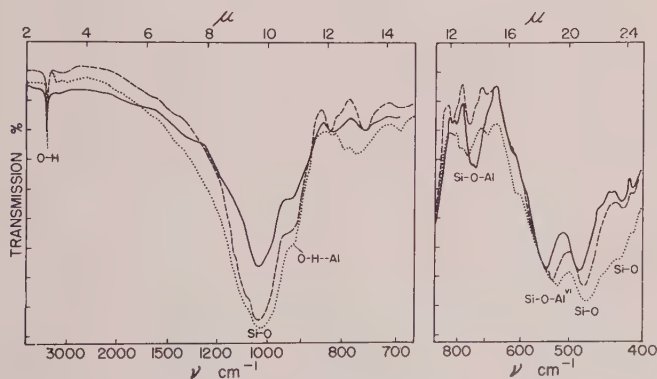


FIG. 11. Infra-red spectra of the members of the muscovite-phengite series: No. 19 (full line), No. 20 (dashed line), No. 21 (dotted line).

In Fig. 11 the infra-red spectra of three synthetic specimens (Nos. 19, 20, 21, Table I) which contained increasing amounts of magnesium ions in the octahedral sites are shown. It is evident that, with entry of magnesium into the octahedral sites, the absorption band with the frequency 935 cm^{-1} becomes more poorly defined, as was also the case with montmorillonites. It seems also that the presence of magnesium ions causes the deactivation of vibrations which give rise to the appearance of the weak absorption bands in the region $600\text{--}850\text{ cm}^{-1}$. The displacement of the absorption band of muscovite at 543 cm^{-1} towards lower frequencies is very marked and can be correlated with the presence of magnesium

ions in the octahedral sites. The quantitative relationship between the amount of magnesia and the frequency center of this band was established (Fig. 12).

III. Trioctahedral 1:1 Minerals

Septechlorites and Chlorites

The chlorites form an extensive isostructural series with extensive ionic substitutions. The natural group comprises mainly magnesium and iron aluminosilicates, but appreciable amounts of chromium, nickel or manganese can also be found in natural specimens.

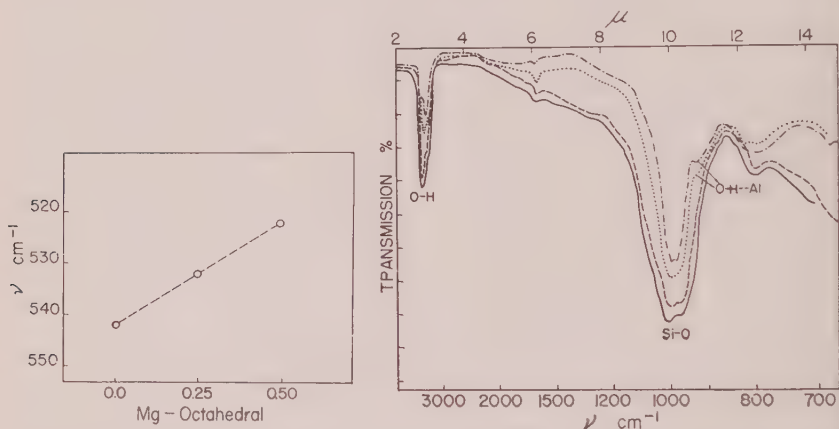


FIG. 12 (left). The relationship between the frequency of the Si-O-Al^{VI} band with the members of the muscovite-phengite series and the amount of magnesium ions in octahedral coordination.

FIG. 13 (right). Infra-red spectra of 7 Å chlorites (septechlorites) in the region 666–5000 cm⁻¹: No. 25 (full line), No. 26 (dashed line), No. 29 (dotted line), No. 30 (dash-dot line).

Our infra-red studies were concerned only with the magnesium aluminum chlorites and specifically with the 7 Å chlorites (septechlorites) and 14 Å chlorites (normal), the synthesis and stability of which have been reported by Nelson and Roy (1958). According to these authors, chlorites are layer lattice silicates of one of two polymorphic types. The one is a trioctahedral two-layer structure type and the other is a four-layer structure comparable to that of mica with substituted brucite sheets replacing K⁺. There is an essentially continuous solid solution in the septechlorites extending between chrysotile and amesite compositions.

Infra-red spectra of 7 specimens of septechlorites (Table I) have been obtained. In this case 1 mg. of the specimen was pressed with 300 mg. of KBr.

With an increasing amount of aluminum ions in the octahedral and tetrahedral sites the most striking change is in the width of the main Si-O bands. Only a weak possible H-O--Al band appears in the richest Al composition at 910 cm^{-1} (Fig. 13). More sensitive to the amount of aluminum ions present is the $\text{Al}^{\text{VI}}\text{-O-Si}$ band with the frequency center at about 535 cm^{-1} . This band can be resolved with all septechnorites from chlinochlore to amesite (Fig. 14). Neither of the above-mentioned absorption bands is sensitive enough for quantitative treatment of isomorphous substitution in this case. Some other strong absorption bands, e.g. the Si-O band at 473 cm^{-1} as well as the Si-O-Mg^{VI} band at 451 cm^{-1}

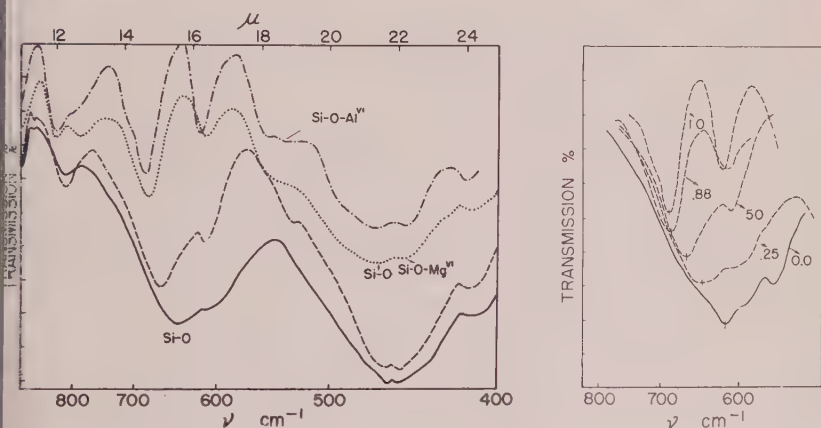


FIG. 14 (left). Infra-red spectra of 7 Å chlorites in the region $450\text{--}910\text{ cm}^{-1}$: No. 25 (solid line), No. 26 (dashed line), No. 29 (dotted line), No. 30 (dash-dot line).

Fig. 15 (right). Absorption bands in the region $550\text{--}800\text{ cm}^{-1}$ with 7 Å chlorites. Numbers on the curves refer to the amount of aluminum ions in octahedral or tetrahedral coordination.

are not affected by the presence of aluminum ions in the lattice. However, characteristic changes in the absorption region between $590\text{--}750\text{ cm}^{-1}$ can be correlated in a quantitative way with the amount of aluminum ions in both coordinations.

Starting from chrysotile (Fig. 15), the strong absorption band at 606 cm^{-1} is gradually shifted in the direction of higher frequencies as the amount of aluminum ions increases till finally with amesite we find the same band at 685 cm^{-1} . Actually bands which are only poorly resolved in this region with chrysotile can be much better resolved with septechnorites as the result of this shift. It seems very probable that all absorption bands in this spectral region can be assigned to metal-metal stretching

vibrations (Stubičan and Roy, 1959). Referring to Fig. 16 it can be noticed that the frequencies of the strongest absorption band in this region can be correlated with the amount of aluminum ions in both coordinations. In this plot the most significant change appears to take in septeclorites between serpentine and chlinochlore, while in septeclorites between clinochlore and amesite the frequency of this Si-O band varies only from 665 to 685 cm^{-1} .

This apparent shape of the curve can easily be seen to be due to the overlapping of two bands which are clearly resolved in amesite but which are affected to different extents by substitution of Si^{4+} by Al^{3+} so that

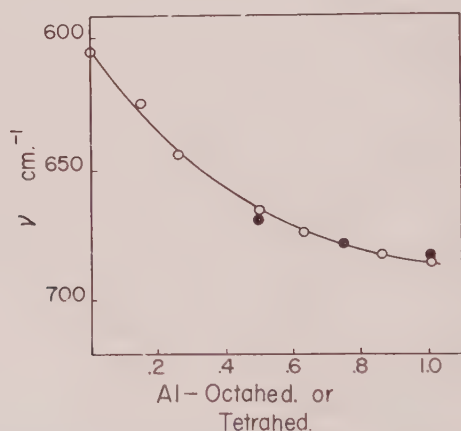


FIG. 16. The relationship between the frequency of the strongest Si-O band in the absorption region 550–800 cm^{-1} with 7 Å chlorites (open circles) and 14 Å chlorites (solid circles) and the amount of aluminum ions in octahedral or tetrahedral coordination.

by the time the composition of penninite is reached they are barely resolvable. Rather than attempt to separate the peaks geometrically the plot is simply made using the *apparent* peak position and gives rise to the apparent non-linear variation.

A series of normal 14 Å chlorite structures extends continuously between one containing about 10% of alumina and amesite. The similarity of the spectra of 14 Å and 7 Å chlorites is evident (Figs. 12, 13, 17, 18). Nevertheless, several distinctions exist. Regardless of alumina content there is generally no resolved band at 910 cm^{-1} with 14 Å chlorites (Fig. 13). It is known that this band is much less pronounced with 2:1 type than with 1:1 clay minerals even in the case when all octahedral positions are occupied by aluminum ions. The main difference is in the frequency region 750–850 cm^{-1} where the two bands are not as well re-

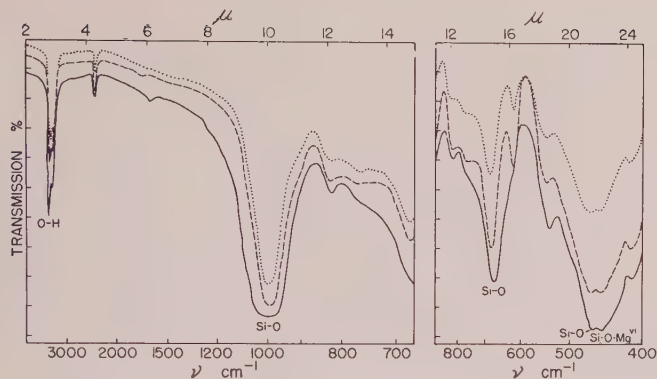


FIG. 17. Infra-red spectra of 14 Å chlorites: No. 26 (full line), No. 28 (dashed line), No. 30 (dotted line).

lved with normal chlorites as with septechlorites. This results in the possibility of using this band also to distinguish between two polymorphs with the same composition. The strongest Si-O band in the frequency region between 665 and 685 cm^{-1} which was used for quantitative treatment of the amount of octahedral and tetrahedral alumina with 7 Å chlorites (vide supra) is found practically in the same position with the corresponding 14 Å chlorites (Fig. 15). The shifts in this band are also analogous. The relatively small shift in this band from the clinochlore to the amesite composition *may* be related to a disproportionation of the Al^{3+} ions between the two octahedral layers. However, much more precise work will be necessary to establish this. Tuddenham and Lyon have recently (1959) published a paper concerned with the relation of infra-

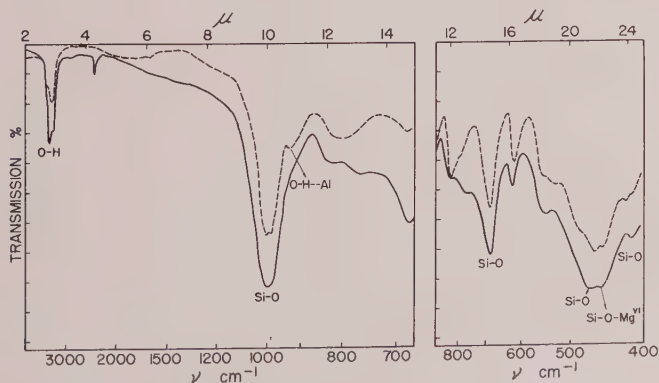


FIG. 18. Infra-red spectra of 7 Å chlorite (dashed line) and 14 Å chlorite (full line) No. 30.

red spectra and chemical composition of some *natural* chlorites. Their spectra extend from 650–5000 cm^{-1} , and they propose the use of the shift in the main Si-O band near 1000 cm^{-1} . The magnitude of the shift is considerably smaller than that shown here, but this shift may be of use to detect Fe^{2+} for Mg^{2+} substitution. Further, it should be noted that in some natural chlorites the band at 1080 cm^{-1} is completely re-established whereas in synthetic chlorites it is well integrated with the main Si-O band. It is more than likely that this is due to Al-Si disorder in the synthetic specimens, although the synthetic specimens are very well crystallized by x -ray diffraction evidence.

IV. Dioctahedral 1:1 Minerals

The type dioctahedral mineral is kaolinite and no appreciable substitutions for Al or Si are known in nature. In the laboratory we have failed to introduce large amounts of Ga^{3+} , Fe^{3+} or Ge^{4+} , and the 3Mg^{2+} for 2Al^{3+} substitution has not been achieved.

THE INFLUENCE OF POLYTYPISM

While gross spectral differences did not appear to exist between clays which differed only slightly in composition it may be anticipated from theory that perhaps more important differences will be found with minor structural variants. It has already been pointed out elsewhere (Stubičan and Roy, 1959) that the use of space group selection rules in such complex structures is very difficult if at all possible. However it seemed worthwhile to record infra-red spectra of several clay minerals which have essentially the same chemical composition but slightly different structure. Of special interest are the polytypic phases with different symmetry. Several polytypes exist in the serpentine group of minerals. Recently Brindley and Zussman (1959) published infra-red absorption data for serpentine minerals in the region 650–5000 cm^{-1} . However, it could be anticipated that better distinction between spectra of these minerals can be obtained in the absorption region between 400–900 cm^{-1} where bending movements are involved since these would be most affected by stacking differences. It can be observed from Figs. 19, 20 that this is, indeed, the case. The platy antigorite (Vermlands, Taberg) and the fibrous antigorite (picrolite, Shipton, Quebec) with approximately the same composition but different morphology* have very similar absorption curves though some important differences can be observed. This can be seen in the different positions of the strong absorption bands in the ab-

* For the data concerning morphology and unit cell parameters, see: Zussman, J., Brindley, G. W., and Comer, J. J. (1957), "Electron Diffraction Studies of Serpentine Minerals," *Am. Mineral.* **42**, 133–153.

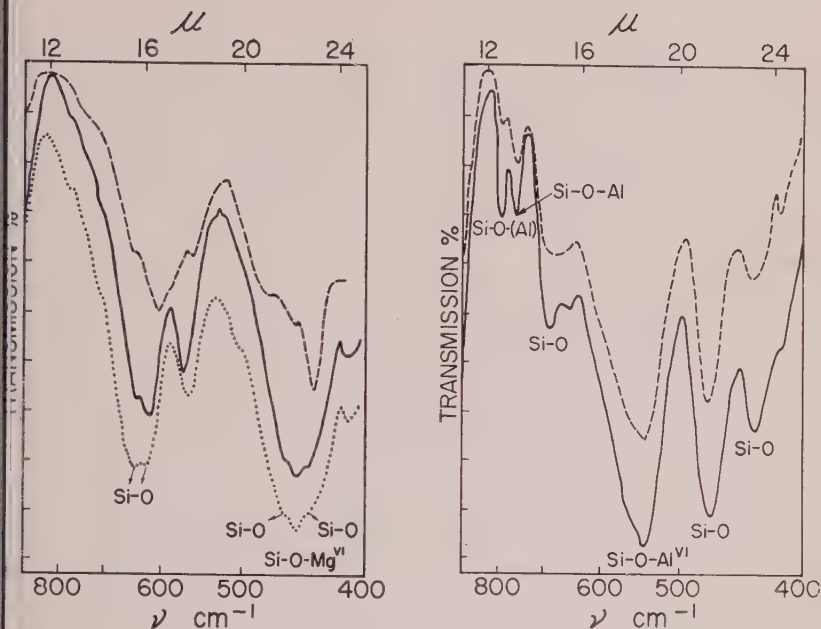


FIG. 19 (left). Infra-red spectra in the $450\text{--}910\text{ cm}^{-1}$ of the fibrous antigorite, Quebec (solid line), chrysotile, Quebec (dashed line), and the platy antigorite, Taberg, Western Sweden (dotted line).

FIG. 20 (right). Infra-red spectra of synthetic kaolinite (full line) and metahalloysite, Breka (dashed line).

absorption region near 700 cm^{-1} as well as in the relative intensities of the bands at about 645 and 625 cm^{-1} .

Chrysotile, (Clinochrysotile, Thelfas, Quebec) with a different structure, shows an apparently different absorption spectrum because the relative intensities of the absorption bands are very much different from those of antigorite. However all absorption bands present in the infrared spectra of antigorites can be found in the spectrum of chrysotile slightly shifted in position, or more poorly resolved, or with different relative intensities. Since the question of composition of these phases raises questions about interpretation, our attempt was made to work with synthetic phases with nearly identical composition. In the infrared spectra of three synthetic polytypes of muscovite, 1M, 2M, and 3T the composition of the 3T phase was $\text{K}_{0.7}\text{Al}_2(\text{Al}_{0.7}\text{Si}_{3.33})\text{O}_{10}(\text{OH})_2$ small differences were obtained (Fig. 21). The most important of these are the presence of a much stronger absorption band at 760 cm^{-1} in the triclinic phase than in the monoclinic forms. Conversely the absence of the shoulder at 640 cm^{-1} in the 3T phase distinguishes it from the 1M and 2M

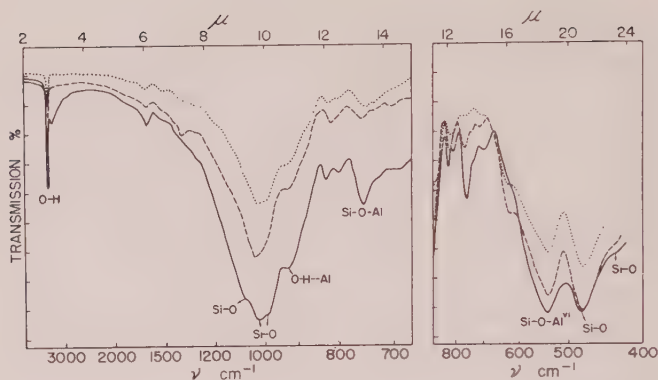


FIG. 21. Infra-red spectra of three polytypes of muscovite: 3T (full line), 2M (dashed line), 1M (dotted line).

phases. Similar effects can be observed if one compares the absorption bands in the same region with pyrophyllite and beidellites (Figs. 1 and 9), as well as in the spectra of kaolinite and halloysite (Fig. 20), which reflect the influence of rather extensive stacking disorder in the latter phases as compared with reasonable order in pyrophyllite and kaolinite.

DISCUSSION

For many years it has been well known that the absorption frequencies in crystalline solutions* vary with the concentration of components. Infra-red spectra of solid solutions of alkali halides contain only one absorption maximum and not two, as could be expected in the case of a true mixture (Krüger *et al.*, 1928). The same result was obtained with solid solutions of NaNO_3 and KNO_3 (Raju, 1945). Likewise in the Raman spectrum only one line appeared with the solid solution for every line of each of its components, the frequency being intermediate. The theoretical approach to the interpretation of the vibration spectra of solid solutions was taken by Matossi (1951). An averaging effect is obtained at least at low concentrations of solute due to the influence of each cation (or anion) upon neighboring cation-anion bonds. In other words, one does not have individual dipoles vibrating independently and giving rise to frequencies corresponding to each cation-anion pair. In one way this is a pity, since other properties such as lattice spacings also reflect this averaging effect; on the other hand, where ionic sizes are similar the infra-red shifts are much more sensitive than lattice shifts. In crystalline solutions with high concentrations of solute separate ab-

* More commonly, though less accurately, referred to as solid solutions.

absorption bands do appear, even though x -ray diffraction properties vary continuously in this region.

In the light of this earlier knowledge one can consider the variation in the spectra caused by crystalline solubility in the layer silicates. As the best example of isomorphous substitution in the clays one can consider the substitution in tetrahedral coordination of Al^{3+} for Si^{4+} .

(Quite different responses were obtained with the two families, di- and octahedral. This different response arises mainly from the fact that vibrations of ions in the crystal lattice are not independent of the rest of the crystal. Up to now no specific band in the spectra of either family could be assigned to the Al-O vibrations with Al^{3+} in tetrahedral coordination.* Hence, only indirect evidence of the presence of aluminum ions in the tetrahedral sites can be observed.

The best examples of this case are found with saponites and beidellites. Farmer (1958) discussed the infra-red spectra of talc, a saponite and a pectorite, and he pointed out only the general broadening of the absorption bands of "smectites" as the result of the isomorphous substitution in the talc structure. According to this author the broadening of bands is the result of the coupling of out-of-resonance vibration. However, more fundamental changes in the spectra of saponites with increasing amount of aluminum ions in the tetrahedral sites can be found. The gradual decreasing of the frequency and intensity of the Si-O band of talc at 668 cm^{-1} reflects the disturbing influence of the presence of the tetrahedral aluminum ions on their Si^{4+} -O neighbors (Fig. 5). With dioctahedral clay minerals, *e.g.* with beidellites, the absorption spectrum in this region is modified due to the presence of trivalent ions in the octahedral sites (Fig. 9). The absorption spectra in this latter case offers less possibility for quantitative treatment of ionic substitution. The presence of aluminum ions in the tetrahedral sites in this case can be correlated only to the decreasing of intensity of the Si-O band at 473 cm^{-1} relative to the bands at 535 cm^{-1} .

(Quite a different response can be observed when the substitution takes place in the octahedral sites. Probably the most radical changes are observed when the substitution of ions *with different charge* takes place. Consider first the substitution in dioctahedral clay minerals. The effect of this kind of substitution on the infra-red spectra of montmorillonites and the members of the muscovite-phengite series can be easily observed (figs. 10 and 11). In this case two spectral regions are very sensitive to substitutions. First, with increasing amount of magnesia in the octa-

* The position of such a band calculated by the method of Dachille and Roy (1959) would indicate a value of $10.5\text{ }\mu$. The band may be slightly shifted due to the environment and obscured by the neighboring bands.

hedral sites, the H-O--Al absorption band at 935 cm.^{-1} decreases in intensity and is more poorly resolved. Second, the frequency and the intensity of the Si-O-Al^{VI} band at 535 cm.^{-1} decreases as the result of this substitution. Both parameters can be useful for the estimation of the amount of magnesium ions in the octahedral sites with dioctahedral clays (Fig. 12). No bands for Mg-O absorption appear clearly in this range of concentration of Mg²⁺.

With trioctahedral clays both above-mentioned bands are absent, though with increasing amount of aluminum ions in the octahedral sites one could expect their gradual appearance. These bands do indeed become visible in the spectra but only in specimens containing large amounts of alumina. With trioctahedral clays the shifts in these regions are not sensitive enough for more quantitative determination of the amount of aluminum ions in the octahedral sites. Nevertheless, even with trioctahedral clays the typical changes of spectra can be correlated with the amount of aluminum ions in the octahedral sites (Fig. 8). Certainly in these cases we have to consider also the combined influence of the octahedral and tetrahedral substitution.

In summary, it can be said that:

1. The ions involved in the vibrations responsible for most of the major absorption bands in the $400\text{--}500\text{ cm.}^{-1}$ infra-red region are now fairly well-established.
2. Shifts in the absorption frequency and/or intensity can be used to indicate the amount and location of substituent ions, providing a sensitive method for the study of layer lattice silicates.
3. Structural changes in the clays in various reactions, e.g. heating (Stubičan, 1959) or chemical leaching, may also be followed by changes in infra-red spectra.

ACKNOWLEDGMENT

This research was supported by the American Petroleum Institute Project 55. It appeared as Technical Report Number 4 of the same Project, dated 20 July, 1959.

REFERENCES

- ADLER, H. H., (1951) Infra-red investigations of clay and related minerals: *Am. Petroleum Inst. Proj.* **49**, *Reference Clay Minerals, Prelim. Rpt.* **8**, pp. 1-72, New York, Columbia University.
- BEUTELSPACHER, H., (1956) Infrarot Untersuchungen an Bodenkolloiden: *6th International Congress of Soil Science. Reports B* (Commission 1 and 2), pp. 329-335.
- BUSWELL, A. M., AND DUDENBOSTEL, B. F., (1941) Spectroscopic studies of base exchange materials: *J. Amer. Chem. Soc.*, **63**, 2554-8.
- BRINDLEY, G. W. AND ZUSSMAN, J., (1959) Infra-red absorption data for serpentine minerals: *Am. Mineral.*, **44**, 185-189.

- ACHILLE, F. AND ROY, R., (1959) The use of infra-red absorption and molar refractivities to check coordination: *Zeit. Krist.*, **111**, 462-467.
- ARMER, V. C., (1958) The infra-red spectra of talc, saponite, and hectorite: *Min. Mag.*, **31**, 829-845.
- ENDRICKS, S. B. AND JEFFERSON, M. E., (1939) Polymorphism of the micas: *Am. Mineral.*, **24**, 729-771.
- ENT, J. M., (1951) Infra-red spectra of clay minerals: *Am. Petroleum Inst. Proj. 49, Reference Clay Minerals, Rpt. 8*, pp. 105-121, New York, Columbia University.
- ENT, J. M., WISHERD, M. P., AND BONHAM, L. C., (1950) Infra-red absorption spectra of minerals and other inorganic compounds: *Anal. Chem.*, **22**, 1478-1497.
- ENT, J. M. AND TURNER, D. S., (1953) The determination of mineral constituents of rocks by infra-red spectroscopy: *Anal. Chem.*, **25**, 1169-1174.
- ELLER, W. D. AND PICKETT, E. E., (1949) The absorption of infra-red radiation by powdered silicate minerals: *Am. Mineral.*, **34**, 855-864.
- ELLER, W. D. AND PICKETT, E. E., (1950) The absorption of infra-red radiation by clay minerals: *Am. Jour. Sci.*, **248**, 264-273.
- IZUMI, M. AND ROY, R. (1959) Synthetic montmorillonoids with variable exchange capacity: *Am. Mineral.*, **44**, 788-805.
- EGGER, F., REINKOBER, O., AND KOCH-HOLM, E., (1928) Reststrahlen von Mischkristallen: *Ann. Physik*, **85**, 110-128.
- UNER, P. J., (1952) Regularities in the infra-red spectra of silicate minerals: *Am. Mineral.*, **37**, 764-784.
- ATOSSI, F., (1951) Interpretation of the vibration spectrum of mix crystal: *J. Chem. Phys.*, **19**, 161-163.
- ATSON, P. G., (1955) Infra-red analysis of clay and related minerals: Clay and Clay Technology. *Bull. 169, Dept. Nat. Resources, Div. Mines, California*, pp. 112-118.
- ELSON, B. W. AND ROY, R., (1958) Synthesis of chlorites and their structural and chemical composition: *Am. Mineral.*, **43**, pp. 707-725.
- JU, M. K., (1945) Raman spectra of mixed crystals sodium and potassium nitrates: *Proc. Indian Acad. Sci.*, **22A**, pp. 150-6.
- AY, D. M. AND ROY, R., (1957) Hydrogen-deuterium exchange in clays and problems in the assignment of infra-red frequencies in the hydroxyl region: *Geochim. et Cosmochim. Acta*, **11**, pp. 72-85.
- AY, R., (1956) Aids in hydrothermal experimentation: II Methods of making mixtures for both "Dry" and "Wet" phase equilibrium studies: *J. Am. Ceram. Soc.* **39**, 145-6.
- AY, R. AND TUTTLE, O. F., (1956): "Investigations under hydrothermal conditions," Ch. VI in *Physics and Chemistry of Earth*, Pergamon Press, London.
- BIČAN, V., (1959) Residual hydroxyl groups in the metakaolinite region: *Min. Mag.*, **32**, pp. 38-52.
- BIČAN, V. AND ROY, R., (1959) A new approach to assignments of the infra-red absorption bands in layer silicates: *Zeit. Krist.*, in press.
- DDENHAM, W. M. AND LYON, R. F. P., (1959) Relation of infra-red spectra and chemical analysis for some chlorites and related minerals: *Anal. Chem.*, **31**, pp. 377-380.

manuscript received March 19, 1960.

MINERALOGY AND PETROLOGY OF THE SYSTEM $\text{Al}_2\text{O}_3\text{-SiO}_2\text{-H}_2\text{O}$ IN SOME PYROPHYLLITE DEPOSITS OF NORTH CAROLINA

E-AN ZEN,* *Department of Geology and Geography,
University of North Carolina.*

ABSTRACT

The mineral assemblages from seven pyrophyllite deposits in the Volcanic Slate belt of the North Carolina Piedmont were studied by x -ray and microscopic methods. These deposits are at Glendon, Robbins, Staley, Snow Camp, Hillsboro, Hager's Mountain, and Bowling's Mountain.

Six of the minerals found in these deposits belong to the ternary system $\text{Al}_2\text{O}_3\text{-SiO}_2\text{-H}_2\text{O}$: quartz, pyrophyllite, andalusite, kyanite, kaolinite, and diaspore. The following are 3-phase assemblages belonging to the ternary system: quartz-kaolinite-pyrophyllite; pyrophyllite-andalusite-quartz; and kaolinite-diaspore-pyrophyllite. All the observed relations, in detail, are consistent with the assumption of mutual equilibrium among the minerals. The occurrence of andalusite-kaolinite assemblage at Hillsboro but of pyrophyllite-diaspore at Staley suggest differences in physical conditions of metamorphism at these localities.

The prevalence of 3-phase assemblages indicates that H_2O behaved as a fixed chemical component during the formation of the pyrophyllite bodies. This conclusion is inconsistent with a hydrothermal-replacement origin for these bodies, as such a theory implies that H_2O belonged to an open system and thus was a mobile component. An alternative mode of origin, consistent with the mineralogical and geological data, starts with saprolite bodies on the weathered surfaces of the volcanic rocks. The saprolite was buried by later volcanic rocks and subsequently the entire sequence was metamorphosed; during recrystallization the saprolite bodies behaved as closed systems. Relative concentrations of Al_2O_3 , SiO_2 , and H_2O at different parts of each deposit account for the difference in mineral assemblages. The regional metamorphism was of low grade; nowhere was the almandite isograd reached.

INTRODUCTION

The pyrophyllite deposits of North Carolina are intimately related geologically to the Volcanic Slate belt of the Piedmont region. The general mode of occurrence of the pyrophyllite deposits and their possible origin, as well as the geology of the surrounding areas, have been discussed by Stuckey (1928) and by Broadhurst and Councill (1953).

The writer has recently studied the detailed mineralogy and petrography of seven of these deposits, as well as their wall rocks. Although the work is yet incomplete, enough has emerged to justify a report on the relations among those minerals that belong to the chemical system $\text{Al}_2\text{O}_3\text{-SiO}_2\text{-H}_2\text{O}$.

The seven deposits reported here are at Glendon (both the Womble and Phillips pits), and Robbins, both in the Deep River region in the northern part of Moore County; at Staley in Randolph County, at

* Present address: Theoretical Geophysics Branch, U. S. Geological Survey, Silver Spring, Maryland.

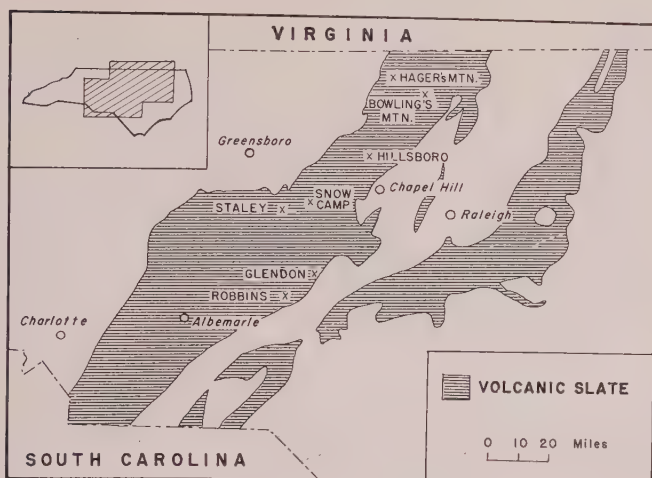


FIG. 1. Map showing location of the seven pyrophyllite deposits reported in this paper (crosses), and principal communities (circles). Inset relates the location of the map to the boundary of North Carolina.

Hillsboro in Orange County, at Hager's Mountain in Person County, at Bowling's Mountain in Granville County, and in several small pits near Snow Camp in Alamance County (Fig. 1; Stuckey, 1928; Broadhurst and Council, 1953; Conley, 1958). The samples were studied both with the petrographic microscope and with a Norelco X-ray Diffractometer; wherever possible results using the two methods are correlated with each other.

MINERALOGY

Introduction

Although many of the minerals in these deposits do not belong to the simple system $\text{Al}_2\text{O}_3\text{-SiO}_2\text{-H}_2\text{O}$, discussion of the other minerals will be omitted. The principal omitted minerals are chloritoid, clinozoisite, chlorite, muscovite, paragonite, hematite, rutile, and pyrite.

Pyrophyllite $\text{Al}_2\text{Si}_4\text{O}_{10}(\text{OH})_2$

Pyrophyllite is one of the commonest and most abundant minerals in the deposits; it is also found in the country rock. It occurs rarely as radiating rosettes of clear pale blue-green crystals up to 2 mm. by 10 mm. in size, and as such has been found at Staley,[†] and at Bowling's Mountain. More commonly, pyrophyllite occurs as fine, felty aggregates. The indi-

[†] The thermochemical properties of the best sample from Staley are being measured by R. A. Robie of the Theoretical Geophysics Branch, U. S. Geological Survey.

vidual crystals are too small to be seen in a hand specimen but the mineral is easily detected by the soapy feel of the rocks containing it. Fine aggregates of pyrophyllite occur in nodules, and in massive as well as banded rocks.

Microscopically, pyrophyllite is easily distinguished from kaolinite by its much higher birefringence, but it can be distinguished from muscovite and paragonite only by x-ray diffraction. The series of diffraction lines due to the (00 l) planes, with the basal spacing of about 9.2 Å, is diagnostic. The only possible mineral with which it might be confused, talc, has not been found in the pyrophyllite deposits.

Kaolinite, $Al_2Si_2O_5(OH)_4$

Kaolinite is a common mineral in all seven deposits. It occurs not only in clearly secondary, cross-cutting veins and joint-fractures, as at Hillsboro, but also occurs in the bulk of the deposits. In fact, few pyrophyllite-rich samples are free of kaolinite. Kaolinite also occurs in the country rock without pyrophyllite.

Microscopically, kaolinite occurs as small lath-shaped crystals of low birefringence, showing at most first-order grey interference color. Where intergrown with pyrophyllite, the sharp contrast in birefringence separates the two phases easily. Many of these intergrowths are on a microscopic scale, with both phases scattered throughout a thin section. There is no textural evidence in any of the samples studied to indicate that either mineral is an alteration product of the other.

The chief basis for the identification of kaolinite in a sample is by its x-ray diffraction pattern, with the strong 7 Å basal reflection and its higher harmonics. As the samples rarely contain chlorite, it causes little confusion in identification.

Diaspore $AlOOH$

Diaspore occurs in the Staley deposit (Broadhurst and Councill, 1953, p. 18). The writer has not found this mineral in the quarry; however, Dr. J. L. Stuckey kindly contributed a small sample from his collection. The sample is grey and shows crude blade-like crystal forms covered by scales of a white mica. Diaspore is identified by its x-ray diffraction pattern; the associated white mica is pyrophyllite with a trace of kaolinite. Due to the unavailability of more samples, no microscopic study has been made.

Andalusite Al_2SiO_5

Andalusite is found at Staley and at Hillsboro, and has been reported by Broadhurst and Councill (1953, p. 15) from Bowling's Mountain. The color is grey in some, but more commonly is light blue or turquoise.

Microscopically, andalusite is characterized by its optical properties (Winchell and Winchell, 1951, p. 521). Its relatively high refringence makes it stand out in strong relief. In most samples, it occurs as anhedral to subhedral masses, strongly poikilitic with inclusions of subhedral quartz, and a few crystals of pyrophyllite or kaolinite scattered both inside and around the andalusite. The andalusite crystals are up to 5 mm. across.

The x -ray pattern of andalusite is compared with that of a standard andalusite from Laws, California, in the Holden Collection of the Mineralogical Museum, Harvard University (no. 95769).

Kyanite Al_2SiO_5

In this study, kyanite has been found only at Hager's Mountain near Roxboro, Person County. Here it is found in two modes of occurrence: as large (up to 6 inches long) crystals in the bulk of the deposit, associated principally with quartz. Such kyanite forms large knobs on slightly weathered surfaces and is commonly pseudomorphed after by white mica. It also occurs as pale blue, clear, blade-like crystals in vein fillings in the rock, and is associated with pyrophyllite and quartz.

Both kyanite and andalusite have been reported from Bowling's Mountain (Broadhurst and Council, 1953, p. 15). In the present study, however, neither was found.

Quartz SiO_2

Quartz is common in the specimens studied, although it is absent in some samples and is subordinate in many others. Quartz occurs both as fine, subhedral grains more or less uniformly disseminated in the rocks, and in veins.

PETROLOGY

Mineral Assemblages

The minerals found at the seven pyrophyllite localities are listed in Table I; for completeness the entire assemblages are given and those minerals belonging to the ternary system Al_2O_3 - SiO_2 - H_2O are set in italics. Each assemblage represents the minerals found in a single thin-section, or a single x -ray mount.

Phase Relationships

The observed phase relationships in the ternary system Al_2O_3 - SiO_2 - H_2O are depicted in Fig. 2. A few comments are necessary.

The first point concerns the anhydrous phase, andalusite. As remarked before, andalusite occurs as stout, poikilitic porphyroblasts in most of the specimens. In a hand specimen it may appear corroded, yet microscopi-

TABLE I

I. Assemblages with four phases in the ternary system	
<i>Pyrophyllite-kaolinite-andalusite-quartz</i>	(Hillsboro, Glendon?)
<i>Pyrophyllite-kaolinite-kyanite-quartz</i>	(Hager's Mountain)
II. Assemblages with three phases in the ternary system	
<i>Pyrophyllite-kaolinite-quartz</i>	(Hillsboro; Glendon; Hager's Mountain; Staley?)
<i>Pyrophyllite-kaolinite-quartz-chloritoid</i>	(Glendon; Robbins)
<i>Pyrophyllite-kaolinite-quartz-hematite</i>	(Glendon)
<i>Pyrophyllite-kaolinite-quartz-muscovite-chlorite (?)</i>	(Robbins)
<i>Pyrophyllite-kaolinite (?) -quartz-chlorite</i>	(Hager's Mountain)
<i>Andalusite-pyrophyllite-quartz</i>	(Staley; Hillsboro)
<i>Andalusite-kaolinite (?) -quartz</i>	(Hillsboro)
<i>Pyrophyllite-diaspore-kaolinite</i>	(Staley)
III. Assemblages with two phases in the ternary system	
<i>Kaolinite-quartz</i>	(Glendon)
<i>Kaolinite-quartz-muscovite</i>	(Hillsboro; Bowling's Mountain)
<i>Kaolinite-quartz-chloritoid-chlorite (?)</i>	(Glendon)
<i>Kaolinite (?) -quartz-muscovite-chlorite (?)</i>	(Snow Camp)
<i>Pyrophyllite-kaolinite</i>	(Glendon; Robbins; Staley)
<i>Pyrophyllite-kaolinite-muscovite</i>	(Glendon)
<i>Pyrophyllite-kaolinite-clinozoisite-chlorite (?)</i>	(Glendon)
<i>Pyrophyllite-kaolinite-chloritoid-muscovite</i>	(Glendon)
<i>Pyrophyllite-kaolinite-chlorite-chloritoid</i>	(Glendon)
<i>Pyrophyllite-kaolinite-chloritoid</i>	(Robbins)
<i>Andalusite-quartz</i>	(Hillsboro; Staley)
<i>Andalusite-kaolinite-muscovite</i>	(Hillsboro)
<i>Pyrophyllite-quartz</i>	(Staley)
<i>Pyrophyllite-quartz-muscovite</i>	(Staley; Robbins; Snow Camp)
<i>Pyrophyllite-quartz-chloritoid-hematite</i>	(Glendon)
<i>Pyrophyllite-quartz-chloritoid</i>	(Glendon; Staley; Robbins; Snow Camp)
<i>Pyrophyllite-quartz-chloritoid-chlorite-muscovite (?)</i>	(Glendon)
<i>Pyrophyllite-quartz-muscovite-chloritoid</i>	(Snow Camp)
<i>Kyanite-quartz-chloritoid</i>	(Hager's Mountain)
IV. Assemblages with one phase in the ternary system	
<i>Pyrophyllite</i>	(Staley)
<i>Pyrophyllite-muscovite</i>	(Staley; Robbins)
<i>Pyrophyllite-chloritoid-chlorite-muscovite</i>	(Staley)
<i>Quartz-muscovite</i>	(Glendon; Bowling's Mountain; Snow Camp)
<i>Quartz-chloritoid</i>	(Glendon; Hager's Mountain)
<i>Quartz-chloritoid-hematite</i>	(Glendon; Staley; Snow Camp)
<i>Quartz-chloritoid-chlorite</i>	(Glendon; Staley)

TABLE I (continued)

Quartz-chloritoid-chlorite-muscovite	(Glendon)
Quartz-muscovite-paragonite	(Hager's Mountain)
Quartz-chlorite-muscovite	(Hager's Mountain)
Quartz-muscovite-chloritoid	(Staley; Snow Camp?)
V. Assemblages with no phase in the ternary system	
Muscovite	(Hillsboro; Glendon; Snow Camp)
Fluorite	(Glendon)
VI. Assemblages with phase questionably in the ternary system	
Montmorillonite (?)	(Glendon)

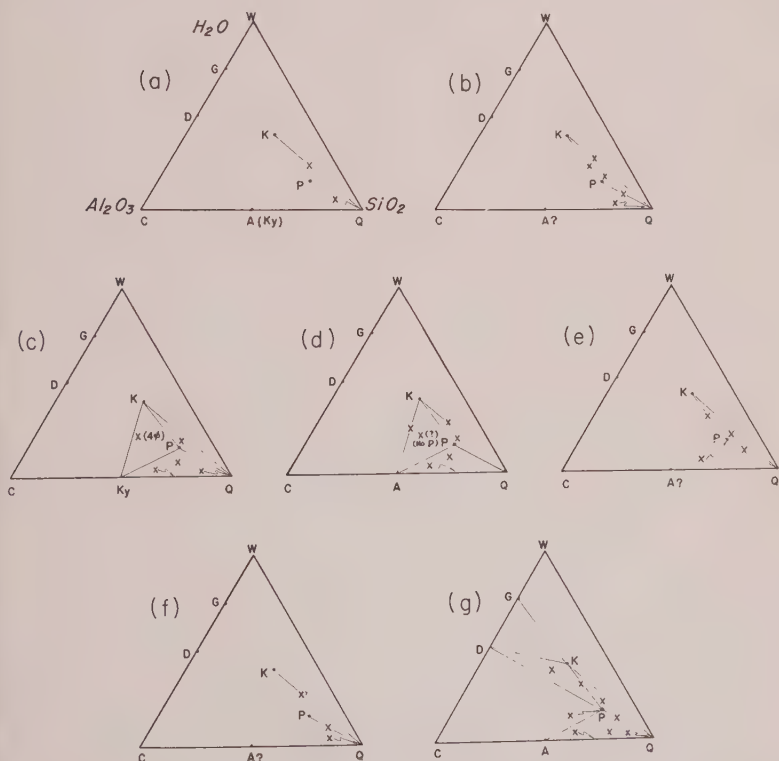


FIG. 2. Observed mineral assemblages (crosses) in the ternary system Al_2O_3 - SiO_2 - H_2O . (a), Bowling's Mountain; (b), Glendon; (c), Hager's Mountain; (d), Hillsboro; (e), Robbins; (f), pits near Snow Camp; (g), Staley. Key to mineral phases: W, a H_2O phase (vapour or liquid); G, gibbsite; D, diaspore; C, corundum; A, andalusite; Ky, kyanite; K, kaolinite; P, pyrophyllite; and Q, quartz. Symbol ϕ stands for "phase."

cally there is no evidence of its conversion to other minerals. Its grain contact is mostly with quartz, but even where it is in contact with pyrophyllite and, more rarely, kaolinite, the contact is clean and the crystals are well-developed. Andalusite therefore is presumably in chemical equilibrium with the surrounding minerals.

The occurrence of the four-phase assemblage, andalusite-kaolinite-pyrophyllite-quartz, at Hillsboro, may therefore seem anomalous, inasmuch as according to Goldschmidt's Phase Rule (Goldschmidt, 1911, p. 123), in general no more than three solids may be expected in a ternary system. Microscopic examination shows, however, that no more than three of these solids occur in direct contact with one another. One of the specimens from Hillsboro showing the four-phase assemblage on the x-ray chart consists of these sub-assemblages, when the mutual contacts are noted: pyrophyllite-andalusite-quartz, kaolinite-andalusite, pyrophyllite-quartz, andalusite-quartz. Thus even though the specimen, on the scale of a thin section, may be out of chemical equilibrium, yet locally such equilibrium prevails, and all the phases present, including andalusite, may be interpreted as stable with their surroundings. The large number of sub-assemblages even in a thin section must then be explained by the immobility of the chemical components during recrystallization. The 3-phase assemblage from Hillsboro, with andalusite-kaolinite-quartz, appears to contradict the phase diagram drawn on the basis of the above discussion; however in this particular sample the identification of kaolinite is questionable and the rock is predominately an andalusite-quartz rock.

The detailed textural relation of kyanite to its associated minerals from Hager's Mountain is as yet unknown. Kyanite and andalusite have not been found together by the writer. This may be due to imperfect sampling, however; for Broadhurst and Councill (1953, p. 13, 16) report both kyanite and andalusite from the Bowling's Mountain deposit.

The second point of interest is that, as far as the ternary system is concerned, the mineralogical assemblages at each locality are mutually compatible; the ternary diagrams (Fig. 2) relating these phases, drawn on the basis of mineralogical data, make sense. None of the other phases listed with these assemblages, moreover, count in this system, since for all such phases other distinct chemical components must be reckoned with. Thus for muscovite, we have K_2O ; for paragonite, Na_2O ; clinozoisite, CaO ; chloritoid and/or chlorite, FeO and MgO ; hematite, Fe_2O_3 ;^{*} and

* If oxygen should turn out to be a mobile component (Korzhinskii, 1950) during the metamorphism, Fe_2O_3 would not count as a distinct component in addition to FeO (Thompson, 1957; Zen, 1960). However, of the three phases, hematite, chlorite, and chloritoid, only two have been found in a given sample.

fluorite, F.* Other phases and their corresponding components are: lazulite, P_2O_5 (Staley, Glendon; Conley, 1958, p. 60, 62); ilmenite, TiO_2 (Glendon, Robbins; Conley, 1958, p. 60); malachite, CuO (Bowling's Mountain; Conley, 1958, p. 32); pyrite, S (all deposits; the writer's own observations). Unfortunately, in the literature the specific mineral associations are not always cited.

The third feature of petrologic interest is the nature and occurrence of some 3-phase assemblages. The assemblage pyrophyllite-kaolinite-quartz is common and occurs at all places except Bowling's Mountain and the pits near Snow Camp. The assemblage diaspore-kaolinite-pyrophyllite is found only at Staley by the writer, whereas andalusite-pyrophyllite-quartz is found both at Hillsboro and at Staley. Textural evidence is consistent with the interpretation that these 3-phase assemblages represent equilibrium assemblages. Kaolinite and pyrophyllite generally are intermixed; more rarely pyrophyllite occurs as clusters in a matrix of kaolinite. Prevalence of such phase assemblages in a finite volume, in a system with H_2O as one of the components, if in internal equilibrium, implies that H_2O behaved as a fixed component (Thompson, 1955, p. 80) during metamorphism. The significance of this point is discussed in the next section.

A final point of petrologic interest is the existence, at Staley, of the assemblage pyrophyllite-diaspore-kaolinite (trace). Diaspore is also reported by Broadhurst and Councill (1953, p. 20) from Holman's Mill, Snow Camp, presumably with pyrophyllite. This mineral pair is incompatible with the pair andalusite-kaolinite (Fig. 2g), which is found at Hillsboro. This fact indicates a crossing of 2-phase tie lines; for even if it be assumed that andalusite is a metastable relict, still if pyrophyllite and diaspore are stable together, hydration of andalusite should result in the formation of this pair before any kaolinite could appear. Since all four phases, kaolinite, pyrophyllite, andalusite, and diaspore, belong, as far as we know, strictly to the ternary system $Al_2O_3-SiO_2-H_2O$, the fact that andalusite-kaolinite and andalusite-kaolinite-pyrophyllite assemblages prevail at Hillsboro and the alternative, pyrophyllite and diaspore, occur at Staley (and possibly Holman's Mill also) suggests therefore that real differences in the *physical* environment (temperature and total pressure) of metamorphism existed between Staley (and Snow Camp) and Hillsboro.

* Topaz has been reported from Bowling's Mountain, Hillsboro and Staley (Broadhurst and Councill, 1953, p. 15, 17, 19). The three phases, topaz, fluorite, and clinozoisite, share the two components, Ca and F, in the enumeration of number of components and phases when we apply the Gibbs Phase Rule. However, no more than two of these are known to occur in any deposit.

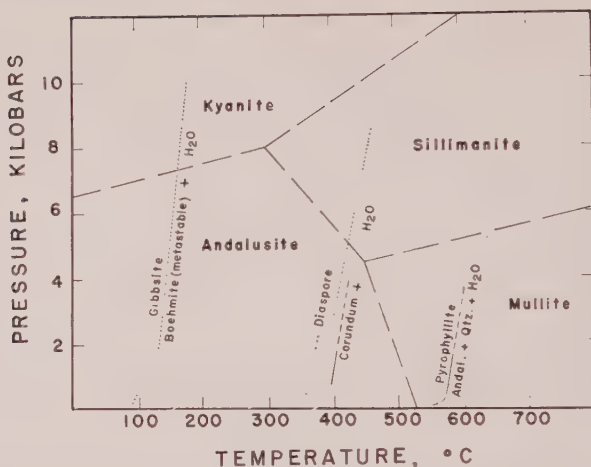


FIG. 3. Experimental data on the system $\text{Al}_2\text{O}_3\text{-SiO}_2\text{-H}_2\text{O}$. Long dashed lines: the extrapolated univariant curves for the dry system, according to Clark, Robertson and Birch (1957). Solid lines and short dashed lines: determined and extrapolated breakdown curves due to Roy and Osborn (1954). Dotted lines: curves due to Kennedy (1959). The discontinuous high-pressure and low-pressure portions of the diaspore breakdown curve due to Kennedy are from his Figs. 1 and 2, respectively, obtained by different experimental techniques. All breakdown curves for hydrous phases are for equilibrium with pure H_2O .

P, T Conditions of Formation of Pyrophyllite Deposits

The mineral assemblage data from the several pyrophyllite deposits afford an estimate on the temperature and total pressure of formation of these deposits.

The high temperature-high pressure portion of the equilibrium diagram for the system Al_2SiO_5 was studied by Clark, Robertson and Birch (1957). These authors determined the kyanite-sillimanite univariant transition curve at $T > 900^\circ \text{C}$. and $P > 17$ kilobars. Using this curve and also available thermochemical data on these phases, the authors extrapolated their results to lower temperatures and total pressures, to include the probable phase region for andalusite. The position of the andalusite field is drawn on the basis that it is probably the relatively low-temperature, low-pressure phase. The lines thus obtained are consistent with the experimental work of Roy (1954) and Aramaki and Roy (1958), and with known geological occurrences.*

The extrapolated diagram of Clark, Robertson and Birch is shown in Fig. 3. It suggests the approximate conditions of formation of the Hills-

* It should be pointed out, however, that Aramaki and Roy (1959) now refer to the phase they obtained as a "disordered" phase with andalusite structure but rather different unit cell dimensions.

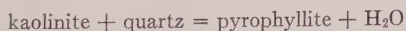
boro, Staley (both with andalusite), and Hager's Mountain (kyanite) deposits. Bowling's Mountain deposit, with reported kyanite and andalusite, may have formed near the univariant transition. Holman's Mill at Snow Camp is reported to yield andalusite (Broadhurst and Councill, 1953, p. 20); although this mineral is not found in the pits near Snow Camp, here reported, the proximity of these pits to Holman's Mill suggests that they, too, formed under conditions in which andalusite was stable.

The breakdown curves of Roy and Osborn (1953, p. 876) for pyrophyllite, forming andalusite, quartz, and vapour, and for diaspore, forming corundum plus vapour, are given Fig. 3 as dashed lines. These curves apply when the fluid phase is pure H_2O . Kennedy (1959, p. 565, 568) presents a breakdown curve for diaspore, forming corundum and vapour, which is slightly lower in temperature than the curve of Roy and Osborn; it is shown as dotted line. The discrepancy between the two sets of data is negligible for our purpose.

Kennedy (1959, p. 565, 568) also gives a breakdown curve for gibbsite, forming vapour plus diaspore (stable) or boehmite (metastable). The stable extension of this curve of course should extrapolate to the left (lower temperature) side of his gibbsite-boehmite curve, thus enlarging the diaspore stability field. The amount of this enlargement is unknown.

Roy and Osborn (1954, p. 876) also give a curve for the breakdown of kaolinite; however, the reaction product is hydralsite, which is metastable (Aramaki and Roy, 1958, p. 1530). Whereas at first sight the curve might seem to give a ceiling to the stability of kaolinite (as the product is a metastable phase), kaolinite is not compositionally equivalent to vapour plus hydralsite (using the probable composition of Roy and Osborn), and the effect of the as yet undetermined additional phase or phases participating in the reaction cannot be evaluated.

The P - T region between the gibbsite breakdown curve (between 100° C. and 200° C.) and the diaspore breakdown curve (around 400° C.) gives the stability field for diaspore (found at Staley and Holman's Mill, Snow Camp) for equilibrium with pure H_2O .^{*} For the other deposits, the breakdown curve for pyrophyllite would give the upper limit. A more realistic reaction to consider, however, is



This reaction curve would occur to the low-temperature side of the breakdown curve for kaolinite alone and thus should impose a lower ceiling on

^{*} The reaction



is more realistic than the breakdown of either pyrophyllite or of diaspore alone; this curve must be located to the left of the breakdown curve for diaspore alone.

the temperature of formation of the pyrophyllite deposits carrying kaolinite.

The metamorphism of the pyrophyllite deposits probably did not occur in equilibrium with pure H_2O , owing to the fact that many of these deposits contain three-solid-phase assemblages in the system Al_2O_3 - SiO_2 - H_2O , apparently in internal equilibrium. This fact precludes a free H_2O phase. Even though addition of other components in the fluid phase could result in its coexistence with the three solids, the value of the chemical activity of H_2O in such a solution is necessarily lower than that of a fluid phase composed of pure H_2O . The temperatures of formation of the pyrophyllite deposits therefore were likely lower than the maximum predictable from the curves in Fig. 3, although by an unknown amount.

This last conclusion is consistent with the coexistence of andalusite and pyrophyllite in the deposits. The diagram of Clark, Robertson and Birch, and of Roy and Osborn indicate (see Fig. 3) that sillimanite or mullite, rather than andalusite, should be the anhydrous aluminum silicate stable with pyrophyllite, for equilibrium with pure H_2O , except at extremely low pressures where the pyrophyllite breakdown curve begins to curve sharply to the left. With dilution of the fluid phase, however, the breakdown curves for the hydrous phases shift progressively to lower temperatures (Thompson, 1955) and thus the breakdown curve for pyrophyllite should eventually enter the stability field of andalusite, resulting in the observed association of andalusite and pyrophyllite.

ORIGIN OF THE PYROPHYLLITE DEPOSITS

Stuckey, after a field and microscopic study of many of the North Carolina pyrophyllite deposits, concludes that these deposits originated from hydrothermal replacement of preëxisting volcanic tuffs and breccias of dacitic and rhyolitic composition (1928, p. 35). The deposits are thought to be located along zones of structural weakness; where no pre-pyrophyllite faults are found, the zones of weakness are attributed to drag folding and shearing along the limbs of folds (1928, p. 41) since some of the deposits are found to occur in such positions (1928, p. 40). Broadhurst and Councill (1953, p. 12) agree with Stuckey's conclusions, without stating supporting evidence.

The present data on mineral assemblages bear upon the possible origin of the deposits. The fundamental assumption is that, unless evidence points to the contrary, the minerals in each assemblage are in mutual equilibrium.

The existence of three-phase assemblages, diaspore-pyrophyllite-kaolinite, andalusite-quartz-pyrophyllite, and pyrophyllite-kaolinite-quartz, excludes the possible existence, during the formation of the

deposits, of a free solution phase which a "hydrothermal solution" implies. Even though the coexistence of four phases (3 solids plus a solution) in a ternary system is permitted by Gibbs' Phase Rule, such an assemblage implies univariant equilibrium and specific combinations of temperature and total pressure. Such combinations are not expected in general to be of geologic importance (Goldschmidt, 1911, p. 123).

One may argue that hydrothermal solutions are probably not pure H_2O but contain other dissolved components; an assemblage like pyrophyllite-kaolinite-quartz-solution therefore is not ternary and more than three phases may be expected in general. However, a hydrothermal solution implies that H_2O behaved as a "mobile" component whose amount is not determined by the initial composition of the local system (Thompson, 1955). Similarly, a hypothetical component whose sole function is to allow an additional solution phase, but which does not manifest itself in the mineralogy of the product, must also have moved in and out of the system and therefore is mobile in the same thermodynamic sense. Thompson (1955) and Korzhinskii (1950) have independently shown that for a system which is thermodynamically open, at arbitrary values of T and P_{total} the maximum number of phases, ϕ_{maximum} , is related to the total number of distinct chemical components, c , and the number of distinct mobile components, c' , by the equation $\phi_{\text{maximum}} = c - c'$. The mobile components therefore cannot contribute to the number of solid phases present. If a hydrothermal solution existed, in fact, in the ternary system $\text{Al}_2\text{O}_3\text{-SiO}_2\text{-H}_2\text{O}$, in general only two solid phases should be found, since $c = 3$ and $c' = 1$ (H_2O). These 2-phase assemblages should be spatially so distributed that they reflect the existence of chemical potential gradients of the mobile components during recrystallization. At Glendon, the sample collection was arranged with this possibility in mind. No systematic mineralogical variation of this sort was found.

The prevalence of the 3-phase assemblages in the ternary system, in fact, indicates strongly that H_2O behaved as a fixed component during the formation of the pyrophyllite deposits, contrary to the general situation in regional metamorphism (Thompson, 1957; Zen, 1960).

An alternative origin, consistent with the mineral assemblage data, and, as far as the writer is aware of, the geologic information, is as follows.

The protolith for the pyrophyllite deposits studied in this report were bodies of saprolite which resulted from the deep weathering of the rhyolitic or dacitic country rock. The residual material would be high in silica, alumina, and ferric oxide. Most of the other components tend to be leached out; among the alkali and alkaline earth oxides, K_2O would be the most stable and lag behind (Goldich, 1938, p. 54). The resulting rock would have the general chemical composition of the pyrophyllite de-

posits. The envisioned condition of weathering is much like the present one in North Carolina.

This picture of surface weathering of volcanic rocks implies discontinuities or unconformities in the Volcanic Slate sequence. Recent mapping (Conley, 1959; Stromquist and Conley, 1959) in the Albemarle and Denton quadrangles in south-central North Carolina has revealed at least one major unconformity in the Volcanic Slate sequence; it would be interesting to see if the same, or a similar, stratigraphic break occurs at the zone of pyrophyllite deposits.

The saprolitic deposits, scattered on the discontinuity surface, were buried by later, additional volcanic eruptions. At a later date, the entire rock sequence was deformed and metamorphosed. In the saprolitic bodies, the alumina:silica ratio varied from one place to another, and the H_2O concentration also varied. For some reason, the component H_2O remained fixed during metamorphism; there was little redistribution of this component even on a very small scale, and certainly none on the scale of the individual deposits. Depending on the relative proportions of the three components, therefore, different mineral assemblages resulted—for instance, andalusite and quartz if the system were free of H_2O , but kaolinite-quartz if the system were very hydrous. A few portions of the bodies were low in silica relative to alumina (approaching a true laterite), and now contain diaspore; by and large however quartz is present.

The metamorphic grade of the rock sequence as a whole was such that, in the country rock, such mineral assemblages as muscovite-pyrophyllite-chlorite-chloritoid-quartz, and pyrophyllite-clinozoisite-muscovite-quartz resulted. Hematite, rather than magnetite, was the predominant iron oxide phase. These are mineral assemblages typical of metamorphism near or just below the almandite isograd; in west-central Vermont (Zen, 1960), similar mineral assemblages characterize phyllites and slates. The country rock of the pyrophyllite deposits is also slate and phyllite (Stuckey, 1928); similarly almandite has not been found in these rocks to date.

It should be stressed that to say H_2O behaved as a fixed component during metamorphism, in no way implies the presence or absence of a free solution phase. The chemical activity of H_2O , for example, might be controlled by the buffering assemblage kaolinite-pyrophyllite-quartz, which being bivariant in the ternary system, possesses a unique value of the chemical activity of H_2O at given temperatures and pressures. On the other hand, if H_2O and also other components in the fluid phase behaved as fixed components, then, according to Gibbs' Phase Rule, a solution phase *could* have been present, although it certainly did not circulate freely through the system to destroy the buffering mineral assemblages.

ACKNOWLEDGEMENTS

I wish to thank Jasper L. Stuckey, Sam Broadhurst, and James F. Conley, all of the North Carolina Division of Mineral Resources, for their assistance in numerous ways. Stuckey kindly furnished me with a sample of diaspore from the Staley pyrophyllite deposit for x -ray study, for this I am especially indebted. Discussions of field relations of the deposits and their possible origin, with Conley, now mapping the bedrock geology of Moore County, have been very illuminating. All the x -ray examinations of the samples were made on a Norelco diffractometer at the Department of Mineralogy and Petrography, Harvard University; for this generous aid I wish to thank Clifford Frondel. A grant from the Smith Fund of the University of North Carolina has helped to defray travel expenses and to prepare thin sections. The manuscript was reviewed by James B. Thompson, Jr., James F. Conley, Fred Barker, Eugene C. Robertson, and Priestley Toulmin III; without their critical and helpful comments this paper would contain many more defects.

REFERENCES

- ARAMAKI, S., AND ROY, R., 1958, Further equilibrium studies in the system $\text{Al}_2\text{O}_3\text{-SiO}_2\text{-H}_2\text{O}$ under hydrostatic and uniaxial pressure (abstract), *Geol. Soc. Amer. Bull.*, **69**, 1530.
- , AND ———, 1959, Detailed x -ray data on mullites and two new anhydrous aluminosilicates As(H)-II and high-temperature sillimanite (abstract). *Geol. Soc. Amer. Bull.*, **70**, 1562.
- BROADHURST, S., AND COUNCILL, R. J., 1953, A preliminary report on high alumina minerals in the volcanic slate series, North Carolina. *North Carolina Dept. of Conservation and Development, Div. of Min. Resources, Inform. Circ.* **10**, 22 p.
- CLARK, S. P., JR., ROBERTSON, E. C., AND BIRCH, F., 1957, Experimental determination of kyanite-sillimanite equilibrium relations at high temperatures and pressures. *Am. Jour. Sci.*, **255**, 628-640.
- CONLEY, J. F., 1958, Mineral localities of North Carolina. *North Carolina Dept. of Conservation and Development, Div. of Min. Resources, Inform. Circ.* **16**, 83 p.
- , 1959, Geology of the Albemarle quadrangle, North Carolina (abstract). *Geol. Soc. Amer. Bull.*, **70**, 1760.
- GOLDICH, S. S., 1938, A study in rock weathering. *Jour. Geol.*, **46**, 17-58.
- GOLDSCHMIDT, V. M., 1911, Die Kontaktmetamorphose in Kristianiagebiet. *Vidensk. i Kristiania, Skrifter, I Mat.-Natur. Kl.*, Bd. **1**, 1-483.
- KENNEDY, G. C., 1959, Phase relations in the system $\text{Al}_2\text{O}_3\text{-H}_2\text{O}$ at high temperatures and pressures. *Am. Jour. Sci.*, **257**, 563-573.
- KORZHIKIN, D. S., 1950, Phase rule and geochemical mobility of elements. *Nineteenth Intern. Geol. Congress Proc., Sec. A*, 50-57.
- ROY, D. M., 1954, Hydrothermal synthesis of andalusite. *Am. Mineral.*, **39**, 140-143.
- ROY, R., AND OSBORN, E. F., 1954, The system $\text{Al}_2\text{O}_3\text{-SiO}_2\text{-H}_2\text{O}$. *Am. Mineral.*, **39**, 853-885.
- STROMQUIST, A. A., AND CONLEY, J. F., 1959, Geology of the Albemarle and Denton quadrangles, North Carolina. *Carolina Geol. Soc. Guidebook*, 36 p.
- STUCKEY, J. L., 1928, The pyrophyllite deposits of North Carolina. *North Carolina Dept. of Conservation and Development, Bull.* **37**, 62 p.

- THOMPSON, J. B., JR., 1955, The thermodynamic basis for the mineral facies concept. *Am. Jour. Sci.*, **253**, 65-103.
- , 1957, The graphical analysis of mineral assemblages in pelitic schists. *Am. Mineral.*, **42**, 842-858.
- WINCHELL, A. N., AND WINCHELL, H., 1951, Elements of optical mineralogy, pt. 2. John Wiley and Sons, 551 p.
- ZEN, E., 1960, Metamorphism of Lower Paleozoic rocks in the vicinity of the Taconic Range in west-central Vermont. *Am. Mineral.*, **45**, 129-175.

Manuscript received March 24, 1960.

* Note added in press: Since the manuscript went to press, two pertinent papers have appeared to which the reader's attention is drawn. (1) Carr, R. M., and Fyfe, W. S., 1960, Synthesis fields of some aluminium silicates, *Geoch. et Cosmoch. Acta* **21**, p. 99-109; (2) Espenshade, G. H., and Potter, D. B., 1960, Kyanite, sillimanite, and andalusite deposits of the southeastern states. *U. S. Geol. Survey Prof. Paper* **336**, 121 p. (see esp. p. 8-16, 109-110).

DIFFERENTIAL THERMAL ANALYSIS OF SHATTUCKITE

MING-SHAN SUN, *New Mexico Institute of Mining and Technology,
Socorro, New Mexico.*

ABSTRACT

The DTA curve of shattuckite from Ajo, Arizona, is characterized by a prominent endothermal peak with a false peak temperature at $774^{\circ}\text{C}.$, and a small exothermal peak with a peak temperature of $980^{\circ}\text{C}.$ Within the dehydration temperature range, shattuckite is decomposed gradually into cryptocrystalline tenorite, some cryptocrystalline α -quartz, and an unknown phase. The exothermal reaction is caused by the crystallization of α -cristobalite. All phases are identified by the x -ray powder diffraction.

Crystallization of tenorite begins at $675^{\circ}\text{C}.$ and ends at $780^{\circ}\text{C}.$ This is a strong exothermal reaction. However, an exothermal peak is obliterated completely by the endothermal dehydration reaction. At the same time, the shape of the dehydration endothermal peak is strongly skewed, and only a false endothermal peak is recorded on the graph. Some tenorite in the sample begins to decompose into cuprite at about $900^{\circ}\text{C}.$ According to the total water content, the formula of shattuckite should be $3\text{CuSiO}_3 \cdot \text{H}_2\text{O}.$ The accepted formula, $2\text{CuSiO}_3 \cdot \text{H}_2\text{O},$ is incorrect, because of an erroneous interpretation of loss of weight of the shattuckite sample by ignition.

INTRODUCTION

The occurrence of hydrated copper silicate minerals in the Southwest is fairly common. The identity of some of these minerals, however, is rather doubtful. Positive identification is often difficult, because the exact nature of these minerals has not been well defined. Therefore, studies have been initiated by the writer in order to learn more about hydrated copper silicate minerals. This paper is the first report on such study.

Dark-blue radiated and spherulitic shattuckite from Ajo, Arizona, has been used in this study. Green ajoite, quartz, and some opal are associated intimately with the shattuckite. The irregular shattuckite spherulites are about 2 mm. in diameter; the individual fibers or acicular crystals are about $2 \times .02$ mm.; and the irregular quartz blebs or grains are about 1.5 mm. across. Samples have been crushed and handpicked with tweezers under a binocular microscope. The green ajoite and most of the quartz and opal may be removed from the sample. However, a small amount of quartz and possibly some opal, which occur between the individual shattuckite crystals, are difficult to remove. The presence of about 3% of quartz in the handpicked shattuckite sample is shown by an x -ray powder diffraction pattern.

DEHYDRATION OF SHATTUCKITE

A handpicked sample of shattuckite, when heated in a cylindrical electric furnace to $1,000^{\circ}\text{C}.,$ loses 3.87% of its weight, 3.71% being caused by loss of water and 0.16% by the decomposition of some tenorite

into cuprite. The amount of cuprite formed from tenorite differs in different samples and under different heating conditions. A minus 100 mesh sample was heated to 200° C., and heating was continued at this temperature for 5 minutes. The sample was removed from the furnace, cooled in a desiccator, and weighed. Heating of the same sample was continued to 300° C., 400° C., and so on. The changes of color and the loss of weight at various temperatures are noted in Table 1. Figure 1D shows a fairly smooth dehydration curve for shattuckite.

TABLE 1. PERCENTAGE LOSS OF WEIGHT OF SHATTUCKITE UPON HEATING

Intermediate temperature	Loss of weight, per cent	Remarks
200° C.	—	Original pale-blue color of shattuckite powder below 100 mesh. (5B 6/2)
300° C.	—	No change in color
400° C.	—	No change in color
500° C.	0.16	Slightly dull blue
600° C.	0.71	Grayish blue-green
700° C.	1.74	Black with greenish hue
800° C.	3.71	Black (N2); maximum loss of water
900° C.	3.87	Black; maximum loss of weight; slightly brownish black streak
1,000° C.	3.87	Grayish black; part of the sample is fused

Because the water content is 3.71 per cent, the chemical formula of shattuckite was first suspected to be $3\text{CuSiO}_3 \cdot \text{H}_2\text{O}$, instead of $2\text{CuSiO}_3 \cdot \text{H}_2\text{O}$ (Shaller, 1915). This will be discussed further with the chemical analysis.

CHEMICAL ANALYSIS

In order to check the chemical composition of shattuckite, about 1 gm. of a handpicked sample was prepared for a complete silicate analysis. The result of the analysis is listed in Table 2. The percentage of H_2O^- was determined from the loss of weight of the sample when dried in an electric oven at 120° C. The percentage of H_2O^+ was determined from the loss of weight of the sample when ignited for 10 minutes in a covered upright platinum crucible, with a Meker burner. The burner temperature was about 1,100° C. to 1,250° C. The total loss of weight by ignition was 6.31 per cent. Usually it is taken for granted that this total loss of weight is caused by the removal of H_2O^+ from the sample. Accordingly, the H_2O^+

content of shattuckite would be recorded to be 6.31 per cent. Based on this analysis, the chemical formula of shattuckite would be calculated approximately as $2\text{CuSiO}_3 \cdot \text{H}_2\text{O}$. Complete chemical analyses by Shaller (see page 72, Ford, 1915) shows that shattuckite contains SiO_2 37.91–39.92%, CuO 53.20–55.51%, H_2O 5.83–6.41%, and minor amounts of FeO , CaO , and ZnO . According to the average of these analyses, the molecular ratio of CuSiO_3 and H_2O of shattuckite is 1.99 to 1. The accepted formula $2\text{CuSiO}_3 \cdot \text{H}_2\text{O}$, however, is erroneous, because the loss of weight by ignition is caused partly by the removal of H_2O^+ and partly by

TABLE 2. CHEMICAL ANALYSIS OF SHATTUCKITE, AJO, ARIZONA
Analyst: Dr. H. B. Wiik, Helsinki, Finland

Wt. per cent		Molecular number	Molecular ratio
SiO_2	35.90	.597	$\text{SiO}_2:\text{CuO}:\text{H}_2\text{O}=1.71:1.98:1$
TiO_2	0.0	.000	
Al_2O_3	0.79	.008	
Fe_2O_3 (total Fe)	0.31	.002	
CaO	0.00	.000	$\text{CuSiO}_3:\text{H}_2\text{O}=1.86:1$
CuO	55.27	.695	
H_2O^+	6.31	.350	
H_2O^- (120° C.)	0.08	.000	
CO_2	0.00	.000	
Total	98.66		

the decomposition of some CuO into Cu_2O . At high temperature, CuO tends to decompose into Cu_2O . Cryptocrystalline cuprite was identified in some shattuckite samples fired to 900 °C. At 1,935° C., Cu_2O will be decomposed into metallic copper under ordinary pressure of oxygen in the air. The entire CuO content of shattuckite may be decomposed completely into Cu_2O if the shattuckite is ignited long enough under favorable conditions. Table 3 shows the loss of weight of shattuckite under different ignition conditions.

In the dehydration curve (Fig. 1D), it is shown that the total water content of the handpicked shattuckite sample is 3.71 per cent. Loss of weight by ignition, in excess of this percentage, is caused by the decomposition of some CuO into Cu_2O . The theoretical maximum loss of weight of shattuckite caused by decomposition of CuO into Cu_2O is 5.49 per cent.

Gaining weight upon heating is also possible. For instance, the oxidation of ferrous iron to ferric iron in stilpnomelane at about 450° C. will produce a gain in weight. The endothermal peak of stilpnomelane occurs

TABLE 3. LOSS OF WEIGHT OF SHATTUCKITE UNDER DIFFERENT IGNITION CONDITIONS

Ignition condition			Per cent loss of weight	X-ray identification
Sample container	Meker burner temperature	Time (minutes)		
Upright, covered porcelain crucible	725° to 900° C.	10	3.07	Tenorite, shattuckite
Platinum crucible, with access of air	1,100° to 1,250° C.	10	3.90	Tenorite, α -quartz
Upright, covered platinum crucible	1,100° to 1,250° C.	10	7.73	Tenorite, cuprite α - quartz, α -cristoba- lite
Upright, covered platinum crucible	1,100° to 1,250° C.	20	8.13	Tenorite, cuprite α - quartz, α -cristoba- lite
Upright, covered platinum crucible	1,100° to 1,250° C.	30	8.47	Cuprite, tenorite, α - quartz, α -cristoba- lite
Upright, covered platinum crucible	1,100° to 1,250° C.	40	8.73	Cuprite, tenorite, α - quartz, α -cristoba- lite
Upright, covered platinum crucible	1,100° to 1,250° C.	50	9.07	Cuprite, α -quartz, α - cristobalite, trace of tenorite
Upright, covered platinum crucible	1,100° to 1,250° C.	60 (or longer)	9.07 (maximum)	Cuprite, α -quartz, α - cristobalite, trace of tenorite

at about 350° C., but may be as high as 500° C. for some samples (Nagy, 1954). If a sample of stilpnomelane is ignited with access to air, the resultant loss of weight will be the loss of weight caused by the removal of water, minus the gain in weight caused by oxidation of ferrous iron into ferric iron.

Analysts who are not aware of this may report an incorrect molecular ratio between water and other constituents of a hydrated substance containing CuO or FeO.

Table 4 lists the impurities that were determined in the shattuckite analyzed. As indicated in the table, barium and aluminum are the chief minor constituents.

According to the chemical and spectrographic analyses, 2.52% of the handpicked shattuckite sample consists of impurities, including mainly Al_2O_3 , Fe_2O_3 , and BaO. According to x-ray powder diffraction analysis, about 3% of the handpicked sample is quartz. Thus, only about 94.48% of the handpicked sample is shattuckite. Dehydration shows that the

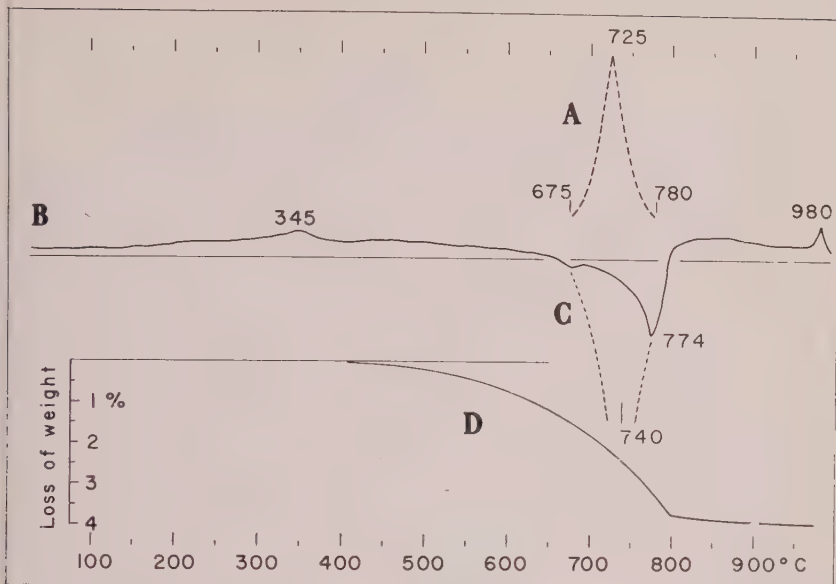


FIG. 1. A. The obliterated exothermal peak of the crystallization of tenorite. B. DTA thermal curve of shattuckite. C. The true endothermal peak of dehydration of shattuckite. D. Dehydration curve of shattuckite, (the sample contains 5.52 per cent impurities.)

handpicked sample contains 3.71% water. Thus, approximately 90.77% of the handpicked sample is CuSiO_3 . The molecular ratio of CuSiO_3 and H_2O^+ of the handpicked sample is .650 to .206, or 3.16 to 1. Therefore, the chemical formula of shattuckite is $3\text{CuSiO}_3 \cdot \text{H}_2\text{O}$.

TABLE 4. SEMI-QUANTITATIVE SPECTROGRAPHIC ANALYSIS OF SHATTUCKITE, AJO, ARIZONA

Spectrographer: A. Davis Odom, Houston, Texas

Element	Per cent	Element	Per cent
Cu	22.	Ti	0.01
Fe	0.03	Mo	0.02
Si	32.	Na	looked for, not detected
Mn	0.06	Ba	0.9
Cr	looked for, not detected	K	looked for, not detected
V	0.02	Sr	trace
Al	1.	Zr	looked for, not detected
B	0.005		
Mg	0.08		
Ca	0.1		
		S and Se are not looked for	

TABLE 5. X-RAY POWDER DIFFRACTION DATA OF SHATTUCKITE

CuK α =1.54178 Å

$d(\text{Å})$ obs	I	$d(\text{Å})$ obs	I	$d(\text{Å})$ obs	I
12.48	3	1.791	7	1.006	3
9.91	4	1.760	1	.990	2
4.95	7	1.730	1	.972	4
4.43	10	1.683	<1	.949	<1
3.63	3	1.625	7	.943 <i>w, b</i>	2
3.50	7	1.596	4	.885 <i>b</i>	1
3.40	2	1.566	6	.847	1
3.31	8	1.506	<1	.823 <i>b</i>	2
3.11	2	1.480 <i>b</i>	2	.314 <i>b</i>	1
2.93	4	1.435	6	.789	<1
2.77 <i>w, b</i>	5	1.398 <i>b</i>	5	.773 <i>b</i> , halo	
2.69	2	1.357	3		
2.59 <i>b</i>	3	1.344	3		
2.46	3	1.297 <i>w, b</i>	5		
2.40	4	1.239	5		
2.36	6	1.227	3	Note:	
2.30	4	1.202	5		
2.22 <i>b</i>	1	1.181 <i>b</i>	1	<i>b</i> means blurred	
2.13	1	1.168 <i>b</i>	1	<i>w</i> means wide band	
2.09	1	1.150	<1		
2.04	1	1.118	1		
1.991 <i>b</i>	1	1.097 <i>b</i>	<1		
1.931 <i>w, b</i>	5	1.073	4		
1.853	<1	1.060	3		
1.821	4	1.036	3		

X-RAY POWDER DIFFRACTION DATA

A total of 61 powder reflections of shattuckite are recorded (Table 5). Several faint reflections of quartz, 4.26 Å, 1.54 Å, and 1.375 Å also appear on the shattuckite picture. Quartz lines of 3.34 Å and 1.817 Å are superimposed on 3.31 Å and 1.821 Å lines of shattuckite, respectively. The three strongest lines of shattuckite are 4.95 Å, 4.43 Å, and 3.31 Å. Some of the low-angle lines of shattuckite may be mistaken for lines of ajoite. The mistake can be avoided by observing a strong line of ajoite (6.19 Å) which does not appear in the shattuckite pattern, and a strong line of shattuckite (4.43 Å) which does not appear in a pattern of ajoite.

DIFFERENTIAL THERMAL ANALYSIS

The thermal curve (Fig. 1B) was traced on a Leeds and Northrup micromax recorder. The heating rate is 12° C. per minute. The scale factor is X20, which corresponds to 10 microvolts per division of the graph paper. The sample was crushed and ground to below 100 mesh.

In order to fit the characteristics of the thermal curve, samples were fired to selected temperatures. The fired samples were examined under a petrographic microscope, and the phases developed at different temperatures were identified by x-ray powder diffraction.

Thermal curve. The thermal curve (Fig. 1B) is fairly persistent for different samples, with slight variation in peak temperature. A minor broad exothermal peak occurs at 345° C., with a peak height of 20 microvolts. Another sample shows a peak temperature of 330° C., with a peak height of 20 microvolts. The cause of this exothermal peak is not known. A major endothermal reaction begins at about 440° C. and increases rather rapidly at 660° C. This endothermal reaction is caused by dehydration of shattuckite. A small false endothermal peak at 675° C. and a minor broad false exothermal peak at 690° C. are recorded on the graph. A major false endothermal peak at 774° C., with a peak height of 210 microvolts, is the most prominent peak of the thermal curve. This endothermal dehydration is greatly affected by an exothermal reaction of the crystallization of tenorite. Therefore, the true endothermal peak of dehydration does not show on the graph, whereas two minor and one prominent false peaks are recorded on the graph. A sharp exothermal peak (Fig. 1A) is obliterated completely by the endothermal dehydration reaction. At about 850° C. the thermal curve begins to show a weak and gradual endothermal reaction. A small and fairly sharp exothermal peak occurs at 980° C. The thermal curve was discontinued at about 995° C. It seems that the exothermal peak at 980° C. is followed closely by a strong endothermal peak beyond 995° C. This has not been verified experimentally because of the limitations of the DTA equipment used.

The obliterated exothermal peak. Because the major false endothermal peak is conspicuously skewed toward the high-temperature end of the thermal curve, an interfering exothermal reaction is suspected. The change of phase of shattuckite upon heating is fairly analogous to that of chrysocolla. (The nature of selected chrysocolla samples will be discussed in another paper.) From an illustration of this analogy, the obliterated exothermal peak of shattuckite will be evident.

(A) Chrysocolla (Tyrone, New Mexico). The DTA curve of a chrysocolla sample from Tyrone, N. Mex., derived under the same condition as the shattuckite sample, consists of (1) an endothermal peak at 154° C.;

peak height 760 microvolts; peak range 60 to 216° C., (2) an exothermal peak at 705° C.; peak height 440 microvolts; peak range 685 to 730° C., (3) an exothermal peak at 950° C.; peak height 130 microvolts; peak range 920 to 980° C. A similar DTA curve of chrysocolla was published by Kauffman and Dilling (1950). When fired to 500° C., all the constituents of the sample become amorphous, as shown by an x-ray powder diffraction pattern. When heated to 685° C., the beginning of the exothermal reaction, the sample becomes dull olive green, and two faint and blurred tenorite powder lines appear at about 2.32 Å and 2.52 Å in the x-ray diffraction pattern. There is also a broad halo at 4.5 Å to 5.5 Å. This halo indicates an incipient crystallization of silica, as in the case of some opal. When fired to the exothermal peak temperature of 705° C., cryptocrystalline tenorite, some cryptocrystalline α -quartz, and an unknown phase appear in the sample. When fired to 730° C., the end of the sharp exothermal peak, crystalline tenorite, some α -quartz, and an unknown phase appear in the sample. The exothermal reaction of chrysocolla is caused by the crystallization of tenorite from amorphous CuO. The exothermal peak of chrysocolla is distinctive and without distortion, because there is no endothermal or other thermal reaction at about 700° C.

(B) Shattuckite (Ajo, Arizona). When fired to 500° C., the sample changes from pale blue to grayish, bluish, green. The fired sample shows a clear x-ray powder diffraction pattern of shattuckite. When fired to 690° C., the sample becomes greenish black. The clear shattuckite x-ray powder diffraction pattern seems unchanged. Two faint, yet discernible, bands of tenorite appear at about 2.40 Å to 2.30 Å, and 2.59 Å to 2.46 Å. There is also a faint broad band at 4 Å to 5 Å. A sample fired to 705° C., the exothermal peak temperature of chrysocolla, shows that the shattuckite x-ray powder diffraction pattern has begun to fade away. Two faint tenorite bands and the faint broad band at 4 Å to 5 Å remain the same as those of the sample fired to 690° C. A sample fired to 715° C. shows that many shattuckite powder lines disappear. Tenorite powder lines at about 2.32 Å and 2.52 Å become darker, but no other tenorite powder lines appear. A sample fired to 740° C. shows a complete disappearance of crystalline shattuckite. Several blurred tenorite powder lines appear; also, a few faint powder lines of an unknown phase appear. A sample fired to 780° C. contains cryptocrystalline tenorite, some cryptocrystalline α -quartz, and an unknown phase. The halo at 4 Å to 5 Å becomes dark; also, a halo at 14 Å appears. The strong endothermal reaction of shattuckite ends at 800° C. A sample fired to 800° C. shows fairly sharp x-ray powder diffraction lines of tenorite, as well as some powder lines of alpha-quartz and an unknown phase.

Because the crystallization of tenorite in fired samples of shattuckite is analogous to the crystallization of tenorite in fired samples of chrysocolla, the existence of a strong exothermal reaction in the DTA of shattuckite becomes evident.

(C) Range and peak temperature of the obliterated exothermal peak. The range of the exothermal peak is 675 to 780°C ., and the peak temperature is estimated to be 725°C . The small false peak at 675°C . indicates the beginning of the exothermal reaction. The exothermal peak range of chrysocolla is narrow, from 685 to 730°C . All of the CuO content of chrysocolla is amorphous when the sample is heated to 500°C . Only a narrow temperature range is required for the amorphous CuO to change into tenorite; on the other hand, a wide temperature range is necessary from 675°C . to about 780°C . for the CuO to shake itself loose gradually from the shattuckite structure. Therefore, the crystallization of tenorite is also a gradual process over this wide temperature range. The estimated obliterated exothermal peak of shattuckite is shown in Fig. 1A. The minor broad exothermal peak at 690°C . may be considered as a remainder of the obliterated true exothermal peak.

The true endothermal peak temperature. By projecting from the false endothermal peaks, one at 675°C . and the other at 774°C ., the true endothermal peak temperature is estimated to be 740°C . Figure 1C shows the true endothermal peak. According to the dehydration curve, shattuckite loses 65% of its total water content by dehydration at 740°C . The loss of water at a dehydration endothermal peak temperature varies a great deal for different minerals. For instance, a goethite sample from Socorro, New Mexico, loses 87.6% of its water at its dehydration endothermal peak temperature of 395°C . A gypsum sample from Lake Lucero, New Mexico, loses 75% at its first endothermal peak temperature of 180°C ., and loses all of its water at the second endothermal peak temperature of 215°C . A chrysocolla sample from Tyrone, New Mexico, loses 66.6% of its water at its dehydration endothermal peak temperature of 154°C . If the dehydration endothermal peak is strong and its range is narrow, the percentage of loss of water at the endothermal peak temperature is large; on the other hand, the percentage is small if the peak range is broad. Because shattuckite has a wide true endothermal peak range, the estimation of 65% loss of its water content at its endothermal peak temperature is reasonable. As interpolated from the dehydration curve, the loss of 65% of water occurs at 740°C . Therefore, the true endothermal peak temperature of dehydration is estimated to be 740°C .

The exothermal peak at 980°C . A sample fired to 950°C . contains tenorite, cryptocrystalline cuprite, and some cryptocrystalline α -quartz; the unknown phase that occurs in a sample fired to 800°C . disappears. A

sample fired to 1,000° C. contains tenorite, cuprite, α -quartz, and α -cristobalite. One fired sample shows that the powder line 4.07 Å of α -cristobalite is darker than the powder line 4.29 Å of α -quartz, whereas the powder line 2.47 Å of cuprite is twice as dark as the powder line 2.54 Å of tenorite. The reverse is shown by another sample. Both samples were fired separately in the same cylindrical electric furnace. Thus, it appears that the decomposition of tenorite into cuprite may be accelerated by the crystallization of α -cristobalite, or vice versa.

The crystallization of α -cristobalite is an exothermal reaction. Alpha-cristobalite is formed in some clays fired to 1,000° C., such as montmorillonite from Chambers, Arizona (Bradley and Grim, 1951). The crystallization of α -cristobalite is usually indicated by a small but sharp exothermal peak at about 950° C. to 1,000° C. It seems likely that the exothermal peak at 980° C. in the DTA curve of shattuckite is caused by the crystallization of α -cristobalite.

Decomposition of tenorite into cuprite. The thermal curve begins to show a weak and gradual endothermal reaction at about 850° C. A sample fired to 900° C. contains a small amount of cryptocrystalline cuprite. The decomposition of tenorite into cuprite is a strong endothermal reaction. The weak and gradual endothermal reaction beginning at 850° C. represents only a gradual decomposition of a small amount of tenorite into cuprite. This decomposition increases rather vigorously above 995° C., the maximum temperature of the DTA. The thermal curve appears to show that the exothermal peak at 980° C. is followed closely by a strong endothermal reaction above 995° C. Heating was continued at 995° C. for a few minutes, and the thermal curve continued to show a strong endothermal reaction. Generally speaking, high temperature and low partial pressure of oxygen in the furnace will favor the decomposition of tenorite into cuprite.

The unknown phase. The unknown phase in shattuckite fired to 800° C. mentioned previously is represented by the following powder lines: 6.81 Å (2), 6.21 Å (2), 4.70 Å (3), 2.68 Å (1.5). The intensity of the tenorite powder line 2.53 Å is (10). These are not powder lines of paramelaconite ($\text{Cu}_2\text{O} \cdot 6\text{CuO}$); possibly they represent a copper silicate of some sort.

ACKNOWLEDGMENT

The writer gratefully acknowledges the assistance of several persons, all of whom are members of the New Mexico Institute of Mining and Technology. Professor Alvin J. Thompson critically read the manuscript. Professor Joseph A. Schutle discussed the thermodynamics of the copper oxides. Dr. Edmund H. Kase, Jr. did the final editing of the manuscript.

REFERENCES

- ADLEY, W. F., AND R. E. GRIM (1951), High temperature thermal effects of clay and related materials: *Am. Mineral.*, **36**, 182-201.
- D, WILLIAM E. (1915), Third Appendix to the Sixth Edition of Dana's System of Mineralogy: 87 p., John Wiley & Sons, Inc., New York.
- FFMAN, A. J., JR., AND E. D. DILLING (1950), Differential thermal curves of certain hydrous and anhydrous minerals, with a description of the apparatus used: *Econ. Geol.*, **45**, 222-224.
- SVY, BARTHOLOMEW (1954), Multiplicity and disorder in the lattice of ekmanite: *Am. Mineral.*, **39**, 946-956.
- ALLER, W. T. (1915), Four new minerals: *Washington Acad. Sci. Jour.* **5**, p. 7.
- THERS, W. J., AND YAO CHIANG (1958), Differential thermal analysis: theory and practice: New York, Chemical Publishing Co., Inc., 444 p.

Manuscript received March 22, 1960.

LATTICE EXPANSION OF KAOLIN MINERALS BY TREATMENT WITH POTASSIUM ACETATE

KOJI WADA, *Faculty of Agriculture, Kyushu University, Fukuoka, Japan.**

ABSTRACT

Grinding with K-acetate ($\text{KC}_2\text{H}_3\text{O}_2$) caused a lattice expansion to 14 Å not only for halloysite but good kaolinite, while the formation of the same complex by drying from a $\text{KC}_2\text{H}_3\text{O}_2$ solution was only observable for halloysite, hydrated or dehydrated without heat. Heating the 14 Å complex at 100° C. caused a collapse to 11.4 Å by dehydration. No comparable result was obtained for kaolinite by grinding with the other NH_4 and K salts which were effective in the formation of the halloysite complex. Also, no complex of $\text{KC}_2\text{H}_3\text{O}_2$ formed with some clay minerals, such as pyrophyllite, talc, antigorite, chrysotile, and chlorites.

The 14 Å complexes of kaolin minerals were subjected to washing with water and air-drying at R.H. 65%. The resulting spacings were 7 Å with good kaolinites, and 10 Å with halloysites, even if they had once dehydrated either with or without heat. The observed difference was interpreted in terms of the regularity in the arrangement of the structural layers affecting the orientation of interlayer water molecules.

INTRODUCTION

Generally it has been considered that the dehydration of halloysite is not reversible and the hydrated form ordinarily can not be formed again. This sometimes presents a problem in identification of 7 Å minerals in clays, and particularly in soil clays. MacEwan (1946, 1948) found that halloysite dehydrated without heat will combine with ethylene glycol, and when the product is treated with water, hydrated halloysite is regenerated. The usefulness of this method, however, is also restricted by the fact that not all forms of halloysite respond to this ethylene glycol treatment.

Earlier studies (Wada, 1958, 1959, Garrett and Walker, 1959) show that salt-halloysite complexes are obtained from the hydrated form of halloysite by drying from solutions, or by grinding with crystals of certain K, Rb, NH_4 , and Cs salts. The complex-forming ability of some of these salts is suggested to be greater than that of the organic reagent. Formation of the salt complexes and regeneration of hydrated halloysite might be utilized as a criterion for differentiation of halloysite from kaolinite. The above consideration has led to the present study on the formation of the salt complex with halloysites which differ in the degree of hydration, and further with some kaolin clays.

EXPERIMENTAL

$\text{KC}_2\text{H}_3\text{O}_2$, NH_4Cl , and HN_4NO_3 were first selected as the complex-

* Present address: Department of Soils, University of Wisconsin, Madison, Wisconsin.

forming salts in view of their greater ability in the complex formation in comparison with other NH_4 and K salts. Basal spacings characteristic to the salt complex of halloysite are 14.3, 10.5, and 11.6 Å, respectively. The following procedures were adopted for the preparation of the salt complexes.

Drying from solutions of complex-forming salts

An aqueous solution containing an appropriate amount of a salt was spread and allowed to dry on the thin layer of a clay (-2μ) formed on a glass plate by sedimentation. In the case of halloysite, maximum intensities of the basal reflections of the salt complex were obtained when it was treated with 3 to 4 m.mols of the salt per gm. of clay.

Dry or wet grinding with salts

One gm. of clay (-150 mesh) was ground in an agate mortar, either mechanically or manually, with 5 to 10 m.mols of the salt. The time necessary for complete formation of the complex varies with the method of grinding, manual or mechanical, dry or wet, and the kind of the minerals and salts. The wet grinding was made in the presence of water just after adding the clay-salt mixture. The dry or mechanical grinding was 3 to 5 minutes as effective as the wet or manual grinding respectively, but caused considerable destruction of the crystal structure. Standing overnight (or longer) after a brief grinding has been found to be as effective in complete complex formation as longer grinding, with less destructive effect. (Andrew, Jackson and Wada, 1960.)

RESULTS AND DISCUSSION

Halloysite

A thin layer of hydrated halloysite from Yoake, Oita, Japan (Aomine and Higashi, 1956) was dried over concentrated H_2SO_4 for two weeks. It combined completely with $\text{KC}_2\text{H}_3\text{O}_2$, but only partly with NH_4Cl and H_4NO_3 by drying from the respective salt solutions (Fig. 1). Although McCowan (1946, 1948) stated that halloysite gently dried without heat combined completely, or almost completely with ethylene glycol, most of it remained unaffected in this experiment. A halloysite from Bedford, Indiana, (API reference specimen), which was partly dehydrated as received, responded to the $\text{KC}_2\text{H}_3\text{O}_2$ treatment, and the hydrated halloysite was readily regenerated from the $\text{KC}_2\text{H}_3\text{O}_2$ complex by treating in water (Fig. 2). A similar result was obtained with a halloysite from Teke, Utah.

Since the result proved that $\text{KC}_2\text{H}_3\text{O}_2$ was most effective to reopen the tightly closed interlayer spaces, this treatment was tried with halloysite



FIG. 1. Effect of pre-drying over conc. H_2SO_4 on the complex formation of the Yoake halloysite.

dehydrated by heating. The Yoake halloysite heated at 100°C . was only partly susceptible, namely, about 80 to 85% remained unaffected, while that heated at 300°C . was almost completely resistant.

After several attempts, grinding with $\text{KC}_2\text{H}_3\text{O}_2$ was found to be most effective for formation of the complex with the halloysite dehydrated by heating (Fig. 3). The time necessary for complete formation of the complex increases with the degree of dehydration, for example, 10 to 40 minutes by the mechanical grinding in the wet state. The amount necessary to obtain the well-developed complex was slightly greater (5 to 6 m.mols/g.) than that in the former drying up treatment. Treating the complex with water, the hydrated form was regenerated (Fig. 3). Therefore, in this sense, the dehydration of halloysite is reversible, and not irreversible as has been generally considered.

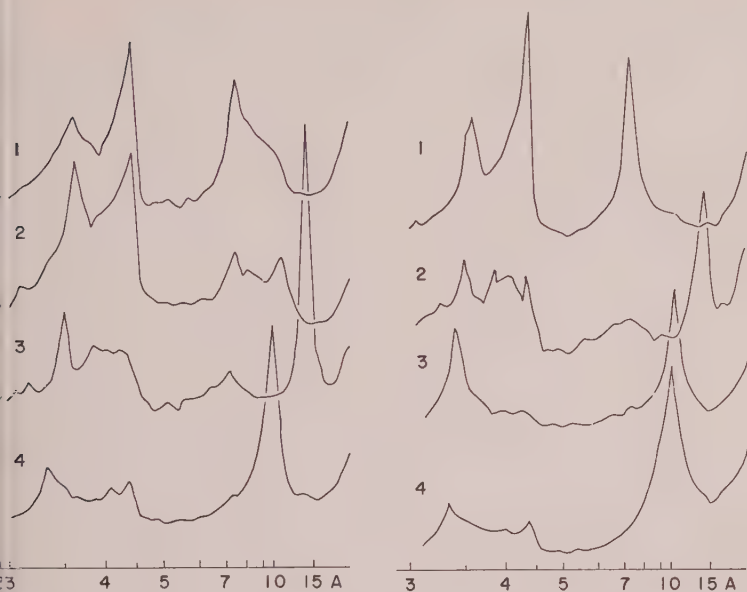


Fig. 2 (left). Bedford halloysite: natural (1); treated with ethylene glycol (2); dried from $\text{KC}_2\text{H}_3\text{O}_2$ solution (3); then, washed with water and air-dried (4).

Fig. 3 (right). Yoake halloysite: heated at 100° C. (1); ground with $\text{KC}_2\text{H}_3\text{O}_2$ (2); then, washed with 1 N NH_4Cl solution (3) or water (4), and dried at R.H. 65%.

Minite

Complex formation by drying from the $\text{KC}_2\text{H}_3\text{O}_2$ solution was tried on platy kaolinite from Macon, Georgia (API reference specimen), but no complex formed. Further, it was subjected to the dry grinding with H_2O_2 . Contrary to expectation, very strong and sharp reflections appeared at 14.2, 7.1, and 3.51 Å (Fig. 4), indicating that the kaolinite structure expanded along its *c*-axis as did halloysite. A comparatively smaller amount of the salt (8 m.mols/g.) was needed to produce the well-developed complex. The time necessary for complete formation of the complex was longer than that needed for metahalloysite, but partial expansion was readily noticed after 20 minutes grinding.

The basal reflections for the kaolinite complex were about eight times stronger as those for the corresponding halloysite complex. This might be interpreted in terms of the higher regularity of the layer stacking and the greater number of the structural layers in the kaolinite complex. Furthermore, smoothing the surface of the specimen packed in the sample holder for x-ray analysis may produce strong orientation of the platy crystallites

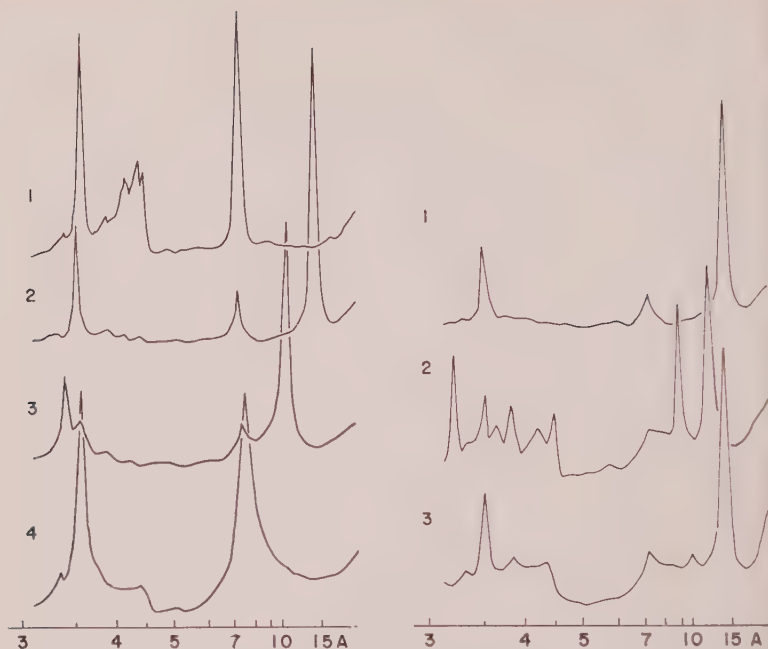


FIG. 4 (left). Georgia kaolinite: natural (1); ground with $\text{KC}_2\text{H}_3\text{O}_2$ (2); then, washed with 1 N NH_4Cl solution (3) or water (4), and dried at R.H. 65%.

FIG. 5 (right). Georgia kaolinite: ground with $\text{KC}_2\text{H}_3\text{O}_2$ (1); then, heated at 100° C (2); and allowed to stand in the laboratory air for 1 hour (3).

in the sticky mass of the clay and $\text{KC}_2\text{H}_3\text{O}_2$, resulting in enhancement of the basal reflections.

An x-ray analysis was made on the clay obtained from the kaolinite complex by washing with water and air-drying. A broad peak appears at about 7 Å instead of 10 Å (Fig. 4), suggesting that there is some difference between kaolinite and halloysite in the stability with which water molecules orient between the kaolin layers. The two triplets of the original kaolinite with spacings, 2.56, 2.53, 2.50 and 2.38, 2.34, 2.29 Å, were replaced by a doublet (2.56 and 2.50 Å.) and a broader reflection at 2.34 Å. Also, a two dimensional diffraction effect appeared on the reflections corresponding to the (020) to (002) reflections of the original kaolinite. The finding indicates that the reversible penetration of $\text{KC}_2\text{H}_3\text{O}_2$ has caused a considerable modification on the disposition of kaolin layers, but it still has some distinctive structural features. These are comparable to those found for "fireclay" (Brindley and Robinson, 1946, 1947) and kaolinite ground in a ball mill for 4 to 10 weeks (Dragsdorf *et al.*, 1951), suggesting the presence of the structural layers being randomly displaced by multiples of $b_0/3$ along the b -axis.

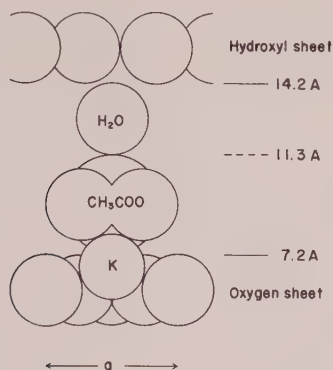


FIG. 6. A cross section of the 14 Å complex, showing a probable position of K^+ , $C_2H_3O_2^-$, and H_2O .

From the foregoing, a mechanical disruption of the kaolinite structure at that of halloysite may be ruled out as a probable cause of the observed expansion. It is certainly true that, in the absence of $KC_2H_3O_2$, the kaolinite structure would be considerably disrupted by only 30 minutes of grinding (Fig. 7). In its presence, however, the kaolinite structure is much more stable probably owing to the lubricating action of interlayer water molecules, as will be shown later. Therefore, the observed expansion to 14 Å by positive penetration of $KC_2H_3O_2$ can be considered as a partial characteristic of kaolinite, and consequently, common to all the members of the halloysite-kaolinite series.*

The effect of heating at 100° C. on the $KC_2H_3O_2$ complex is interesting in view of the configuration of the interlayer material and the preference for $KC_2H_3O_2$ in the reaction. The heating caused a collapse of the complex to 11.4 Å (Fig. 5). The reflections due to the excess salt appeared at 4.44, 3.55, and 3.21 Å. The decrease in the basal spacing and the ease of its restoration by allowing the heated complex to stand in the laboratory air indicates the presence of a monomolecular layer of water rather than that of $KC_2H_3O_2$. The cation size was found to be of primary importance in the reaction in relation to the size of the cavity in the hydroxyl sheet (Wada, 1958, 1959), so $KC_2H_3O_2$ and water molecules probably are oriented in a configuration, such as that illustrated in Fig. 6, in which the potassium ion is in the cavity of the oxygen hexagon and the clearance space is not equal to the sum of the CH_3 and H_2O *van der Waals* radii.

Such longer grinding of the Georgia kaolinite with NH_4Cl resulted in the appearance of a diffuse reflection at about 10 Å. The effect of mechanical destruction was found to be greater as illustrated by some of the

A recent study (Andrew, Jackson and Wada, 1960) has shown that dickite is also expanded upon grinding with $KC_2H_3O_2$.

rather diffuse and generally weakened (*hkl*) reflections. The partial formation of the hydrated form from the complex by washing with water may be related to this. Since the well-developed NH_4Cl complex can readily be obtained by washing the $\text{KC}_2\text{H}_3\text{O}_2$ complex with an NH_4Cl solution (Fig. 4), the result seems to indicate difficulty in the penetration into the kaolinite structure, and not the unstable nature of the resulting configuration.

The dry grinding was also tried with the following salts; NH_4NO_3 , $(\text{NH}_4)_2\text{HPO}_4$, $(\text{NH}_4)_2\text{SO}_4$, K_2HPO_4 , NH_4 -formate, NH_4 -acetate, and $(\text{NH}_4)_2$ -citrate. These were effective in the formation of the halloysite complex (Wada, 1959), but none was comparable to $\text{KC}_2\text{H}_3\text{O}_2$ in the penetration into the kaolinite structure.

The reason of this preferential penetration is as yet not clear. The presence of interlayer water molecules owing to its strong deliquescent nature might have an effect in the penetration as a lubricant and or as a stabilizing agent in the complex formation. Lubricating action of interlayer water was also assumed by Mackenzie and Milne (1953) in the explanation of the relative stability of vermiculite to grinding in comparison with muscovite. However, it alone could not account for the observed preference, because the deliquescent salts, $\text{NH}_4\text{C}_2\text{H}_3\text{O}_2$ and K_2HPO_4 , fail to form the complex upon dry grinding.

RELATIONSHIPS OF COMPLEX FORMATION TO CLAY STRUCTURE

In view of a common peculiarity of their crystal structures, salt-complex formation was previously tried with montmorillonites as well as with halloysite (Wada, 1959), but no complex was found. The difference between both the minerals was ascribed to the differences in the density of the interlayer charge and in the atomic configuration of the interlayer surface.

Further, in this study, dry grinding with $\text{KC}_2\text{H}_3\text{O}_2$ was tried with the following minerals:

1. Pyrophyllites from Fukue, Nagasaki and Mitsuishi, Okayama.
2. Talc from Sasaguri, Fukuoka.
3. Antigorite from Sasaguri, Fukuoka (Table 1).
4. Chrysotile from Kashii, Fukuoka (Table 1).
5. Chlorites from Sanno, Fukuoka, and Okushi, Nagasaki (Shirozu, 1958).

There is no indication of the lattice expansion with these minerals. Pyrophyllite and talc were used in view of the absence of the interlayer charge and the difference in the atomic configuration at the interlayer

face. The fact that no complex formation occurred with these minerals could be attributed to their atomic configuration of the interlayer surface, namely, the oxygen and oxygen sheets in these minerals instead of oxygen and hydroxyl sheets in the kaolin minerals. It is also evident that the absence of the interlayer charge may contribute, but it alone cannot cause the penetration and orientation of the salt molecule. Considering their structural similarity, a sharp difference in the complex formation between the kaolin and serpentine minerals is particularly

TABLE 1. THE EFFECT OF DRY GRINDING ON THE X-RAY DIFFRACTION PATTERNS OF CHRYSOTILE AND ANTIGORITE

Chrysotile (Kashii)				Antigorite (Sasaguri)			
Before grinding		After 2.5 hrs. grinding		Before grinding		After 2.5 hrs. grinding	
$d(\text{\AA})$	I	$d(\text{\AA})$	I	$d(\text{\AA})$	I	$d(\text{\AA})$	I
7.25	56	7.25	38	7.20	200	7.20	35
4.53	18	4.54	14				
3.64	41	3.63	26	3.60	184	3.60	22
2.62	10	2.61	8				
2.50	31	2.50	20	2.52	42	2.52	23
2.43	18	2.44	12	2.41	14	2.41	3
2.33	15	2.33	7	2.16	10	2.16	5
2.15	3			2.15	10		
1.96	5			1.81	8		
1.53	20	1.53	12	1.56	8	1.57	4
				1.54	8	1.54	4

The samples were mounted by packing into the hollow of the A1-holder and smoothing the surface. Intensities were measured from the peak height on the automatic recording

instrument. So far as the 1:1 layer structure is assumed, there seems no significant difference in the strength of the interlayer bonds between both minerals. The effect of cation substitution is practically negligible in connection. On the other hand, the configuration of the oxygen and hydroxyl layers are different as seen in their b_0 parameters 8.93 and 9.24 for kaolinite and antigorite respectively, and this might affect the stability of the resulting complex. It seemed still questionable, however, that the striking difference in the complex formation could be ascribed to a rather small difference.

In relation to this, the result of grinding of these mineral samples alone should be noted (Fig. 7). Under comparable conditions (dry, mechanical), 001 reflections of the kaolinite, talc, and pyrophyllite markedly

reduced their intensities in the first 30 minutes. At the end of 2 hours they completely collapsed with disappearance (kaolinite) or marked blurring (talc and pyrophyllite) of all the (*hkl*) reflections. In the meanwhile, the chrysotile showed little change in the sharpness and intensity of its (001) reflection, and contrary to what expected from its hypothesized tubular structure, was reasonably stable to grinding (the Yoak halloysite completely collapsed within 1 hour). In the case of antigorite, marked degradation was observed at first, but the (001) reflection max

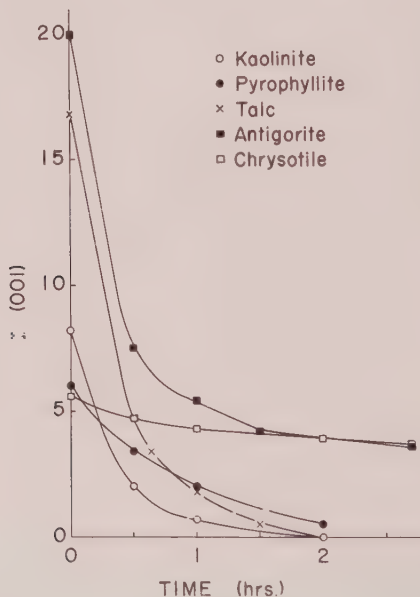


FIG. 7. Effect of dry grinding on the (001) intensities of kaolinite (Georgia), pyrophyllite (Fukue), talc (Sasaguri), antigorite (Sasaguri), and chrysotile (Kashii).

ima remained more resistant on further grinding in comparison with the other platy materials. The coincidence of the (001) intensities of both the minerals after prolonged grinding may be meaningful, although there is no comparable agreement in other reflections (Table 1). These results seem to indicate the presence of some fundamental fiber-crystallites in these minerals, such as that suggested by Pundsack (1956) on the basis of the density measurement for massive chrysotiles.

At any rate, it seems apparent that both the serpentine minerals react to grinding differently from the kaolin minerals, and this would be the cause for the inhibition of the formation of a salt complex. There may be some significant differences in their crystalline arrangement and therefore

the strength of the interlayer bonds, although this seems difficult to understand on the basis of the structural and morphological analogy between the kaolin and serpentine minerals (e.g. Bates, 1959). The absence of the chlorite complex could be used in determination of kaolin minerals in the presence of chlorite minerals. Unfortunately, the 001 reflections of the $\text{KC}_2\text{H}_3\text{O}_2$ complex of the kaolin minerals are close to the corresponding spacings of the chlorites, but the shift of 14 \AA reflection to 10 or 11 \AA is easily seen by forming the NH_4Cl or NH_4NO_3 com-

STABILITY OF WATER COMPLEX

The foregoing data suggest that the stability of the water complex derived from the $\text{KC}_2\text{H}_3\text{O}_2$ complex closely relates to its source minerals; Georgia kaolinite forms only a very unstable water complex, while the synthetic halloysite, even after it has been heated, readily regenerates its hydrated form. If it is generally correct, the difference in the stability of the water complex would aid in differentiation of 7 \AA minerals in clay minerals, and provide useful informations on their genesis.

The proposed method is the following. Clay samples are subjected to grinding with $\text{KC}_2\text{H}_3\text{O}_2$. The resulting complexes are washed twice with water (water complex) or a 1 N NH_4Cl solution (NH_4Cl complex) by centrifuge technique, spread on a glass plate, allowed to stand in a desiccator at R.H. 65%, and x-rayed.

Whether the kaolinite or halloysite forms its NH_4Cl complex (Figs. 3 and 4) permits a check of the formation of the complex with $\text{KC}_2\text{H}_3\text{O}_2$. While, the stability of the water complex is much different for the minerals; no complex formed with well-crystallized kaolinites, such as those from Macon, Georgia (Fig. 4); Mesa Alta, New Mexico; and Ibukishi, Japan. Even a transient formation of their fully-hydrated complexes could hardly be followed by x-ray analysis made while the clays were kept moistened. On the other hand, several natural hydrated and partially dehydrated halloysites (formed either by weathering of volcanic rocks or by hydrothermal action) gave water complexes which were stable at R.H. 65%, even after they had been dehydrated by heating (Fig. 3). The observed difference in the stability of the water complex derived from the $\text{KC}_2\text{H}_3\text{O}_2$ complex seems to reflect the difference in the arrangement of their structural layers that is inherited from the original minerals. The probably associated with environmental conditions of their formation. Random displacements of successive kaolin layers along both *b*- and *c*-axes in halloysite may favor relatively stable orientation of water molecules, whereas the higher degree of regularity, such as that found for the kaolinite complex derived from kaolinite may not. It suggests that the inter-

layer water molecules of halloysite are in a regular crystalline array that is related in some way to the clay structure, but not in the state of two-dimensional liquid.

Of all the specimens examined, the Spruce Pine kaolin (API reference specimen) is interesting in showing an intermediate character between kaolinite and halloysite, and in suggesting a possible transition from the poorly crystalline halloysite to the well-ordered kaolinite. Electron microscopic studies of this material revealed a predominance of tubular

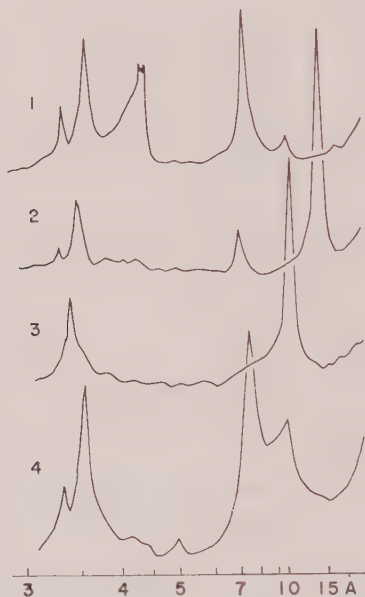


FIG. 8. Spruce Pine kaolin: natural (1); ground with $\text{KC}_2\text{H}_3\text{O}_2$ (2); then, washed with 1% NH_4Cl solution (3) or water (4), and dried at R.H. 65%.

crystals (Davis *et al.*, 1950; Sand and Ormsby, 1954; Taggart *et al.*, 1955). Further, the electron diffraction studies made by Honjo and his collaborators (1954) showed that these tubular crystals have a regular structure different either from that of halloysite, or of kaolinite. The x-ray diffraction pattern shows a rather sharp (001) reflection at 7.20 Å, and two triplets with spacings at 2.56, 2.53, 2.50 and 2.38, 2.34, 2.29 Å are fairly well-separated. These x-ray characteristics are also indicative of a high degree of crystallinity than that commonly attributed to halloysite minerals.

Partial formation of the water complex was observed by washing the $\text{KC}_2\text{H}_3\text{O}_2$ complex with water (Fig. 8), while only 15 to 20% of this material

ial (-2μ) and even less of that included in the coarser fraction (-150 sh) formed the complex by drying from the $\text{KC}_2\text{H}_3\text{O}_2$ solution.

Sand (1956) analyzed the material believed to be of the same origin kept in moist conditions and gave the ratio of *hydrated halloysite*:kaolinite as approximately 7.5–6.9:1.0–2.1. In this district, all halloysites are found in the hydrated form, and not its dehydrated form. He interpreted his data to indicate that environmental conditions in weathering feldspathic rocks that are conducive to the formation of the hydrated halloysite, have not changed appreciably since Tertiary time. On the other hand, he noted that the Spruce Pine halloysite dehydrates much more rapidly than the compact hydrothermal hydrated halloysite (personal communication). A similar observation was also made by Kerr, Lipp, and Hamilton (1950).

These data are interesting in indicating the presence of a particular kaolin mineral that is derived from its hydrated form but exhibits rather a low degree of regularity in the stacking of the structural layers. As has been well-known, environmental conditions, such as humidity, temperature, and pressure cause the dehydration of halloysite (Brindley and Goodyear, 1948; Brindley, Robinson, and Goodyear, 1948). In view of the present results, it seems very probable that the dehydration of halloysite is also a function of its crystallinity, and the ready and irreversible hydration of the Spruce Pine material might be interpreted as due to a long period of crystallization time.

CONCLUSION

The formation of the interlayer complex resulting in lattice expansion to 14 \AA by grinding with $\text{KC}_2\text{H}_3\text{O}_2$ can be considered as a potential characteristic common to all the minerals of the kaolinite-halloysite series, as well as to serpentine minerals, 2:1 and 2:2 type minerals, either with or without interlayer charge. So far as tested, no well developed complexes were formed with other NH_4 and K salts, although the reason for this preference for $\text{KC}_2\text{H}_3\text{O}_2$ is as yet not known. Contraction of the 14 \AA complex to 11.4 \AA by heating indicates the presence of a monomolecular layer of water between the layers together with that of $\text{KC}_2\text{H}_3\text{O}_2$.

The water complexes of kaolin minerals could be obtained from each mineral by washing with water, and their stability has a relation to the degree of randomness of the stacking of the structural layers. The water complexes derived from good kaolinites are far less stable, than those from poorly crystalline halloysites are stable, even if they are once dehydrated with or without heating. Differentiation between the two types of 7 \AA minerals on this basis could be of considerable significance in studying kaolin minerals in clays and soil clays.

ACKNOWLEDGMENT

The author would like to acknowledge the help and encouragement received during the study from Professor S. Aomine. The research was supported in part by a grant from the Asahi Science Research Fund. API specimens were kindly furnished by Dr. T. Sudo through Professor Aomine, Ibuski kaolin and talc samples by Drs. N. Tanaka and T. Muta, serpentine and chlorite minerals by Dr. H. Shirozu, respectively. The author is also grateful to Dr. L. B. Sand who has provided the Utah halloysite and valuable informations on the Spruce Pine kaolin.

REFERENCES

- ANDREW, R. W., JACKSON, M. L., AND WADA, K. (1960), Intersalation as a technique for differentiation of kaolinite from chloritic minerals by x -ray diffraction; *Soil Sci. Soc. Am. Proc.*, **24**, 422-424.
- AOMINE, S. AND HIGASHI, T. (1956), Clay minerals of decomposed andesitic agglomeratic lava at Yoake: *Mineral. Jour. (Japan)*, **1**, 278-289.
- BATES, T. F. (1959), Morphology and crystal chemistry of 1:1 layer lattice silicates: *Am. Mineral.*, **44**, 78-114.
- BRINDLEY, G. W. AND GOODYEAR, J. (1948), X -ray studies of halloysite and metahalloysite (II): *Min. Mag.*, **28**, 407-422.
- BRINDLEY, G. W. AND ROBINSON, K. (1946), Randomness in the structures of kaolinitic clay minerals: *Trans. Faraday Soc.*, **42B**, 198-205.
- BRINDLEY, G. W. AND ROBINSON, K. (1947), An x -ray study of some kaolinitic fireclays: *Trans. Brit. Ceramic Soc.*, **46**, 49-62.
- BRINDLEY, G. W., ROBINSON, K., AND GOODYEAR, J. (1948), X -ray studies of halloysite and metahalloysite (III): *Min. Mag.*, **28**, 423-428.
- DAVIS, D. W., ROCHOW, T. G., AND ROWE, F. G. (1950), Electron micrographs of reference clay minerals: *A.P.I. Proj. 49, Prelim. Rep't.*, No. 6.
- DRAGSDORF, R. D., KISSINGER, H. E., AND PERKINS, A. T. (1951), An x -ray study of the decomposition of kaolinite: *Soi. Sci.*, **71**, 439-448.
- GARRETT, W. G. AND WALKER, G. F. (1959), The cation exchange capacity of hydrated halloysite and the formation of halloysite salt complexes: *Clay Minerals Bull.*, **4**, 75-80.
- HONJO, G., KITAMURA, N., AND MIHAMA, K. (1954), Study of clay minerals by means of single-crystal electron diffraction diagrams—the structure of tubular kaolin: *Clay Minerals Bull.*, **2**, 133-141.
- KERR, P. F., KULP, J. L., AND HAMILTON, P. K. (1950), Differential thermal analyses of reference clay mineral specimens: *A.P.I. Proj. 49, Prelim. Rep't.*, No. 3.
- MAC EWAN, D. M. C. (1946), Halloysite-organic complexes: *Nature*, **157**, 159-160.
- MAC EWAN, D. M. C. (1948), Complexes of clays with organic compounds (I): *Trans. Faraday Soc.*, **44**, 349-367.
- MACKENZIE, R. C. AND MILNE, A. A. (1953), The effect of grinding on micas: *Clay Minerals Bull.*, **2**, 57-62.
- PUNDSACK, F. L. (1956), The properties of asbestos (II): *J. Phys. Chem.*, **60**, 361-364.
- SAND, L. B. (1956), On the genesis of residual kaolins: *Am. Mineral.*, **41**, 28-40.
- SAND, L. B. AND ORMSBY, W. C. (1954), Evaluation of methods for quantitative analysis of halloysite-kaolinite clays: *Proc. Second National Clay Conference, Natl. Acad. Sci.—Natl. Res. Council Publ.*, **327**, 277-284.

- ROZU, H. (1958), X-ray powder patterns and cell dimensions of some chlorites in Japan, with a note on their interference colors: *Mineral. Jour. (Japan)*, **2**, 209-223.
- GGART, M. S., MILLIGAN, W. O., AND STUDER, H. P. (1955), Electron micrographic studies of clays: *Proc. Third National Clay Conference, Natl. Acad. Sci.—Natl. Res. Council Publ.*, **395**, 31-64.
- DA, K. (1958), Adsorption of alkali chloride and ammonium halide on halloysite: *Soil and Plant Food* (Tokyo), **4**, 137-144.
- DA, K. (1959), Oriented penetration of ionic compounds between the silicate layers of halloysite: *Am. Mineral.*, **44**, 153-165.

manuscript received April 5, 1960.

SOME OBSERVATIONS ON "IDDINGSITE"

P. GAY AND R. W. LEMAITRE,* *Department of Mineralogy
and Petrology, University of Cambridge, Cambridge,
England.*

ABSTRACT

Specimens of "iddingsite" for many localities have been examined by x-ray, chemical, and optical methods in a study of the alteration of olivine to "iddingsite." This proves to be a continuous transformation, and although at any stage it is possible to recognize embryonic structures, the pseudomorph is throughout a disordered atomic arrangement, and at no stage can it be assigned a definite structure or chemical composition or be regarded as a simple submicroscopic mineral intergrowth. The mechanism of the alteration appears to be one of cationic diffusion and replacement, the anion framework suffering little change; the presence of a high proportion of mobile hydrogen ions is probably an important factor. Some speculations are offered regarding the physical and chemical conditions under which alteration takes place.

INTRODUCTION

The name "iddingsite" was proposed by Lawson (1893) for certain phenocrysts occurring in the eruptive, basaltic rocks of Carmelo Bay, California. In thin section they were described as ranging in color from deep chestnut-brown to citron-yellow and occasionally clear yellowish green, with marked pleochroism in sections transverse to the cleavage; in hand specimen "iddingsite" is described as soft but brittle, with a very well developed cleavage. Lawson was not convinced that the phenocrysts had altered from olivine, as he thought that the absence of residual olivine, and the presence of appreciable amounts of lime and soda were difficult to explain on the basis of alteration. Ross and Shannon (1925) in a detailed study give optical data for a considerable number of specimens and several chemical analyses; they deduce the formula of "iddingsite" to be $\text{MgO} \cdot \text{Fe}_2\text{O}_3 \cdot 3\text{SiO}_2 \cdot 4\text{H}_2\text{O}$ with MgO replaced by CaO in the ratio $\text{CaO}:\text{MgO} = 1:4$. They also point out that "iddingsite" is confined almost entirely to extrusive or hypabyssal rocks and is practically absent from deep-seated rocks. They conclude that "iddingsite is most probably a deuteric mineral formed in the presence of heat, water and gases after the magma has reached a horizon near enough the surface to give oxidizing conditions." Later Edwards (1938) described three lines of evidence that "iddingsite" formed during consolidation of the magma. Firstly, rims of augite commonly surround "iddingsitized" olivine crystals; secondly, zones of fresh olivine can be seen enclosing embayed and "iddingsitized" olivine phenocrysts; and finally, a boulder from a "boulder tuff," Victoria, Australia, contained fresh olivine in the tachylitic outer

* Now at Department of Geology, King's College, University of London.

ne, and an "iddingsitized" olivine in the crystalline core. Unlike Ross and Shannon, Edwards does not consider that the formation of "iddingsite" is dependent on the original composition of the olivine. He concludes that the formation of "iddingsite" is a process of oxidation and hydration and that the magma should not only be rich in water vapor, but should also have differentiated to give an iron-rich liquid.

The first *x*-ray data on "iddingsite" were published by Ming-Shan Sun (1957). Using powder methods only, he concluded that "iddingsite" consisted of cryptocrystalline goethite and amorphous material and gives a few chemical analysis and optical data. With regard to the conditions of formation, he states that "the alteration of olivine to iddingsite occurs most likely in a highly oxidizing solution containing HCl, at high temperatures and under high pressure." Further *x*-ray powder data on the alteration of olivine are given by Wilshire (1958). Unfortunately he does not clearly distinguish the various types of alteration. He concludes that "iddingsite" consists mainly of "mixed layer smectite-chlorite with a variety of accessory minerals"; among the accessory minerals are feldspar, quartz and calcite which strongly suggest that the material was contaminated. Recently Brown and Stephen (1959) have presented structural observations on an "iddingsite" from New South Wales, Australia, examined by single-crystal *x*-ray methods. Their results are in good agreement with those for some specimens examined during the present study, and will be referred to in more detail at the appropriate point. Smith (1959) has recently described the single crystal examination of pseudomorphs after olivine in the Markle basalt.

The object of the present study was to obtain more information on the structural arrangements in "iddingsites," so as to examine the process of alteration and to attempt to define the conditions under which "iddingsitization" takes place. To do this, a large number of specimens of "iddingsite" were examined from many different localities by single-crystal *x*-ray methods; chemical analyses, together with the optical properties, were obtained for several of the specimens. The results are now presented in this paper.

DESCRIPTION OF SPECIMENS

The selection of specimens of "iddingsite" for examination is difficult owing to the complexity of the possible alterations of olivine e.g. to serpentine, bowlingite and "iddingsite," and to the uncertainty of the exact physical and chemical conditions required for these alterations. Further, the optical characterization of "iddingsite" is not well defined. The specimens available from many different localities were divided into two groups. In the first group, the "iddingsites" conformed to the following

conditions:—(a) they were optically homogeneous in plane polarized light, and crystalline; (b) they ranged from orange-red to red-brown in thin section; (c) they were obviously pseudomorphing olivine and unaccompanied by any other obvious alteration product of olivine and (d) they occurred in basic or intermediate, volcanic or hypabyssal rocks. Six different specimens satisfying these conditions have been examined in some detail; x-ray, optical and, where possible, chemical data have been obtained. In the second group of seven specimens, the examination has not been so full, and has usually only consisted of single crystal x-ray studies. Some of these specimens, although described as "iddingsite," show deviations which suggest that they may not be the product of an identical alteration process as the others. Their relationship to specimens of the first group will be commented on after the results have been described.

The six specimens of the first group will now be described with brief petrographic comments on the rocks in which they occur.

"Iddingsite," G.133 from a picrite basalt: Gough Island:

In thin section the rock is strongly porphyritic with phenocrysts of diopsidic augite and olivine set in a groundmass of pyroxene, plagioclase, ilmenite, magnetite and alkali feldspar. The "iddingsite" occurs as thin shells to the otherwise perfectly fresh olivine phenocrysts. It is a red-brown to orange-brown in color and is only very slightly pleochroic. No new cleavage is developed.

"Iddingsite," V. 3, from a nepheline-bearing basalt: Vogelsberg, Hesse, Germany:

In thin section (see Fig. 5), the rock is micro-porphyritic with abundant microphenocrysts of euhedral to subhedral "iddingsitized" olivine, up to 1 mm. long, and a few highly zoned, titaniferous augites. In the smaller crystals the original olivine has been completely altered to an orange-brown slightly pleochroic "iddingsite," which in plane polarized light appears to be perfectly homogeneous. Between crossed nicols, however, it often shows a patchy extinction and in places has a slightly fibrous appearance. In the larger crystals where there is still some olivine present in the core, the junction between olivine and "iddingsite" is very gradational and consists of numerous, exceedingly minute hair like fingers of "iddingsite" penetrating into the olivine. This border zone is usually about 0.02 mm. wide. Closely associated with the "iddingsitized" olivine are equidimensional grains of iron ore up to 0.2 mm. across.

The groundmass consists of abundant, euhedral to subhedral crystals of highly zoned titaniferous augite poikilitically enclosed in large clear crystals of plagioclase and nepheline. Iron ore is absent from the groundmass.

"Iddingsite," 57303, from an olivine basalt: Tahiti:

In thin section this rock is very similar to V.3 except that the nepheline is absent and the plagioclase occurs as laths. It is a microporphyritic rock with abundant microphenocrysts of "iddingsitized" olivine, up to 1 mm. across, and euhedral to skeletal iron ore, up to 0.5 mm. across. The "iddingsite" is identical to that described for V.3 except that the junction between the olivine and the "iddingsite" is often perfectly gradational with no sign of the penetrating hair-like growth of the "iddingsite."

The groundmass consists of abundant small euhedral to subhedral crystals of titaniferous augite, and basic plagioclase laths.

"iddingsite," G. 50 from a trachybasalt: Gough Island:

In thin section, the rock is porphyritic, with phenocrysts of plagioclase, "iddingsite" and titanite. The plagioclase is irregularly veined with an isotropic material, which is probably analcite, but the titanite is perfectly fresh. The "iddingsite" occurs as pseudomorphs after euhedral to subhedral olivine, although very few remnants of the original olivine are present. It is an orange-brown in color, and under crossed nicols it has a rather patchy and fibrous extinction.

The groundmass consists of plagioclase, pyroxene, "iddingsite" and iron ore.

"iddingsite," 11537, from an olivine basalt: Dunchideock, nr. Exeter, Devon:

A general petrographic description of this rock has been given by Tidmarsh (1932). "iddingsite" is a very rich ruby-red to orange-red color and is moderately pleochroic in these colors; maximum absorption occurs when the light vibrates parallel to the mica-schist cleavage, which is fairly well developed. Some of the grains are so dark as to be almost opaque, and in some of the crystals there is a central rounded core of almost opaque, amorphous material.

"iddingsite," FEAE No. 124 from a pyroxene trachyte, Mount Moroto, Uganda:

In thin section the rock is porphyritic with phenocrysts of strongly zoned titanite up to 3 mm. across, and "iddingsite," up to 1 mm. across, and iron ore. The "iddingsite" is a bright orange-red and is moderately pleochroic. In plane polarised light it appears homogeneous but between crossed nicols it has a patchy extinction. No remnants of the original olivine are present and no micaceous cleavage is developed.

The groundmass consists of titanite, iron ore, plagioclase, and interstitial zeolitic material, probably analcite.

The specimens of the second group are described much more briefly in Table 1.

TABLE I. DESCRIPTIONS OF "IDDINGSITES" OF THE SECOND GROUP

Specimen No.	Locality	Rock type	Comments on "iddingsite"
A	Gough Island	Gabbroic xenolith in tuff	Dark red brown, weak pleochroism. Occurs in thin films and hair-like rods. (See Fig. 6)
6	Juan Fernandez Island (Quensel 1952)	Olivine basalt	Reddish-brown to greenish-yellow
I-15	Carmelo Bay, Calif., U.S.A.	Carmeloite (olivine basalt)	Medium to dark orange-brown. Moderately pleochroic with new cleavage slightly developed
I-17	Carmelo Bay, Calif., U.S.A.	Carmeloite (olivine basalt)	As above but no new cleavage.
(C)	Gough Island	Gabbroic xenolith in lava flow	Bright ruby-red. Moderately pleochroic but no new cleavage developed
1378	Rungwe, Southern Province, Tanganyika	Olivine basalt	Orange-brown, only very slightly pleochroic

X-RAY METHODS

The optical homogeneity of many "iddingsites" suggests that, even if the material is not to be regarded as a definite compound with relatively fixed chemical constitution, there is some structural control over the alteration process. It appears, therefore, that the identification of the alteration products and the structural character of the "iddingsite" are advantageously studied by single-crystal, rather than powder x-ray methods. Similar methods for the identification of oriented intergrowths have been applied previously to pyroxenes by Bown and Gay (1959).

Oscillation photographs taken about the x - or z -crystallographic directions of the original olivine with $\text{FeK}\alpha$ radiation have been mainly used; the oscillation ranges were usually selected to be symmetrically across diad directions. The single crystals examined were carefully chosen from the most optically homogeneous part of the specimen; as far as possible, it was ensured that no unaltered olivine was present. It was also found necessary to examine a number of crystals from the same specimen for the alteration process in some specimens had proceeded to a different extent in different local areas. For such specimens, the results to be described below may be regarded as representing the average state of alteration of the specimen.

CHARACTERISTICS OF DIFFRACTION PATTERNS

The original olivine from which the "iddingsite" has been derived has an orthorhombic structure (space group $Pbnm$) determined first by Bragg and Brown (1926) and later refined by Belov *et al.* (1951). The dominant feature apparently controlling the structural rearrangements of the alteration process is the hexagonal sequence of approximately close-packed oxygen sheets; these oxygen layers are perpendicular to the x -axis, with one of the close-packed directions parallel to the z -axis of the olivine cell. Whilst it is not our purpose in this paper to discuss the structural rearrangements in detail, it must be emphasised that, just as in the pyroxenes described by Bown and Gay (1959), it is the anion arrangement which controls the structural orientation of the alteration products.

The characteristic x-ray diffraction patterns of various phases which occur in "iddingsites" will now be described.

(a) Olivine-like structures

Often a pattern can be recognized which retains features of the photographs of an unaltered olivine, despite the fact that the specimen shows the strong coloration of an "iddingsite." The patterns vary from those which are barely distinguishable from true olivine patterns, through those where the diffraction maxima have become diffuse, to patterns

h very diffuse spots and obvious discrepancies in the relative intensities of various reflections when compared with the corresponding intensities from an unaltered olivine.

Structurally, these patterns must represent the stages in the breakdown of the original olivine structure with the chemical changes introduced by the alteration. The diffuse character of the reflections could be attributed to a mosaic texture or to a distorted structure; it would seem probable that the atomic replacements taking place give a very distorted atomic arrangement.

Goethite-like structures

The occurrence of goethite (α -FeOOH) in "iddingsites" has been reported both by Ming-Shan Sun (1957) and Brown and Stephen (1959). The latter authors have presented a full analysis of the orientation of the goethite with respect to the original olivine. Goethite belongs to the same space group as olivine, and has similar cell dimensions except that the c -axis length is halved; there is a structural equivalence in that the approximately hexagonal close-packed oxygen sheets form the basis of the arrangement. The mutual orientation of goethite and olivine deduced by Brown and Stephen, and confirmed in the present investigation, is as expected if the structural control is exerted by the anion framework. Goethite grows within the olivine so that the close-packed planes are common to both structures, but with three different orientations corresponding to the effectively close-packed z -direction of the goethite being parallel to the three "close-packed" directions of the olivine oxygen sheet. Full details of the complex diffraction patterns produced by this arrangement are given by Brown and Stephen.

Often the diffraction spots due to the goethite are rather diffuse, although the material is quite well oriented; in a few specimens, however, the orientation of the goethite seems to be linked with sharper diffraction maxima. The relative amounts of goethite in the three possible orientations vary from specimen to specimen, suggesting that the three "close-packed" directions in the olivine sheet are not exactly equivalent; the parallel orientation with the z -axis of olivine and goethite coincident seems to be preferred. The poor quality of the goethite patterns from "iddingsites" makes the comparison with patterns from single crystals of goethite difficult, but it is apparent that the relative intensities are not always correct, and the cell dimensions are slightly variable. This suggests that it would be better to call this phase of the alteration product "goethite-like" for, like the olivine, it may well be defective and distorted, and variable in chemical constitution depending on the state of the alteration process. The size of the equi-dimensional goethite-like particles can be as

small as a few hundred Ångströms when estimated from the breadth of the reflection maxima, but this must be regarded as a lower limit as it takes no account of broadening due to the probable lattice distortion.

(c) *Hematite structures*

Hematite ($\alpha\text{-Fe}_2\text{O}_3$) occurs in some specimens (see Smith, 1959), usually in place of goethite. Although trigonal, it may again be regarded as having an approximately hexagonal close-packed oxygen framework, and its orientation is that expected from its similarity to the olivine structure. It is "twinned" in accordance with the intergrowth symmetry principle (Bown and Gay, 1959) so that its orientation may be described as

$$a_{0l} \parallel c_H, \quad b_{0l} \parallel \pm [01.0]_H, \quad c_{0l} \parallel \pm [21.0]_H$$

In all specimens, the hematite is very well oriented, though the breadth of the reflections is variable from quite diffuse to relatively sharp. Comparison with standard hematite photographs show no obvious relative intensity discrepancies, nor any detectable change in cell size; it seems more probable that this phase may be identified with $\alpha\text{-Fe}_2\text{O}_3$ with little impurity. The origin of the hematite cannot be regarded as being established. It is possible that it is formed by dehydration of a goethite-like phase formed during the alteration; indeed heating experiments have been carried out in which this transformation occurred. However other experiments (to be described elsewhere) have shown that hematite can be exsolved directly from olivine under suitable oxidizing conditions. Whatever its origin, its occurrence, as with the other structures so far described, points to the high stability of the anion framework through while the cations can be made to migrate. It is important to realize that the strength of the silicon-oxygen bond is not so great as to prevent a structural reorganization in which the Si O tetrahedra do not remain as discrete structural units.

(d) *Spinel structures*

Multiple oxide structures of this type are cubic, with the oxygen atoms in approximately cubic close packing. The orientation of such phases with respect to the original olivine is controlled by a correspondence of the close-packed sheets, with a "twinned" orientation required by the intergrowth symmetry principle; it is

$$a_{0l} \parallel (111)_{Sp}, \quad b_{0l} \parallel \pm (\bar{1}\bar{1}2)_{Sp}, \quad c_{0l} \parallel \pm (1\bar{1}0)_{Sp}$$

These phases are rarely present in "iddingsites," but when they are, their diffraction spots are sharp, but with an appreciable range of disorientation. It is difficult from x-ray data alone to distinguish the different mixed oxides of the spinel group, but it seems likely that the phase present in

"iddingsites" is probably magnetite (Fe_3O_4) or a magnesioferrite (MgFe_2O_4); the cell dimensions and intensity relationships are roughly in agreement with these compositions. It seems probable that these phases are directly exsolved by the olivine (possibly before the alteration has begun) when it is heated in an oxidizing atmosphere. Experiments to be described elsewhere have shown that a spinel phase can be developed within an olivine crystal in this way, though spinel phases in other orientations and entirely different products can also be obtained if the oxidizing conditions are too severe.

(e) *Silicate structures*

These structures are represented on the diffraction pattern in a manner more variable than any other phase identified in the "iddingsites."

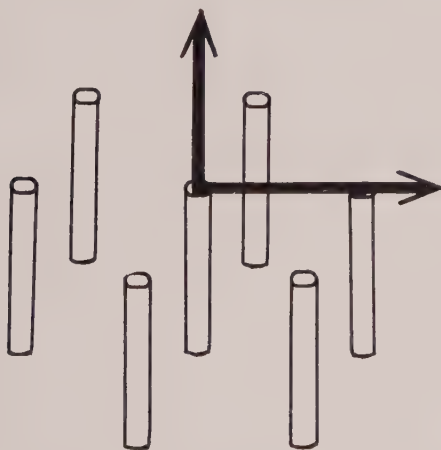


FIG. 1. Schematic representation of reciprocal space relationship between the hexagonal array of cylinders due to the silicate phase and the axes of the original olivine. (x-axis vertical, z-axis horizontal)

Brown and Stephen (1959) have described some of the characteristics of the pattern and have suggested that in their specimen a layer lattice silicate is present, probably belonging to the vermiculite or smectite group.

The diffraction effects may be considered in two parts. First, there occurs a hexagonal pattern of cylinders in reciprocal space (Fig. 1). The length of the cylinders is parallel to the x-axis of the original olivine; the side of the hexagonal "cell" marked out by these cylinders in reciprocal space is parallel to the z-axis of the original olivine. The "cell" side of the hexagonal array is slightly variable around a value of about 5.3 \AA . Along

the length of the cylinders, the intensity distribution, which is usually continuous, fades away sharply at about $\zeta=0.5$ for $\text{FeK}\alpha$ radiation. Radially the intensity falls away fairly quickly, so that rods with low ξ values are the only ones which are seen, unless fairly heavy exposures are made. The diameters of the rods in reciprocal space are variable from specimen to specimen, some even being relatively sharp. Others with relatively large diameter have a marked asymmetric intensity distribution, with a sharp cut-off on the low angle side. Diffraction effects of this general character seem to be present on most specimens containing a silicate phase; associated with them, however are low angle effects, which again show a marked degree of variability. Broadly these low angle effects fall into two categories. For the majority of specimens, there is a strong broad streak extending continuously from 70–80 Å down to about 10 Å, where it appears to tail off; the streak probably extends to even higher spacings than have been experimentally detected, for it shows no sign of diminished intensity at the limit of the present experimental observation. The streak extends in the x -direction of the olivine, and is thus parallel to the hexagonal array of cylinders. However for a few specimens, although the continuous streak still remains it appears to be considerably diminished in intensity, and fades away in the region 20–30 Å; intensity maxima, at times not very well defined, are then found at spacings of about 14–15 Å, with higher orders of this reflection also present.

The specimen described by Brown and Stephen (1959) gives a pattern showing both the hexagonal cylinders and sharp basal spacings. These authors suggest that the diffraction effects are due to the formation of a sheet silicate structure with a highly disordered stacking of the layers; the collapse of the basal spacing to ~ 10 Å by heating at 500° C. for one hour indicates that the sheet silicate may belong to the vermiculite or smectite groups. However, the variability of the diffraction patterns of this phase, identified in the present study, in which very few "iddingsites" seem to have developed a basal spacing, and the chemical evidence to be given in a later section suggest that it is highly speculative to attempt to identify this phase with any recognized sheet silicate group. The diffraction patterns showing only the continuous low angle streak could be interpreted as being due to effectively two-dimensional crystals of the silicate phase; rough calculations from the extent of the cylinders and streaks in reciprocal space show that, if the particles of this phase are perfect, they are 50–100 Å in diameter, and about 5 Å thick. At the early stages of development, they represent an embryonic silicate structure, which has not achieved any three dimensional regularity; they are probably very variable in constitution. At this stage, too, the possibility must be considered that the embryonic silicate should not be regarded as a sheet silicate

structure at all, but rather as a random local linkages of chain and band structures (the development of oriented pyroxene structures from heat treated olivines will be described in another publication). The close packed oxygen framework of the olivine does not require severe atomic rearrangement to form the oxygen arrangement of chain, band or sheet silicate, whilst the Si atoms appear to have considerable freedom of migration during the alteration process, so that local concentration of Si atoms may form embryonic linked tetrahedra structures which do not conform to the ordered arrangements recognized in silicate minerals.

The occurrence of basal spacings of 14–15 Å for some specimens containing a silicate phase indicates that some three dimensional regularity of the silicate structure can be achieved. However, it is not certain whether this can be obtained under the conditions of alteration which lead to the disordered structures of the majority of specimens. Apart from its rarity of occurrence in specimens which can be said to be "iddingsitized" olivine, the silicate pattern with sharp basal spacings seems to be characteristic of material described by other workers as bowlingite, another alteration product of olivine. It is possible that the processes which alter olivine to "iddingsite" or bowlingite cannot be sharply distinguished, and that the specimens which show basal spacings should be described as being partly "bowlingitized." The silicate phase occurring in the pseudomorphs after olivine in Markle basalt (Smith, 1959) has a basal spacing of 14.5 Å and is considered by the author to be a true chlorite of the pennine series. These pseudomorphs are unusual in that they are reported to contain quartz, which is not detected at all in the present investigation. It seems unlikely that they could have formed solely by the process of "iddingsitization" defined by the present investigation; for the Markle pseudomorphs the effects of weathering may be important.

EXPERIMENTAL RESULTS AND CLASSIFICATION OF SPECIMENS

The results of the *x*-ray examination are summarised in Table 2; for each specimen, the phases identified are shown together with a brief comment on the diffraction patterns. While the patterns (Figs. 2 and 3) cannot be divided into rigid categories, these data, together with the optical and chemical data on the specimens of the first group, allow some inferences as to the structural changes taking place during the alteration process.

To trace out these changes, we shall confine discussion for the moment, to the first group of selected typical "iddingsites." In the first stages of alteration, the anion framework of the original olivine remains unchanged; initially the diffusion through this framework of the cations

TABLE 2. RESULTS OF X-RAY EXAMINATION

Specimen No.	Phases Present	Comments
G.133	O _S +G _D	Relative intensities of "olivine" effectively normal; very little "goethite."
V.3	O _D	Relative intensities of "olivine" effectively normal.
57303	O _D	Relative intensities of "olivine" effectively normal.
G.50	O _D +G _D +H _D	Very little "olivine" and hematite; marked discrepancies of relative intensities of "olivine" from normal.
11537	G _D +S _L +H _D	There are also sharp powder rings of "goethite."
FEAE 124	G _D +S _L +H _D	Only a trace of hematite.
X11 A	O _S +S _L +H _D +Sps	Specimen may contain unaltered olivine. Very little "silicate," with low angle streak barely visible. There are also powder rings of spinel phase.
87366	O _{S-D} +C _D	"Olivine" sharp in some specimens, diffuse in others; when diffuse, relative intensities incorrect, and small amounts "goethite" present.
303-I-15	G _S +S _L	"Goethite" poorly oriented and sharp.
303-I-17	G _D +S _L	
X18C	O _{S-D} +S _L +H _D	"Olivine" showing both sharp and diffuse spots within same single crystal specimen
DH 1378	O _D +S _B	"Olivine" has relative intensity discrepancies; "silicate" has basal basing of 14.1 Å.

Key to Table:

- O indicates olivine-like phase
- G indicates goethite-like phase
- S indicates silicate phase
- H indicates hematite phase
- Sp indicates spinel phase.

The subscripts S and D give some indication of whether the diffraction spots are sharp or diffuse; the subscripts L and B after the symbol S, indicate continuous low angle streak and basal spacing respectively.

only slightly changes the structure (G.133), though as the chemical reconstitution becomes more drastic, the structure becomes more and more distorted, and less and less like true olivine (V.3 and 57303). The presence of increasing numbers of hydroxyl ions (see next section) allows the formation locally in areas effectively denuded of silicon of increasing amounts of a goethite-like structure (G. 50); this phase may appear as hematite if at any time during or after the alteration process the goethite-like structure is dehydrated. At this stage it would not appear that there is any order in the arrangement of the silicon atoms remaining within the "iddingsite." As the goethite or hematite regions increase, local silicon concentrations increase to the point where they begin to organize into a

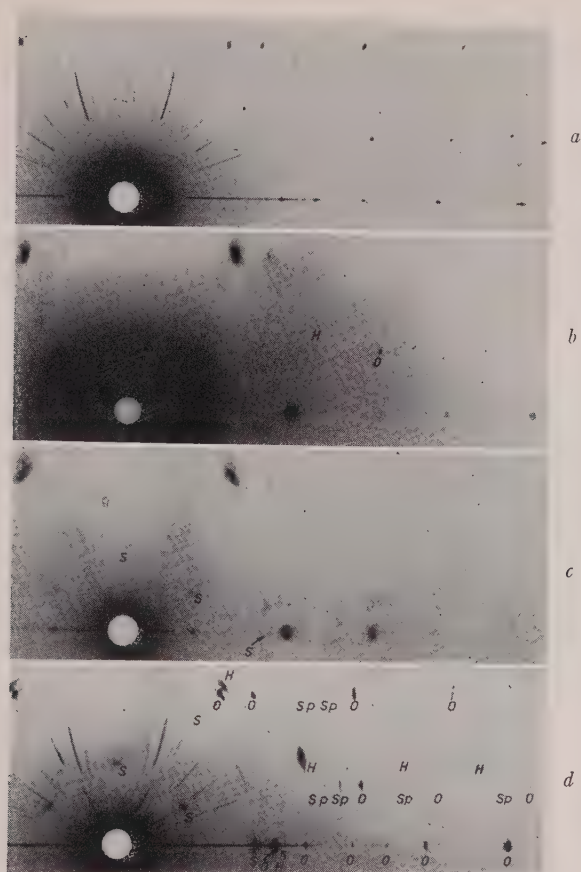


FIG. 2. X-ray diffraction photographs of "iddingsites." All the photographs are taken on camera of 3 cm. radius with $\text{FeK}\alpha$ radiation. The oscillation axis is in all cases the z -axis of the original olivine, the 15° oscillation range is symmetrically across the x -axis of the original olivine. Only a part of the photographs is shown (magnification $\times \frac{3}{4}$).

- (a) An unaltered olivine for comparison. Skaergaard Intrusion, East Greenland. EG 4265.
- (b) Specimen G.50, Gough Island. Some of the spots of the remaining olivine-like structure is labelled O, a weak hematite spot H. The formation of the "goethite-like" structure is shown by the diffuse regions almost coincident with "olivine" spots.
- (c) Specimen FEAE 124, Mount Moroto, Uganda. All spots other than those marked are due to "goethite" structure in three orientations. Spots marked S are due to silicate phase. In this specimen, diffraction spots due to hematite are barely visible.
- (d) Specimen X11A, Gough Island. Diffraction spots are marked as O, olivine-like, S, silicate, H, hematite, Sp, spinel. All rings belong to misoriented spinel structure, except for short spotty arcs which are due to misoriented olivine fragments.

kind of local order, with consequent rearrangement of the anion framework, this marks the appearance of the silicate phase (11537 and FEAE 124). So far as the specimens of the first group are concerned, this appears to denote the end of the alteration process. We cannot be certain whether specimens in which the silicate structure has gained some kind of three-dimensional regularity (as exemplified by the formation of a definite basal spacing) represent a further development of this particular alteration process or whether they have been formed by some different

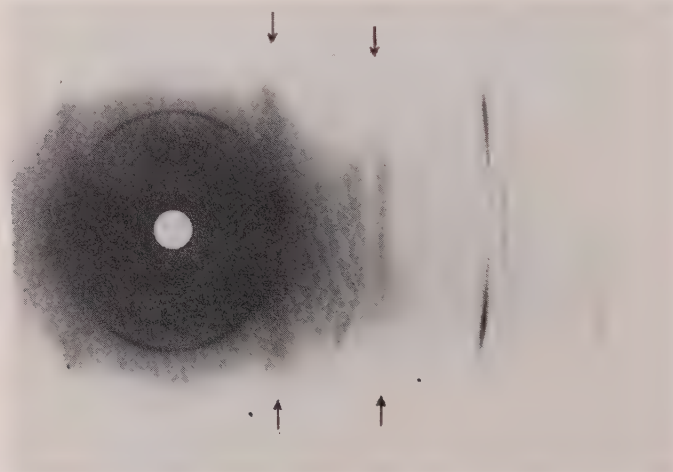


FIG. 3. Specimen 303-I-15, Carmelo Bay, Calif., Oscillation photograph, 3 cm. camera, FeK α ; oscillation axis, x -axis of original olivine, the 15° oscillation range is symmetrically across the z -axis of the original olivine. The sharp, poorly oriented preferred orientation pattern is due to "goethite." Note particularly the continuous blackened regions (arrowed) due to the silicate phase.

but related alteration; the limited chemical evidence given later can be interpreted as showing that specimens like 11537 and FEAE 124 will change little more.

Commenting briefly on the second group, it seems probable that in specimen X11A small regions of olivine have been "iddingsitized," leaving other regions of unaltered olivine. Reheating has then caused the dehydration of the "goethite" to hematite in the "iddingsitized" regions with the simultaneous precipitation of the spinel phase from the unaltered olivine regions. No. 87366 shows the early stages of alteration (like G.133 and V.3) which has been local, to give different degrees of alteration in different parts of the specimen. 303-I-15 and 303-I-17 are probably products of the same changes as the specimens of the first

group though other alteration products are also present in thin section; for 303-I-15, the structural control of the orientation of the products has been disturbed. X18C represents another example of local alteration, together with reheating of the specimen as evidenced by the hematite phase. DH 1378, in addition to the basal spacing, does not show either the "goethite" or hematite usually observed at the stage in alteration when a "silicate" phase is present, and must be regarded as anomalous.

The results can be summarized in the following manner. The structural changes involved suggest that the alteration process proceeds continuously through the various stages which are marked by the occurrence of poorly crystalline but characteristic phases. Individual specimens of "iddingsite" may differ from one another by being at different points of the structural change, though there may also be minor variations caused by different geological histories. We shall now examine chemical and optical data to see if they can be reconciled with a classification of this kind.

THE CHEMICAL COMPOSITION OF SOME OF THE "IDDINGSITES"

Two of the specimens of the first group, V.3 and G.50 were analyzed, and the analysis of a third, FEAE 124, was kindly supplied by K. Hytönen. These analyses are given in Table 3, together with the ideal composition of an olivine (Fa_{20}) approximating to the chemical composition before alteration. Qualitatively the changes involve a decrease in SiO_2 , FeO and MgO with an increase in Al_2O_3 , Fe_2O_3 and H_2O as the alteration process proceeds. It is interesting also, as first pointed out by Lawson (1893), that small quantities of CaO , Na_2O and K_2O enter the "iddingsite."

In Fig. 4 the proportions of the major constituents of the olivine and the three "iddingsites" have been plotted against their β refractive indices. It is seen that MgO , Fe_2O_3 and Al_2O_3 all show a reasonably smooth variation, whilst SiO_2 and Al_2O_3 vary rather more irregularly. If it is assumed that the chemical process is essentially one of addition of Fe_2O_3 and removal of MgO from the original olivine, the end product of the "iddingsitization" process would have a composition corresponding to the removal of all the MgO . On this assumption it is possible to derive an approximate composition for the hypothetical end product of $\text{SiO}_2=16\%$, $\text{Al}_2\text{O}_3=8\%$, $\text{Fe}_2\text{O}_3=62\%$ and $\text{H}_2\text{O}=14\%$, with a corresponding β refractive index of just over 1.9. The x-ray data suggests that this bulk composition must be interpreted in terms of goethite-like and silicate structures. If the bulk composition is rewritten in terms of atoms it is

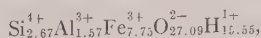


TABLE 3. CHEMICAL ANALYSES OF "IDDINGSITES"

	1	2	3	4
SiO ₂	39.3	37.9	25.59	17.52
TiO ₂	—	0.7	0.61	0.42
Al ₂ O ₃	—	5.6	6.53	8.00
Fe ₂ O ₃	—	20.7	31.44	55.09
FeO	18.9	3.3	4.64	0.00
MnO	—	n.d.	n.d.	0.45
MgO	41.8	24.0	15.83	2.73
CaO	—	3.6	1.30	1.29
Na ₂ O	—	n.d.	0.31	0.18
K ₂ O	—	n.d.	0.28	0.31
H ₂ O ⁺	—	4.2	9.09	13.74
H ₂ O ⁻	—		3.74	
Total	100.0	100.0	99.36	99.73
R.I. (β)	1.694	1.766	1.816	1.885

1. Ideal composition of olivine (Fa₂₀).
2. Specimen V.3. Nepheline bearing olivine basalt, Vogelsberg, Germany. Analyst R. W. LeMaitre. (The "iddingsite" was taken into solution with HCl from a mixture containing pyroxene. The H₂O was determined on the mixture assuming zero water content of the pyroxene.)
3. Specimen G.50. Trachybasalt, Gough Island. Analyst: R. W. LeMaitre.
4. Specimen FEAE 124. Pyroxene trachyte, Mt. Moroto, Uganda. (Hytönen, 1959). Analyst: P. Ojanperä.

it is clear that the hydrogen content is very high. The ratio of the number of hydrogen ions to the number of oxygen ions present in the silicate can be fixed between two limits. If all the Fe³⁺ ions are associated with the goethite-like phase, an upper limit of 0.67 for this ratio is derived for the

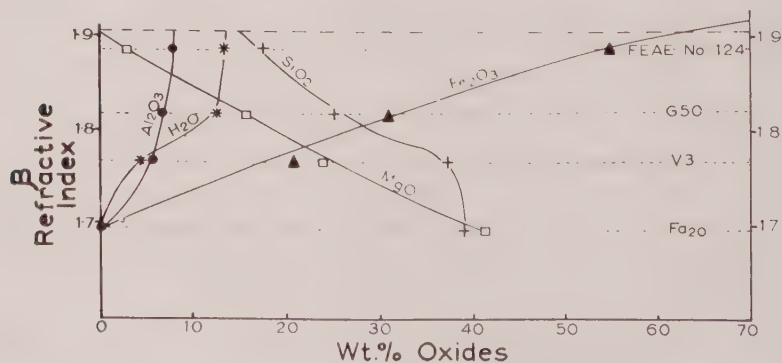


FIG. 4. The relation between the major chemical constituents of an olivine (Fa₂₀) and the three analyzed "iddingsites" and the value of the β refractive index.

silicate phase; on the other hand, if the equally unlikely assumption is made that no goethite-like phase is present, the lower limit of the H^+/O^{2-} ratio for the silicate phase is about 0.57. Now for most recognized sheet silicate minerals this ratio is usually well below 0.5; only for partially hydrated halloysite does it have the high values of the highly altered "iddingsites." While it is undoubtedly possible to express this bulk composition in terms of a recognized mineral assemblage such as goethite and a hydrated halloysite, the authors must stress that this does not mean that recognizable or even identifiable areas of a hydrated halloysite exist within the "iddingsite." All the data suggest that the silicate structure is very irregular and disordered and should not be equated, at this stage of alteration at least, with any recognized mineral species. Whether the development of a basal spacing leads to a more regular and recognizable silicate structure merits further investigation. The data of Brown and Stephen (1959) on the properties of the phase are to be resolved.

OPTICAL PROPERTIES

Some of the characteristic optical properties of the first group of typical "iddingsites," is given in Table 4. The most notable feature is the increase in the β refractive index as the alteration proceeds; this is also ac-

TABLE 4. OPTICAL PROPERTIES OF "IDDINGSITES" OF THE FIRST GROUP

Specimen No.	Depth of alteration (mm.)	Color	Pleochroism	Cleavage	Amount of alteration	Dispersion	Other alterations	R.I. (β)
133	0.2	Red-brown to orange-brown	Slight	None	Partial	—	None	1.76 ± 0.01
13	0.2	Orange-brown	Slight	None	Partial	—	None	1.766 ± 0.003
1303	0.3	Orange-brown	Slight	None	Partial	—	None	1.762 ± 0.005
550	0.5	Red-brown to orange brown	Slight	None	Complete	—	Feldspar analcitized	1.816 ± 0.003
537	0.4	Deep ruby-red to orange-red	Moderate, maximum absorption parallel to cleavage	Micaceous	Complete	Strong	Calcite and chlorite present	1.86 ± 0.01
EAE 124	0.5	Orange-red	Moderate	None	Complete	Very strong $r > v$	Amygdales and slight alteration of feldspar	1.885 ± 0.005

accompanied by an increase in the total birefringence and dispersion. The color in plane polarized light is almost the same at all stages, though there is a tendency for it to be darker in the later stages of alteration, where the pleochroism, though never marked, is stronger. Where "iddingsite" and olivine are present in the same crystal it is always found that their optic orientations are identical.

The development of the micaceous cleavage, characteristic of the material from Carmelo Bay described by Lawson (1893), does not appear to be diagnostic of the late stages of alteration. It is interesting to note that when the micaceous cleavage is developed (as in the material of Brown and Stephen (1959) and some specimens of Ross and Shannon (1925)), the refractive indices are considerably lower than would be expected; it appears that this lowering of refractive indices is to be correlated with the development of a basal spacing in the silicate. Since these "iddingsites" are often accompanied by other ill-defined alteration products of olivine, it is difficult to be certain if such effects are to be regarded as part of the process of "iddingsitization."

THE ALTERATION PROCESS

From the evidence presented, it seems clear that the mechanism for the alteration of olivine to "iddingsite" is one of ionic diffusion. As with the hydration of dicalcium silicate (personal communication, Dr. J. D. C. McConnell), under suitable conditions of temperature, pressure and chemical environment, highly mobile hydrogen ions can diffuse into the olivine structure. By temporary attachment to the oxygen ions, they are capable of releasing magnesium, ferrous and silicon ions from their sites in the olivine structure, and allowing their replacement by ferric, aluminum and calcium, etc., ions, provided that suitable concentration gradients exist across the boundary.

The structural changes involved are only slight. For some of the phases recognized, only cation changes are needed; for the others, only slight rearrangement of the essential oxygen framework is necessary. The continuity of the oxygen framework throughout the "iddingsite" and the short range order of the cations could undoubtedly account for the optical homogeneity of most of the "iddingsites" (see Brown and Stephen, (1959)). It must be emphasized again that this alteration process represents another example of the ability of silicon ions to diffuse fairly readily from their tetrahedral sites in the oxygen framework, and shows that in consideration of transformations in silicate structure, the SiO_4 tetrahedra cannot always be regarded as rigid units of structure (cf. Taylor (1957)).

The conditions under which the alteration takes place are still a matter for some speculation, except for the pressure, which can be assumed to be relatively low (see however Sun (1957)), as "iddingsite" is confined to volcanic and hypabyssal rocks. So far as the temperature of formation is concerned, considerable evidence has been accumulated which suggests that the alteration took place in the deuteric stage, before consolidation of the magma (Edwards (1938), Ross and Shannon (1925)). Rims of fresh olivine mantling "iddingsite," which have been observed by Edwards, can also be seen in some of the basaltic rocks from Gough Island and imply that the "iddingsite" formed before the olivine finished crystallizing. However it seems unlikely that a crystal with small domains of "goethite" and "silicate" structures, having a relatively high free energy, would be stable at high temperatures; it would tend to reorganize itself into a more ordered structure. It can only be concluded that "iddingsite" is formed at intermediate temperatures, below those necessary for structural reorganization, and above those at which the rock has completely solidified. The chemical environment is undoubtedly one of strong oxidizing conditions, with most of the iron in the ferric state, Fe^{3+} , but the suggestion by Edwards (1938) that the magma must differentiate to give an iron-rich liquid cannot be completely valid, for "iddingsite" occurs in many non-iron enriched basaltic rocks. The formation of "iddingsite" with a high Fe^{3+} content requires only the oxidizing conditions and does not necessarily imply the presence of an iron-rich liquid.

During the present investigation attempts to synthesize "iddingsite" from olivine in iron-rich, aqueous and acid solutions, at temperatures up to 600°C . and pressure up to 1000 atmospheres, were unsuccessful. When alteration rims were produced, x-ray examination showed they were of the serpentine type.

In conclusion, it must be made clear that "iddingsite" is not a mineral with a definite structure and chemical composition as implied by Ross and Shannon (1925); neither can it be regarded, as other workers have done, as a simple sub-microscopic intergrowth of two or more well characterized minerals. "Iddingsitization" is a continuous transformation in the solid state, during which the original olivine crystal may pass through various stages of structural and chemical change; it may be possible at any stage to recognize embryonic structural arrangements, some of which approximate to normal ordered mineral structures, but the altered olivine is at all times a disordered, irregular arrangement which cannot be described as a simple sub-microscopic mineral intergrowth. In view of these difficulties it is proposed that the term used for any member of the alteration series should be written "iddingsite."

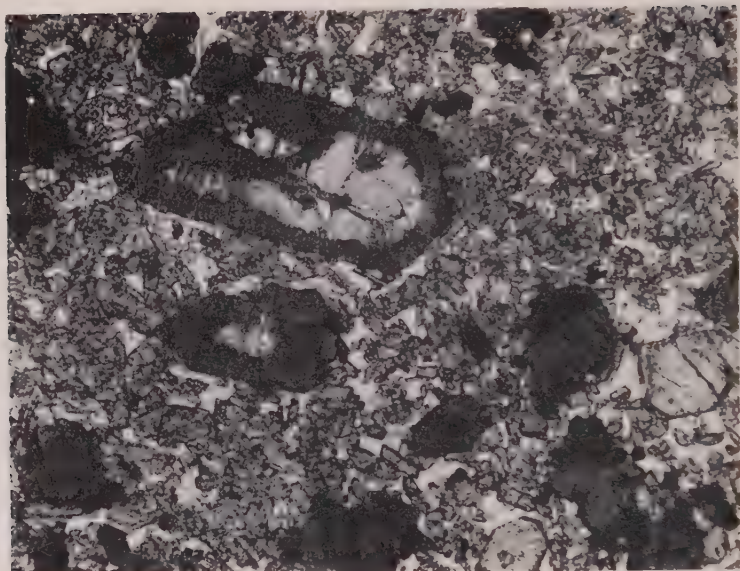


FIG. 5. Photomicrograph of a typical "iddingsite" in a basic lava. Specimen V.3, Vogelsberg, Hesse, Germany. Ordinary light, magnification $\times 65$.



FIG. 6. Photomicrograph of an olivine exsolving iron ores. Specimen X11A, Gough Island. Note the difference in appearance between this and the "iddingsite" shown in Fig. 5. Ordinary light, magnification $\times 65$.

ACKNOWLEDGMENTS

The authors wish to express their thanks to Professor C. E. Tilley, F. R. S., for his encouragement throughout this work. They are also indebted to Dr. J. D. C. McConnell for many helpful discussions. Specimens and other data were kindly provided by Dr. S. O. Agrell, Dr. K. Hytönen, Mr. D. McKie, and Dr. P. Quensel.

Mr. K. O. Rickson took many of the x-ray photographs. The work was carried out while one of the authors (R. W. LeM.) was in receipt of a maintenance award from the Department of Scientific and Industrial Research.

REFERENCES

- BELOV, N. V., BELOVA, E. N., ANDRIANOVA, N. H. AND SMIRNOVA, P. F., 1951, Determination of the parameters in the olivine (forsterite) structure with the harmonic three-dimensional synthesis: *Dokl. Akad. Nauk. SSSR*, **81**, 399-402.
- BROWN, M. G., AND GAY, P., 1959, Identification of Oriented Inclusions in Pyroxene Crystals: *Am. Mineral.*, **44**, 592-602.
- BRAGG, W. L. AND BROWN, G. B., 1926, Die struktur des olivine: *Zeits. für. Krist.*, **48**, 538-556.
- BROWN, G. AND STEPHEN, I., 1959, A structural study of iddingsite from New South Wales, Australia: *Am. Mineral.*, **44**, 251-260.
- EDWARDS, A. B., 1938, The formation of iddingsite: *Am. Mineral.*, **23**, 277-281.
- HYTÖNEN, K., 1959, On the petrology and mineralogy of some alkaline volcanic rocks of Toror Hills, Mt. Moroto, and Morulinga in Karamoja, N. E. Uganda: *Bull. Comm. Geol. Finland*, **184**, 75-132.
- LAWSON, A. C., 1893, The geology of Carmelo Bay: *Bull. Dept. Geol. Univ. Calif.*, **1**, 1-59.
- MING-SHAN SUN, 1957, The nature of iddingsite in some basaltic rocks of New Mexico: *Am. Mineral.*, **42**, 525-533.
- QUENSEL, P., 1952, Additional comments on the geology of Juan Fernandez Islands: *Nat. Hist. Juan Fernandez and Easter Island*, **1**, 37-87.
- ROSS, C. S. AND SHANNON, E. V., 1925, The origin, occurrence, composition and physical properties of the mineral, iddingsite: *Proc. U. S. Nat. Mus.*, **67**, 1-19.
- SMITH, W. W., 1959, Pseudomorphs after olivine in Markle basalt: *Min. Mag.*, **32**, 324-331.
- TAYLOR, H. F. W., 1957, Summarised proceedings of a conference on x-ray analysis—Cardiff, April, 1957: *Brit. J. Appl. Phys.*, **8**, 431-432.
- WIDMARSH, W. G., 1932, The Permian lavas of Devon: *Quart. J. Geol. Soc.*, **88**, 712-775.
- VILSHIRE, H. G., 1958, Alteration of olivine and orthopyroxene in basic lavas and shallow intrusions: *Am. Mineral.*, **43**, 120-147.

Manuscript received April 8, 1960.

SYNTHESIS AND ORIGIN OF CHALCEDONY*

J. F. WHITE AND J. F. CORWIN, *Departments of Geology
and Chemistry, Antioch College Yellow Springs, Ohio.*

ABSTRACT

Synthetic chalcedony has anomalous properties similar to those of natural chalcedony. These properties have been explained by submicroscopic holes and inferred disordered regions between fiber interfaces. The properties and origin of synthetic chalcedony are compatible with these concepts.

The chalcedony was made by transformation of solid silica in the presence of hydrothermal solutions at moderate temperature and pressure. Chalcedony was not directly precipitated from solution, but formed only by transformation of silica glass or cristobalite. In general, no conversion took place in slightly acid solutions, while complete, rapid conversion occurred in slightly alkaline solutions. The transformation proceeds indirectly by way of cristobalite and keatite.

Chalcedony is regarded as a secondary, metastable, transitional phase. The peculiar properties differentiating chalcedony from ordinary quartz may be a result of nucleation and growth in solid material (silica glass, opal, silica gel, or cristobalite).

INTRODUCTION

Chalcedony has certain distinguishing properties such as low, variable refractive indices and fibrous appearance or undulose extinction. In addition, it is commonly brown in transmitted light, biaxial, chemically more reactive than quartz, and shows suppression of the low-high transition of quartz as commented on by Peltó (1956), Hoss (1957), and Tuttle and Keith (1952). In this paper, the term chalcedony is restricted to material with the quartz structure but with refractive indices less than those of quartz. This essentially follows Peltó (1956). The term "chalcedonic quartz" probably should not be used for chalcedony, but can be conveniently used for textural varieties of quartz which look like chalcedony; e.g., fibrous quartz which has the refractive indices of quartz.

In previous work, a chalcedonic variety of GeO_2 (quartz type), which was analogous to chalcedony, was produced hydrothermally (White, Shaw, and Corwin, 1958). Probably, the first acceptable synthesis of chalcedony was by Nacken (1948) who discussed the laboratory preparation of chalcedonic, geode-like structures and their bearing on the origin of agates.

SYNTHETIC CHALCEDONY

Description and Comparison with Natural Chalcedony

The synthetic material, shown in Fig. 1, consists of microscopic, fibrous, fan-shaped aggregates which appear similar to natural chalced-

* Summary in "Synthetic Chalcedony," Nov. 1959 meeting Geol. Soc. Am., Pittsburgh, Pa.

ony. The fibers range from approximate parallelism to strongly divergent groups. Most of the fiber groups show straight extinction, but some have inclined and undulose extinction. The fiber groups are usually length-fast, but some are length-slow, and correspond to the variety quartzine. Commonly, one or the other predominates in a given concentric zone. The complexity is similar in natural chalcedonic materials as considered by Braitsch (1957). The birefringence is about that of quartz. Some of the material is biaxial, optically positive, with $2V$ about 25° . Jones (1952) reported optically positive chalcedony with $2E$ about 50° .



FIG. 1. Synthetic chalcedony showing texture, rhythmic banding, and gradation to quartz. Crossed nicols. $\times 25$.

Much of the synthetic material is concentrically banded (Fig. 1) with changes of color and texture perpendicular to the length of the fiber groups. Rhythmic banding is also commonly present. In transmitted light, the color ranges from colorless, to a distinct brown, to murky along the length of the fiber groups.

The refractive indices are variable, but are mostly in the range 1.51 to 1.52. Indices of some of the fiber groups are gradational along the length ranging from as low as 1.48 to 1.55. Measurements of refractive indices and their comparison to natural chalcedony and quartz are given in table I.

Folk and Weaver (1952) by using the electron microscope showed that water-filled submicroscopic holes, ranging from about .02 to .30 microns,

TABLE I. REFRACTIVE INDICES OF SYNTHETIC CHALCEDONY,
CHALCEDONY, AND QUARTZ

Synthetic Chalcedony	Chalcedony
	1.470 (heat-treated, Pelto, 1956)
n_1 1.48	
n_2 1.49	
n_1 1.50	
n_2 1.51	
n_1 1.51	
n_2 1.52	1.528 (heat-treated, Pelto, 1956)
n_1 1.53	1.530 (Winchell, 1951)
n_2 1.54	1.533-1.539
n_1 1.54	
n_2 1.55	
Synthetic Quartz	Quartz
ω 1.544	1.544
ϵ 1.553	1.553

are present in chalcedony, and that these can account for the low indices as well as the brown color. The refractive index was shown to vary in proportion to the abundance of holes. Later, Pelto (1956), showed that the brown color is due to holes of suitable size which result in preferential scattering of blue light. Pelto also suggested there should be no sharp break between quartz and chalcedony. In describing the synthetic germanium analogue of chalcedony, White, Shaw, and Corwin (1958) noted low refractive indices and gradual change up to those of the quartz form of GeO_2 . A relation between change in refractive index and color was also present. Synthetic chalcedony grades into ordinary quartz along with gradual changes in refractive index which in places accompany color changes.

The low-index material (Table I) is comparable to the heated natural material (Pelto, 1956) which develops a comparable range of indices and is as low as 1.47. Apparently upon heating, some of the water is lost and the index is lowered. A similar explanation appears reasonable for the low-index material which occurs in the central parts of the transformed glass and thus might contain less water.

X-ray powder patterns of the chalcedonic material indicate almost

pure quartz, but lines indicating minor amounts of cristobalite and keatite (Keat, 1954) are present in many samples.

CONDITIONS OF ORIGIN

Silica glass, or in some experiments cristobalite, was placed in a 250 ml., stainless-steel autoclave containing 125 ml. of water solution of usually 0.025 N salt concentration. The pH of the solutions was varied in different experiments from about 3.5 to 12 by adding HCl or NaOH. The temperature, pressure, and time were respectively 400° C., 340 atm., and usually 48 hours, although longer and shorter runs were also made. De-

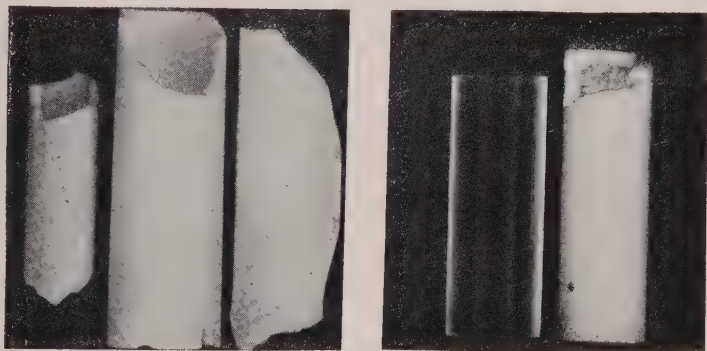


FIG. 2 (left). Glass tubing completely converted to chalcedony and quartz. Diameter of large tube 1.5 mm.

FIG. 2 (right). Unconverted glass rod on left. At right, partially replaced rod with unconverted core. Diameter of rods 13 mm.

tails of the equipment and procedure have been given by Swinnerton, Owen, and Corwin (1949) and Yalman and Corwin (1957). The silica was silica glass tubing and rods, and "standard" and "hyflo super-cel" (Johns-Manville) which are processed natural silica. This material is cristobalite as shown by x-ray powder patterns. The glass was high purity silica glass made by Thermal American Fused Quartz Co., transparent, one-half inch diameter. In some experiments, a quartz seed was also present.

Examination of the autoclave after a run generally showed crystalline material in one or more of the following places: on the quartz seed, on the walls of the autoclave, and as a replacement of original silica. Petrographic study of the material deposited on the walls of the autoclave and on the seed revealed in 30 samples the common presence of quartz or cristobalite, but no chalcedony. In contrast, the glass or cristobalite was commonly converted to chalcedonic quartz and chalcedony. In many cases glass tubing and rods maintained their original shape after conversion (Fig. 2).

A sequence of concentric layers is commonly shown by the converted silica (Fig. 3). When fully developed, the sequence from the outer surface inward is fibrous quartz, chalcedony, keatite, a thin zone of cristobalite, and finally a glass core if conversion is not complete. In detail, the cristobalite-glass contact is made up of hemispherical lobes of cristobalite directed into the glass. Identification is based on presence of cristobalite lines in the powder patterns, refractive index of 1.49, isotropic character, and assumed silica composition. The results are similar to those of Carr and Fyfe (1958), who found that the conversion of amorphous silica proceeded by way of cristobalite, keatite, and quartz. Similarly in the pres-

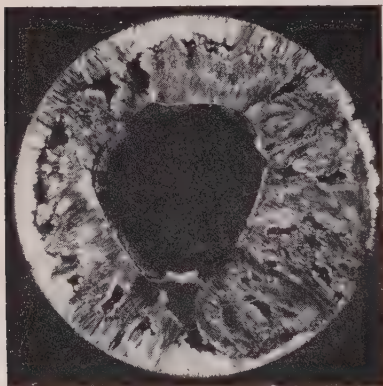


FIG. 3 (left). Cross section showing concentric layers of fibrous quartz, chalcedony, keatite, cristobalite and glass core. Growth proceeded from outer surface inward. Crossed Nicols. Diameter 13 mm.

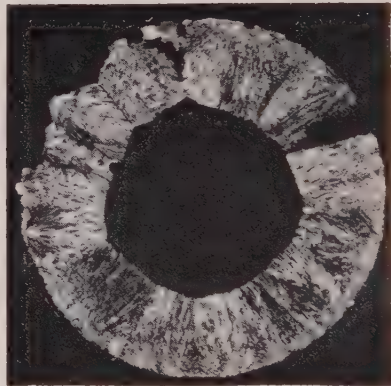


FIG. 3 (right). Cross section of partially converted silica rod. Note radial fibrous texture and growth centers on outer surface. Core is glass. Crossed nicols. Diameter 13 mm.

ent work, the transformation proceeded as follows: *glass*—*cristobalite*—*keatite*—*chalcedony*—*quartz*.

Although chalcedony formed only by conversion of solid material, the character of the hydrothermal solutions determined whether the replacement or transformation would or would not take place under the given conditions of time, temperature and pressure. In pure water or very dilute acids, no reaction occurs. However, in very slightly alkaline solutions, the reaction is rapid and complete. This is in general agreement with Nacken (1948), and a similar control has been noted in experiments on the growth of quartz by precipitation from solution, *e.g.*, Yalman and Corwin (1957). A summary of data from 30 experiments pertaining to the influence of hydrothermal solutions and in particular the effect of pH on the presence or non-presence of chalcedony is given in Table II.

NATURAL CHALCEDONY AND CHERT

Conditions of Origin

It is known that natural chalcedony forms under near surface conditions at low temperatures. These conditions are restricted to sedimentary and low-temperature hydrothermal environments. Further well recognized features are the common and widespread association with opal and similar material and the conversion of opal to chalcedony (Pettijohn,

TABLE II. HYDROTHERMAL SOLUTIONS AND THE PRESENCE OR NON-PRESENCE OF CHALCEDONY

Number of Experiments	Solution	pH _f *	Product
4	Pure H ₂ O	6.0-7.5	Glass. No change in source material
3	HCl, .025 N	6.7-7.5	
2	MgCl ₂ , .025 N	4.0-4.5	
2	BaCl ₂ , .025 N	4.0	
2	BaCl ₂ , .025 N + Ba(OH) ₂ to pH 10	4.0	
2	BeF ₂ , .025 N	3.5	
3	KOH, .025 N	10.3	Chalcedony and Quartz. Replacement of original glass
4	NaOH, .025 N	10.2	
6	NaCl, .025 N + NaOH to pH 10	8.0-9.0	
2	NaF, .025 N	5.0-8.0	

Source material—silica glass. Temp. 400° C.; Pressure 340 atm.; Time 48 hrs.

* pH_f is the final pH (measured).

1957; Barth, 1952; Williams, Turner, and Gilbert, 1954; White, 1955; Pittman, 1959; and others). The experimental data support and complement these observations.

Although chalcedony and quartz were formed rapidly at 400°, petrographic examination shows chalcedony is being converted to fibrous quartz and cannot persist. This was confirmed by longer runs (96 hours) which showed only fibrous quartz. From a consideration of solubility data (Kennedy, 1950) such transformations should take place at temperatures as low as about 300°, but below about 250° the recrystallization would be appreciably slower. That the critical temperature of water is not a factor is shown by the formation of the germania chalcedony (White, Shaw, and Corwin, 1958) at 200° C. Also Carr and Fyfe (1958) observed complete conversion of amorphous silica to quartz at 250° C. in a few hours in the presence of dilute alkaline solutions. Thus, an upper

limit for the formation and persistence of chalcedony is suggested at about 300°. Concerning the lower limit, it has not been possible to grow quartz at temperatures below 100° C. This is also in line with natural occurrences, opal being the mineral present at lower temperature. White (1955) noted the rarity of opal in hot spring deposits at temperatures greater than 100°; its place being taken by chalcedony and quartz. White, Brannock, and Murata (1956) observed that opal probably forms at temperatures as high as 140° C. but is unstable and changes to chalcedony or quartz. Thus a temperature of formation on the order of 100–300° C. is indicated for chalcedony.

Pressure may be more important than temperature in controlling the occurrence of chalcedony. The important effect of pressure on the transition of amorphous silica to quartz has been demonstrated by Carr and Fyfe (1958). The pressure factor would restrict chalcedony to shallow depths.

In the formation of both synthetic and natural chalcedony, water solutions are necessary. Further, the nature of the solution seems to be of critical importance in determining whether chalcedony and quartz will form in a given time interval, or whether amorphous silica or cristobalite will persist. While many different ions may affect the rate of transformation, the experimental data suggest the presence or absence of chalcedony and secondary quartz in opaline, near-surface deposits may be primarily dependent on solutions of appropriate pH.

Flörke (1955), Hoss (1957), and others consider that much opal is essentially disordered low-cristobalite. In a study of cherts, Hoss concludes that the sequence of changes is probably: amorphous silica (or opal), to cristobalite, to chalcedony (or microcrystalline quartz). Braitsch (1957) describes natural examples of the apparent conversion of cristobalite to chalcedony, and notes silica gel may change to cristobalite-opal or directly to chalcedonic material, or in some instances cristobalite-opal later changes to chalcedony. The experimental results are similar but suggest keatite also may be found associated with opal and chalcedony.

This study supports the concept that most chalcedony and chert are secondary products and require the former presence of gelatinous silica, silica glass, opal or cristobalite. The extensive work on transport and precipitation of silica by Krauskopf (1956, 1959) is in agreement with these conclusions.

In the conversion, quartz may crystallize with submicroscopic holes because of negative volume change. Disordered regions between crystallite interfaces also might be expected. Nucleation and growth, as shown by the synthetic chalcedony, would generally start from a surface and proceed to other parts of the material producing the typical fibrous and radial textures.

REFERENCES

- BARTH, TOM, F. W., 1952, *Theoretical Petrology*: John Wiley & Sons, New York.
- BRAITSCH, OTTO, 1957, Über die natürlichen Fasen- und Aggregationens-typen beim SiO_2 , ihre Verwachsungsformen, Richtungsstatistik und Doppelbrechung: *Heidelbg. Beitr. Mineral. u. Petrogr.*, **5**, 331-372.
- CARR, R. M. AND FYFE, W. S., 1958, Some Observations on the Crystallization of Amorphous Silica: *Am. Mineral.*, **43**, 908-916.
- FLÖRKE, O. W., 1955, Zur Frage des Hoch-Cristobalit in Opalen, Bentoniten, und Gläsern: *Neues Jahrbuch für Mineralogie, Mh.*, H **10**, 217-223.
- FOLK, ROBERT K. AND WEAVER, CHARLES EDWARD, 1952, A Study of the Texture and Composition of Chert: *Am. Jour. Sci.*, **250**, 489-510.
- HOSS, H., 1957, Untersuchungen über die Petrographie kulkmischer Kieselschiefer: *Beiträge zur Min. u. Petrog.*, **6**, 59-88.
- JONES, FRANCIS T., 1952, Iris Agate: *Am. Mineral.*, **37**, 578-587.
- KEAT, PAUL B., 1954, A New Crystalline Silica: *Sci.*, **120**, 328.
- KEITH, M. L. AND TUTTLE, O. F., 1952, Significance of Variation in the High-Low Inversion of Quartz: *Am. Jour. Sci.*, *Bowen Volume*, **250**, 203-280.
- KENNEDY, GEORGE C., 1950, A Portion of the System Silica Water: *Econ. Geol.*, **45**, 629-653.
- KRAUSKOPF, K. B., 1956, Dissolution and Precipitation of Silica at Low Temperatures: *Geochim. Cosmochim. Acta*, **10**, 1-26.
- KRAUSKOPF, K. B., 1959, The Geochemistry of Silica in Sedimentary Environments: Silica in Sediments, Soc. Econ. Paleon. and Mineralogists, Am. Assoc. Petroleum Geologists, 4-19.
- LACKEN, R., 1948, Über die Nachbildung von Chalcedon-Mandeln: *Natur und Volk*, **B**, 78, 2-8.
- MELTO, CHESTER R., 1956, A Study of Chalcedony, *Am. Jour. Sci.*, **254**, 32-50.
- PETITJOHN, F. J., 1957, *Sedimentary Rocks*: 2nd Edition, Harper and Bros., New York..
- PITTMAN, J. S., JR., 1959, Silica in Edwards Limestone, Travis County, Texas: Silica in Sediments, Soc. Econ. Paleon. and Mineralogists, Am. Assoc. Petroleum Geologists, 121-134.
- WINNERTON, A. C., OWEN, G. E., AND CORWIN, J. F., 1949, Some Aspects of the Growth of Quartz Crystals: *Disc. Far. Soc.*, **5**, 172-180.
- WHITE, DONALD E., 1955, Thermal Springs and Epithermal Ore Deposits: *Econ. Geology, Fiftieth Anniversary Volume*, Part I, Bateman, editor, 99-154.
- WHITE, D. E., BRANNOCK, W. W., AND MURATA, K. J., 1956, Silica in Hot-Spring Waters: *Geochim. Cosmochim. Acta*, **10**, 27-59.
- WHITE, J. F., SHAW, E. R., AND CORWIN, J. F., 1958, A Chalcedony-like Variety of Germania: *Am. Mineral.*, **43**, 580-584.
- WILLIAMS, HOWELL, TURNER, FRANCIS J., AND GILBERT, CHARLES M., 1954, *Petrography*: Freeman and Company, San Francisco.
- WINCHELL, ALEXANDER N. AND WINCHELL, HORACE, 1951, *Elements of Optical Mineralogy*, Part II. Description of Minerals: 4th Edition, John Wiley & Sons, Inc., New York, New York.
- ALMAN, RICHARD G. AND CORWIN, JAMES F., 1957, Hydrothermal Reactions under Supercritical Conditions, III—The Effect of pH on the Crystallization of Silicon Dioxide: *Jour. Phy. Chem.*, **61**, 1432-1437.

Manuscript received March 5, 1960.

FLUORESCENT X-RAY SPECTROGRAPHIC ANALYSES OF AMPHIBOLITE ROCKS

A. A. CHODOS, *California Institute of Technology, Pasadena, Calif.*

AND

CELESTE G. ENGEL, *U. S. Geological Survey, University of
California, La Jolla, Calif.*

ABSTRACT

Fluorescent x-ray spectrographic analyses have been made for the oxides Fe_2O_3 , CaO , MgO , K_2O , TiO_2 , and MnO on 27 samples of amphibolite rock. The amphibolites vary appreciably in mineralogical composition but all have a chemical composition approximating that of a saturated basalt. Variations in mineralogy are from hornblende-andesine amphibolites to two pyroxene-labradorite-hornblende gneisses with 0.2 to 5.0 per cent opaque minerals.

Mean deviations of the fluorescent x-ray spectrographic analyses from classical wet chemical analyses in per cent of the amount reported are: Fe_2O_3 , 3.1; CaO , 1.3; MgO , 3.0, K_2O , 3.2; TiO_2 , 3.2; and MnO , 7.7. Precision of the analyses is equivalent to, or better than, that achieved by wet chemical methods.

Preliminary work indicates equivalent precision can be obtained for most common rocks and minerals.

INTRODUCTION

This paper is a report on analytical studies of amphibolites (hornblende, plagioclase, pyroxene-bearing rocks) using fluorescent x-ray spectrographic analyses. An earlier report on these studies discusses the basic concept involved in fluorescent x-ray spectrographic analysis. Refinements have been made in equipment and the technique has been modified since that report (Chodos, Branco, and Engel, 1957).

Our studies are based upon the obvious need for a rapid, relatively inexpensive method of obtaining precise and accurate chemical analyses of rocks and minerals. Costs and time factors have resulted in a serious reduction in the number of analytical laboratories and of rocks and minerals analyzed by conventional chemical techniques. Moreover, in most analyses that employ classical techniques, neither the precision nor accuracy of the data can be estimated; and the recent studies of the rocks G-1 and W-1 have demonstrated the wide variations in values that may be reported for a given element in these rocks (Fairbairn, *et al.*, 1951). Attempts to reduce the time and costs of silicate analyses include the so-called "rapid" method of chemical analysis developed by Shapiro and Brannock (1952, 1956) and the emission spectrographic techniques formulated by Kvalheim (1947), Ahrens (1950), Dennen *et al.* (1951), Dennen and Fowler (1955), and others. Although the "rapid" method of chemical analysis is more rapid than classical procedures it remains a time consuming technique which requires an enormous amount of "dishwashing." The

mission spectrographic methods greatly reduce the time and costs of analyses but at too large a price in precision for the major elements.

The fluorescent x-ray spectrographic analytical methods employed in this study permit the rapid determination of total Fe, Mn, K, Ti, Ca, and Mg in rocks and minerals with a precision and accuracy as good as that obtained by a single analyst using classical chemical methods and better than the precision among a number of different analysts (*see* Fairbairn, *et al.*, 1951). The standard working curves used for the determinations have been established by using the values from wet chemical analyses by G. Engel. These analyses also included the rock W-1 so that both wet chemical analytical data and those obtained by fluorescent x-ray analyses might be keyed to the adjusted mean composition of W-1 (Fairbairn, 1953). This comparison is particularly significant because the composition of the rock W-1 is very close to the composition of the amphibolites under discussion.

Si and Al can be determined by the fluorescent x-ray method but with only limited success due to limitations in techniques and apparatus. Very probably, precise determination of Si and Al can be obtained by slight improvements of the methods we are using. Values for Na may be obtained quickly and with considerable precision by use of the flame photometer. Separate determinations are required for the ratio of ferrous to ferric iron and for total H_2O .

ROCK TYPE

The present work has been confined to amphibolites and pyroxenite-bearing "amphibolites" which have the chemical composition of many gabbros. In so doing we have eliminated those problems that are inherent in fluorescent x-ray spectrographic analyses of rocks of very diverse mineralogy, chemical composition, and texture. Actually any rock or mineral may be analyzed by the fluorescent x-ray technique but best results are obtained in analyses of a given rock or mineral for which standard working curves have been constructed.*

The range in chemical compositions of the amphibolites reported in this work are: Fe_2O_3 8–22%; CaO 7–13%; MgO 4–9%; K_2O 0.3–2.5%; Na_2O 1–3%; and MnO 0.12–0.35%.

Variations in mineralogical composition of the amphibolites are shown in Table 1. Modal analyses of these rocks are being published separately in a study of the progressive metamorphism of amphibolite rocks by Engel and Engel. In general, the specimens A 1EF, A 3A, A 4D, A 14B,

* We have also prepared standard working curves for quartz-biotite-oligoclase gneisses and for the minerals garnet, biotite, and hornblende, with results equivalent to those recorded in this paper.

TABLE 1. VARIATIONS IN MINERALOGICAL COMPOSITION OF AMPHIBOLITE ROCKS USED IN FLUORESCENT X-RAY SPECTROGRAPHIC AND CHEMICAL ANALYSES

Mineral	Range in volume per cent
Quartz	0 -16.9
Plagioclase*	15.2-57.5
Hornblende	12.4-69.6
Clinopyroxene	0 -31.6?
Orthopyroxene	0 -15.5?
Opaque minerals†	.2- 5.1
Biotite	0 -24.8
K-feldspar	0 - 3.8
Garnet	0 -11.4
Sphene	0 - 1.6

* Partly sericitized.

† Chiefly ilmenite, pyrite, and magnetite.

and A 15DE (Table 2) contain in volume per cent; hornblende 65, andesine 20, quartz 10, and opaque minerals 2. There are gradations in mineralogical composition between these rocks and the remaining specimens in Table 2 which contain as much as 40% combined ortho- and clinopyroxene and as little as 12% hornblende. Sample A 9A is a garnetiferous, pyroxene-rich "amphibolite" with about 11% garnet 35% ortho- and clinopyroxene, 17% hornblende and 28% plagioclase.

It is obvious from comparison of Tables 1 and 2 that these are far greater variations in the mineralogical composition of the amphibolites than in their chemical composition. Iron displays the largest variation in concentration and occurrence among the samples analyzed. Total Fe (as Fe_2O_3) varies from about 8 to 22 weight per cent in the amphibolites and is an important constituent in hornblende, clino- and orthopyroxene, biotite, garnet, ilmenite, pyrite, and magnetite. Despite this diversity in the crystallographic distribution of Fe, its concentration in the rock can be obtained rather precisely by the fluorescent x-ray spectrographic technique.

SAMPLE PREPARATION AND PARTICLE SIZE

All samples of amphibolites were reduced to -100 mesh as described elsewhere (Engel and Engel, 1958). These -100 mesh fractions were then split into two parts using a high purity aluminum micro-split. One part, of approximately 10 grams, was used for wet chemical analyses; the other fraction, about 5 grams, was ground to a very fine powder for use in fluorescent x-ray analyses.

TABLE 2. COMPARISON OF WET CHEMICAL AND FLUORESCENT
X-RAY SPECTROGRAPHIC ANALYSES OF AMPHIBOLITE ROCKS

The working curves shown in Fig. 1 to 6 were derived from the wet chemical analyses given in this table.

Sample	Type of Analysis	Oxide (weight per cent)					
		Total Fe as Fe ₂ O ₃	CaO	MgO	K ₂ O	TiO ₂	MnO
A 1EF	Chem.	14.30	9.83	6.59	1.66	1.58	.22
	X-ray	15.14	9.77	7.20	1.71	1.62	.25
A 3A	Chem.	13.14	11.27	7.21	.81	1.20	.23
	X-ray	13.69	11.26	7.40	.75	1.25	.23
A 4D	Chem.	12.53	9.47	7.57	2.29	1.07	.20
	X-ray	13.28	9.38	7.90	2.25	1.18	.24
	X-ray*	12.92	9.38	7.90	2.30	1.15	.24
A 14B	Chem.	19.21	8.93	4.76	1.85	2.64	.31
	X-ray	19.60	8.99	4.88	1.87	2.70	.31
A 15DE	Chem.	16.34	7.86	6.32	1.89	2.05	.24
	X-ray	15.98	7.87	6.58	1.92	2.06	.32
A 19A	Chem.	13.58	8.54	7.63	2.27	1.60	.27
	X-ray	14.61	8.43	7.73	2.34	1.63	.26
	X-ray*	13.90	8.34	7.66	2.37	1.52	.24
A 20A	Chem.	12.46	11.25	8.60	1.19	1.93	.20
	X-ray	12.76	11.25	8.60	1.17	1.86	.20
	X-ray*	12.25	10.96	9.10	1.73	1.80	.19
A 21	Chem.	12.88	9.84	7.14	1.67	1.20	.22
	X-ray	13.35	9.68	7.26	1.73	1.23	.24
	X-ray*	13.20	9.72	7.20	1.73	1.21	.24
A 65A	Chem.	10.59	7.96	3.72	1.38	1.57	.14
	X-ray	10.26	7.93	4.00	1.34	1.63	.13
A 67A	Chem.	10.91	12.77	6.85	.35	.99	.20
	X-ray	10.57	12.63	6.90	.37	1.06	.22
	X-ray*	10.42	12.45	6.91	.36	1.04	.22
A 68	Chem.	12.57	11.17	7.99	1.35	1.18	.20
	X-ray	12.23	11.09	8.13	1.40	1.21	.20
A 104	Chem.	13.57	11.68	7.36	.47	1.60	.25
	X-ray	13.79	11.73	7.16	.47	1.53	.23
	X-ray*	13.68	11.92	7.40	.47	1.53	.23
A 105	Chem.	13.78	11.96	7.43	.57	1.56	.25
	X-ray	13.76	12.72	7.10	.59	1.57	.24
A 10E	Chem.	14.40	11.92	7.46	.58	1.40	.25
	X-ray	14.24	11.95	7.48	.59	1.40	.23
	X-ray*	14.05	12.14	7.77	.78	1.39	.23
A 9A	Chem.	21.06	10.01	5.46	.41	2.73	.35
	X-ray	20.74	10.49	5.43	.44	2.72	.34
	X-ray*	20.81	10.67	5.53	.44	2.77	.35

Note: Mineralogical composition of the rocks is discussed in the text.

* A second split of the sample prepared by A. E. Engel and submitted under a different number to test reproducibility of x-ray methods.

Analyses obtained by fluorescent x-ray spectrographic techniques may be strongly biased by alternate methods of preparation of samples and by the size of constituent particles. Some of these problems have been discussed by Claisse (1956). Because mineralogical composition and surface homogeneity strongly influences the behavior of the sample during x-ray analysis, precision may be increased by very fine grinding. Many grinding problems are presented by different rock types. Minerals such as sulfides and quartz are brittle and powder rapidly; others, such as mica are flexible and resistant to grinding. When all of these minerals coexist in a rock, the resultant powder may show a wide range in particle size that can be correlated with mineral composition. Relatively coarse flakes of mica in a very fine powder of other minerals may induce errors in the analysis of mica-bearing rocks. Obvious analogies may be drawn from other rock types.

The data in Fe are instructive as an example of the relationship of grain size to precision of analyses of elements. Iron occurs in sulfides and silicates (including biotite). Analyses of biotitic amphibolites ground to successively finer fractions below -100 mesh size show an increase in the Fe/Ca intensity ratio which does not level off until the flakes of biotite can no longer be resolved at $\times 20$ magnification. The increase in the ratio Fe/Ca with increased grinding below -100 mesh is from 0.58 to 0.70.

All samples analyzed by the fluorescent x-ray spectrographic technique were ground in an automatic agate mortar until the entire sample appeared as a homogeneous powder at $\times 20$ magnification under a binocular microscope. Measurements indicate that the average grain size is about 15 microns and the maximum grain size does not exceed 45 microns. Most of the non-biotitic amphibolites could be ground to this approximate size in 2 to 4 hours. Biotitic amphibolites required from 4 to 10 hours of grinding to reduce the biotite to this size. Similar time requirements have been recorded for other mica-bearing rocks.

ANALYTICAL METHODS

Each sample of amphibolite analyzed by classical chemical methods and by x-ray fluorescent spectrographic methods was handled as an unknown prepared by A. E. Engel. At the outset 15 amphibolites were analyzed by C. G. Engel using analytical methods described in Engel and Engel, 1958. The precision of this analytical work was tested by the introduction of masked splits of the rock W-1 introduced as unknowns along with samples of amphibolites. The results of analyses of W-1 are tabulated in Table 3 and compared with the adjusted mean composition of the rock W-1. They indicate for the elements given the reproducibility of the silicate analyses by classical techniques and any major bias in the determina-

on of the elements relative to the presumed composition of the rock W-1. Inspection of the chemical analytical data in Tables 2 and 4 indicates that the elements, Fe, Ca, Mg, Ti, K, and Mn as determined in the amphibolite are accurate relative to the presumed concentration in the rock W-1. This analytical work suggests that the analyses of amphibolites by classical methods may be used to construct standard working curves for the fluorescent x -ray analytical studies.

Wet Chemical Analyses.—Determinations of CaO and MgO were done by conventional gravimetric methods employing a 1.0000 gram sample of

TABLE 3. REPLICATE CHEMICAL ANALYSES OF THE ROCK W-1 MADE WITH ANALYSES OF AMPHIBOLITES AND INDICATIVE OF PRECISION OF ANALYTICAL METHODS (Analyst, C. G. Engel)

Oxide	Date										Mean*	Mean deviation
	10/56	1/57	5/57	12/57	1/58	4/58	11/58	4/59	5/59	Mean		
O ₂	1.05	1.09	1.09	1.11	1.12	1.08	1.09	1.04	1.06	1.08	1.10	.02
Total Fe as Fe ₂ O ₃	10.80	10.74	10.84 10.76 10.88	10.86	—	10.65	—	10.84	—	10.80	11.17	.37
MnO	.17	.15	.16	.17	—	.17	.16	.17	.16	.17	.165	.00
TiO ₂	11.02	—	—	11.00	—	10.90	—	11.04	—	10.99	10.96	.03
K ₂ O	6.55	—	—	6.39	—	6.59	—	6.67	—	6.55	6.63	.08
CaO	.68 .69	.66	—	.66	—	.66	—	.64	.67	.67	.63	.04

* Arithmetic mean of replicate analyses by 35 laboratories of the rock W-1 (see Fairbairn, 1953, table 1, 146-147).

rock. This weight of sample was fused in Na₂CO₃ in a platinum crucible and the fusion was dissolved in HCl.

Total Fe (as Fe₂O₃), TiO₂, and MnO were determined on a 0.4000 gram sample dissolved in a platinum crucible on a steam bath in sulfuric and hydrofluoric acids. The resulting solution was increased to 200-ml. volume with distilled water. Aliquots were taken to determine Fe₂O₃*, TiO₂, and MnO on the Beckman Model B spectrophotometer using the methods described by Shapiro and Brannock (1956). Another aliquot of

* Analyses of total Fe as Fe₂O₃ made in this way were checked by 13 analyses with a ferri-reductor. In this method, iron from the R₂O₃ group, in a HCl solution, was reduced by passing the solution down a column of metallic silver. The determinations of Fe₂O₃ that need about 12 weight per cent that are made on the spectrophotometer require a saturated solution of orthophenanthroline. A 0.1% solution of orthophenanthroline is satisfactory where concentrations of Fe₂O₃ do not exceed about 12%.

TABLE 4. COMPARISON OF WET CHEMICAL AND FLUORESCENT X-RAY SPECTROGRAPHIC ANALYSES IN WHICH THE SAMPLES WERE RUN AS UNKNOWN FOR BOTH ANALYSTS

The analyses are of amphibolite rocks similar in chemical and mineralogical composition to those in Table 2.

Sample	Type of analysis	Oxide (weight per cent)					
		Total Fe as Fe ₂ O ₃	CaO	MgO	K ₂ O	TiO ₂	MnO
AE 317	Chem.	13.15	11.49	7.45	1.20	1.17	.23
	X-ray	13.20	11.37	7.77	1.23	1.23	.23
	X-ray*	13.17	11.29	7.48	1.22	1.23	.23
AE 326	Chem.	15.86	9.54	6.29	.94	2.05	.24
	X-ray	16.08	9.81	6.30	.94	2.14	.26
	X-ray*	16.10	9.84	6.48	.96	2.13	.26
AE 334	Chem.	16.49	9.74	6.32	.88	2.11	.29
	X-ray	16.40	9.84	6.45	.92	2.15	.25
AE 337	Chem.	15.98	9.54	6.51	.98	2.07	.27
	X-ray	16.00	9.76	6.40	.99	2.07	.27
AE 338	Chem.	15.63	9.71	6.04	.99	2.04	.25
	X-ray	16.20	9.84	n.d.	.95	2.04	.25
AE 320	Chem.	8.84	7.78	5.49	2.11	1.11	.15
	X-ray	8.60	7.67	6.20	2.05	1.27	.13
	X-ray*	8.64	7.58	6.00	2.06	1.27	.12
AE 411	Chem.	11.91	n.d.	n.d.	1.76	1.76	.12
	X-ray	11.80	8.40	5.67	1.66	1.77	.14
AE 414	Chem.	8.84	n.d.	n.d.	1.89	1.76	.12
	X-ray	8.74	7.10	5.40	1.92	1.28	.10
AED 404	Chem.	12.44	11.90	8.20	.60	.94	.22
	X-ray	12.18	11.98	8.04	.65	1.04	.20
AC 342	Chem.	15.67	10.65	6.99	.75	1.69	.24
	X-ray	15.60	10.79	7.00	.77	1.71	.25
AC 348	Chem.	14.78	11.46	7.40	.58	1.73	.24
	X-ray	14.67	11.65	7.34	.58	1.78	.23
	X-ray*	14.55	11.59	7.56	.59	1.77	.23
AC 362	Chem.	14.91	10.92	7.38	.47	1.66	.24
	X-ray	15.11	11.37	7.38	.47	1.74	.25
	X-ray*	14.95	11.21	7.14	.46	1.68	.25

Note: Mineralogical composition of the rocks is discussed in the text.

* A second split of the sample prepared by A. E. Engel and submitted under a different number, to test reproducibility of x-ray methods.

this same solution was used to determine K₂O and Na₂O on the Perkin-Elmer flame photometer.

Fluorescent X-Ray Spectrographic Technique. -The finely ground rock (or mineral) powder is pressed into the sample aperture of a standard

orelco sample holder (Zytel boat) and the surface of the powder is toothed off. After some practice it is possible to make highly reproducible packs of each sample. Tests show that samples prepared by two practiced technicians will yield analytical results which agree within 1%. This sample preparation is used for the analysis of Fe, Ca, Mg, K, Ti, and Mn. As noted below, a modification of this technique is required to achieve adequate precision in the analysis of Si and Al.

The sample holder is inserted into the x-ray spectrograph and the goniometer is set at the proper angular position necessary to measure the peak of the desired elements. This peak position is previously determined by a stepwise scanning of the approximate region in which the

TABLE 5. OPERATING CONDITIONS FOR FLUORESCENT X-RAY SPECTROGRAPHIC ANALYSES

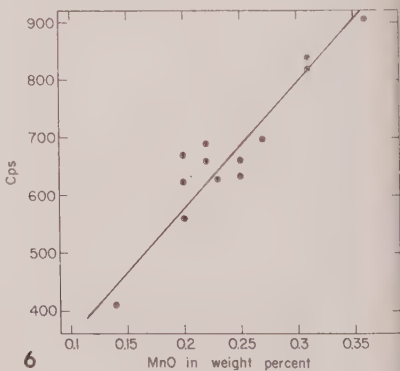
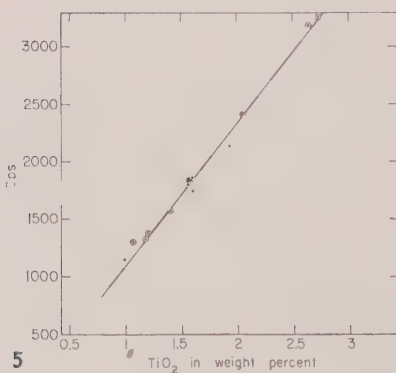
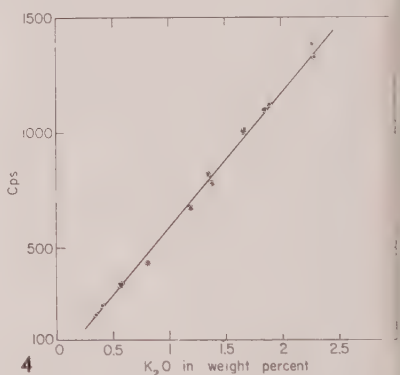
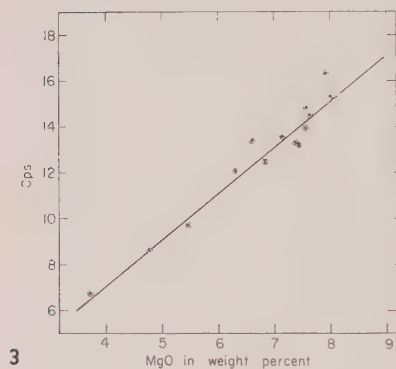
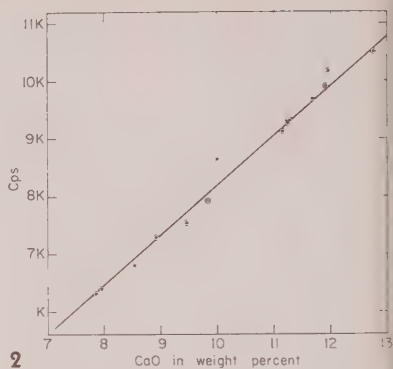
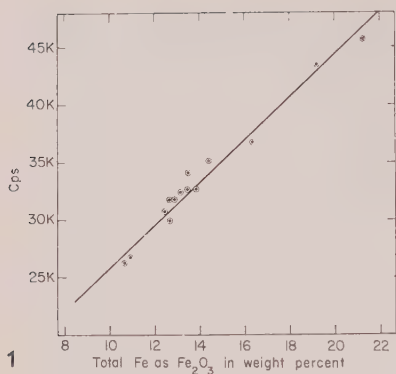
Element	Crystal	FPC* v	Pulse height analyzer		Element peak	Peak location $^{\circ} 2 \theta$	Back-ground location $^{\circ} 2 \theta$	Counts peak (thousands)	Counts back-ground (thousands)
			Base v	Window v					
Fe	EDT	1825	—	—	K α	25.45	—	500	—
Mn	EDT	1660	4	9	K α	27.65	28.75	20	5
Ti	EDT	1750	10	12	K α	36.46	—	50	—
Ca	EDT	1825	—	—	K α	44.89	—	100	—
K	EDT	1750	7	9	K α	50.33	—	20	—
Si	EDT	1825	5	18	K α	108.10	—	100	—
Al	EDT	1825	5	18	K α	142.63	—	50	—
Mg	ADP	1825	6	9	K α	136.90	135.5 138.0	10	1

* * Flow proportional counter.

Note: EDT (ethylene diamine D-tartrate).

ADP (ammonium dihydrogen phosphate).

peak occurs. A crystal of ammonium dihydrogen phosphate (ADP) is used for the analysis of Mg; all other elements are obtained by use of a crystal of ethylene diamine D-tartrate (EDT). After appropriate crystal and instrumental conditions are chosen, a measurement is made of the time required to accumulate a specific number of counts. The number of counts which must be made for each element is a function of the position of measurement required for that element. Background readings are made for those elements which require them by counting at some distance from the peak location (Table 5). Counting times are calculated to counts per second (cps) and the background intensity is subtracted from peak intensity to yield the net peak intensity. The intensity values obtained for the standard samples are plotted against weight per cent of element to obtain the calibration curves as shown in Figs 1 to 6 inclusive. Values for the unknowns are obtained by interpolation from the calibration curves. This procedure permits the determination of the



FIGS. 1-6. Calibration curves for fluorescent x-ray analysis.

x elements: Fe, Ca, Mg, K, Ti, and Mn, in approximately one-half hour.

Initial phases of our fluorescent x-ray spectrographic studies were begun with a Norelco x-ray spectrograph, using its standard electronic panel and a Baird-Atomic pulse height analyzer. It soon became apparent that the desired electronic stability necessary to obtain reproducible values over extended periods could not be obtained with the original electronic panel. Accordingly, an electronic system was constructed from standard components by our colleague E. V. Nenow. The equipment used is commercially available and is listed in Table 6. One of the principal modifica-

TABLE 6. EQUIPMENT FOR FLUORESCENT X-RAY SPECTROGRAPHIC ANALYSES

Norelco standard x-ray spectrograph equipped for helium atmosphere
Helium flow rate 2 liters/minute
FA-60 tungsten target x-ray tube
50 KV and 35 ma
Flow proportional counter
P-10 gas flow rate 0.02 cu. ft./hr. (air)
EDT and ADP analyzing crystals
0.02"×3" collimator
Baird-Atomic model 219A preamplifier
Baird-Atomic model 218 linear amplifier
Baird-Atomic model 510 pulse height analyzer
Hamner model N401 high voltage power supply
Baird-Atomic model 134 high speed scaler
Nuclear-Chicago model 1620 rate meter
Norelco interval timer
Leeds and Northrup model G recorder

tion was intended to increase the stability needed for pulse height analysis for light elements. The original system had a pulse height drift of several volts per day. The addition of a high voltage stabilizer, stable to plus or minus 0.01 per cent, decreased this daily drift to less than 0.5 volts per day, and the drift per week on the order of 0.2 volts. This drift may be ignored.

Initial analytical techniques emphasized speed and simplicity and used only the crystal of ADP as required for analyses of Mg. Use of the ADP crystal is not desirable in the analysis of Si and Al inasmuch as phosphorus from the crystal contributes to the background. The high background increases abnormally the counting times necessary for desired precision and also decreases the reliability of the results. Recently a crystal inter-

changer has been developed which will permit the rapid change from a crystal of ADP to one of EDT without either shutting off the x-rays or opening the helium bag. The crystal of EDT is used for all elements other than Mg.

The pulse height analyzer is not used for determinations of Fe and Ca because there are no interfering lines and the intensity is sufficient to completely eliminate the need for background readings. In the analyses for K, Ti, and Mn, the pulse height analyzer settings were such that more than 95% of the energy of the element lay within the chosen energy range. The settings for Mg are chosen so as to exclude the maximum possible phosphorus energy. This asymmetric setting of the pulse height analyzer is made possible by the use of the stable electronic components added by Nenow. The conditions under which measurements were made are also listed in Table 5, although it must be remembered that these are unique to the apparatus as modified by Nenow.

Both the electronic components and the gas flow to the flow proportional counter are allowed to run continuously. During periods of analysis references are made every hour to a standard rock slab to check intensity and pulse height. During the warmup period of the equipment slight adjustments are made in the milliamperes to keep the intensity at a constant value.

The methods of analysis described above fall short of achieving desirable precision for Si and Al. Analyses of silica are accurate only to within about 3-5% of the amount present and for alumina only to about 5-10% of the amount present. This precision obviously does not compare favorably with results obtained by careful wet chemical analyses. Presumably serious matrix effect reduces the precision of analyses of Si and Al as indicated by the scatter of determinations on our calibration curves. Attempts to compensate for matrix effects by the use of ratios of the elements have proved unsuccessful.

Probably adequate analyses of Si and Al require fusion of the samples. Various alternative methods of fusing samples were tried with limited success. Best results to date have been obtained by sintering one part with one part sodium carbonate. Analyses of freshly sintered samples appear to be quite precise but the sinter appears to be unstable and there is considerable difficulty in reproducing identical sinters of the same sample.

The borax fusion technique described by Claisse (1956) is not entirely adequate because of the loss in intensity of the light elements due to the large dilutions of the sample. At present we are experimenting with types of borax fusions which vary in detail from those described by Claisse.

ANALYTICAL RESULTS

Results of analyses of amphibolites, using both fluorescent x-ray spectrographic and chemical techniques are shown in Tables 2 and 4. In Table 2 each of the analyses labelled "chem" represents the results of wet chemical analyses by C. G. Engel. As noted previously these analyses were used to construct the working curves reproduced in Figs. 1 to 5. The fluorescent x-ray analyses of these same samples are labelled "x-ray" in Table 2.

Comparisons of the two types of analyses indicate the deviation involved. The mean and maximum deviations respectively of the x-ray analyses from the chemical analyses in per cent of the amount reported are as follows: Total Fe as Fe_2O_3 3.1, 7.6; CaO 1.3, 6.4; MgO 3.0, 9.3; K_2O 3.2, 7.4; TiO_2 3.2, 10.3; and MnO 7.7 and 33.3. The deviations tend to be fairly symmetrically distributed on either side of the chemical analyses. The mean and maximum deviations in every instance are as small or smaller than deviations in analyses by classical chemical techniques where different analysts are involved. There has been little testing of the precision of a single analyst over long periods of time using classical methods.

X-ray analyses marked with an asterisk in Table 2 represent analyses made at a much later time of identical splits of 8 of the samples. Comparison of these numbers with the earlier x-ray data in Table 2 indicate precision over a 4 month time interval. The mean and maximum deviation respectively of x-ray analyses of the same samples at 4 months intervals are as follows: total Fe as Fe_2O_3 2.1, 4.9; CaO 1.3, 2.6; MgO 1.4, 7.7; K_2O 7.9, 32.4; TiO_2 2.3, 6.7; and MnO 2.0, 7.7.

Analyses in Table 4 are of samples first run by x-ray methods and checked by subsequent wet chemical analyses. A second split was made of some of the samples and submitted for x-ray analyses under a separate number. This second split was run at the same time and serves as a test of precision of the fluorescent x-ray analytical method where there is no time variance.

The chemical analyses obtained after the x-ray data were made on masked samples prepared by A. E. Engel so that the analyst did not know the identity of the sample. Duplicate x-ray analyses of any sample yields essentially identical results. Accordingly, where two x-ray analyses have been made of any sample, the results have been averaged in the comparison made below. The mean and maximum deviation of the x-ray analyses from the chemical analyses in per cent are as follows: total Fe as Fe_2O_3 1.2, 3.7; CaO 1.8, 3.4; MgO 2.6, 11.1; K_2O 3.3, 8.3; TiO_2 2.0, 27.3; MnO 7.6, 16.7. With the exception of data from several samples

(notably 414, 320), the data in table 4 are very comparable with those in Table 2. Samples AE 320 and AE 414 are biotitic amphibolites in which the flakes of biotite were not reduced to a uniformly small size. This spread in grain size with relatively coarse biotite in a finer matrix appears to be the cause of the rather large errors reported for TiO_2 , MnO , and MgO . These results again emphasize the need for fine grinding of the sample to achieve precise analytical results.

CONCLUSIONS

Analyses of rocks and minerals attempted to date point up major advantages and disadvantages to the x -ray techniques we have employed. It is obvious that where working curves are available x -ray methods permit a rapid analysis and comparison of the compositions of large numbers of samples where data on Fe, Ca, Mg, K, Ti, and Mn are critical.

It is equally obvious that there are important limitations to this method of x -ray analysis. Commonly, solution of mineralogical and petrologic problems requires the determinations of Si, Al, Na, H_2O , and the valence states of Fe, and so on. These data cannot be obtained with the equipment and techniques described earlier. At present the most satisfactory method is the classical gravimetric technique.

The working curves necessary for x -ray analyses must be prepared by an independent method having a high degree of precision. Moreover, the best working curves usually are obtained on either rock or minerals where there is a rather large continuous variation in chemical composition without major changes in crystal structure (*i.e.*, matrix differences). For this reason working curves prepared for granites are not wholly satisfactory for the analyses of clays or for feldspars. In effect, the x -ray technique must be supplemented and constantly rechecked by either wet chemical analysis or some other independent, precise analytical method. We have found (Engel and Engel, in preparation) x -ray techniques invaluable as a supplement to classical methods of analysis for a chemical reconnaissance of the concentration of heavy elements in both minerals and rocks. Presumably this is at present where the chief value of the x -ray technique lies.

ACKNOWLEDGMENTS

This work was initiated as part of a research program at the California Institute of Technology on the origin of amphibolite rocks, made possible, in part, by a grant from the National Science Foundation and support from the U. S. Geological Survey. The authors are indebted to E. V. Nenow for modifications and care of the x -ray unit and to A. E. Engel for suggestions and assistance throughout the work. The manuscript has

been read and greatly improved by the constructive comments of M. Fleischer, I. Adler, and H. J. Rose, Jr.

REFERENCES

- AHRENS, L. H. (1950), *Spectrochemical Analyses*: Addison-Wesley, Cambridge, Mass.
- CHODOS, A. A., BRANCO, J. J. R., AND ENGEL, C. G. (1957), Rock analysis by x-ray fluorescence spectroscopy: Proceedings, 6th Annual x-ray conference, Denver Research Institute, University of Denver, 315-327.
- CLAISSE, F. (1956), Accurate x-ray fluorescence analyses without internal standard: *Département of Mines, Province of Quebec, Canada, P. R.* **327**.
- DENNEN, W. H., AHRENS, L. H., AND FAIRBAIRN, H. W. (1951), Spectrochemical analysis of major constituent elements in rocks and minerals: *U. S. Geological Survey Bull.*, **980**, 25-52.
- DENNEN, W. H. AND FOWLER, W. C. (1955), Spectrographic analysis by use of a mutual standard method: *Bull. Geol. Soc. Amer.*, **66**, 655-662.
- ENGEL, A. E. J. AND ENGEL, CELESTE, G. (1958), Progressive metamorphism and granitization of the major paragneiss, Northwest Adirondack Mountains, New York, Part I: Total Rock: *Bull. Geol. Soc. Amer.*, **69**, 1369-1414.
- FAIRBAIRN, H. W. (1953), Precision and accuracy of chemical analyses of silicate rocks: *Geochem. et Cosmochim. Acta*, **4**, 143-156.
- FAIRBAIRN, H. W., *et al.* (1951), A cooperative investigation of precision and accuracy in chemical, spectrochemical and modal analysis of silicate rocks: *U. S. Geol. Survey Bull.* **980**.
- KVALHEIM, A. (1947), Spectrochemical determination of the major constituents of minerals and rocks: *Jour. Op. Soc. Amer.*, **37**, 585.
- SHAPIRO, LEONARD, AND BRANNOCK, W. W. (1956), Rapid analysis of silicate rocks: *U. S. Geol. Survey Bull.* **1036-C**, 56 p.
- (1952), Rapid analysis of silicate rocks: *U. S. Geol. Survey Circ.*, **165**, 17 p.

Manuscript received April 23, 1960.

TITANOMAGHEMITE IN IGNEOUS ROCKS

TAKASHI KATSURA, *Tokyo Institute of Technology*

AND

IKUO KUSHIRO, *Geological Institute, University of Tokyo.*

ABSTRACT

Titanomaghemite, an oxidized titanomagnetite having compositions near the $\text{TiFeO}_3\text{-Fe}_2\text{O}_3$ join or even within the $\text{TiFe}_2\text{O}_5\text{-TiFeO}_3\text{-Fe}_2\text{O}_3$ triangular field in the system $\text{TiO}_2\text{-FeO-Fe}_2\text{O}_3$, has been found in some Japanese igneous rocks. Microscopically the mineral can be distinguished from titanomagnetite by its bluish gray color in reflected light and the abundance of cracks. Titanomaghemite so far observed occurs largely in rocks in which olivine and hypersthene are partially or completely altered to chlorite and serpentine, but it occurs also in some unaltered lava flows. It is concluded that titanomagnetite crystallizing from magma is oxidized to produce titanomaghemite under a certain condition which may be easily obtained during the cooling process. It is not necessary to consider the special solid solution series between $\gamma\text{-FeTiO}_3$ and Fe_3O_4 in order to explain the formation of titanomaghemite in igneous rocks. The titanomaghemite possesses vacancies of two or three metal ions in a unit cell. The lattice parameters vary with the ratios $\text{Fe}/(\text{Fe}+\text{Ti})$ and $32(\text{Fe}+\text{Ti})/0$, and range from 8.359 to 8.419 Å.

INTRODUCTION

Titanomagnetites in igneous rocks are generally considered to have compositions within a triangular field $\text{TiFeO}_3\text{-TiFe}_2\text{O}_4\text{-Fe}_3\text{O}_4$ in the system $\text{TiO}_2\text{-FeO-Fe}_2\text{O}_3$. Their compositions are explained as belonging either to the $\text{TiFe}_2\text{O}_4\text{-Fe}_3\text{O}_4$ solid solution or to the $\gamma\text{-TiFeO}_3\text{-Fe}_3\text{O}_4$ solid solution (Chevallier and Girard, 1950; Vincent *et al.*, 1957). However, some titanomagnetites have compositions outside of the triangular field, lying even near the $\text{TiFeO}_3\text{-Fe}_2\text{O}_3$ join. Such compositions cannot be explained by the two simple solid solution series. Recently, Akimoto and Katsura (1959) discussed the origin of the titanomagnetites outside the triangular field $\text{TiFeO}_3\text{-TiFe}_2\text{O}_4\text{-Fe}_3\text{O}_4$ on the basis of their experiments (Akimoto, Katsura and Yoshida, 1957) and concluded that they were formed by oxidation of the normal titanomagnetite belonging to the $\text{TiFe}_2\text{O}_4\text{-Fe}_3\text{O}_4$ solid solution. But they did not discuss the extent to which the spinel phase can exist as a single phase. Basta (1953; 1959) named the titanomagnetites having compositions close to the $\text{TiFeO}_3\text{-Fe}_2\text{O}_3$ join and the $\text{TiO}_2\text{-Fe}_2\text{O}_3$ join the "titanomaghemites" and also concluded that they were formed by oxidation of the titanomagnetite of the $\gamma\text{-TiFeO}_3\text{-Fe}_3\text{O}_4$ solid solution.

Titanomaghemite in igneous rocks has been described only rarely. Frenzel (1953) reported maghemite (titanomaghemite) in shonkinite in Katzenbuckel in Odenwald. Basta (1959) summarized the titanomaghemites in South Africa which were early investigated by Wagner (1928), Walker (1930), Frankel and Grainger (1941) and Schweltnus and

TABLE 1. DESCRIPTIONS OF TITANOMAGHEMITE-BEARING ROCKS

Sp. No.	Rock	Locality	Main constituent minerals (titanomagnetite is replaced by titanomaghemite)
11003	Olivine analcite dolerite (sheet)	Atumi, western coast of Yamagata Pref.	Olivine (altered), titanaugite, plagioclase, titanomagnetite, ilmenite, zeolite, hypersthene (partially altered).
22502 6	Quartz-bearing olivine titanaugite dolerite (sheet)	Kingosi in Sidara Basin, Aiti Pref.	Olivine (altered), titanaugite, plagioclase, titanomagnetite, ilmenite, quartz.
22403-3	Olivine andesite (dike)	Orimoto-toge in Sidara Basin, Aiti Pref.	Phenocrysts; olivine (partially altered), augite, plagioclase, titanomagnetite, ilmenite. Groundmass: plagioclase, titanomagnetite, olivine, augite, glass.
HK53051602	Dacitic welded tuff	Kogasira, 8 km. NW of Kagosima, Kagosima Pref.	Phenocrysts; hypersthene, plagioclase, quartz, titanomagnetite, biotite.
	Olivine titanaugite dolerite (sheet)	Warabidaira, 20 km. SSW of Kohu, Yamanashi Pref.	Olivine (altered), titanaugite, plagioclase, ilmenite, titanomagnetite, zeolite.
	Augite hypersthene andesite (lava flow)	Central cone of Hakone Volcano, Sizuoka Pref.	Phenocrysts; augite, hypersthene, plagioclase, titanomagnetite. Groundmass; plagioclase, titanomagnetite, augite, hypersthene, glass.
	Olivine augite andesite (lava flow)	North-western caldera wall of old somma of Hakone Volcano, Sizuoka Pref.	Phenocrysts; olivine (mostly altered), augite, plagioclase. Groundmass: augite, plagioclase, titanomagnetite, glass.
	Scoria	North-western caldera wall of Hakone Volcano.	Phenocrysts; plagioclase. Groundmass: plagioclase, titanomagnetite, glass.
	Augite hypersthene andesite (lava flow)	Usami, eastern coast of Izu Peninsula, Shizuoka Pref.	Phenocrysts; augite, hypersthene, plagioclase, titanomagnetite. Groundmass: plagioclase, hypersthene, augite, titanomagnetite.
	Augite hypersthene andesite (lava flow)	Iwanuma, 20 km. S of Sendai, Miyagi Pref.	Phenocrysts; augite, hypersthene, plagioclase, titanomagnetite. Groundmass: plagioclase, hypersthene (partially altered), titanomagnetite, glass.
	Ferrogabbro (cone intrusion)	Skaergaard in Greenland	Olivine, augite, titanomagnetite (quartz), (hypersthene). (After Wager and Deer, 1939).

Willemsse (1943). In this paper, titanomaghemite is defined as a mineral with the spinel structure having a composition close to the $\text{TiFeO}_3\text{-Fe}_2\text{O}_3$ join or within the $\text{TiFe}_2\text{O}_5\text{-TiFeO}_3\text{-Fe}_2\text{O}_3$ triangular field in the $\text{TiO}_2\text{-FeO-Fe}_2\text{O}_3$ system. This mineral was first found by the present authors in dolerite of Atumi, Yamagata Pref., northern Japan and in welded-tuff of Kogasira, Kagosima Pref., Kyūsyū. Afterward, they also found it in dolerites of Sidara and Warabidaira and in several andesite dikes and lavas of Izu-Hakone district and Sidara in central Japan. It appears that titanomaghemite is not a rare mineral in igneous rocks. The mineral will be found commonly in both intrusive and extrusive rocks, if the reflection microscope is more widely used and chemical analysis made on iron oxide minerals. In the present paper, the mode of occurrence of titanomaghemite in igneous rocks is described, its physical and chemical properties are given and are compared with the previous data.

MODE OF OCCURRENCE OF TITANOMAGHEMITE

Titanomaghemite-bearing igneous rocks so far investigated are the dolerites of Atumi and Warabidaira, the dolerites and andesite of Sidara, the lavas of Izu-Hakone and Iwanuma, the welded-tuff of Kogasira, scoria of Hakone and gabbro of the Skaergaard complex in Greenland. Brief descriptions of the host rocks are given in Table 1. In these rocks, titanomaghemite replaces partially or completely titanomagnetite.

Titanomaghemite in the Atumi dolerite which has been studied by one of the authors (Kushiro, 1959) occurs in olivine-analcite-dolerite of Kayaoka Sheet and analcite-syenite in Sumiyosizaki Sheet. The dolerite and syenite have been subjected more or less to hydrothermal alteration as inferred from the existence of altered olivine, hypersthene and plagioclase. Titanomaghemite 1003, No. 1 in Table 3, which has been analyzed and observed in detail was separated from the surface of the dolerite, 55 m. above the base of the Kayaoka Sheet. The chemical composition of this dolerite is given in Table 2, No. 1. The dolerite is situated near the center of the sheet where hydrothermal solution may have been concentrated at the later stage of magmatic differentiation. Furthermore, the surface of the dolerite has suffered more or less weathering. In this case titanomaghemite replaces titanomagnetite almost completely.

Titanomaghemite 2403 in olivine-andesite dike of Orimoto-toge in the Sidara basin, No. 3 in Table 3, has been partially analyzed. It occurs in the central part of the dike as both phenocrysts and in the groundmass. The degree of replacement of titanomagnetite by the titanomaghemite decreases towards the margin of the dike. Olivine associated with the titanomaghemite is partially or completely altered to carbonate. It is supposed that the central part of the dike has been permeated by hydrothermal solutions or by volatiles. The chemical composition of the central part of the dike is given in Table 2, No. 3.

Titanomaghemite 2502 6 in olivine-titanaugite-dolerite of Kingosi in the Sidara basin, No. 2 in Table 3, occurs near the margin of a sheet. It is associated with chloritized olivine. The relation between the existence of the titanomaghemite and unstable magnetization of this sheet has recently been discussed (Akimoto and Kushiro, 1960). The chemical composition of this dolerite is given in Table 2, No. 2.

In ferrogabbro of the Skaergaard intrusion of which samples were kindly offered by Drs. Uyeda and Akimoto, a small amount of titanomaghemite replaces titanomagnetite along the cracks and the boundary of ilmenite lamellae. The titanomagnetite has fine exsolution lamellae of ulvöspinel. The composition of the titanomagnetite in the ferrogabbro given by Vincent and Phillips (1954) should be corrected in view of the presence of the titanomaghemite.

TABLE 2. CHEMICAL COMPOSITIONS OF HOST ROCKS

	No. 1	No. 2	No. 3	No. 4
SiO ₂	49.03	50.74	56.69	71.64
TiO ₂	1.48	1.75	0.88	0.43
Al ₂ O ₃	17.43	15.76	16.43	14.88
Fe ₂ O ₃	2.89	4.74	1.30	1.83
FeO	5.32	4.64	7.07	0.50
MnO	0.15	0.14	0.18	0.01
MgO	6.07	4.25	1.63	0.15
CaO	6.25	8.15	4.69	2.10
Na ₂ O	4.45	3.34	4.70	3.95
K ₂ O	1.95	0.99	1.58	3.30
H ₂ O(-)	1.18	2.81	0.20	0.35
H ₂ O(+)	3.60	0.86	0.50	0.98
P ₂ O ₅	0.31	0.26	0.42	0.10
CO ₂	0.05	1.25	4.02	0.02
Total	100.16	99.68	100.29	100.24

No. 1. Olivine-analcite-dolerite 1003, Atumi.

No. 2. Olivine-titanaugite-dolerite 2502-6, Kingosi.

No. 3. Olivine-andesite 2403, central part of the dike, Orimototoge.

No. 4. Dacitic welded-tuff HK53051602, Kogasira.

TABLE 3. CHEMICAL COMPOSITIONS OF TITANOMAGHEMITES

	No. 1	No. 2	No. 2-a	No. 3	No. 4	No. 3-a	No. 3-b
FeO	11.89	20.25	19.89	15.98	14.84	33.32	45.02
MgO	0.45	n.d.	n.d.	n.d.	0.35	n.d.	n.d.
MnO	2.29	0.99	n.d.	n.d.	0.81	0.76	n.d.
CaO	1.58	n.d.	n.d.	n.d.	0.05	n.d.	n.d.
Fe ₂ O ₃	56.53	45.94	42.76	41.91	66.97	35.02	29.60
Al ₂ O ₃	1.94	n.d.	n.d.	n.d.	1.53	n.d.	n.d.
V ₂ O ₃	0.73	0.53	0.41	0.17	0.38	0.15	0.12
TiO ₂	22.63	26.92	20.95	25.45	13.83	20.82	18.63
SiO ₂	2.01	0.78	7.30	n.d.	0.87	3.35	n.d.
P ₂ O ₅	0.00	0.00	n.d.	n.d.	0.01	n.d.	n.d.
Total	100.05	95.41	91.31	83.51	99.64	93.42	93.37

No. 1. Titanomaghemite from olivine-analcite-dolerite 1003, Atumi.

No. 2. Titanomaghemite from olivine-titanaugite-dolerite 2502-6, Kingosi.

No. 2-a. Titanomaghemite from another part of the same sheet as No. 2.

No. 3. Titanomaghemite from the central part of the dike 2403, Orimototoge.

No. 4. Titanomaghemite from dacitic welded-tuff HK53051602, Kogasira.

No. 3-a. Titanomagnetite from the margin of the dike 2403, Orimototoge.

No. 3-b. Titanomagnetite from the margin of the dike 2403, Orimototoge.

In most cases, if not all, the titanomaghemite occurs in more or less altered rocks in which olivine and hypersthene are partially or completely altered to chlorite, serpentine and other minerals. This indicates that most titanomaghemite has been formed by the reaction of hydrothermal solutions or volatiles with titanomagnetite primarily formed from magma. Though the minimum oxygen partial pressure necessary to oxidize titanomagnetite at a given temperature is not known, the hydrothermal solutions or volatiles derived from magma may be able to oxidize titanomagnetite. From the fact that the amount of titanomaghemite increases towards the weathered surface of the Atumi dolerite, it is suggested that some titanomaghemite may have been formed by weathering.

It must be noted that titanomaghemite occurs in some apparently unaltered lava flows. In this case, the volatiles or solutions may have attacked only the titanomagnetite, but not silicate minerals.

It is suggested that titanomaghemite and the transitional variety between titanomaghemite and TiFe_2O_4 - Fe_3O_4 solid solution are common in intrusive as well as extrusive igneous rocks.

OBSERVATIONS WITH MICROSCOPE

In thin section titanomaghemite is opaque, and in polished section it is isotropic and shows intermediate reflectivity between those of titanomagnetite and hematite. The color is bluish gray for the extremely oxidized one which has composition near the TiFeO_3 - Fe_2O_3 join or in the triangular field TiFe_2O_5 - TiFeO_3 - Fe_2O_3 in the system TiO_2 - FeO - Fe_2O_3 . The difference in color between titanomagnetite and titanomaghemite is emphasized by using oil immersion lens. In most cases, titanomaghemite develops from the margin or cracks of titanomagnetite grains. The boundary between them is generally sharp but complete gradation is sometimes observed. Titanomaghemite often shows irregular cracks. Figure 1 shows gradual change from titanomagnetite to titanomaghemite as revealed by the gradual change in color and in the number of irregular cracks. The analyzed titanomaghemites are generally homogeneous but occasionally contain small amounts of titanomagnetite in the inner parts of some grains which are considered as unoxidized parts of the original titanomagnetite. The titanomaghemites from the Atumi and Kingosi dolerites contain ilmenite exsolution lamellae less than about 4%. Hence the chemical compositions of the titanomaghemites must be slightly different from those suggested by the analyses.

METHODS OF SEPARATION AND CHEMICAL ANALYSIS

The separation of titanomaghemites was carried out by the same method as described in a previous paper (Akimoto and Katsura, 1959)

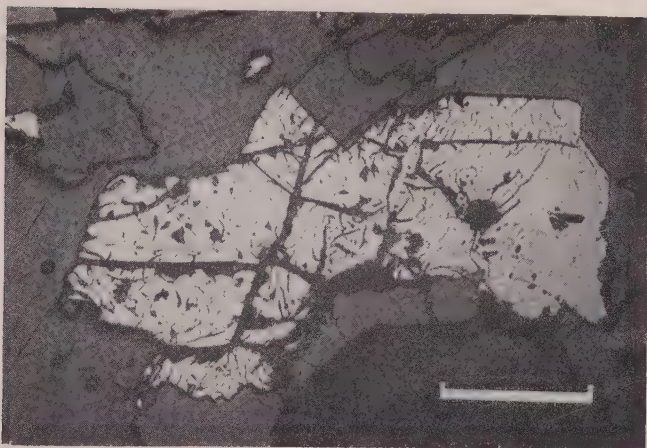


FIG. 1. Titanomaghemite in olivine-analcite-dolerite 1003, Atumi. Gradual change from titanomagnetite (right) to titanomaghemite (left) is revealed by the increase in reflectivity and in the number of cracks. The unit line at lower right indicates 0.1 mm.

except titanomaghemite No. 2 in Table 3. Specimen No. 2 is very fine grained and could not be separated by the same method. Therefore it was purified as follows: 1 gm. of the titanomaghemite roughly separated was suspended in 50 ml. of water held in a platinum dish, then half a ml. of hydrofluoric acid (45%) was added, and the mixture was stirred vigorously. After 5 minutes, a hand magnet was attached to the dish at the bottom from outside in order to fix the ferromagnetic deposit and the solution was removed by decantation. The ferromagnetic fraction thus obtained was washed several times with dilute hydrochloric acid. The purification was thus nearly complete as will be seen by the low SiO_2 content. The chemical analysis of titanomaghemites was made by the method devised by Iwasaki, Katsura, Yoshida and Tarutani (1957). The precision and accuracy of this analytical method are sufficient for the present study.

CHEMICAL COMPOSITIONS OF TITANOMAGHEMITES

Chemical compositions of the titanomaghemites separated from the Japanese igneous rocks are shown in columns Nos. 1, 2, 3-a, 3 and 4 of Table 3. In the last two columns of the same table, compositions of unoxidized titanomagnetite and of fairly oxidized titanomagnetite in the dike from Orimoto-toge, Sidara are given for comparison with that of titanomaghemite No.3. Nos. 3-a and 3-b are from the margin of the dike whereas No. 3 is from the center of the same dike. A gradual increase in

TABLE 4. MOLECULAR PROPORTIONS OF OXIDES, ATOMIC RATIOS OF Fe AND Ti, LATTICE PARAMETERS AND CURIE TEMPERATURES OF TITANOMAGHEMITES

	No. 1	No. 2	No. 2-a	No. 3	No. 4
	Mol. %				
FeO	20.62	31.09	34.31	27.69	26.06
Fe ₂ O ₃	44.10	31.74	33.19	32.67	52.56
TiO ₂	35.28	37.17	32.50	39.64	21.38
	Atomic ratio				
Fe/(Fe+Ti)	0.755	0.718	0.756	0.701	0.860
32(Fe+Ti)/O	20.63	21.01	21.43	20.71	21.55
	Mol. %				
FeO } MgO } RO MnO }	23.93	—	—	—	27.13
Fe ₂ O ₃ } Al ₂ O ₃ } R ₂ O ₃ V ₂ O ₃ }	43.48	—	—	—	52.19
TiO ₂	32.59	—	—	—	20.68
	Atomic ratio				
R/(R+Ti)	0.773	—	—	—	0.864
32(R+Ti)/O	20.96	—	—	—	21.64
Lattice parameter (Å)	8.359 (8.394)	8.405	8.419	8.373 (8.470)	8.360 (8.430)
Curie temperature (°C.)	460	580	520, 560	430	545

Nos. are same as those in Table 3. The lattice parameter values in parentheses are those of the titanomagnetites present in small amount. Curie temperatures are determined by the extrapolation of thermomagnetic curves for the heating process.

the degree of oxidation is recognized in the order No. 3-b→No. 3-a→No. 3.

The SiO₂ content in the specimens is due largely to pyroxene and feldspar. The presence of small amounts of such impurities obviously introduces a slight error in the calculation of the titanomaghemite compositions, but in the following calculations the silicate compositions are not subtracted from the analyses. Table 4 shows the molecular proportions and atomic ratios of the analyzed titanomaghemites. RO means the sum of FeO, MgO and MnO, and R₂O₃ that of Fe₂O₃, Al₂O₃ and V₂O₃. The

difference between the ratios $\text{FeO}:\text{Fe}_2\text{O}_3:\text{TiO}_2$ and $\text{RO}:\text{R}_2\text{O}_3:\text{TiO}_2$ is small as shown in Nos. 1 and 4 of Table 4, and is insignificant for the interpretation of the relation between chemical compositions and physical properties of titanomaghemite. The value of $32(\text{Fe}+\text{Ti})/\text{O}$ ($=32(\text{Fe}^{2+}+\text{Fe}^{3+}+\text{Ti})/\text{O}$) which is a measure of the degree of oxidation ranges between 24 and 23 in the titanomagnetites from volcanic rocks (Akimoto and Katsura, 1959), whereas the value for the titanomaghe-

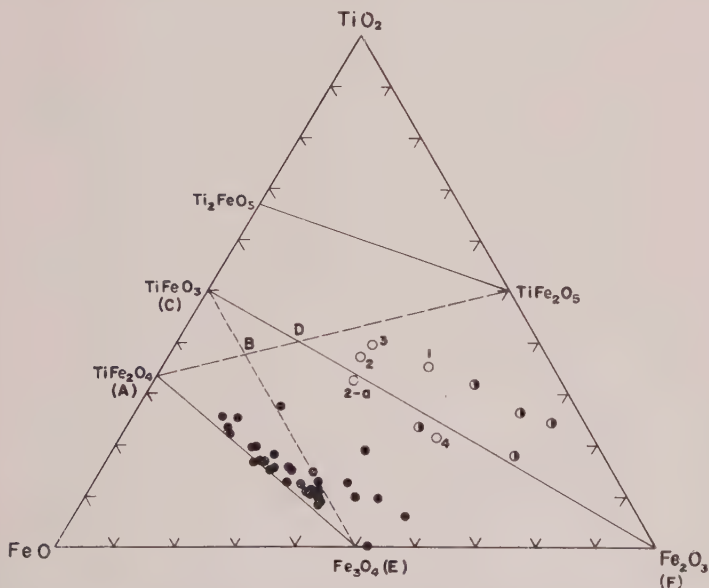


FIG. 2. Compositions of titanomagnetites and titanomaghemites in molecular per cent FeO , Fe_2O_3 and TiO_2 . Solid circles represent titanomagnetites (data from Akimoto and Katsura, 1959). Open and half solid circles represent titanomaghemites from Japanese rocks and from South Africa respectively. (Data for latter from Basta, 1959.) The numbers refer to those in Tables 3 and 4.

ites listed in Table 4 ranges from 20.6 to 21.6. Thus in the titanomaghemites there are vacancies of 2 or 3 metal ions in a unit cell with 32 oxygen atoms. The same result is obtained even when the ratio $32(\text{RO}+\text{Ti})/\text{O}$ is used.

Figures 2 and 3 show with open circles the chemical compositions of the titanomaghemites in the ternary system $\text{TiO}_2\text{-FeO-Fe}_2\text{O}_3$ and the relation between the values $\text{Fe}/(\text{Fe}+\text{Ti})$ ($=\text{Fe}^{2+}+\text{Fe}^{3+}/(\text{Fe}^{2+}+\text{Fe}^{3+}+\text{Ti})$) and $32(\text{Fe}+\text{Ti})/\text{O}$ respectively. Available analyses of titanomagnetites from Japanese igneous rocks are also plotted with solid circles. The lines

EF and ABD in Fig. 3 represent the courses of oxidation of magnetite and ulvöspinel respectively. The lines AE and CBE represent the binary $\text{TiFe}_2\text{O}_4\text{-Fe}_3\text{O}_4$ and $\gamma\text{-TiFeO}_3\text{-Fe}_3\text{O}_4$ solid solutions assumed by Chevallier and Girard (1950) and the compositional field CAE includes the intermediate titanomagnetite of Vincent *et al.* (1957). Figure 2 shows that the Japanese titanomaghemites have compositions close to the $\text{TiFeO}_3\text{-Fe}_2\text{O}_3$ join or within the $\text{TiFe}_2\text{O}_5\text{-TiFeO}_3\text{-Fe}_2\text{O}_3$ triangular field. Figure 3 shows

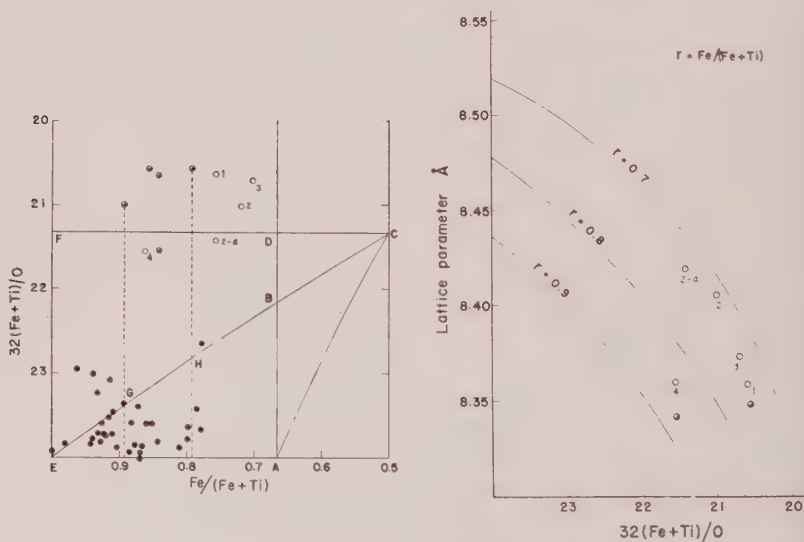


FIG. 3 (left). Relation between $32(\text{Fe}+\text{Ti})/\text{O}$ and $\text{Fe}/(\text{Fe}+\text{Ti})$ of titanomagnetites and titanomaghemites. Symbols are same as in Fig. 2. Fe includes Fe^{2+} and Fe^{3+} .

FIG. 4. (right) Relation between lattice parameters and $32(\text{Fe}+\text{Ti})/\text{O}$ of titanomaghemites. Symbols same as in Fig. 2.

that the titanomaghemites have much more vacancies in metallic positions than the titanomagnetites.

Recently Basta (1959) reported titanomaghemites from South Africa and suggested that they were formed mainly by oxidation of titanomagnetite of the $\gamma\text{-TiFeO}_3\text{-Fe}_3\text{O}_4$ series (titanomagnetite II of Chevallier and Girard) but not of the $\text{TiFe}_2\text{O}_4\text{-Fe}_3\text{O}_4$ series. Table 5 gives recalculated Basta's data on the South African titanomaghemites. They are also plotted in Figs. 2 and 3. The South African titanomaghemites have the values of $\text{Fe}/(\text{Fe}+\text{Ti})$ ranging from 0.79 to 0.89 and those of $32(\text{Fe}+\text{Ti})/\text{O}$ from 20.5 to 21.3. Thus, there are almost the same numbers of vacancies

TABLE 5. MOLECULAR PROPORTIONS OF OXIDES, ATOMIC RATIOS OF Fe AND Ti, AND LATTICE PARAMETERS OF TITANOMAGHEMITES FROM SOUTH AFRICA (AFTER BASTA, 1959)

	No. 1	No. 2	No. 3	No. 4	No. 5
			Mol. %		
FeO	14.41	27.83	5.45	9.64	14.81
Fe ₂ O ₃	53.53	48.57	69.93	64.00	67.18
TiO ₂	32.05	23.60	24.62	26.36	18.01
			Atomic ratio		
Fe/(Fe+Ti)	0.791	0.841	0.855	0.839	0.892
32(Fe+Ti)/O	20.55	21.54	20.56	20.63	21.20
			Mol. %		
FeO } MgO } RO MnO }	17.26	30.12	7.90	10.20	
Fe ₂ O ₃ } Al ₂ O ₃ } R ₂ O ₃ V ₂ O ₃ }	52.50	47.55	69.70	64.23	
TiO ₂	30.24	22.33	22.40	25.57	
			Atomic ratio		
R/(R+Ti)	0.802	0.849	0.868	0.844	
32(R+Ti)/O	20.74	21.72	20.74	20.69	
Lattice parameter (Å)	8.3475	8.342			

in the unit cells as those in the Japanese titanomaghemites. If the South African titanomaghemites were oxidized from titanomagnetites of the γ -TiFeO₃-Fe₃O₄ series as postulated by Basta, the original titanomagnetites should have the values of Fe/(Fe-Ti) from 0.79 and 0.89 and 32(Fe Ti)/O from 22.9 to 23.4, in other words, they should be represented by points between H and G of Fig. 3. These titanomagnetites should have vacancies of 0.6–1.1 in the unit cells. It is clear from the experiment by Akimoto and Katsura (1959) that such titanomagnetites may be easily formed by oxidation of the titanomagnetite of the TiFe₂O₄-Fe₃O₄ solid solution under suitable conditions. In consideration of this, the postulation of the special solid solution series between γ -FeTiO₃ and Fe₃O₄ is not needed to explain the formation of titanomaghemite from normal titanomagnetite.

LATTICE PARAMETERS OF TITANOMAGHEMITES

The lattice parameters of the present titanomaghemites were determined by the measurement of diffraction angles for (440), (511, 333), (400), (311) and (220) by the "Norelco" x -ray diffractometer with $\text{FeK}\alpha$ radiation. Instrumental errors were calibrated by using a standard specimen of silicon. The lattice parameters are listed in Table 4. Those in parentheses are for titanomagnetites present in small amount. As reported previously (Akimoto *et al.*, 1957; Akimoto and Katsura, 1959), the change in lattice parameters of titanomagnetites depends not only on their TiO_2 content but also on the degree of oxidation. So far as we know, the relation between the lattice parameters of the Fe-Ti spinels and their TiO_2 content is not yet established. But if titanomaghemites are compared with titanomagnetites having the same Fe (Fe+Ti) values, a certain definite relation is obtained between the lattice parameters and the degree of oxidation. Figure 4 shows the relation between lattice parameters and $32(\text{Fe}+\text{Ti})/\text{O}$ for titanomaghemites and titanomagnetites with $\text{Fe}/(\text{Fe}+\text{Ti}) (=r)$ equal to 0.7, 0.8 and 0.9. As will be seen in the figure, for any given values of $32(\text{Fe}+\text{Ti})/\text{O}$, the lattice parameter increases with the decrease of the r value. Basta (1953, 1959) gives a value 8.3475 Å for the cube edge of a titanomaghemite from Transvaal (No. 1 in Table 5). This value also fits the diagram.

ACKNOWLEDGMENTS

The authors wish to express their thanks to Dr. S. Akimoto of the Geophysical Institute, University of Tokyo, who kindly allowed them to use the data of Curie temperatures. They thank cordially Prof. H. Kuno who kindly gave them a sample of Kogasira welded tuff, offered much valuable suggestions and discussions from the petrological point of view, and also read the manuscript. They are indebted to Prof. T. Watanabe for suggestions in microscopic observations. Their thanks are also due to Prof. I. Iwasaki of the Tokyo Institute of Technology, and to Mr. M. Yoshida for his fruitful discussion throughout the study.

REFERENCES

- AKIMOTO, S., KATSURA, T. AND YOSHIDA, M. (1957), Magnetic properties of TiFe_2O_4 - Fe_3O_4 system: *Jour. Geomag. Geoelect.*, **9**, 165-178.
 AKIMOTO, S. AND KATSURA, T. (1959), Magnetochemical study of the generalized titanomagnetite in volcanic rocks: *Jour. Geomag. Geoelect.*, **10**, 69-90.
 AKIMOTO, S. AND KUSHIRO, I. (1960), Natural occurrence of titanomaghemite and its relevance to unstable magnetization of rocks: *Jour. Geomag. Geoelect.*, **11**, 94-110.
 BASTA, E. Z. (1953), Mineralogical aspects of the system $\text{FeO-Fe}_2\text{O}_3\text{-TiO}_2$: Ph.D. thesis, Bristol.

- (1959), Some mineralogical relationships in the system $\text{Fe}_2\text{O}_3\text{-Fe}_3\text{O}_4$ and the composition of titanomaghémite: *Econ. Geol.*, **54**, 698–719.
- CHEVALLIER, R. AND GIRARD, J. (1950), Synthèse de titanomagnétites: *Bull. Soc. Chim. France*, **17**, 576–581.
- FRENZEL, G. (1953), Die Erzparagenese des Katzenbuckel im Odenwald: *Heidel. Beitr. Min. Petrogr.*, **3**, 409–444.
- IWASAKI, I., KATSURA, T., YOSHIDA, M. AND TARUTANI, T. (1957), Rapid chemical analysis of magnetite and ilmenite: *Jap. Analyst*, **6**, 211 (in Japanese).
- KUSHIRO, I. (1959), Preliminary note on alkali-dolerite of Atumi District, northern Japan: *Jap. Jour. Geol. Geogr.*, **30**, 259–272.
- SCHWELLNUS, C. M. AND WILLEMSE, J. (1943), Titanium and vanadium in the magnetic iron ores of the Bushveld complex: *Geol. Soc. South Africa Trans.*, **46**, 23–38.
- VINCENT, E. A. AND PHILLIPS, R. (1954), Iron-titanium oxide minerals in layered gabbros of the Skaergaard intrusion, East Greenland: *Geoch. Cosmoch. Acta*, **6**, 1–26.
- VINCENT, E. A., WRIGHT, J. B., CHEVALLIER, R. AND MATHIEU, S. (1957), Heating experiments on some natural titaniferous magnetites: *Min. Mag.*, **31**, 624–655.
- WAGNER, P. A. (1928), The iron ore deposits of the Union of South Africa: *Mem. Geol. Surv. South Africa*, **26**, 29–34.
- WALKER, T. L. (1930), Lodestone from Bon Accord, Transvaal: *Toronto Univ. Studies, Geol. Ser.*, **29**, 17–19.

Manuscript received April 11, 1960.

VERNADSKITE DISCREDITED: PSEUDOMORPHS OF ANTILERITE AFTER DOLEROPHANITE*

MARY E. MROSE, *U. S. Geological Survey, Washington 25, D. C.*

ABSTRACT

Vernadskite crystals from Vesuvius, Italy, are shown to be pseudomorphs of antlerite, $\text{Cu}_3(\text{SO}_4)(\text{OH})_4$, after dolerophanite. Experimental work indicates that these pseudomorphs were formed by the action of moisture from fumaroles on crystals of dolerophanite.

Indexed x-ray powder data are given for synthetic and natural dolerophanite and antlerite.

INTRODUCTION

During a mineralogical investigation of specimens recently obtained from the walls and ceiling of the abandoned Ecton mine in Pennsylvania, several unidentified copper sulfate minerals were observed. In order to attempt to identify them, x-ray powder diffraction patterns were taken of a number of rare copper sulfate minerals. Among these was a pattern of vernadskite (originally spelled vernadskijite and vernadskyte by Zambonini, 1910) obtained from crystals from the only known specimen in the United States. This micromount-sized specimen from Vesuvius, Italy, was the gift of Zambonini to the late Colonel Washington A. Roebeling. It was accompanied by the original label on which Zambonini had written, "part of the original lot." The minerals associated with the vernadskite crystals on this tiny specimen were found to be dolerophanite, anglesite, and conichalcite.

Vernadskite was described by Zambonini as a basic hydrated sulfate of undetermined crystal system. It was found as an alteration product of dolerophanite which had formed during the eruption of Vesuvius in October, 1868. The mineral was said to occur there as aggregates of pale-green birefringent crystals in close association with dolerophanite. The hardness of vernadskite was reported to be $3\frac{1}{2}$; the specific gravity, > 3.3 . The formula given for vernadskite, $4\text{CuO} \cdot 3\text{SO}_3 \cdot 5\text{H}_2\text{O}$ ($= \text{Cu}_4(\text{SO}_4)_3(\text{OH})_2 \cdot 4\text{H}_2\text{O}$), was derived by Zambonini from the following chemical analysis made by Serra (in per cent): CuO 49.15, SO_3 37.01, H_2O [13.84], total [100.00]. Zambonini suggested that vernadskite was produced by the action of acid vapors from the fumaroles on dolerophanite, with the following reaction taking place:

dolerophanite

vernadskite



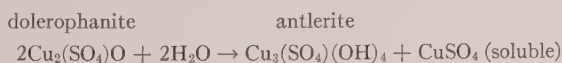
* Publication authorized by the Director, U. S. Geological Survey.

VERNADSKITE DISCREDITED (= ANTLERITE)

Sample preparation of "vernadskite" crystals for an x -ray powder diffraction pattern revealed the presence of included remnants of a light-brown, glassy mineral, thus necessitating very careful handpicking of the material for the powder spindle. The x -ray powder pattern obtained from the carefully selected fragments of "vernadskite" was that of antlerite, $\text{Cu}_3(\text{SO}_4)(\text{OH})_4$; from the minute, light-brown, glassy inclusions, that of dolerophanite.

Closer re-examination of the "vernadskite" crystals on the specimen indicated that they are pseudomorphs of antlerite after dolerophanite. Several crystals were found that were partly dolerophanite and partly antlerite, where the change to antlerite was incomplete.

Experiments then were performed to show that dolerophanite may be converted to antlerite by the reaction of moisture with dolerophanite. Crystals of dolerophanite from Vesuvius, Italy (USNM R8317), averaging 1.00 mm. by 0.50 mm. by 0.25 mm. in size, changed to antlerite slowly and incompletely in distilled water at room temperature over a period of three days. They were completely converted when left immersed in distilled water in an oven at 80°C . for 12 hours, and also when placed in a dry vessel in the presence of a moist atmosphere in an oven at 80°C . for 24 hours. The results of these experiments were checked by means of x -ray powder patterns; in each case a pattern of antlerite was obtained. The experimental work indicates that the following reaction must have taken place near the fumaroles at Vesuvius to result in the formation of these pseudomorphs:



SYNTHESIS OF DOLEROPHANITE, ANTLERITE, AND HYDROCYANITE

Dolerophanite was synthesized so that sufficient material would be available for carrying on experimental work that would check the validity of the proposed reaction. Dolerophanite was easily synthesized (Binder, 1936) by placing finely-powdered $\text{Cu}(\text{SO}_4) \cdot 5\text{H}_2\text{O}$ in an open porcelain crucible in a muffle furnace for one hour at a temperature about 660°C . Synthetic dolerophanite produced in this manner is orange-brown. At a temperature about 640°C . synthetic hydrocyanite (chalcocyanite), CuSO_4 (Hey, 1955), was formed; it is pale greenish gray in color.

When distilled water, hot or cold, was added to the synthetic dolerophanite, the orange-brown powder immediately turned light green. The light-green residue gave the powder pattern of antlerite. The pale-blue filtrate was brought to dryness in an oven at 80°C .; the x -ray powder

TABLE 1. X-RAY POWDER DATA FOR DOLEROPHANITE, $\text{Cu}_2(\text{SO}_4)\text{O}$

MONOCLINIC, $C2/m$
 $a=9.355 \pm 0.010 \text{ \AA}$, $b=6.312 \pm 0.005$, $c=7.628 \pm 0.005$, $\beta=122^\circ 17'_{\frac{1}{2}}$

Borchardt and Daniels (1957) ³		Present Study ²					
Synthetic $\text{Cu}_2(\text{SO}_4)\text{O}$		Synthetic $\text{Cu}_2(\text{SO}_4)\text{O}$ [f. 14347]		Vesuvius, Italy USNM R6084; [f. 14391]			
Measured		Measured		Measured		Calculated	
I	<i>d</i>	I	<i>d</i>	I	<i>d</i>	<i>d</i>	<i>hkl</i>
78	6.46	50	6.451	50	6.443	6.447	001
6	4.91	2	4.937	2	4.935	4.933	110
25	4.75	13	4.755	11	4.760	4.757	111
14	4.63	6	4.659	2	4.659	4.658	201
4	4.02 ⁴	4	3.950	2	3.956	3.954	200
100	3.63	100	3.617	100	3.623	3.619	202
15	3.41	9	3.408	4	3.408	3.407	111
						3.238	112
8	3.29	4	3.220	2	3.228	3.224	002
16	3.15	13	3.153	9	3.156	3.157	020
21	2.83	8	2.840	8	2.835	2.835	021
						2.796	022
47	2.78	30	2.776	21	2.776	2.774	201
8	2.67	3	2.680	2	2.678	2.677	312
94	2.62	50	2.614	42	2.615	2.612	221
34	2.54	25	2.546	18	2.546	2.543	203
10	2.47 ⁴	4	2.468	4	2.468	2.466	220
		1	2.431	1	2.432	2.432	310
8	2.38 ⁴	4	2.381	4	2.377	2.379	222
		4	2.365			2.362	112
6	2.32 ⁴	4	2.324	2	2.331	2.328	402
						2.266	113
52	2.25	35	2.254	30	2.256	2.258	401
						2.255	022
5	2.14	4	2.151	2	2.151	2.254	313
						2.149	003
						2.137	311
						2.128	403
26	2.02	1	2.087	1	2.087	2.084	221
		18	2.028	13	2.028	2.033	130
						2.024	202
						2.020	131
10	1.97	9	1.979	4	1.979		
4	1.86	2	1.870	1	1.868		
7	1.82	4	1.821	3	1.819		
23	1.76	13B	1.769	13	1.767		
5	1.70	3	1.709	1	1.704		

¹ Single-crystal data obtained in this study from a crystal of dolerophanite from Vesuvius, Italy (USNM R6060).

² Films corrected for expansion. B=broad. Camera diameter, 114.59 mm. Nickel-filtered copper radiation ($\lambda=1.5418 \text{ \AA}$). Lower limit of 2θ measurable: approximately 7° (12.6 \AA).

³ Camera diameter, 114.59 mm. Nickel-filtered copper radiation. The relative intensities listed are the ratios of peak heights obtained on a diffractometer trace. The designated bands appeared as a broad line in the x-ray photograph but were resolved in a diffractometer trace.

⁴ These lines correspond to intense lines in the CuSO_4 or CuO x-ray pattern and were thought to be due to the presence of these materials as impurities.

TABLE 1 (continued)

Borchardt and Daniels (1957) ³		Present Study ²					
Synthetic Cu ₂ (SO ₄)O		Synthetic Cu ₂ (SO ₄)O [f. 14347]		Vesuvius, Italy USNM R6084; [f. 14391]			
Measured		Measured		Measured		Calculated	
I	d	I	d	I	d	d	hkl
15	1.67	13	1.678	6	1.678		
4	1.64	2	1.648	6	1.642		
7	1.62						
11	1.61	8	1.616	4	1.615		
14	1.60	6	1.600	4	1.600		
16	1.58	9	1.579	6	1.579		
		5	1.574	3	1.573		
5	1.55	2	1.556	1	1.556		
5	1.53	3	1.535	2	1.534		
4	1.51	3	1.510	2	1.512		
9	1.48	4	1.480	2	1.482		
15	1.47	8	1.469	4	1.469		
7	1.45	2	1.450	2	1.448		
		3	1.430				
8	1.41	4	1.407	3B	1.407		
17	1.39	8	1.389	6	1.387		
		2	1.374	3	1.374		
		2	1.366	1	1.366		
		2	1.343	3	1.342		
		2	1.321	2	1.321		
		2	1.304	2	1.305		
		2	1.293	2	1.292		
		1	1.277	1	1.278		
		2	1.248	2	1.245		
		2	1.233	2	1.232		
		< 1	1.219	< 1	1.217		
		< 1	1.203				
		1	1.188	< 1	1.188		
		1	1.176	1	1.178		
		3	1.166	3	1.166		
				1	1.136		
		4B	1.129	3	1.128		
		2	1.116	1	1.116		
		1	1.106	1	1.106		
		2	1.095	2	1.094		
		2	1.080	2	1.079		
		1	1.062	1B	1.065		
		1	1.052	1	1.052		
		1	1.041	1	1.041		
				1	1.029		
		1B	1.026	1	1.025		
		3B	1.013	2B	1.013		
		2B	1.000	2B	1.001		
Plus additional weak lines all with I < 1.							

data for this dried salt was identical with those given in the ASTM card file for the compound Cu(SO₄)·H₂O. When the dried salt was subjected to a temperature of 100° C. for 24 hours, the x-ray powder pattern remained unchanged. When the temperature was raised to 150° C. and the

TABLE 2. X-RAY POWDER DATA FOR ANTLERITE, $\text{Cu}_3(\text{SO}_4)(\text{OH})_4$
 ORTHORHOMBIC, $Pnam$
 $a=8.24 \text{ \AA}$, $b=11.99$, $c=6.03^1$

de Wolff (1955) ²	Present Study ³							
	Synthetic $\text{Cu}_3(\text{SO}_4)(\text{OH})_4$ [f. 14347]	"Vernadskite" = Antlerite Vesuvius, Italy USNM R6084; [f. 14353]	Antlerite Chuquicamata, Chile USNM C5472; [f. 15077]					
Measured	Measured	Measured	Measured		Calculated			
I d_{hkl}	I d_{hkl}	I d_{hkl}	I	d_{hkl}	I	d_{hkl}	d_{hkl}	hkl
11 6.80	11 6.792	11 6.795	11	6.792	6.789	110		
26 6.01	30 6.021	30 6.018	35	6.026	6.030	001		
					5.995	020		
23 5.40	21 5.405	18 5.406	15	5.405	5.385	011		
100 4.86	100 4.858	100 4.855	100	4.853	4.847	120		
9 4.52	6 4.517	6 4.519	6	4.515	4.509	111		
8 4.13	11 4.125	9 4.127	11	4.122	4.120	200		
					3.897	210		
16 3.79	13 3.785	13 3.783	15	3.788	3.778	121		
77 3.60	71 3.597	71 3.604	71	3.597	3.596	130		
31 3.40	25 3.401	25 3.401	25	3.403	3.403	201		
					3.396	220		
9 3.34	7 3.339	6 3.339	6	3.333	3.331	031		
					3.272	211		
16 3.09	13 3.084	13 3.089	15	3.089	3.089	131		
					3.015	002		
18 3.00	21 2.998	21 3.003	21	3.003	2.998	040		
					2.959	221		
					2.869	230		
	3 2.819	3 2.827	3	2.823	2.817	140		
12 2.762	9 2.765	9 2.763	9	2.763	2.756	112		
9 2.698	9 2.698				2.694	022		
77 2.683	60 2.683	71 2.683	71	2.683	2.677	310		
					2.591	231		
85 2.566	71 2.564	71 2.564	71	2.567	2.560	122		
					2.552	141		
26 2.503	21 2.501	21 2.502	21	2.502	2.497	320		

¹ X-ray crystallographic data obtained by Richmond (Palache, 1939) by the Weissenberg method on a crystal from Remolinos, Vallenar, Chile. Original kX values have been converted to Ångstrom units by the present author.

² Camera diameter, 114.6 mm. Copper radiation ($\lambda=1.5418 \text{ \AA}$). Intensities determined by photometer (Guinier camera).

³ Films corrected for expansion. B=broad. Nickel-filtered copper radiation ($\lambda=1.5418 \text{ \AA}$). Lower limit of 2θ measurable: approximately 7° (12.6 \AA).

TABLE 2 (continued)

de Wolff (1955) ²		Present Study ³					
Synthetic Cu ₃ (SO ₄)(OH) ₄		Synthetic Cu ₃ (SO ₄)(OH) ₄ [f. 14347]		"Vernadskite" = Antlerite Vesuvius, Italy USNM R6084; [f. 14353]		Antlerite Chuquicamata, Chile USNM C5472; [f. 15077]	
Measured		Measured		Measured		Measured	Calculated
I	<i>d</i> _{hkl}	I	<i>d</i> _{hkl}	I	<i>d</i> _{hkl}	I	<i>d</i> _{hkl} <i>hkl</i>
6	2.439						2.447 331
13	2.430						2.439 202
4	2.398	9	2.433	11	2.430	9	2.428 240
7	2.315	2	2.395	3	2.392	2	2.392 212
4	2.307						2.384 212
		7	2.307	7	2.307	9	2.311 132
							2.307 321
							2.303 150
13	2.259	9	2.259	9	2.259	11	2.259 222
							2.249 241
							2.229 051
							2.224 330
							2.151 151
69	2.131	50	2.129	50	2.127	60	2.127 042
							2.119 331
6	2.083	3	2.083	3	2.080	2	2.083 232
							2.073 250
18	2.065	9	2.062	9	2.065	11	2.062 400
							2.058 142
20	2.034	21	2.034	15	2.034	15	2.034 410
							2.025 340
							2.010 003
4B	2.004	6	2.006	6	2.004	6	2.002 312
2	1.951						
9	1.946	13	1.947	11	1.946	13	1.945
7	1.927	3	1.926	4	1.925	3	1.929
3	1.893	3	1.892	3	1.893	3	1.892
12	1.835	9	1.834	11	1.833	8	1.833
15	1.814	11	1.818	13	1.814	9	1.813
2	1.801						
1	1.758	2	1.760	1	1.761	2	1.762
6	1.711	3	1.712	3	1.711	2	1.712
9	1.687	5	1.684	3	1.687	4	1.687
3	1.667	2	1.669	2	1.668	2	1.669
16	1.634	15	1.634	15	1.634	18	1.634
6	1.617	4	1.618	4	1.617	4	1.618
2	1.599	2	1.596	2	1.595	2	1.593
13	1.566	11	1.566	13	1.567	9	1.568

de Wolff (1955) ²		Present Study ³							
		Synthetic Cu ₃ (SO ₄)(OH) ₄ [f. 14347]		"Vernadskite" = Antlerite Vesuvius, Italy USNM R6084; [f. 14353]		Antlerite Chuquicamata, Chile USNM C5472; [f. 15077]			
Measured		Measured		Measured		Measured		Calculated	
I	d _{hkl}	I	d _{hkl}	I	d _{hkl}	I	d _{hkl}	d _{hkl}	hkl
15	1.551	15	1.557	13	1.554	13	1.551		
4	1.525	3	1.527	3	1.526	3	1.526		
12	1.511	9	1.512	7	1.512	6	1.513		
9	1.500	9	1.499	9	1.499	9	1.499		
21	1.481	21	1.482	15	1.483	18	1.483		
2	1.467	2	1.469	2	1.464	2	1.469		
2	1.455	2	1.455	3	1.455	3	1.454		
9	1.438	6	1.438	5	1.436	6	1.438		
1	1.426								
4	1.390	4	1.392	4	1.390	4	1.391		
1	1.365	2	1.363	2	1.364	3	1.361		
3	1.360								
7	1.316	7	1.318	6	1.317	8	1.318		
1	1.281	2	1.281	2	1.280	2	1.282		
3	1.277	3	1.277	4	1.277	4	1.277		
		1	1.251	1	1.254	1	1.253		
		1	1.236	1	1.237	1	1.237		
		1	1.224	1	1.224	1	1.224		
		2	1.215	2	1.214	2B	1.213		
		2	1.200	2B	1.200	2B	1.199		
		2	1.170	2B	1.168	2B	1.170		
		1	1.152	1	1.153	1B	1.154		
		1	1.130	1	1.131	1B	1.131		
		5	1.107	5	1.107	6	1.107		
		2	1.082	1	1.083	1	1.083		
		3	1.073	2	1.074	2	1.073		
		3	1.065	3	1.065	2	1.065		
		3	1.060	2	1.060	2	1.060		
		2	1.051	2	1.051	2	1.050		
		3	1.026	3	1.028	2B	1.027		
		3	1.012	2	1.011	2B	1.012		
		2	0.9995	2	0.9993	3B	0.9991		
		2	0.9878	1	0.9880	1	0.9878		
		2	0.9813			2	0.9810		
		4	0.9723	3	0.9723	3	0.9723		

Plus additional weak lines all with I < 3.

dried salt was held at this temperature for 24 hours, a pattern of CuSO_4 , synthetic hydrocyanite, was obtained.

X-RAY DATA FOR DOLEROPHANITE AND ANTLERITE

All the x -ray powder films made in connection with this study were taken with Cu/Ni radiation ($\lambda = 1.5418 \text{ \AA}$) in Debye-Scherrer powder cameras (114.59 mm. diameter) using the Straumanis and Wilson techniques. Measurements made on the patterns of dolerophanite and antlerite necessitated correction for expansion. Intensities were estimated visually by direct comparison with calibrated intensity film strips of successive step line-exposures related to each other by a factor of $\sqrt{2}$. Interplanar spacings listed in the tables were calculated down to values of $d_{hkl} \geq 2.000 \text{ \AA}$.

A single-crystal x -ray study of dolerophanite from Vesuvius, Italy (USNM R6060), was made with a quartz-calibrated Buerger precession camera using Mo/Zr radiation ($\lambda = 0.7107 \text{ \AA}$). Film measurements were corrected for both vertical and horizontal shrinkage. The cell constants derived from single-crystal x -ray examination are given in Table 1; these data are in excellent agreement with those cited by Richmond and Wolfe (1940) for Vesuvius material.

No indexed x -ray powder data have previously been published for dolerophanite. Table 1 presents observed and calculated interplanar spacings obtained in this study for synthetic and natural dolerophanite. These are compared with the data given by Borchardt and Daniels (1957) for the compound $\text{Cu}_2(\text{SO}_4)\text{O}$ and were found to be in good agreement.

Indexed x -ray powder data for synthetic and natural antlerites are given in Table 2, which lists observed and calculated interplanar spacings, the latter down to $d_{hkl} = 2.002 \text{ \AA}$. These were found to be in excellent agreement with the data obtained by de Wolff (1955) for synthetic antlerite.

ACKNOWLEDGMENTS

I am indebted to Dr. George Switzer of the U. S. National Museum for his kindness in making available the specimens used in this study; and to Howard T. Evans, Jr., of the U. S. Geological Survey who provided helpful discussion.

REFERENCES

- BINDER, OSIAS (1936), Definition des sulfates basiques de cuivre: *Ann. chim.*, 5, ser. 11, 337-409.
- BORCHARDT, HANS J. AND DANIELS, FARRINGTON (1957), Differential thermal analysis of inorganic hydrates: *J. Phys. Chem.*, 61, 917-921.

- HEY, MAX (1955), Chemical Index of Minerals (p. 274). London, British Museum (Natural History).
- PALACHE, CHARLES (1939), Antlerite: *Am. Mineral.*, **24**, 293-302.
- RICHMOND, W. E. AND WOLFE, C. W. (1940), Crystallography of dolerophanite: *Am. Mineral.*, **25**, 606-610.
- WOLFF, P. M. DE (1955), ASTM card 7-407.
- ZAMBONINI, FERRUCCIO (1910), Mineralogia Vesuviana: *Mem. R. Accad. Sci. Fis. Mat. Napoli*, **14**, ser. 2, no. 7, 337-339.

Manuscript received May 1, 1960.

HELIUM IN LIMESTONE AND MARBLE*

FRASER FANALE AND J. L. KULP, *Geochemical Laboratory,
Lamont Geological Observatory, Columbia University
Palisades, New York.*

ABSTRACT

The helium and uranium content of a number of specimens of marble, Iceland spar and fossil shell of known age have been determined. The sedimentary calcite specimens contained only a small fraction of the helium expected, indicating that most of the uranium is external to the lattice. The marbles in contrast contain much more helium than is calculated from the age and the alpha activity. This appears related to the gaseous inclusions in these materials.

INTRODUCTION

This work was undertaken to evaluate the potential use of the alpha-helium method in the dating of carbonate materials. Such mineral phases as marble in metamorphic rocks, crystals of calcite associated with the gangue of hydrothermal deposits and fossil shells are common so that a means of directly dating them would have considerable value.

Earlier theoretical work has shown that reasonably perfect calcite crystals should not permit diffusion of helium at surface temperatures (Keevil, 1940). On the other hand, pioneer measurements on such materials (Keevil, 1950) showed both more and less helium than would be expected from the uranium-thorium content and the age. In view of the imposing experimental difficulties in accurately measuring the extremely small quantities of helium by the older volumetric techniques, the uncertainty in the age of the specimens and the limited selection of mineral types, further investigation was desirable. In the work described below, the helium was determined by the method of isotope dilution and the alpha activity by the radium emanation and fluorimetric techniques.

The terms "excess" and "deficiency" of helium in this study refer to the amount of helium observed compared to the amount expected from the rate of production and the age of the mineral. If either existed it was hoped that the causes could be defined so that evaluation of the potential age method could be made.

EXPERIMENTAL TECHNIQUES

Helium Determination

The helium was determined by isotope dilution using He^3 as a spike. The vacuum systems used for preparation of the He^4 standards and the He^3 spikes have been described by Damon (1956). Two He^3 spikes from

* Lamont Geological Observatory Contribution No. 475.

each set of thirty were calibrated with primary He^4 standards. The average deviation from the mean of the calibrations was about 2% and indicates uniformity of He^3 pressure throughout the set.

The gas liberation and purification system is similar to that described by Damon. The carbonate samples are not actually fused but merely decrepitated at about 800° C. in which process the helium is liberated with the carbon dioxide. When the sample has begun to decrepitate, the He^3 tracer is admitted to the furnace side of the system. Since pure carbonates have such a low uranium content, it is often necessary to process 10–30 gm. samples. Thus, up to a third of a mole of CO_2 may be liberated. Essentially all the CO_2 freezes at liquid nitrogen temperatures in the large cold trap adjacent to the furnace. Other gases are pumped out of the furnace by a mercury diffusion pump specially designed to pump against high back pressures. They pass through a U-tube filled with CuO and maintained at a temperature of 600° C. where any hydrogen reacts to form water. The diffusion pump is allowed to continue pumping out the furnace side after decrepitation is complete, until a vacuum of 10^{-6} mm. of Hg is achieved in the furnace volume. Still more pumping time is allowed to ensure equilibration and quantitative transfer of helium out of the furnace. The furnace is then isolated from the sample purification side by means of a stopcock and gases condensed on the charcoal trap at liquid nitrogen temperatures are successively sublimed and recondensed, as an aid to equilibration. Final purification is achieved by allowing these gases to react with metallic calcium at 700° C. When this process is completed, the helium is compressed into a sample breakseal by allowing mercury to rise into a 500 ml. reservoir at the top of which is attached the breakseal. All of the helium is thus compressed into the sample breakseal which is then detached and transferred to the sample introduction system of the mass spectrometer.

The standard deviation on individual helium measurements was 6%. Blank runs on the fusion system included mock fusions with Pleistocene coral and barnacle samples. All blanks were negative (see Table 1); however, the amount of atmospheric helium introduced to the system during the operation of the CuO furnace cannot be tolerated for very low level measurements. Hence, in the case of fossils, removal of impurities by adsorption on charcoal at liquid nitrogen temperatures must be substituted for the chemical removal of the impurities.

Regardless of which procedure is used, gross fusion system leaks can be effectively monitored by scanning the Ne^{20} peak during the spectrometer measurement. This is not applicable to diffusion leaks however, since neon will not diffuse significantly through quartz and vycor at elevated temperatures, whereas helium will.

TABLE 1. HELIUM CONTENT OF SPECIMENS OF CALCIUM CARBONATE

Sample	Description	Procedure used to purify helium	Blank as- soc. with procedure (microliters He ⁴)	Total He ⁴ in sample (microliters)	Weight of sample (g)	He ⁴ (microliters/g. rock)
I. <i>Sedimentary or Low Temperature Origin</i>		Charcoal at Liq. Air temp.	.002			
KT-1	Ammonite composite from U. Cret. Pierre Shale, Mobridge, S. Dakota, Baculites (sp.)			.034 ± .006	10.6	.0032 ± .0006
SB-3	U. Cret. Belemnite from N.J. coastal plain.			< .0024	14.4	< .0002
No. 475A	Pleistocene Barnacles, Van- couver Island, British Columbia			< .0020 < .0030	13.5 10.4	< .0002 < .0003
JS-1	Iceland Spar, Joplin, Missouri			< .002	20.6	< .0002
II. <i>Metamorphic Origin</i>		CuO	.02			
IN-1	Inwood Marble, Thornwood, N.Y., crystal size ~5 mm.			.30 .88	10.4 31.6	.029 ± .002 .028 ± .002
RC-1	Pink Carbonate from Sterling Zinc Mine, Ogdensburg, N.J. 2550' level. Avg. crystal size 5-10 mm.			.90	33.3	.027 ± .002
BH-3C	Same as RC-1 except sample colorless.			.61	25.6	.024 ± .002
55K	Grenville marble from No. 1 pit along Rt. 7 about 4 mi. east of Deloro turnoff on Rt. 7 east of Marmora, Ont. Avg. grain size ~2 mm. contains about 3% tremolite.			4.34 6.75 11.5 18.2 7.10 12.7 18.5 25.7 6.00 5.09	8.343 10.81 22.98 39.56 11.20 26.39 33.01 47.57 12.75 9.83	.52 .62 .50 .46 .64 .48 .56 .54 .47 .51
						Avg. .53 ± .02
55K						
200 mesh				2.31	10.71	Avg. .21 ± .02

Helium measurements were made using the first order, 60°, 6 inch radius mass spectrometer described by Carr and Kulp (1957). The present helium sensitivity of the instrument is about one millivolt per 10⁻⁵ c.c. before the molecular leak using a 10" ohm reed lead resistor. The half time of helium before the leak is about 40 minutes. Thus fractiona-

tion of the helium isotopes through the leak can, during the course of a normal run, alter the ratio by as much as 3%. The observed ratios, however, are extrapolated back to the time of presentation of the sample before the leak, or a fixed time thereafter. Since this procedure is followed both in the initial spike calibration and in sample runs, the fractionation effect is essentially canceled. The introduction system is static leak-tested prior to liberation of the sample using the A^{40} peak and, as stated earlier, the fusion system can be checked for gross leaks by scanning the Ne^{20} peak during the course of the run. In addition, the H_2 peak is scanned to insure that there is no significant contribution to the mass-3 peak from HD.

Radium Measurement

Radium was determined by dissolving samples in phosphoric acid and counting the radon gas in equilibrium with the dissolved radium. Radium determinations were reproducible to within 10%. Assuming complete secular equilibrium in the rock, the uranium content of the rock can be calculated and compared with that measured by other techniques. The agreement is good considering the extremely low concentrations of uranium in these materials and the uncertainty in the absolute level of fluorimetric analysis (Table 2).

It appears that the radium measurement can be used to assess the helium production rate in these samples. This is largely because the average limestone has a thorium:uranium ratio of only 0.5 as compared to 3.5 for an average granite. Furthermore, any given amount of thorium produces alphas at less than one-fourth the rate of an equal amount of ordinary uranium. It would be expected then, that the total rate of helium production would be within about 10% of that predicted on the basis of uranium or radium analyses alone.

Fluorimetric Procedure

Uranium determinations by the fluorimetric method were performed on all samples. A combination of dilution and solvent extraction was used to separate the uranium from possible interferences and quenchers. Aluminum nitrate was used as a salting agent and the uranium was extracted into ethyl acetate. The ethyl acetate was evaporated off gold dishes and the uranium then incorporated into buttons of flux containing sodium fluoride. The intensity of fluorescence was then determined using a Jarrell-Ash G-M Fluorimeter. Samples were run in groups of ten including three standards and a blank. Reproducibility was about 10% in this concentration range.

TABLE 2. MEASUREMENTS OF THE ALPHA ACTIVITY
parts per million uranium

Sample	Radium given as 10 ⁻¹² g. Ra/g.	Calculated from Radium Content	Fluorimetric Measurement	Alpha activity of rock based on fluorimetric U anal- ysis α 's/mg./hr.
KT-1	.44 \pm .04 (unleached) .36 \pm .04 (leached)	1.2 \pm .01 1.0 \pm .01	1.3 \pm .1 (unleached)	.48 \pm .05
SB-3			.31 \pm .03 .25 \pm .03 — .28 \pm .03 Av.	.10 \pm .01
ML-1†	.31 \pm .03 .29 \pm .03 — .30 \pm .03 Av.	.87 \pm .09 .82 \pm .08 — .85 \pm .09 Av.	1.10 \pm .10 1.25 \pm .10 — 1.18 \pm .10 Av.	.44 \pm .04 .38 \pm .01*
JS-1	.046 \pm .005	.13 \pm .01	.13 \pm .01 .10 \pm .01 .11 \pm .01 .16 \pm .01 — .12 \pm .01 Av. .19 \pm .01 (<200 mesh, leached)	.045 \pm .005
RC-1	.0035 \pm .0004 .0037 \pm .0004 — .0036 \pm .0004 Av.	.010 \pm .001 .010 \pm .001 — .010 \pm .001 Av.	< .02 — < .02	< .007
SH-3H			< .02 < .02	< .007
EN-1	.034 \pm .004 .039 \pm .004 — .037 \pm .004 Av.	.10 \pm .001 .11 \pm .001 — .11 \pm .001 Av.	.12 \pm .01 .10 \pm .01 — .11 \pm .01 Av.	.041 \pm .004
GSK	.056 \pm .006 .051 \pm .005 — .054 \pm .006 Av.	.16 \pm .02 .14 \pm .01 — .15 \pm .02 Av.	.39 \pm .04 .23 \pm .03 .27 \pm .03 — .30 \pm .03 Av.	.11 \pm .01

* Isotope Dilution Method performed by J. C. Cobb, Lamont Geochemical Laboratory gave 1.02 \pm .02 ppm uranium.

† Oolitic limestone from the Spergin formation (Mississippian). See Sackett 1958.

RESULTS

The sample descriptions and the helium concentrations are given in Table 1. Sample KT-1 was found to be entirely aragonite by x-ray diffraction. The sample of Pleistocene barnacles represents a blank. SB-3 and JS-1 also showed negligible helium. The reproducibility shown by

samples IN-1 and G5K are satisfactory. The error given on the average of the determinations of G5K is the standard error on the mean.

The radium and uranium determinations are given in Table 2. The estimated uranium content from the fluorimetric measurements and that inferred from the radium measurement assuming radioactive equilibrium is the same within the experimental uncertainties for all samples, except the Grenville marble where the uranium content from the fluorimetric determination is double that calculated from the radium content. This implies radioactive equilibrium for all cases except the Grenville marble. The ML-1 sample was also analyzed for uranium by isotope dilution. The figure obtained agreed with the average of the uranium content calculated from the radium and fluorimetric analyses. The alpha activity of the rock was estimated in each case from the fluorimetric analyses and the assumption that the thorium content is negligible.

The alpha activity of most of these samples is too low for direct determination except in the case of KT-1 and ML-1. Using the method described by Kulp *et al.* (1952) ML-1 was counted after calibration of the system with NBS standards. The alpha activity agree with that predicted from the fluorimetric analysis within the experimental errors of both methods suggesting that the Th:U ratio was less than 0.4. This is in agreement with the result of Sackett (1958) who obtained a ratio Th:U of .15 by neutron activation analysis. The Th:U ratio is normally less than 0.5 in reasonably pure carbonates. Since the specific alpha activity of the thorium is only one-fourth that of uranium, the contribution from thorium to the total alpha activity in these samples is probably negligible.

The alpha activities reported in Table 2 are 10^{-1} to 10^{-3} times that for typical granitic rocks.

HELIUM LOSS IN ROCKS AND MINERALS

Keevil (1940) has treated the diffusion of helium in various crystal lattices from a theoretical point of view. In the absence of suitable experimental data such an approach is necessary to estimate potential losses of helium.

Distances of approach of helium to neighboring ions in a crystal lattice depend on weak attractive forces resulting from perturbations or induced polarizations (~ 130 cal/g mole) and important repulsive forces which change sharply with distance and which determine the effective "size" of the helium atom. Equilibration separation from oxygen corresponds to an interatomic distance of about 2.3 \AA and to bring the helium atom within the range corresponding to an effective helium radius of $.95 \text{ \AA}$ would require 13 k cal/mole . Experimentally determined values indicate that this

is a minimum radius but even this is large compared with spacings in most crystal structures. This is indicated by the fact that diffusion experiments with glasses show that the diffusion rate is strongly dependent on the radius of the inert gas (T'sai and Hogness, 1932). In silica glass the average pore openings larger than the helium atom are about 1.3 Å in radius. It is generally true that if the channels are less than 2 Å in diameter the energy of activation to move helium along the channel is very high and rises sharply with decreasing channel width. In old glasses that have partially recrystallized it has been observed that the rate of diffusion is greatly reduced. When glasses completely recrystallize with disappearance of the larger metastable holes, the activation energy would be expected to greatly exceed that which the helium atom possesses as the result of its thermal agitation

$$\left(\bar{E}_{km} = \frac{3}{2} kT\right).$$

On the other hand, the helium atom impinges, with some energy, on the potential barrier between it and the next potential valley with a frequency which is very high ($\sim 10^{13} \text{ sec}^{-1}$) throughout the entire course of geologic time. Knowing the frequency of vibration and taking $e^{-E/kT}$ as the probability that, at any instant, a given helium atom possesses enough energy to get it over an opposing potential hill of height E , the number of times a helium atom vibrating between two such hills could surmount one in any length of time can be calculated. The probable distance of diffusion of a helium atom in a crystal in any time is then, according to the Einstein relation, the product of the time, the mean path length from one valley to the next, and the average velocity of the vibrating helium atom. Keevil (1940) performs these calculations considering the effect of thermal motion of the bordering ions in temporarily widening the channel so that the helium atom might pass. There is required synchronicity of vibration of all the ions away from the channel rim while at the same time the helium atom possesses enough energy to allow it to pass through the temporarily widened channel. The probability that all this will happen is the product of two terms. The first is the probability that all the n atoms around the rim will vibrate a given distance away from the rim at a given moment and is, of course, the n th power of the probability that this will occur for any one individual which in turn depends on the vibrational force constant of the ions. The second is the probability that at just this moment the helium atom will possess enough energy to get it through the channel before it narrows again. At any temperature this product, which represents the key rate determining step in the diffusion process, reaches a maximum value at a certain vibrational

amplitude. Because Keevil (1940) uses this vibrational amplitude corresponding to the highest diffusion rate and because of the relation used for dependence of repulsive force on distance, his calculations can be regarded as conservative. Even so, they indicate that the diffusion path of a helium atom through most crystal lattices at 600° K. during geologic periods of time would only be a few interatomic distances long.

It is improbable that helium is "exsolved" since it is present in such low quantities. Thus it has never been possible to correlate helium "retentivity" with helium content except where minerals are actually metamict. Some loss might be expected where alpha tracks end in minute cracks resulting from substitution of different sized ions or from surface tension during growth. These cracks may be spaced on a very fine scale down to about 10^{-6} cm., but, barring reflection phenomena at phase boundaries, there is no reason to expect the per cent of the alpha tracks which end in these cracks to exceed the volume per cent of the mineral represented by the cracks and this is very low. If cracks were present with a spacing of 10^{-6} cm. throughout a crystal, and a sharp rise in structural strength at these edge lengths for some crystals indicates that this may be the case, the diffusion constants are still about a factor of 10,000 too low at 300° to allow much diffusion; but at 600° it would be significant. The barrier height implied in this calculation is based on measured distances between oxygen atoms and is about a factor of ten higher than the lower limit set by Rayleigh for calcite; but ordinarily, since the diffusion rate is such a sensitive function of channel width, it is not only the equilibrium interatomic distance between oxygen atoms but also the ability of the oxygens to vibrate about this mean position that determines the diffusion rate. Thus critical factors include the force constant for vibration of oxygen atoms and the effect of local distortion due to the presence of the large foreign helium atom in the structure.

All attempts to force helium through common minerals, including calcite, have failed. Rayleigh (1936) succeeded in setting a lower limit on the activation energy of 21.5 k cal mole. Unfortunately, calculations based on a non-rigid lattice model show that it is still just possible that, if the activation energy is no greater than this, the diffusion distances might, in geologic time, approach the crack spacing in the crystal. Rayleigh also had determined the activation energy for mica at a similar value but was later able to raise the limit to 47 k cal mole which prohibits significant helium diffusion in mica perpendicular to the cleavage. It is important to note that all of the experimental results on diffusion through minerals were negative which means that the activation energy is probably higher than 21.5 k cal/mole. At least, although they are not very definitive, the experimental data accumulated to date have not contradicted the

theoretical conclusions of Keevil. Diffusion theory and experiment, then, indicate negligible helium loss by diffusion through ordinary crystal lattices in geologic time.

In contrast, essentially all of the helium age determinations made during the last thirty years seem to indicate that, in most rock forming minerals, the ratio of observed helium to expected helium is less than unity. This suggests that the answer lies in the location of the uranium atoms.

If the activity is surficially concentrated (Hurley, 1956), in intergranular microcrystals of uranium and thorium minerals in igneous rocks, in association with a free organic phase in sediments or merely on grain boundaries, the helium from this uranium-thorium and their decay products would be expected to leave the rock. Thus even if the helium produced within the calcium carbonate lattice were quantitatively retained, the ratio of observed to expected helium would be less than unity.

DISCUSSION

It may be seen from Table 3 that the specimens of calcium carbonate crystal formed at low temperature all show a deficiency of helium, whereas those found in a metamorphic environment show an excess of helium.

The alpha activity and the helium content are taken from Tables 1 and 2.

Probable ages were assigned to the samples on the basis of regional U-Pb and K-A dates. The absolute ages assigned to the fossils are consistent with an age of 90 m.y. for the base of the Santonian (U. Cret.)

TABLE 3. HELIUM RETENTION IN FOSSIL SHELLS AND LOW TEMPERATURE DOG-TOOTH SPAR

Sample	Alpha Activity α 's/mg./hr.	Geologic Age	Expected He ⁴ content mic./g.	Measured He ⁴ content mic./g.	% Retained
KT-1	.48 \pm .05	90	.014 \pm .001	.0032 \pm .0006	22
SB-3	.10 \pm .01	90	.0030 \pm .0003	< .0002	< 7
JS-1	.045 \pm .005	100	.0015 \pm .0007	< .0002	< 13
<i>Helium Excess in Marble</i>					(% Excess)
G5K	.11 \pm .01	1040	.041 \pm .004	.53 \pm .03	\sim 1200
IN-1	.041 \pm .004	360	.0050 \pm .0005	.029 \pm .002	\sim 600
RC-1	< .007	850	< .002	.027 \pm .002	>1000
SH-3C	< .007	850	< .002	.024 \pm .002	>1000

(Kulp, 1959). Concordant U-Pb dates on zircon and uraninite indicate a probable date of about 1040 for the Grenville event (Eckelmann and Kulp, 1957). Potassium-argon ages on Sterling Hill micas give an age of about 850 m.y. (Long and Kulp, 1959) for the last major metamorphism of the area. Potassium-argon ages on phlogopite from the Inwood marble and surrounding rocks (Long and Kulp, in press) indicate a major event at about 360 m.y. It is possible that the Inwood marble was formed as early as 850 m.y. and that the 360 event did not heat the rock sufficiently to cause loss of helium. The fact that the 360 event produced widespread pegmatites, however, points to a significant metamorphic event. It is also possible that the Sterling Hill marbles may have been produced at about 1100 m.y. ago and survived the 850 m.y. event. As will be shown below, the uncertainties in the true age are not critical to the argument.

On the basis of the ages and the alpha activities listed in Table 3, the "expected" helium content of the rock is calculated. This is the amount of helium produced in the rock by radioactive decay since its formation. The per cent "excess" helium is defined as

$$\frac{\text{He}_{\text{measured}} - \text{He}_{\text{expected}}}{\text{He}_{\text{expected}}} \times 100.$$

Likewise in case the mineral contains less than the expected amount and hence has lost helium, the per cent retained is,

$$\frac{\text{He}_{\text{measured}}}{\text{He}_{\text{expected}}} \times 100.$$

The results on the fossil shells KF-1 and SB-3 show that most of the uranium must be located on the surface of grains or in association with the organic phase. Since the ammonite composite, KT-1, is still aragonite the loss of helium cannot be explained by loss during recrystallization of the primary calcium carbonate to calcite. Some evidence for the surficial uranium may be the lower radium content observed for KT-1 after leaching with acid (Table 2). In most cases, as in JS-1, it is unlikely that leaching can be sufficiently selective to determine the fraction of uranium in surficial sites.

The dog-tooth spar from the Joplin, Missouri lead deposits was surely formed at low temperature and atmospheric pressure. It shows loss of at least 85% of its helium if the time of formation is accepted. The latter is probably uncertain by a factor of two but this does not alter the picture.

It is concluded that the helium produced from the uranium atoms and their decay products in the calcite or aragonite lattice is quantitatively retained. In shells and other low temperature products this may represent only a small fraction of the total helium generated in the sample in the course of its geologic history, thus accounting for the low retentivity.

Since the ratio of external to internal uranium is highly variable, no retentivity factor can be defined to correct the experimental He/U ratio to the actual one for the system as a whole throughout its geological history. As a result it appears that the helium age method cannot be used in sedimentary carbonates. It is probable that this conclusion applies to all minerals with low uranium content and high internal surface area.

The results on the helium content of a selected group of marbles indicate that there may generally be a large excess of helium. The Grenville sample (G5K) has twelve times the helium expected from the uranium content. The samples from New Jersey Highlands (RC-1 and SH-3C) appeared to have an equally large excess but here the uranium analysis is

TABLE 4. EXCESS HELIUM AND ARGON IN MARBLES AND BERYL

Sample	He^4 micro'iter /g.	$\text{He}^4/\text{A}^{40}$
G5K	.53	>2000
G5K (<200 mesh)	.21	
IN-1	.029	
SH-3C	.024	
RC-1	.027	
Average of 12 beryls (Damon and Kulp, 1958)	27	21 ± 15

too low to permit an accurate estimate to be made. The sample from the Inwood marble shows six times the expected helium content.

The presence of "excess" helium in these samples is evidence for the inherent high retentivity of the calcite lattice. Under magmatic-metamorphic conditions it appears that helium can be trapped in inclusions in the growing calcite crystals. The quantity that is trapped is far less than is observed in beryl and cordierite lattices (Damon and Kulp, 1958) which contain channels of sufficient size to incorporate large foreign ions readily. For example, the Grenville marble shows 10 times less non-radiogenic helium than the average beryl (Table 4). This is probably present in small vacuoles in the calcite since all of these marbles showed liquid-gas inclusions frequently localized on sharply defined planes traversing intergrain boundaries. Microscopic examination of a <200 mesh fraction revealed some tendency to preferred breakage along these inclusion-rich planes. Thus it was not surprising that grinding to less than 200 mesh decreased the helium content by more than a factor of two.

If the uranium were fairly homogeneously distributed in the rock, the produced helium should be even more so because of the range of the alpha particles. Hence for nearly perfect crystals the loss of helium on

grinding should not be significant unless the resulting fragments were of unit cell dimensions. The observed loss confirms the conclusion that the excess helium is largely located in inclusions. If significant diffusion had occurred it might be expected that the helium would be more homogeneously distributed.

It is particularly interesting to note that after grinding, the helium content of the Grenville limestone dropped by more than a factor of two although a significant fraction of the inclusions remained intact. Thus it appears that it may be possible to obtain an approximation to the true age of marbles from the uranium-helium ratio under certain conditions, particularly if the sample had only large inclusions and no small ones. Nevertheless, the method does not appear to have much practical value due to the large uncertainties involved.

A single determination of the argon content of the Grenville specimen indicates a much higher ratio of helium to argon than the average for the beryls formed in the pegmatite environment. Possibly this reflects the U/K ratio of the immediate environment during metamorphism but more measurements would be required to establish this hypothesis.

CONCLUSIONS

1. The gross helium retentivity in shells and sedimentary carbonate crystals appears to be small and highly variable. Although the actual retentivity of the calcite lattice is considered to be essentially 100%, the low gross retentivity is due to the high ratio of external to internal uranium.

2. Coarse-grained marbles appear to retain their helium quantitatively, but "excess helium" is present due to fluid inclusions containing gases present in the metamorphic environment. Upon grinding, the marble may break along the planes containing the fluid inclusions and thus reduce the helium/uranium ratio.

3. The helium method does not appear to be a practical geochronometer for carbonates.

ACKNOWLEDGMENTS

This research was supported by the Atomic Energy Commission under Contract AT(30-1)-1669.

The authors are grateful to Professor Paul E. Damon, University of Arizona, for his suggestions on technique and interpretation. Professor K. K. Turekian, Yale University, kindly provided the ammonite composite KT-1. Professor H. A. Potratz of Washington University supplied sample ML-1. Discussions with Professor W. S. Broecker, Dr. L. E. Long and G. Erickson of the Lamont staff were helpful.

REFERENCES

- CARR, D. R. AND KULP, J. L. (1957), The potassium-argon method of geochronometry: *Geol. Soc. America Bull.*, **68**, 763-784.
- DAMON, P. E. (1956), Helium and argon in the lithosphere and atmosphere: Ph.D. thesis, Dept. of Geology, Columbia University.
- AND KULP, J. L. (1958), Excess helium and argon in beryl and other minerals: *Am. Mineral.*, **43**, 433-459.
- ECKELMANN, W. R. AND KULP, J. L. (1957), Uranium-lead method of age determination, Part II: North American Localities: *Geol. Soc. America Bull.*, **68**, 1117-1140.
- HURLEY, P. M. (1956), Variations in isotopic abundances of strontium, calcium and argon and related topics: *M.I.T. Annual Progress Report for 1955-56*, U. S. Atomic Energy Commission Contract AT (30-1)-1381.
- KEEVIL, N. B. (1940), Interatomic forces and helium in rocks: *Proc. Am. Acad. Arts and Sci.*, **73**, No. 11, 311-359.
- (1950), Radioactivity and mineral deposits: *Am. Mineral.*, **35**, 816-833.
- KULP, J. L., HOLLAND, H. D. AND VOLCHOK, H. L. (1952), Scintillation alpha counting of rocks and minerals: *Amer. Geophys. Union Trans.*, **33**, No. 1, 101-113.
- (1959), Absolute age determination of sedimentary rocks: *Proc. Fifth World Petroleum Congress, Section I, Paper 37*, 689-704.
- LONG, L. E. AND KULP, J. L. (in press), Isotopic age study of the metamorphic history of the Manhattan and Reading Prongs: *Geol. Soc. America Bull.*
- RAYLEIGH, J. W. S. (1936), Studies on the passage of helium at ordinary temperature through glasses, crystals, and organic materials: *Proc. Roy. Soc. (London)*, **156**, Series A, 350-357.
- SACKETT, W. M. (1958), Ionium-uranium in marine deposited calcium carbonates and related minerals: Ph.D. thesis, Dept. Chemistry, Washington University, St. Louis, Mo.
- T'SAI, L. S. AND HOGNESS, T. (1932), The diffusion of gases to fused quartz: *Jour. Phys. Chem.*, **36**, 2595.

Manuscript received April 21, 1960.

NEW DATA ON DEWEYLITE .

DAVIS M. LAPHAM,* *Bureau of Topographic and Geologic Survey, Harrisburg, Pennsylvania.*

ABSTRACT

The several sub-varieties of deweylite from Cedar Hill, Pennsylvania, formed from aqueous, possibly colloidal, low temperature solutions by the alteration of pre-existing magnesium silicates in serpentinite. Fluorescent white deweylite, pseudomorphs of deweylite after aragonite, and iron and nickel bearing varieties are described. Molecular water is characteristic of deweylite and is present in varying amounts. The ratio of tetrahedral cations to octahedral cations is approximately 1:1. The structure of deweylite is similar to that of antigorite, containing a superlattice probably in the a direction of about $8\frac{1}{2} a_0$. Line broadening is extreme and characteristic, and many of the antigorite reflections are weakly diffuse or absent. Analysis of the data suggests that Cedar Hill deweylite may be a dioctahedral modification of antigorite with an undulant character in the ab plane and containing crystallites on the order of a few hundred Angstroms. No single crystals or well crystallized samples of deweylite have been discovered.

INTRODUCTION

During the course of a Pennsylvania Geological Survey field mapping project in the serpentinized ultramafics of southeastern Pennsylvania two previously undiscovered minerals were found in a serpentinite fault breccia in the Cedar Hill serpentinite quarry in Lancaster County. One of these is bright emerald green, massive and possesses a conchoidal fracture. The other occurs as small, white radiating crystal groups found in cavities within the breccia matrix. A cursory x-ray examination showed that Debye-Scherrer patterns for both of these minerals correspond to previously published diffraction patterns for deweylite. Since the color and crystal form of these specimens differ from other known occurrences, and since the properties and structure of deweylite are not well known, this investigation was undertaken to shed more light on this rather unusual mineral.

Several occurrences and analyses of deweylite have been described in the literature (Rogers, 1918; Ross and Shannon, 1925; Daly, 1935; Selfridge, 1936; Konta, 1951). Rogers (1918) and Daly (1935) report an occurrence in limestone associated with a calcite-brucite rock and spatially related to a nearby quartz monzonite porphyry dike. Rogers (p. 584) states that the sequence of mineral formation, from oldest to youngest, is periclase-brucite-hydromagnesite-deweylite. Daly (p. 651) questions the supergene origin ascribed to this deweylite by Rogers, stating "that the genesis of these silicates (chrysotile and deweylite) can be assigned to the action of solutions emanating from this dike on previously formed

* Published by permission of the State Geologist, Pennsylvania Geological Survey.

minerals (epidote or diopside . . .) and thus in this case their origin would be hypogene." However the majority of deweylite occurrences are associated with serpentinites in fractures which post date at least initial serpentinization and are generally believed to be of supergene origin from colloidal suspensions (Konta, 1951, p. 420).

Optical, differential thermal, x-ray, and chemical data have been given for deweylite, but only on the specimens described by Konta have all these analyses been performed for each sample. In general, deweylites reported in the literature have the following characteristics: 1) a close resemblance to the serpentine structure but with the absence of many (*hkl*) reflections and a characteristic line broadening; 2) a chemical composition approaching that of serpentine but with a higher Si/Mg ratio and more molecular water, and 3) variable indices of refraction lower than those for chrysotile or antigorite.

GEOLOGIC OCCURRENCE

The Cedar Hill Quarry from which these deweylite samples came is located $\frac{1}{2}$ mile east of Pennsylvania Route 222-72 just north of the Pennsylvania-Maryland state line, in Lancaster County. Deweylite may also be found at the old Wood chromite mine about one mile to the east and has been reported on by Selfridge (1936, p. 483, 484, 499).

The Cedar Hill Quarry is composed of serpentinitized dunite which has been intruded by siliceous pegmatites, highly fractured, faulted, and deeply weathered along fault and fracture planes. This serpentinite is part of a NE-SW trending belt of ultramafics, mafics, and granitic pegmatites which extend from the Susquehanna River eastward about 15 miles.

There are three distinct occurrences of deweylite at Cedar Hill: 1) reddish brown deweylite associated with limonite in a steeply dipping fault, often slickensided so that it has the appearance of fault gouge; 2) red, yellowish green, and pale yellow in a nearly horizontal fracture and crudely zoned with red along the contact and pale yellow in the center of the fracture, and 3) white pseudomorphs, massive white, and massive green in a vertical fault breccia containing open cavities with small magnesite stalactites, brucite crystals, and deweylite pseudomorphs.

The breccia matrix in the latter occurrence contains blebs of green and white fluorescent deweylite surrounded by a mixture of magnesite and dolomite. Angular fragments of spotted serpentine from a few millimeters to several feet in size are present, often with a narrow rim of chalcedony between the serpentine and the magnesite-dolomite matrix. The spotted appearance of the serpentinite in the breccia is the result of differential weathering of serpentine and olivine.

Assuming that the red-brown deweylite samples in the two unbrecciated fracture systems are contemporaneous, the paragenesis of the deweylite and associated minerals in the above three occurrences may be divided into two groups. (1) In the unbrecciated fractures the red-brown deweylite was followed by both yellow and white fluorescent varieties. A similar paragenetic sequence has been described by Konta (1951, p. 420). This fracture system has been displaced by a later fracture system containing chlorite and vermiculite. (2) In the breccia, the following sequence was observed, from oldest to youngest: chalcedony, dolomite and magnesite, replaced by white fluorescent and green deweylite, brucite, botryoidal and stalactitic magnesite, aragonite, deweylite pseudomorphs, and lastly, opal and hydromagnesite which coat the pseudomorphs (Fig. 1, *b-e*). Sepiolite is associated with some of the deweylite, but its paragenetic relations are not known.

Although the solutions from which deweylite formed are often considered to have contained colloidal suspensions, their source has been variously thought to be both hypogene and supergene. One of the reasons for these two hypotheses lies in its association with both contact metamorphic magnesium silicates and also with supergene magnesium carbonates and hydroxides. The occurrence of the Cedar Hill deweylite in fractures and in a serpentinite breccia indicates that it formed after at least some of the faulting occurred, and that this faulting itself postdates serpentinitization. Numerous vertical faults and fractures contain chlorite borders and vermiculite centers. The relation between these and the deweylite is not clear. Although one horizontal fracture containing deweylite ends abruptly at a chlorite-vermiculite fracture filling, another, a horizontal deweylite fracture, appears to continue through the chlorite-vermiculite. The time of the deweylite formation relative to the chlorite-vermiculite crystallization is further obscured by the fact that the vermiculite is probably a supergene alteration product of an earlier hydrothermal mineral assemblage (Klup and Brobst, 1954; Bassett, 1959, p. 293-295).

Several observations bear upon the temperature of deweylite formation. The dolomite-magnesite-deweylite matrix in the fault breccia does not appear to have replaced the angular fragments of serpentine and thus temperatures of formation for this assemblage must have been within the stability range of serpentine, below 500° C. (Bowen and Tuttle, 1949; Gillery 1959, p. 144-146). Numerous cavities in the breccia also indicate that these minerals formed in an open fracture rather than by replacement. Magnesite, brucite, opal, and hydromagnesite, and to a lesser extent deweylite, are found throughout this serpentine belt as a surficial coating on open fracture surfaces and appear to be secondary

minerals of supergene origin. In addition to these data the spotted appearance of the serpentine in the breccia well below the zone of surficial weathering, the presence of limonite associated with the reddish brown deweylite, and also a possibly supergene vermiculite nearly 100 feet below the surface all attest to the activity of supergene ground water solutions migrating along fractures.

Magnesite within the breccia cavities is typically stalactitic and botryoidal, with a glassy appearance and a conchoidal fracture. Deweylite has a similar appearance and is composed of aggregates of colloidal size. Such physical features are characteristic of low temperature mineralization and may represent crystallization from a colloidal gel formed by the alteration of pre-existing magnesium silicates. Likewise, Konta (1951, p. 420) concludes that the very similar Mladotice deweylites in serpentine are of low temperature origin from colloidal suspensions.

DEWEYLITE PSEUDOMORPHS

Representative examples of the deweylite forms are shown in Fig. 1. Sketches (a), (b), and (d) indicate an orthorhombic, or possibly monoclinic, habit; (c) is orthorhombic (pseudo-hexagonal); (e) is the most common form and consists of a central plate of deweylite coated with hydromagnesite. Pseudomorphs are typically grouped in radial clusters. The associated botryoidal and stalactitic 'pencils' of magnesite are illustrated in (d).

A search of the literature was undertaken to determine the original crystal which the pseudomorphs represent. Although positive identification is not possible, the pseudomorphs most closely resemble aragonite (see Goldschmidt, 1913, p. 97, 98, 104) which is relatively common in crystal clusters both at Cedar Hill and the nearby Wood chromite mine.

A survey of the literature and of the excellent collection of serpentine pseudomorphs at the Mineralogical Museum at Columbia University revealed pseudomorphs after pectolite, chrysolite, chlorite, chondrodite, dolomite, calcite, garnet, enstatite, hornblende, tremolite, pyroxene, brucite, apatite, and magnetite. This, however, is believed to be the first report of deweylite after aragonite.

OPTICAL PROPERTIES

Indices of refraction (Table 1) were determined in white light with a daylight blue filter. The accuracy of determination is considered to be ± 0.003 .

Birefringence is on the order of 0.004 to 0.006. Two types of structures were noted: very fine-grained aggregates, and fibrous bands resembling chalcedony. Where both materials occur together, the banded deweylite

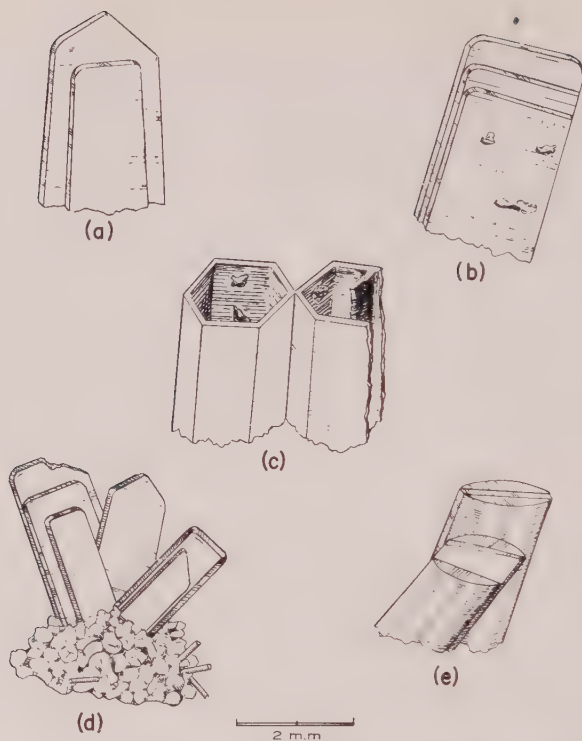


Fig. 1. Pseudomorphs of deweylite after aragonite, Cedar Hill Pennsylvania.

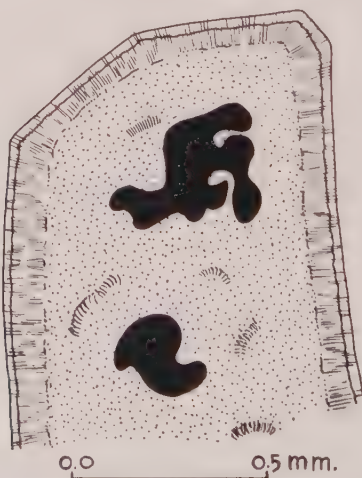


Fig. 2. Pseudomorph of deweylite after aragonite illustrating an earlier aggregated deweylite (center) and a later banded, fibrous deweylite (rim). The black mineral is opal. \times nicols.

forms an outer rim (Fig. 2). The white pseudomorphs of deweylite (#3b in Table 1) are closely associated with opal (Fig. 2). The reddish brown deweylite (#2 in Table 1) did not exhibit any limonite in either transmitted or reflected light, hence at least some of the reddish brown color is believed to be inherent in the deweylite itself.

The indices of refraction of the Cedar Hill Material are compared with published values in Table I. The indices range in value from very near that of opal at 1.48 to approximately the values for well crystallized antigorite at 1.548. All of the material from Pennsylvania (Table I, 1-8) is in

TABLE I. INDICES OF REFRACTION FOR DEWEYLITE

	(1)	(2)	(3a)	(3b)	(4)	(5a)	(5b)	(6)
α	1.504	1.511	1.500	1.511	1.507	1.511	1.522	1.500
γ	1.509	1.516	1.506	1.517	1.512	1.518	1.527	1.509
	(7)	(8)	(9)	(10)	(11)	(12)	(13)	(14)
α	1.500	1.487	1.538	1.505 to	1.528 to	1.532	1.548	1.546
γ		1.510	1.546	1.525	1.555	1.540		

- (1) White fluorescent deweylite in fibrous bands; $\pm .003$; Cedar Hill.
- (2) Reddish brown deweylite; indices from fibrous bands on edges; no indices determined on inner aggregates; $\pm .003$; Cedar Hill.
- (3a) White pseudomorphs; outer fibrous bands; $\pm .003$; Cedar Hill.
- (3b) White pseudomorphs; inner aggregate; $\pm .003$; Cedar Hill.
- (4) Yellow green; aggregates; no fibrous bands; $\pm .003$; Cedar Hill.
- (5a) Emerald green (nickeliferous); outer fibrous bands; $\pm .003$; Cedar Hill.
- (5b) Pale green; inner aggregates; $\pm .003$; Cedar Hill.
- (6) Texas, Pa. (Selfridge, 1936, p. 483).
- (7) Lancaster County, Pa. (Selfridge, 1936, p. 483).
- (8) Delaware, Pa. (Selfridge, 1936, p. 483).
- (9) Pseudomorph after pectolite, Jersey City, N. J. (Selfridge, 1936, p. 483).
- (10) Variation of indices; average at 1.510; Webster, N. C. (Ross and Shannon, 1925, p. 445) for a nickeliferous deweylite.
- (11) Considered to be a mixture with chrysotile; E. Chino Quarry, Riverside, Calif. (Daly, 1935, p. 651).
- (12) Brown; Mladotice, Czech. (Konta, 1951, p. 413).
- (13) Green; Mladotice, Czech. (Konta, 1951, p. 413).
- (14) White; Mladotice, Czech. (Konta, 1951, p. 413).

lower portion of this range. In addition, where there is a rim of banded fibers, this material has a lower index than the inner, fine-grained aggregates. Within any one sub-variety of deweylite the indices vary: in the Cedar Hill material over a narrow range; in the Webster, N. C. material (Ross and Shannon, 1925, p. 445) and the Riverside, Calif. samples (Daly, 1935, p. 651) over a much wider range.

The influence of molecular water in decreasing the index of refraction may be seen from the data given by Konta (1951, p. 414, 415) and is similar to that observed in the opal-quartz series. It seems highly probable that this wide variation in the indices of deweylite is the result of variable H_2O content and that the conchoidal fracturing observed in deweylite is evidence of hydration. If this is the case, then the outer rims of deweylite either represent a hydration stage in which more water was available, or a rehydration of previous deweylite. The former interpretation is preferred by the author for the Cedar Hill samples. This is based both on the appearance of the rims (Fig. 2) and by analogy with the paragenetic sequence given by Konta (1951, p. 415, 420) which also suggests that the youngest deweylite contains the most molecular water.

With respect to the green deweylite (Table I, 5a, b), the higher index material contains the deepest green coloration. Since this green variety contains significant amounts of nickel, there may also be a correlation between indices and nickel content, or with the amounts of nickel and H_2O present if the nickel were in a structural position such that an $(OH)^--Ni$ attraction would be significant. As yet, this remains a moot question.

CHEMICAL COMPOSITION

Material selected for chemical analysis was examined both optically and with the aid of x-ray powder photographs to obtain samples free from impurities. A small amount of magnesite was present in the two samples selected. A negligible amount of opal may also have been present. Because of the difficulty of obtaining sufficient amounts of pure deweylite, only the white, fluorescent (1) and reddish brown (2) deweylites were analyzed (Table II).

The x-ray spectrographic methods utilized both external and internal standards. Wet chemical analyses were used as external standards to determine total iron content based on the FeK_{α} line. For nickel, $NiCO_3$ was used as an internal standard based both on the NiK_{α} and NiK_{β} lines. The matrix used was white, fluorescent deweylite. Three runs were averaged at each frequency and the slope of the resulting graph was used to obtain the results listed in Table II. Since the Mn content was quite low and consistently uniform for all the deweylite samples, the amount present was estimated from the slopes of the iron and nickel curves.

The calculation of the chemical formulas (Table II) is based on three tetrahedral cations per unit cell since this yields more nearly whole number octahedral cation values than would two tetrahedral cations per unit cell. The structural formulas are written with $(OH)_4$ plus molecular water to conform to the serpentine structure, rather than expressing all the water as H_2O .

Three steps were performed in obtaining the corrected chemical analyses listed in Table II. Sufficient Mg was subtracted to utilize all of the CO_2 as magnesite, present as an impurity. The iron was recalculated from Fe_2O_3 to FeO on the assumption that all the iron is within the

TABLE II. CHEMICAL ANALYSES, CEDAR HILL DEWEYLITE
Analyses by L. E. Gingerich, Pa. R. R.

(1) Massive, white, fluorescent deweylite (a)

	Analysis	Corrected	Atomic Ratio	Atoms/unit cell
% SiO_2	49.64	52.43	.8748	3.000
% Al_2O_3	0.00			
% Fe_2O_3	2.40			
% FeO		2.16	.0301	0.1036
% MgO	32.07	31.62	.7841	2.6997
% NiO	tr	0.16*	.0021	0.0072
% CO_2	2.34			
% H_2O	12.90	13.62	3.0238	10.4109
Total	99.35	99.99		

Formulas: 1. $(\text{Mg}_{2.70}\text{Fe}_{.10}\text{Ni}_{.01})_{2.81}\text{Si}_{3.0}\text{O}_7 \cdot (\text{OH})_{4.0} \cdot 3.2\text{H}_2\text{O}$

2. $(\text{Mg, Fe, Ni})_3\text{Si}_3\text{O}_7 \cdot (\text{OH})_4 \cdot 3\text{H}_2\text{O}$

(2) Reddish brown deweylite (b)

	Analysis	Corrected	Atomic Ratio	Atoms/unit cell
% SiO_2	44.82	48.69	.8124	3.000
% Al_2O_3	0.67	0.73	.0286	
% Fe_2O_3	3.29			
% FeO		3.23	.04495	0.1600
% MgO	33.38	32.72	.81099	2.893
% NiO	tr	0.11*	.00147	0.005
% CO_2	3.56			
% H_2O	13.36	14.51	3.22176	11.492
Total	99.08	99.99		

Formulas: 1. $(\text{Mg}_{2.9}\text{Fe}_{0.16})_{3.1}(\text{Si}_{2.9}\text{Al}_{0.1})_{3.0} \cdot (\text{OH})_{4.0} \cdot 3.75\text{H}_2\text{O}$

2. $(\text{Mg, Fe})_3(\text{Si, Al})_3\text{O}_7 \cdot (\text{OH})_4 \cdot 4\text{H}_2\text{O}$

* Analyses by x-ray spectrograph.

deweylite and not present as limonite, since optical observations did not reveal any limonite or hematite. However, small amounts are probably present and hence the iron content listed in Tables II and III is a maximum value. The resulting values were then recalculated to total 100 per cent.

An interesting feature is the high nickel content of the emerald green deweylite (Table III, #5). The intensity of the green coloration is directly proportional to the amount of nickel present. The analyzed sample was selected from material which was largely emerald green. However, since small amounts of pale green and white deweylite could not be completely separated, the value of 4.53% NiO is not the maximum nickel content, although the maximum probably does not exceed 5%. Previously Ross and Shannon (1925, p. 445) have reported a green deweylite from Webster, N. C., containing 4.2% NiO.

Perhaps the most interesting result from the chemical analyses is the

TABLE III. X-RAY SPECTROGRAPHIC ANALYSES OF DEWEYLITE

	% Cr ₂ O ₃	% NiO	% FeO	% MnO
(1) White fluorescent	nil	0.16 ± .03	2.16	.03 ± .01
(2) Reddish brown	nil	0.11 ± .03	3.23	.02 ± .01
(4) Yellow-green	nil	0.11 ± .03	2.38	.02 ± .01
(5) Emerald green	nil	4.53 ± .04	2.13	.03 ± .01

Ni Analyses: NiCO₃ internal standard on NiK_α and NiK_β.

Fe Analyses: Wet chemical external standard FeK_α.

Mn Analyses: Estimate based on slope of Ni and Fe curves.

high Si:(Mg+Fe+Ni) ratio. In most chrysotiles and antigorites this ratio is approximately 2:3, representing a trioctahedral structure. The Cedar Hill deweylites in Table II have a ratio very close to 1:1. Analyses given by Ross and Shannon (1925, p. 445), Daly (1935, p. 650), Selfridge (1936, p. 449), and Konta (1951, p. 414) for deweylite generally fall between these ratios. One consequence of this ratio will be discussed under the differential thermal analysis data in reference to the formation of clinoenstatite (1:1 ratio) as opposed to forsterite (1:2 ratio). Another consequence lies in the speculation that octahedral cation holes may exist in deweylite. In the case of the two analyzed Cedar Hill deweylites, a 1:1 tetrahedral to octahedral cation ratio would represent a dioctahedral serpentine, while the values reported by other analysts would be more trioctahedral in character. Bates (1959, p. 95) has discussed the possibility of cation deficiencies as it relates to serpentine morphology, but did not note a completely dioctahedral serpentine.

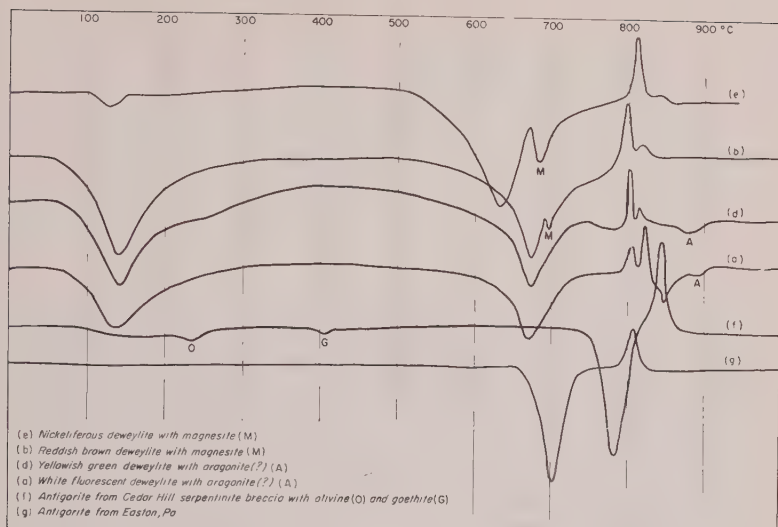


FIG. 3. Differential thermal curves of deweylite and antigorite.

No chemical explanation has been found for the fluorescence of the white deweylite. Neither manganese (Table III) nor chromium (not present) is responsible.

DIFFERENTIAL THERMAL ANALYSIS

The DTA curves reproduced in Fig. 3 were run on a commercial instrument, the Deltatherm, at 10° C/min. The sample head accommodates four samples. Both quartz and kaolinite were used as standards. The accuracy is $\pm 10^{\circ}$ C. One deweylite and one Cedar Hill serpentine from the breccia were also kindly rerun by Robert C. Bolger to serve as a further check.

In Fig. 3 several deweylite curves are compared with two antigorite curves. There is a general correspondence between them, although the transformation temperatures serve to differentiate them. The endothermic reaction at 125° – 140° C. represents the loss of molecular water. The endothermic reaction at 625° – 675° for deweylite and at 700° and 775° C. for antigorite represents the loss of structural water. Magnesite tends to lower the peak temperature of this endothermic reaction. Between this endothermic and the following exothermic reactions, x-ray powder photographs do not exhibit diffraction lines, indicating that the short range order of a crystal structure has disappeared. The exothermic reactions at 800° to 850° C. represent the crystallization of anhydrous magnesium silicates.

Several features are of interest. The lower temperature for the second endotherm of deweylite, as contrasted with a higher temperature for antigorite, is probably in part a consequence of its greater degree of disorder. Nickel also appears to lower this peak temperature as has been noted by Caillere and Henin (1957, p. 221–224). If, as Caillere and Henin believe (1948, p. 114–118), this peak temperature is related to the composition of the octahedral layer, nickel may be the cause of this lower decomposition temperature. It may also be related to the extent to which the cation octahedral sites are filled.

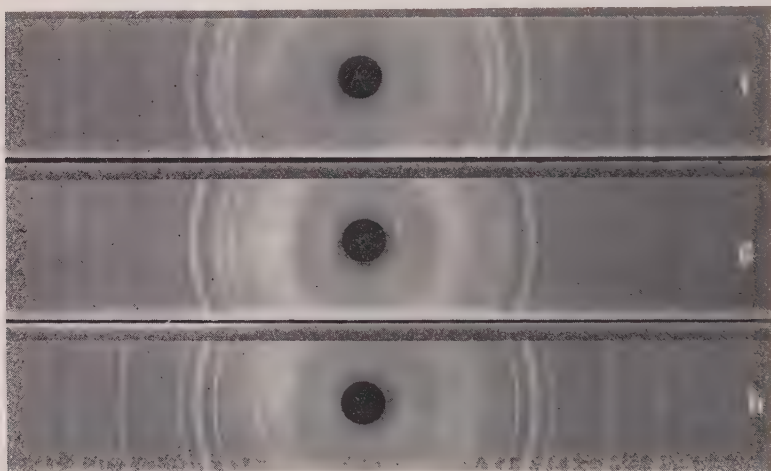


FIG. 4. X-ray powder patterns of (f) clinoenstatite with minor forsterite, (g) forsterite with clinoenstatite and (h) forsterite from differential thermal treatment of samples (b), (a), and (f) (brown deweylite, white fluorescent deweylite, and antigorite respectively) in Fig. 3.

Another interesting feature is the occurrence of two exothermic peaks for deweylite, at about 800° and 820° C., while antigorite exhibits only a single exothermic reaction between 805° and 840° C. Post DTA x-ray powder patterns of the antigorite samples contain only forsterite. Similarly Aruja (1945, p. 72) notes that only forsterite is produced by heating antigorite until a run of 25 hours at 1000° C. exhibited a faint line at the position of the strongest line of enstatite. From this, he was not able to differentiate between enstatite and clinoenstatite. Konta (1951, p. 416) reporting on the differential thermal analysis of deweylites presents curves with a single exothermic reaction at about 800° C., noting that "the crystallization of the orthosilicate Mg_2SiO_4 " predominates but that MgSiO_3 is also shown to be present in the x-ray powder photographs. Post DTA x-ray photographs corresponding to DTA curves of deweylites (b) and (a), and of antigorite (f) in Fig. 3 are reproduced in Fig. 4,

labelled (f), (g) and (h) respectively. The DTA curves show an increase in the area under the curve for the higher temperature exotherm, and the *x*-ray photographs show a corresponding change from predominantly clinoenstatite in (f) to predominantly forsterite in (h). This correspondence is taken to mean that the lower exotherm represents forsterite formation dominantly from antigorite, and the higher temperature that of clinoenstatite from deweylite.

The formation of forsterite at a temperature below that of clinoenstatite is quite interesting. From the points of view both of mineral structures and paragenetic field evidence, forsterite is often considered to be the higher temperature mineral. In the case of the deweylite and antigorite thermal products it is believed by the author that initial chemical composition is the controlling factor. Clinoenstatite has a Si: Mg ratio of 1:1, whereas the ratio in forsterite is 1:2. The former ratio corresponds almost exactly to that of the two Cedar Hill deweylites (Table II), while the latter corresponds more closely to the 2:3 ratio of serpentines. There is, however, an even closer correlation within the deweylites themselves. The white fluorescent deweylite contains more silica than the reddish brown deweylite (Table II). This correlates very well with the greater area under the higher temperature endotherm for clinoenstatite from the white deweylite as compared to that from the reddish brown deweylite. It also correlates with the relative amounts of clinoenstatite in the *x*-ray patterns (Fig. 4). Further support is lent to the supposition that chemical composition controls the decomposition products by the apparently amorphous nature of the deweylite preceding the exothermic reactions. Thus structural control does not seem to be significant.

STRUCTURAL DATA AND INTERPRETATIONS

General Discussion

Several *x*-ray powder techniques were utilized in an attempt to determine the structural characteristics of deweylite. Two or more powder photographs were taken for each sample using Cu K α radiation, a Ni filter, approximately a 3-hour exposure time, and Duco Cement as the bonding medium. As a result of the extreme line broadening (Fig. 5) measurements of 2θ are accurate only in the first decimal place, despite the fact that they have been checked by diffractometer runs calibrated by a Si standard. Intensities listed in Table IV were estimated visually, and modified somewhat by diffractometer runs between 5° and 60° 2θ . The (N20) or (02N) series listed in Table IV are all weak reflections.

A general structural correspondence between the serpentine minerals and deweylite may be seen from Fig. 5 and Table IV. The assigned indices are based on those of antigorite as given by Brindley and von Knor-

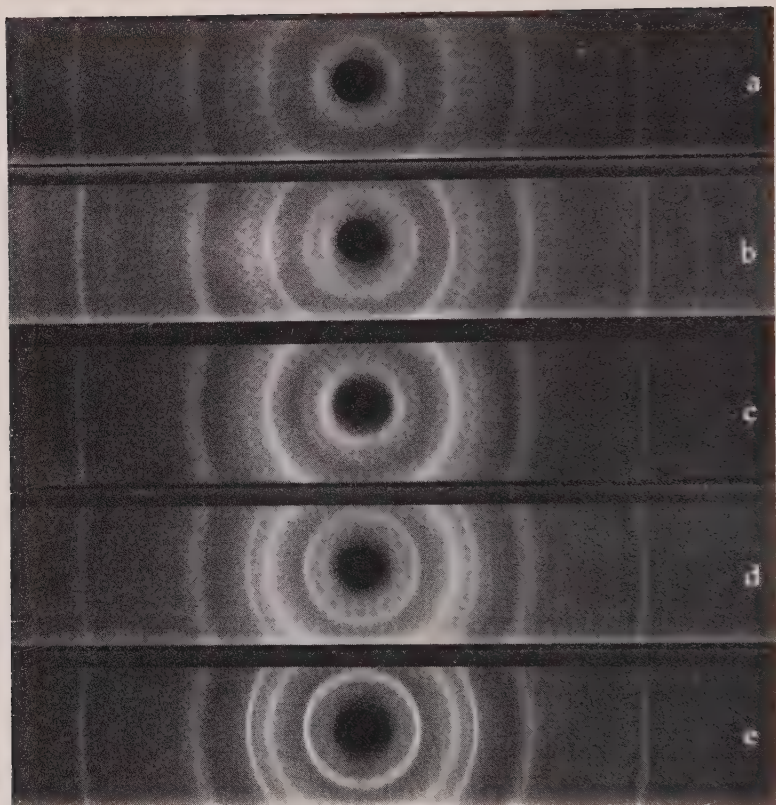


FIG. 5. X-ray powder patterns of deweylite: (a) white fluorescent; (b) reddish brown; (c) pseudomorphs after aragonite; (d) yellowish green, and (e) nickeliferous. Letters correspond to Table IV.

ring (1954, p. 799) and will be discussed later. The reflections which are present in deweylite are also present in the serpentine minerals. However many of the serpentine reflections are absent in deweylite, notably among the $(20l)$ series. Those present are all broad and diffuse in character. In comparison with the serpentines, all of the deweylite samples in Table IV exhibit lattice expansion in the c direction and a small contraction along the b axis. Such a contraction as that of the (060) may be another indication of a tendency toward dioctahedral character for deweylite as suggested by an M^{+2} cation deficiency calculated from the chemical analyses. As may be seen from Fig. 5 and Table IV there are significant variations in intensity within the deweylites themselves, notably between the $(00l)$ and $(0k0)$ series of reflections. These differences between serpentine and deweylite in x-ray characteristics appear to be consistent

and should serve to differentiate deweylite from both antigorite and chrysotile whose characteristics recently have been summarized by Eitel (1958, p. 131–138).

The 10 Å reflections visible in Fig. 5 are believed to represent the presence of sepiolite and are most noticeable in patterns (*a*) and (*c*), white fluorescent and white pseudomorphic deweylite respectively. Those reflections which may in part be a combination of sepiolite and deweylite are denoted in Table IV. Magnesite is nearly always present in small amounts, and it seems probable that at least one of the reflections (1.717 Å) listed by Selfridge (1936, p. 469) and Konta (1951, p. 419) for deweylite belongs to magnesite.

Influence of M^{+2} Cations

The deweylite *x*-ray powder photographs in Fig. 5 and Table IV have been arranged to show a progressive increase in intensity of (002) (020). A possible explanation may exist in a correlation between M^{+2} cation substitution and the effect of this substitution on the absolute structure factor, $|F|$. If it is assumed that substitutional changes in either the octahedral or a possible interlayer site will not affect the (020) intensity, and this seems probable, then semi-quantitative *F* calculations based on a modification of the basic units of the chlorite structure show that increasing degree of substitution, or the substitution of heavier atoms, will increase the (00 l) intensity for at least the first four orders. Such a calculation also shows that the effective increase in intensity will be greater for octahedral than for interlayer substitution. The evidence for such a cause and effect is slight, but worth noting.

The chemical analyses of the white (*a*) and reddish brown (*b*) deweylites in Table II show that the latter contains more M^{+2} cations. Similarly, there is a noticeable increase in the (002) (020) intensity ratio. The nickeliferous deweylite (*c*) yields the highest intensity ratio of those analyzed. This may be explained easily either by degree of octahedral (or interlayer) substitution or by the substitution of Ni which has a greater atomic weight than Mg. Since this intensity ratio cannot be explained for the non-nickeliferous, iron deweylites (*a*–*d*) solely on the basis of total Fe content, it seems logical to assume that the unit cell quantity of all the M^{+2} cations is as important as the substitution of a heavier cation for Mg. It is also interesting to note that most serpentine minerals have a high (002/020) intensity ratio and also have significantly more M^{+2} cations than deweylite, suggesting that the observed intensity changes in deweylite may be the result of octahedral substitutions which approach that of serpentine in the degree to which the octahedral sites are filled.

There is also a noticeable increase in most of the deweylite lattice spac-

ings as compared with those of antigorite and chrysotile. This may well be the result, in part, of interlayer molecular water, which helps to explain the variability of the (00l) spacings. It is also possible that a correlation may exist with the M^{+2} cations. For example the nickeliferous deweylite appears to have the smallest c_0 value. However, the diffuse character of the reflections does not allow a sufficient accuracy of measurement to draw conclusions in this regard.

Line Broadening and Crystallite Size

Measurements of line broadening for comparison among the deweylite samples and for crystallite size calculations were made at one half the peak height ($\beta_{\frac{1}{2}}$) from diffractometer traces. This is often inaccurate because of pronounced peak asymmetry and because the establishment of a background base-line is difficult as a result of the extreme broadening. In addition, superlattice reflections (to be discussed below) often are superimposed upon the flanks of major peaks. As a consequence of these limitations quantitative calculations are highly inaccurate as far as absolute numerical values are concerned. It is hoped, however, that relative comparisons are useful if used with caution.

Line broadening in deweylite could be, and probably is, the result of several factors, rather than any single one. Limited randomness in the packing of the layers (stacking disorder resulting in crystallites) may be a significant factor. The colloidal size and aggregated optical character of the deweylites may be a large scale consequence of such a disorder. Aruja (1945, p. 71) in connection with antigorite also mentions the possibility of variation in the structure factor from one unit cell to the next as a result of two different types of octahedral cavities. However, the deweylite line broadening is much greater than that in antigorite and hence this cannot be the major factor. Extreme warping of atomic planes will also result in line broadening. A double half wave structure, such as that proposed by Kunze (1957, p. 104) for antigorite, may be contributory but again seems unlikely as an explanation for the more pronounced broadening of deweylite. However, warping of atomic planes might also be caused by incomplete lattice substitution or by "stuffing." Evidence has been presented previously that incomplete octahedral substitution may exist. The extent to which this may be a cause of deweylite line broadening is not known.

Calculations of crystallite size were carried out for all five deweylite samples (a-e) assuming all line broadening to be the result of the presence of crystallites. The values thus obtained are minimal values. The formula used was

$$D_{hkl} = \frac{K\lambda}{\beta_{1/2} \cos \theta} \quad \text{where } K = 0.9$$

on the assumption that the crystallites sufficiently approach sphericity so that no significant errors are introduced in the shape factor. Data are presented in Table V only for the nickeliferous (*e*) and yellowish green (*d*) deweylite samples since all others yield values similar to that for yellowish green deweylite. Useful determinations in the *c* direction were not obtainable.

From Table V it can be seen that the minimal crystallite size is on the order of 100 Å. It also can be seen that the *k* dimension is somewhat greater than the *l* for all except the nickeliferous deweylite where the situation is reversed. If, as Aruja suggests for antigorite (1945, p. 66), the *b* axis is the fiber axis, then the longer dimension of the majority of the deweylite crystallites parallels this direction. That this is not the case for the nickeliferous deweylite suggests that crystallite dimensions may be compositionally or structurally controlled by the presence of Ni ions in the lattice.

TABLE V. CRYSTALLITE SIZE (*D*) DETERMINATIONS FOR DEWEYLITE

(d) Yellowish green (similar for white and reddish brown)				
$D_{(006)}$	$D_{(020)}$	$D_{(0.0.12)}$	$D_{(060)}$	$D_{(206)}$
80 Å	115 Å	82 Å	98 Å	
$k > l$				
(e) Nickeliferous				
106 Å	81 Å	105 Å	77 Å	56 Å
$l > k(> h)$				

Superlattice Structure

Diffraction traces of the Cedar Hill deweylite samples contain numerous small peaks belonging to an (*h*20) or (02*l*) series of reflections (Table IV). This series suggests a superlattice for deweylite similar to the superlattice structures of antigorite. Aruja (1945) proposed a superlattice in the *a* axis direction for antigorite, while Brindley and von Knorring (1954, p. 801–802) also discuss the possibility of a *c* axis superlattice.

Since x-ray powder analysis cannot distinguish between a superlattice in the (*h*20) planes from one in the (02*l*) series, calculations of the superlattice dimension (*S*) were carried out for comparison with *a*₀ and *c*₀ according to the expression

$$(1/d)^2 = (2/b)^2 + (N/S)^2$$

for both the yellowish green (*d*) and nickeliferous (*e*) deweylite samples. For (*d*), the value of *b*₀ used was 9.18 Å, and for (*e*), 9.15 Å. Calculations of *S* were made for *N* = 2, 4, 5, 6, 12, and 15 (Table IV) with their corre-

sponding d spacings. These values are compared with $3c_0$, $8a_0$, $8\frac{1}{2}a_0$, and $8\frac{3}{4}a_0$ for both yellowish green (d) and nickeliferous (e) deweylites (Table VI). The a_0 values were calculated and averaged from the (201) and (202) planes for each sample according to the expression.

$$a_0 = \frac{hd_{(h0l)}}{\cos \left(89^\circ - \cos^{-1} \frac{d_{(h0l)}}{1/c_0} \right)}$$

where β has been assumed to have a value of 91° . This assumption probably falls within the limits of error of the d spacing measurements, and hence within the average value of c_0 .

TABLE VI. COMPARATIVE SUPERLATTICE CALCULATION FOR DEWEYLITE

Yellowish Green (d)	Nickeliferous (e)
$S_{(d)} = 45.0 \pm 1.0$	$S_{(e)} = 45.5 \pm 1.0$
$3c_0 = 44.0$	$3c_0 = 44.10$
$8a_0 = 42.16$	$8a_0 = 42.24$
$8\frac{1}{2}a_0 = 44.80$	$8\frac{1}{2}a_0 = 44.88$
$8\frac{3}{4}a_0 = 46.11$	$8\frac{3}{4}a_0 = 46.20$

The best fit for the data is between a superlattice in h (a_0) and the S dimension for both deweylite samples. Both also correlate best with an $8\frac{1}{2}a_0$ superlattice dimension. This fractional correlation of a_0 suggests that undulations may be a necessary part of the deweylite structure as proposed by Onsager (1952) for serpentinite. Such undulations, or warping of atomic planes, have been mentioned as a possible contributor to line broadening and would conform to the suggestions of Kunze (1957) regarding possible types of wave structures in antigorite. However, as Brindley and von Knorring have noted (1954, p. 802), analysis of the data from x -ray powder analysis cannot conclusively distinguish between an a_0 and a c_0 superlattice, nor is the accuracy of the data sufficient to confirm an undulating structure in deweylite.

High Temperature X-Ray Diffraction Data

High temperature powder x -ray diffractometer scans and oscillations were run on several deweylite samples using the instrument and techniques described by Bassett and Lapham (1957). The purposes of this method of analysis were to determine 1) if line broadening is a function of mechanical or structural strain, 2) the relative persistence in maintaining crystallinity of the various (hkl) planes under heat treatment, 3) if the deweylite structure might exercise a control over the formation of an-

hydrous magnesium silicates and 4) if any significant* difference exists among the Mg-Fe deweylites.

In general, there are no d spacing shifts, intensity changes, or changes in the amount of line broadening for any of the major reflections previous to the collapse of any one atomic plane. The lack of peak sharpening upon heating indicates that line broadening is not a function of mechanical strain. Aruja (1945, p. 72-73) arrived at a similar conclusion from single crystal studies of antigorite.

The thermal stability of various (hkl) planes varies considerably. Planes with even h and l indices are most stable, ($hkl0$) planes slightly less stable, while ($00l$) planes are the least stable. The latter collapse at about 500° C., while the other atomic planes persist to approximately 600° C. This suggests that linkages in the ab plane are strongest and again coincides with the conclusion of Aruja (1945, p. 73) for antigorite. The superlattice reflections begin to disappear at a lower temperature, between 400° C. and 500° C., indicating the relative instability of the superlattice structure. Also, the (201), (202), and (15.2.0) planes merge into one reflection approximately coinciding with the position of the (202) reflection.

Although all the deweylite samples behaved in similar fashion, small differences were noted for the Ni deweylite. It must be borne in mind, however, that the magnitude of these differences is so small that they may be more apparent than real. A slight tendency was noted toward greater stability of the ($00l$) planes in the Ni deweylite than in the other samples. There also appeared to be a small increase in line broadening upon heating which was not noted for other deweylite samples. These data are much too indefinite to draw any conclusions.

As noted previously, there were no reflections present at scans higher than 650° C. and hence the influence of the deweylite structure on the formation of clinoenstatite relative to forsterite is probably not significant.

CONCLUSIONS

Several methods of investigation have been combined in an attempt to elucidate the nature of deweylite based upon samples from Cedar Hill, Pa. All of the methods confirm that deweylite is a member of the serpentine group of minerals closely related to antigorite. It is suggested that both indices of refraction and c_0 are related to molecular water content. Deweylite with at least 4.5% NiO is reported. The onset of the 660° C. endotherm is probably lowered slightly by the presence of this nickel. The nickel is believed to be present in the octahedral site although the evidence from chemical, differential thermal, and x-ray powder analyses is far from conclusive. The high ratio of tetrahedral to octahedral cations is offered as an explanation for the predominance of clinoenstatite relative

to forsterite at about 820° C., which is slightly higher than the temperature of forsterite crystallization.

The deweylite structure is similar to that of antigorite with a superlattice probably in the a direction of $8\frac{1}{2}a_0$ although a $3c_0$ superlattice is a plausible alternative. Line broadening is taken to be indicative of the presence of crystallites 100 Å or 200 Å in size. An undulant structure in the ab plane and distortion of atomic linkages associated with octahedral cation holes may be a contributing factor. Analysis of differential thermal, chemical, and x -ray data suggest that the Cedar Hill deweylite may be a dioctahedral variety of antigorite. The alternative explanations of cation stuffing or tetrahedral cation deficiencies to explain the nearly 1:1 ratio of M^{+4} to M^{+2} cations seems less plausible.

Geological evidence indicates that deweylite is of low temperature origin and at Cedar Hill has formed by the alteration of pre-existing serpentine minerals. Physical characteristics suggest formation from a colloidal suspension concomitant with a gradual decrease in the amount of available water.

Pseudomorphs of deweylite after aragonite are discussed and are believed to be the first report of such an occurrence.

ACKNOWLEDGMENTS

The chemical analyses were performed by the Geology Division of the Pennsylvania Railroad through the courtesy of Mr. Richard Teichman. Appreciation is extended to Professor Paul F. Kerr, Columbia University, for permission to use the high temperature diffraction equipment and to Mr. Robert Bolger for several differential thermal analyses of deweylite and serpentine. The writer is also grateful to William A. Bassett for helpful discussions and criticism.

REFERENCES

- BARUJA, ENDEL (1945), An x -ray study of the crystal structure of antigorite: *Min. Mag.* **27**, 65-75.
- BASSETT, WILLIAM A. AND LAPHAM, DAVIS M. (1957), A thermal increment diffractometer: *Am. Mineral.* **42**, 548-555.
- BASSETT, WILLIAM A. (1959), Origin of the vermiculite deposit at Libby, Montana: *Am. Mineral.* **44**, 293-295.
- BATES, THOMAS F. (1959), Morphology and crystal chemistry of 1:1 layer silicates, *Am. Mineral.* **44**, 78-114.
- BOWEN, NORMAN L. AND TUTTLE, O. F. (1949), The system $MgO-SiO_2-H_2O$: *Bull. Geol. Soc. America*, **60**, 439-460.
- BRINDLEY, G. W. AND VON KNORRING, O. (1954), A new variety of antigorite (ortho-antigorite) from Unst, Shetland Islands: *Am. Mineral.* **39**, 794-804.
- CHAILLIERE, S. AND HENIN, S. (1948), Significance of d. t. a. results: *Terre et silic. industr.* **13**, 114-118.

- CAILLERE, S. AND HENIN, S. (1957), The chlorite and serpentine minerals: The Differential Thermal Investigation of Clays, Mineralogical Society, London, p. 221-224.
- DALY, JOHN W. (1935), Paragenesis of the mineral assemblage at Crestmore, Riverside County, California: *Am. Mineral.* **20**, 650-651.
- EITEL, WILHELM (1958), Polytypism of layer structure silicates, in Structural Conversions in Crystalline Systems: *Geol. Soc. Amer. Spec. Pa.* **66**, 131-138.
- GILLERY, F. H. (1959), X-ray study of synthetic Mg-Al serpentines and chlorites: *Am. Mineral.*, **44**, 144-146.
- GOLDSCHMIDT, VICTOR (1913), Atlas der Krystallformen, Heidelberg, Band I, Tafel 97-104.
- KONTA, JIRI (1951), Investigation of the deweylite from the fissure fillings in the serpentine of Mladotice: *Bull. Internat. Classe des Sci. Math. Nat. et Med.*, **I** (1953), Academic Tcheque Sci. Prague, p. 411-424.
- KULP, J. L. AND BROBST, D. A. (1954), Notes on the dunite and the geochemistry of vermiculite at the Day Book dunite deposit, Yancey County, North Carolina: *Econ. Geol.*, **49**, 211-220.
- KUNZE, GUNTHER (1957), Die gewellte struktur des Antigorits: *Zeits fur. Krist.* **108**, 82-107.
- ONSAGER, L. (1952), Report of a conference on structures of minerals by K. Robinson and E. R. S. Shaw (1952): *Jour. Sci. Instr.*, **3**, 281-282.
- ROGERS, AUSTIN F. (1918), An American occurrence of periclase and its bearing on the origin and history of calcite-brucite rocks: *Am. Jour. Sci.*, **46**, 4th ser., p. 581-586.
- ROSS, CLARENCE S., AND SHANNON, EARL V. (1925), The so-called genthite from Webster N. C.: *Am. Mineral*, **10**, 444-446.
- SELFIDGE, GEORGE C., JR. (1936), An x-ray and optical investigation of the serpentine minerals: *Am. Mineral.*, **21**, 467-471, 483, 484, 496, 499-500.

Manuscript received May 2, 1960.

Note added in press: A reddish brown deweylite from Cedar Hill has the following x ray characteristics indicative of a greater dioctahedral character than any previously found:

$$\frac{(002)}{(020)} = \frac{15}{100}, \text{ and } (060) = 1.525 \text{ \AA.}$$

A tan deweylite from the Sparvetta quarries one mile west of Nottingham, Pa., associated with serpentinite cut by a feldspar pegmatite, is relatively trioctahedral:

$$\frac{(002)}{(020)} = \frac{85}{100}, \text{ and } (060) = 1.536 \text{ \AA.}$$

The indices are $n_a = 1.517 \pm 0.003$ and $n_\beta = 1.523 \pm 0.003$.

CELESTITE AND CALCIOSTRONTIANITE FROM WISE COUNTY, VIRGINIA

RICHARD S. MITCHELL, *University of Virginia*

AND

RICHARD F. PHARR, *Virginia Division of Mineral
Resources, Charlottesville, Virginia.*

ABSTRACT

Celestite and calciostrontianite occur in vugs in dolomite of the Cayuga group (Silurian) in a quarry one half mile east of East Stone Gap, Wise Co., Virginia.

Light blue, well developed celestite crystals average about one inch in length. Most crystals are elongated parallel to the a axis, and the $\{011\}$ faces predominate. Vectorial etching is common. A blue fibrous crust of celestite was also observed.

The calciostrontianite occurs as radiating globular masses up to a half inch in diameter. A quantitative spectrographic analysis shows approximately 10% CaO. X-ray diffraction data show a significant departure from pure SrCO_3 .

OCCURRENCE

Although strontium minerals are known to occur at several places in the United States, only recently have they been found in Virginia. One of the writers (RFP) first noticed celestite and calciostrontianite in Wise County in 1958. A preliminary report on this occurrence was presented at the 1959 meeting of the Virginia Academy of Science, and has been published in abstract form (Pharr and Mitchell, 1959).

Both celestite and calciostrontianite occur along State Road 613 about one half mile east of East Stone Gap, Wise County, in a quarry in dolomite of the Cayuga group (Upper Silurian) owned by Mr. G. H. Belton. The beds here consist of a succession of intercalated, fine-grained, medium- to dark-gray, dolomites and magnesian limestones which are nearly horizontal. Eby (1923) described the geology of the region and also gave a section of the formation at a place some yards west of the quarry. In his description there is no mention of strontium minerals.

The strontium minerals are found in vugs in thick-bedded dolomite. The vugs range from very small to over 10 inches across, and occur in a horizontal zone across the quarry. The vugs examined by the writers were rather barren of good material. They did contain etched celestite crystals and small globular calciostrontianite masses. Most of the better celestite crystals described in this paper were collected by Mr. Belton and his son over a period of several years, and their exact location in the quarry is not certain.

DESCRIPTION OF THE CELESTITE

Most of the celestite is pale-blue in color and occurs as well-developed crystals which average from $\frac{1}{2}$ to $\frac{3}{4}$ inch in length with a maximum of

about 2 inches. Most of the crystals are elongated parallel to their a axes, and the $\{011\}$ faces predominate. They can be conveniently classified into two main habits.

Habit A (Figs. 1A and 2A) is the most common, and exhibits the greatest number of crystal forms. In addition to the prominent $\{011\}$ faces, which are frosted due to slight etching, they have relatively large, bright $\{101\}$ faces and small $\{122\}$, $\{210\}$, $\{211\}$, $\{100\}$, $\{001\}$, and $\{010\}$ faces. Lying between $\{122\}$ and $\{210\}$ (also $\{211\}$) is a dull flat

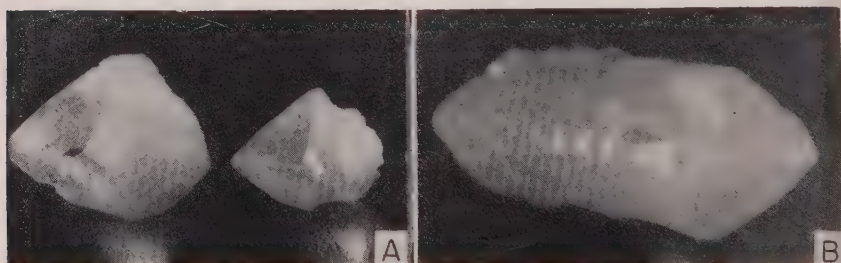
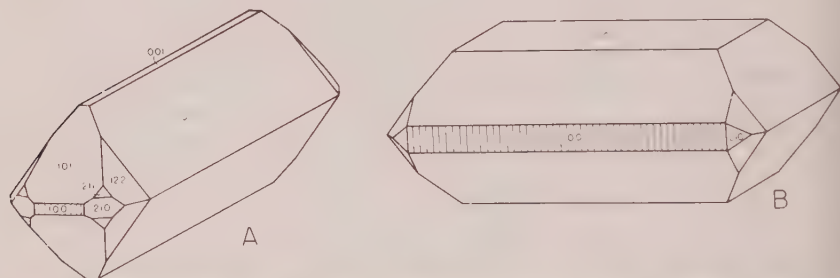


FIG. 1 (above). Idealized drawings of the two habits exhibited by celestite crystals from Wise County, Virginia.

FIG. 2 (below). Celestite crystals illustrating fig. 1.

nonreflective area which may correspond to $\{111\}$. This plane, which may be a result of etching, is not represented in Fig. 1A. The $\{100\}$ faces characteristically show vertical striations. On some crystals, reflections from these faces in the optical goniometer are continuously blurred for several degrees parallel to the b crystallographic axis. In this blurred region the brightest light falls at the $\{100\}$ position and at positions approximately 11° on each side of it, or at positions near the $\{810\}$ form. Other crystals show striations due in part to re-entrant $\{210\}$ faces on the $\{100\}$ plane.

A common modification of this habit has only three forms. The large $\{011\}$ faces are conspicuously etched. The $\{101\}$ faces are brilliant, and the $\{100\}$ faces vertically striated. A second modification is similar, but

without the brilliant {101} faces. The {011} faces are frosted and exhibit deep irregular etch pits. Several of these crystals have globular calciostrontianite attached to them. These two modifications may represent progressive etching.

Habit B (Figs. 1B and 2B) is less common. They are elongated parallel to b , and flattened parallel to {001}. Other important faces are {101}, {011}, {111}, {210}, {010}, and vertically striated {100}. No evidence of etching was observed.

The vectorial etching is an outstanding property of the type A crystals. The area between {122} and {210}, which may correspond to {111}, is affected the most, {122} is next, and then {011}. Contrasted with these are the bright {100}, {101}, {210}, {211}, and {001}. Apparently the faces have different susceptibilities to natural acids (probably carbonic) which circulated in the rock. Solution channels, roughly parallel to {010}, deeply penetrate some of the crystals. No good etch figures were observed.

A fragment of blue fibrous celestite, resembling satin spar gypsum, was found loose in the quarry. The piece is tabular, measuring about an inch across and $\frac{1}{8}$ inch thick, and probably represents a cross-fiber vein; the fiber axes being perpendicular to the tablet surface. A study of thin sections of this material showed that the fibers are all elongated parallel to c . Thin sections cut perpendicular to the fibers showed bundles with nearly parallel orientation, but adjacent bundles may have quite different orientation of the a and b axes. The individual fibers measure from 0.02 to 0.12 mm. across, and the bundles are from 1 to 2 mm. across. Quite perfect cleavage, {001}, was observed across the fibers, and less perfect inclined cleavage, presumably prismatic, {210}, was observed in thin sections cut perpendicular to the fiber direction.

Cleavable masses of blue and white celestite up to $1 \times 4 \times 5$ inches were also observed filling veins and vugs in the quarry. Thin sections of the dolomite show embedded microscopic euhedral celestite crystals.

X-ray diffraction powder data for the celestite showed no significant departure from that of pure strontium sulfate as reported by Swanson and Fuyat (1953). However, a semiquantitative spectrographic analysis of a specimen did reveal 0.15% CaO and 0.002% BaO.

DESCRIPTION OF THE CALCIOSTRONTIANITE

Calciostrontianite occurs intimately associated with celestite in the quarry, especially with celestite which is frosted or deeply corroded. Calciostrontianite forms vitreous to dull globular masses which possess an internal radial structure (Fig. 3). The size of the globules ranges from very small to a half inch in diameter. They vary in color from a light

grayish-white to light buff. Bright pale-green to cream fluorescence is exhibited under long-wave ultraviolet light (3600 to 3650 Å. U.). The majority of the globules are rough and are terminated by small acicular crystals. Because of their extremely small size (width from 0.02 to 0.08 mm. and length from 0.1 to a little over 0.3 mm.) a precise determination of the morphology was not obtained. However, goniometric measurements, combined with measurements made on the microscope stage, show that the crystal needles consist mainly of an orthorhombic bipyra-

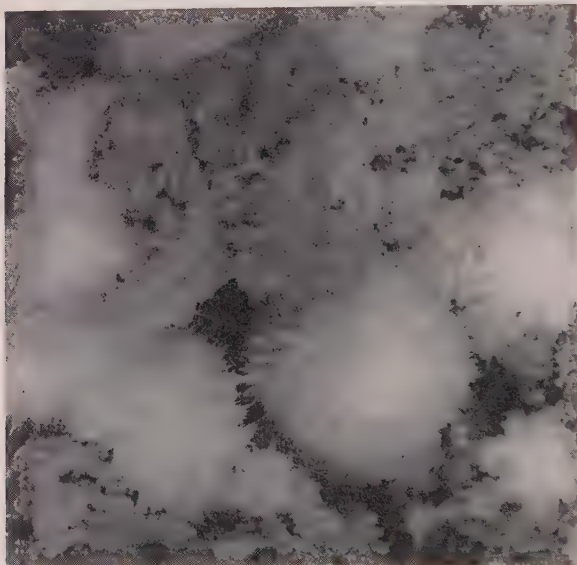


FIG. 3 (left). Calciostrontianite globular masses attached to porous dolomite.

FIG. 4 (right). Idealized drawing of pseudo-hexagonal calciostrontianite crystal.

mid, either {881}, or a form close to it, and a brachydome, possibly {0.15.1}. These forms combine to give a steep pseudo-hexagonal pyramid (Fig. 4). In some cases the pyramidal needles were somewhat curved and at times showed horizontal striations like material from Tyrol, described by Cathrein (1888). According to Palache, Berman, and Frondel (1951) steep pyramidal forms are frequently found in highly calcian strontianite.

The presence of considerable amounts of calcium in the strontium carbonate was first suspected from the x-ray diffraction data. Quantitative spectrographic analyses of specially selected and cleaned material revealed $10.6 \pm 1.0\%$ CaO for a tan colored specimen, and $9.1 \pm 1.0\%$ CaO for a white specimen.* Traces of Ba, Mg, Al and Cu, listed here in the

* These quantitative analyses were performed by the American Spectrographic Laboratories, Inc., San Francisco, California.

order of decreasing amounts, were also noted by semiquantitative spectrographic analyses. The name calciostrontianite was introduced into the literature by Cathrein (1888) for a type of strontianite, from Brixlegg, Tyrol, which contains up to 7.36 per cent CaO. The name emmonite was given by Thomson (1836) to a material from "Massachusetts" (probably from New York, according to Palache, Berman, and Frondel, 1951) with nearly an identical amount of CaO. Although the name emmonite was introduced earliest, the writers prefer to use calciostrontianite.

TABLE I. A COMPARISON OF X-RAY POWDER DATA FOR CALCIOSTRONTIANITE FROM WISE COUNTY, VIRGINIA WITH PURE SrCO_3
CuK α radiation; camera diameter 11.46 cm.

<i>hkl</i>	Calciostrontianite		SrCO_3^* <i>d</i> Å	<i>hkl</i>	Calciostrontianite		SrCO_3^* <i>d</i> Å
	<i>d</i> _{obs} Å	<i>I</i> _{obs}			<i>d</i> _{obs} Å	<i>I</i> _{obs}	
110	4.33	vw	4.37	132	1.88	m	1.91
020	4.16	vvw	4.21	113	1.81	mw	1.83
111	3.51	vvs	3.54	023	1.79	w	1.81
021	3.40	vs	3.45	222	1.75	vw	1.77
002	2.98	mw	3.01	042	1.70	vvw	1.73
012	2.81	m	2.84	310	1.65	vw-	1.67
102	2.58	w	2.60	311	1.60	mw	1.61
200	2.53	mw	2.55	241	1.55	mw	1.57
130	2.46	m	2.46	151	1.53	w	1.54
022	2.43	s-	2.45	004	1.49	vvw	1.51
211	2.25	vw	2.26	223	1.47	vvw	1.48
220	2.16	mw	2.18	330	1.44	vw	1.46
040	2.07	vw	2.10	242	1.41	vw	1.43
221	2.04	s	2.05	060	1.38	vvw	1.40
041	1.96	mw	1.99	332	1.30	mw	1.31
202	1.93	mw	1.95	313	1.27	mw	1.28
				134			

* Taken from Swanson, Fuyat and Ugrinic (1954).

The x-ray data in Table I represent an average of measurements made on four films from four different specimens. The unit cell constants are $a_0 = 5.070$, $b_0 = 8.300$ and $c_0 = 5.970$ Å (all ± 0.005 Å); $a_0 : b_0 : c_0 = 0.611:1:0.719$. These data show a significant departure from pure SrCO_3 . The data of Swanson, Fuyat and Ugrinic (1954) for pure SrCO_3 are also given in Table I. Their values are $a_0 = 5.107$, $b_0 = 8.414$ and $c_0 = 6.029$ Å. No significant departure of refractive indices from values reported in the literature for natural strontianite was found.

Calciostrontianite globules occur attached to the large blue celestite crystals, especially in the vicinity of solution channels, or along seams

where two crystals are joined. Masses of porous dolomite also contain globules of calciostrontianite attached to the walls of cavities, as well as tiny gemmy celestite crystals up to $\frac{1}{8}$ inch, and gemmy calcite scalenohedrons. Most evidence suggests that the calciostrontianite is secondary after celestite, and was probably formed by the reaction of carbonic acid on the sulfate. A thin section across a spherulite, which was situated at the junction of two celestite crystals, showed a channel leading out from the celestite with the globule perched at the orifice. Perhaps these relationships suggest a mechanism whereby the globule of radial needles was formed.

ASSOCIATED MINERALS

Other minerals found in the quarry include sphalerite, fluorite, glauconite, illite, dolomite and quartz. A white efflorescent material, which had formed on dolomite, gave x-ray patterns for starkeyite ($\text{MgSO}_4 \cdot 4\text{H}_2\text{O}$) (Grawe, 1956) and hexahydrate. Because the iron analogs of these compounds have nearly identical diffraction patterns, the presence of magnesium was verified by semiquantitative spectrographic analyses.

OTHER OCCURRENCES OF CELESTITE AND CALCIOSTRONTIANITE IN VIRGINIA

Lozenge-shaped celestite crystals, up to $\frac{1}{2}$ inch across occur in vugs in a quarry in Tonoloway limestone, of the Cayuga group, at Hayfield, Frederick County. Near Fulks Run, Rockingham County, small vugs and cavities in Tonoloway limestone contain celestite crystals. The discovery of these three occurrences of celestite in rocks of the Cayuga group in widely separated sections of Virginia strongly suggests that strontium minerals may be found at other places in the state in rocks of this age.

Dietrich (1960) has recently reported calciostrontianite, with small amounts of celestite, in vugs and on joint surfaces in dolomite (Elbrook limestone, Cambrian), from the Salem Rock Corporation Quarry south of Dublin, Pulaski County. One of the writers (RFP) has recently noticed thick fibrous veins of celestite, as well as vugs containing good crystals up to $\frac{1}{4}$ inch across, in a road cut near the same quarry. Dietrich (1960) also observed calciostrontianite in vugs in a limestone drill core from the Athens formation (Middle Ordovician) obtained near Harrisonburg, Rockingham County.

ACKNOWLEDGMENTS

The writers wish to express their gratitude to Mr. G. H. Belton for his cooperation in allowing them to examine and collect from his quarry; and also for making all the specimens he and his son collected for several

years available for study. Special thanks are due Dr. Bruce Hobbs, of the Virginia Division of Mineral Resources, for taking the photographs of celestite and calciostrontianite which are reproduced in this paper.

REFERENCES

- CATHREIN, A. (1888) Ueber Calciostrontianit (Emmonit) von Brixlegg: *Z. Krist.*, **14**, 366-374.
- DIETRICH, R. V. (1960), Calciostrontianite from Pulaski and Rockingham Counties, Virginia: *Am. Mineral.*, **45**, 1119-1124.
- EBY, J. B. (1923), The geology and mineral resources of Wise County and the coal-bearing portion of Scott County, Virginia: *Virginia Geol. Survey, Bull.*, **24**, 36-40.
- GRAWE, O. R. (1956), Starkeyite, a correction: *Am. Mineral.*, **41**, 662.
- PALACHE, C., BERMAN, H. AND FRONDEL, C. (1951), *Dana's System of Mineralogy* (7th): New York, John Wiley, **2**, 196-200.
- PHARR, R. F. AND MITCHELL, R. S. (1959), Celestite and strontianite from Wise County, Virginia: *Virginia J. Sci.*, **10**, 295.
- SWANSON, H. E. AND FUYAT, R. K. (1953), *Natl. Bur. Standards (U. S.) Circ.* 539, **2**, 61-62.
- AND UGRINIC, G. M. (1954), *Natl. Bur. Standards (U. S.) Circ.* 539, **3**, 56-57.
- THOMSON, T. (1836) Description and analysis of emmonite, a new species of carbonated strontium from America: *Records of General Science*, **3**, 415-417.

Manuscript received April 12, 1960.

PHASE TRANSFORMATIONS IN SILICA AS EXAMINED BY CONTINUOUS X-RAY DIFFRACTION

F. M. WAHL, R. E. GRIM, AND R. B. GRAF,
University of Illinois, Urbana, Illinois.

ABSTRACT

The phase transformations of six different varieties of silica were examined by continuous x-ray diffraction while heated to 1400° C.

The (101) peak intensity changes which often accompany the α - β quartz inversion are a function of particle size. There is, however, no correlation between these changes and the gradual increase in the (101) d -spacing as the material is heated.

The crystallization temperature of β -cristobalite from a siliceous material is a consequence of the crystallinity and initial structural perfection of that material—the better the crystallinity, the higher the transition temperature. Rock crystal quartz gives β -cristobalite at 1200° C.; whereas, amorphous silica gel produces this phase of 900° C.

Tridymite was not detected as a transitional phase mineral in the silica system.

INTRODUCTION

During the past few decades many persons have studied the silica system and have presented data regarding the stability conditions of polymorphic silica minerals.

Previous methods and techniques used in examining the silica system were diversified. In an early fundamental investigation of this system, Fenner (1913) used static equilibrium conditions. Since that time, the thermochemical measurements of Mosesman and Pitzer (1941), the differential thermal studies of Keith and Tuttle (1952), and numerous other investigations by Sosman (1927), Jay (1933), Buerger (1954), Flörke (1955 and 1956), and Holmquist (1958), to mention only a few, have contributed greatly to our knowledge and understanding of this system.

The design and inception of continuous heating x-ray diffraction techniques now permit a new approach to the examination of certain problems regarding phase transformations within the SiO_2 system. This report is based on data obtained using this heating-diffraction technique. Of principal interest is the alpha-beta quartz inversion and the crystallization temperature for different initial forms of silica, and also the establishment of this technique for studying the effect of inherent structure of material upon consequent mineral phase transformations.

SAMPLES AND PROCEDURE

Six varieties of silica representing different degrees of structural perfection and crystallinity were examined by continuous x-ray diffraction as they were heated to 1400° C. These were rock crystal quartz from near Hot Springs, Arkansas; chert from Dover, England; chalcedony

from Middle Park, Colorado; opal from Guanajuato, Mexico; silica gel, grade 42, Davison Chemical Company; and, silicic acid, 100 mesh, A. R. grade, Mallinckrodt Chemical Works.

Each of these materials was heated in the furnace in the x-ray diffraction unit at a program rate of 5° C. per minute. During the heating operation, diffraction data were logged for the 2θ interval containing the major diffraction reflections of the material under investigation. This traverse was normally restricted to a 2θ range of 19° to 27° and thus provided a continuous diffraction record of the (100) and (101) quartz peaks and the diagnostic (111) β -cristobalite reflection.

The furnace used was constructed on the same principle as that designed by G. Kulbicki and described by Grim and Kulbicki in 1957. It was adapted for use with a Philips recording diffractometer. All data to be presented herein were obtained using this type furnace and nickel-filtered copper radiation at 45 Kvp. and 18 ma.

The data curves shown in this report are a measure of the intensities of the diagnostic diffraction peaks as plotted against the temperatures at which they occurred. The resultant plot is a series of points representing the presence of a specific mineral phase at various temperatures. By connecting these representative points a curve is obtained for that particular mineral (Fig. 1). From the nature and configuration of this curve one can ascertain (a) the initial nucleation and growth of any new mineral phase, (b) the prevalence of any initial mineral with its consequent breakdown upon heating, and (c) the apparent rate of any structural inversion or new phase mineral formation.

EXPERIMENTAL DATA

Rock Crystal Quartz

The α - β inversion in quartz was examined in detail. Rock crystal quartz was first crushed and then fractionated to obtain different size-grade materials. In addition to the unsized material the less-than-74 micron and less-than-2 micron fractions were isolated. Each of these fractions was x-rayed continuously while being heated to 1400° C.

A gradual shift in the d -spacing of the (101) reflection was observed as the quartz samples were heated. These values as recorded at specific temperatures are listed in Table 1, and plotted in Fig. 2. They show a gradual increase in the α -quartz (101) value of 3.34 \AA as the sample is heated up to about 600° C. at which temperature a value of 3.38 \AA is attained. Above this temperature, which is the temperature usually given for the α - β quartz inversion, there is again a gradual increase in this same value with the rate of increase becoming greater at higher temperatures. Taken as a whole there is a gradual increase in this dimension as the sample is

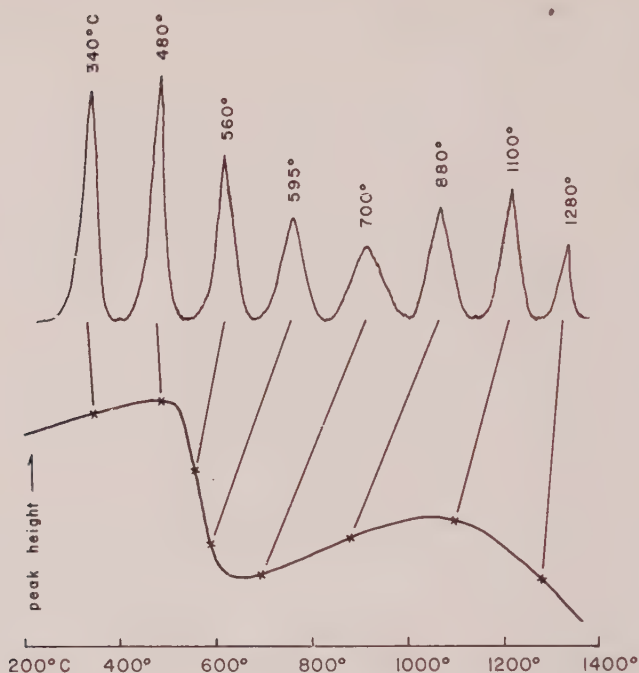


FIG. 1. Method used in plotting x-ray diffraction data. The intensities of a characteristic diffraction peak at different temperatures are transferred to a curve.

heated upward from 200° C. with a slight break at about 600° C., which is essentially a reduction in rate of increase, and a final increase in rate just prior to the transformation to β -cristobalite. D.T.A. curves show an endothermic reaction at about 570° C. indicating some structural rearrangement at this temperature. A 3.42 Å β -quartz spacing was eventually

TABLE 1. SPACING VALUES OF THE (101) QUARTZ REFLECTION AT VARIOUS TEMPERATURES

Temperature	<i>d</i> -value of (101) reflection
20° C.	3.34 Å
220° C.	3.35 Å
390° C.	3.36 Å
490° C.	3.37 Å
595° C.	3.38 Å
1120° C.	3.39 Å
1280° C.	3.40 Å
1340° C.	3.41 Å
1370° C.	3.42 Å

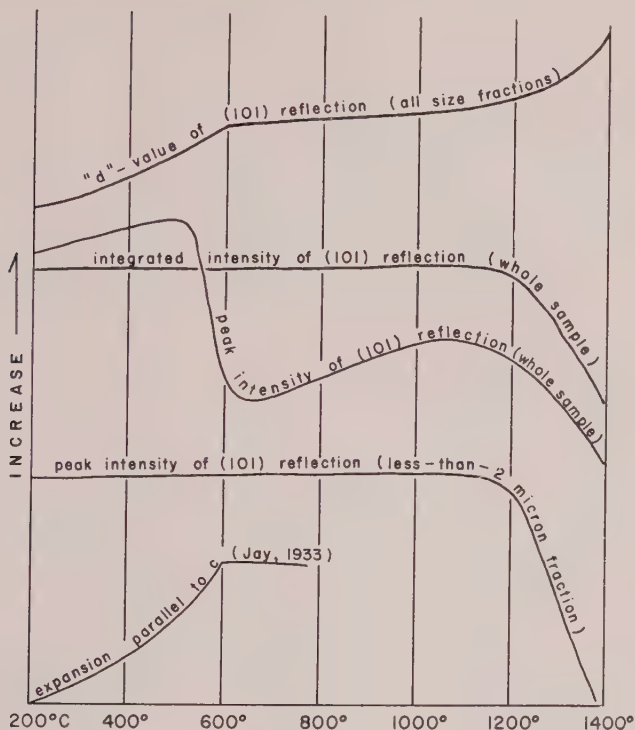


FIG. 2. Changes in quartz as heated to 1400° C.

reached at 1370° C. at the rate of firing used. It is important to note that the same increase in the (101) d -spacing of quartz was observed as each of the three different size fractions was heated.

Diffraction results from these three quartz fractions are shown in Fig. 3. The unsized fraction and the less than -74 micron fraction show a slight gradual increase in the peak height of the (101) quartz reflection with an increase in temperature up to about 500° C. Accompanying heating from 500° to 600° C. there is a sharp drop in peak height, but on heating to higher temperatures the intensity of this reflection gradually increases again. As the temperature of formation of cristobalite is approached the intensity of the quartz reflection decreases. Thus, there is a gradual increase in the intensity of this peak immediately preceding both the break in dimension change in α - β quartz (and the temperature of the thermal reaction) and the transformation to β -cristobalite. The change in the (101) quartz dimension between 500° and 600° C. is accompanied by an abrupt change in peak height, but not an overall change in diffrac-

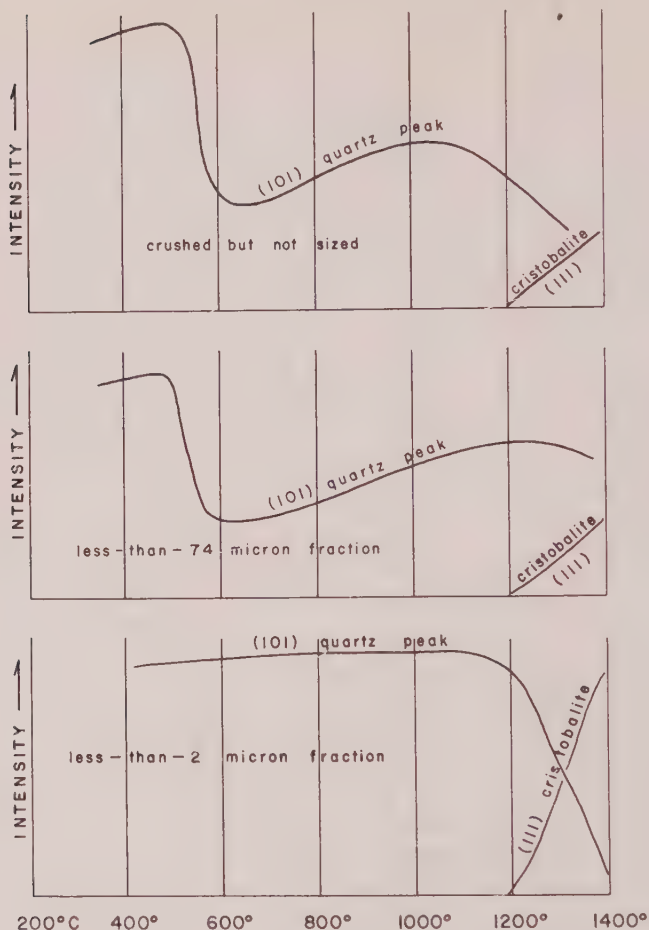


FIG. 3. Continuous x-ray diffraction results from rock crystal quartz.

tion intensity. The abrupt change in peak height is accompanied by an increase in peak width (Fig. 1) so that the integrated intensity is the same.

Rock crystal quartz (less-than-2 micron fraction), shows no comparable intensity change of the (101) reflection as the sample is heated from 400° to 800° C. In general there is only a slight increase in peak height prior to the formation of β -cristobalite at 1200° C. Following cristobalite nucleation the intensity decrease representing break-down of the existing phase is compatible with the intensity increase of the (111) cristobalite reflection indicative of the corresponding growth of this phase mineral. This loss of quartz and consequent formation of β -cristobalite was the same for all size fractions of the specimen.

In order to determine the effect of prolonged heating on the (101) d -spacing shift, less-than-2 micron quartz was held at various temperatures for different periods of time. After 20 hours at 520° C. the (101) reflection maintained a 3.37 Å dimension—the same value that was initially measured at 520° C. during the regular heating cycle. When held at 650° C. the same relationship was observed; namely, there was no additional shifting of the (101) reflection value from 3.38 Å, the initially recorded value at that temperature. With an additional temperature increase the d -spacing continues to increase, slowly at first but more rapidly above 1200° C.

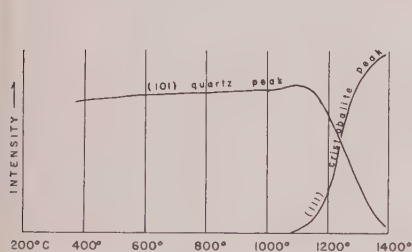
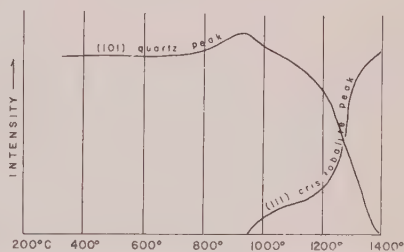


FIG. 4 (left). Continuous x-ray diffraction results from less-than-2 micron chert as heated to 1400° C.

FIG. 5 (right). Continuous x-ray diffraction results from less-than-2 micron chalcedony as heated to 1400° C.



Chert

The heating curve for the less-than-2 micron chert sample (Fig. 4) is similar in configuration to that of less-than-2 micron quartz. No intensity variation of the initial α -quartz (101) diffraction peak accompanies heating from 400° to 800° C. There is a slight increase in the intensity of the (101) reflection just prior to cristobalite nucleation at 1050° C.

Chert also exhibits a gradual shift in the d -spacing as it is heated. The rate of this change is of the same approximate magnitude as that observed from rock crystal quartz; however, the maximum dimension attained at 1370° C. was only 3.39 Å instead of the 3.42 Å value recorded for the beta modification as derived from rock crystal quartz at that temperature.

Chalcedony

The less-than-2 micron chalcedony (Fig. 5) initially showed diffraction effects for α -quartz. There was no gradual intensity change of the (101) reflection on heating from 400° to 800° C. An increase in diffraction peak intensity suggesting an increase in structural perfection is indicated,

however, just prior to the initial appearance of β -cristobalite at 950°C . With the nucleation and growth of cristobalite, there is a comparable decrease in the intensity of the quartz peak. That is, the quartz progressively decreases as the cristobalite increases. With the ultimate disappearance of quartz there is a leveling out of the β -cristobalite curve signifying complete conversion. A gradual shift in the d -spacing of the (101) reflection again accompanied the heating of this material. As with chert the maximum value attained for β -quartz was only 3.39 \AA .

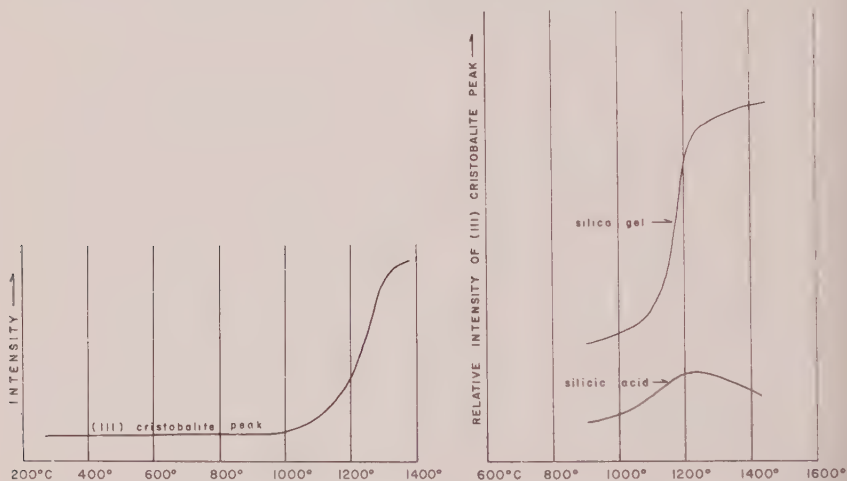


FIG. 6 (left). Changes in the cristobalite (111) peak intensity as opal is heated to 1400°C .

FIG. 7 (right). Curves depicting the formation of beta-cristobalite from silicic acid and silica gel.

Opal

Opal showed diffraction effects only for cristobalite. When heated, a definite increase in structural perfection of the initial cristobalite framework was indicated by a sharpening and increase in intensity of the (111) peak. This perfection and consequent intensity rise of the (111) reflection is not prominent, however, until the opal has been heated to 1000°C . Above this temperature the intensity increase is quite rapid until at 1400°C a maximum is reached representing optimum structural perfection (Fig. 6).

Silicic acid

On heating, silicic acid showed no diffraction effects prior to 900°C . At that temperature, however, beta-cristobalite began forming. The cristobalite diffraction peaks increased gradually in intensity with continued

heating and attained a maximum at 1250° C. (Fig. 7). A measure of the beta-cristobalite (111) reflection peak intensity is regarded as an indication of the amount of nucleation of, or the degree of transformation to this modification: thus, the maximum intensity at 1250° C. represents the most complete conversion of the silicic acid to beta-cristobalite under these conditions of heating. At temperatures above 1250° C. there is a decrease in the peak intensity which accompanies partial fusion. It is noted that no diffraction data for other SiO₂ polymorphs were observed prior to the formation of beta-cristobalite, *i.e.*, no quartz or tridymite formed prior to the cristobalite.

Silica gel

Silica gel also gave no diffraction peaks prior to 900° C. At that temperature beta-cristobalite began forming (Fig. 7). The most rapid cristobalite growth as indicated by the (111) reflection peak intensity occurred between 1100° and 1200° C., and nearly complete transformation was reached by 1400° C. Neither α nor β -quartz, nor tridymite formed prior to the nucleation of β -cristobalite.

DISCUSSION

The sharpness and intensity of an x-ray diffraction peak can usually be regarded as an indication of the degree of crystallinity and perfection of atomic arrangement within the structural framework of a mineral. Thus, the nature of the (101) quartz reflection should be acceptable as a standard upon which the perfection of atomic arrangement of the alpha and beta forms of this mineral can be compared. Of particular interest are the diffraction data obtained while heating rock crystal quartz, chert, and chalcedony. Prior to heating each of these materials gave relatively sharp 3.34 Å diffraction peaks.

There was an abrupt decrease in peak height intensity of the (101) reflection as crushed-but-unsized quartz was heated from 400° to 800° C. which includes the temperature interval usually given for the alpha-beta quartz inversion; whereas, there was no intensity decrease of this same reflection when the less-than-2 micron fraction of the same specimen was heated through the identical temperature interval. Integrated peak area intensity measurements through the inversion interval are, however, the same for both fractions. Keith and Tuttle (1952) report that in the coarser-grained chert and novaculite samples which they examined, the observable heat effects were only weak; whereas, after fine grinding these same materials showed a measurable heat adsorption through the inversion.

The diffraction intensity data, dimensional values, and thermal data all suggest a relatively pronounced structural inversion at about 600° C.

It seems logical that in an aggregate the larger particles should require more time for complete inversion, especially if the actual transition starts at the surface of a grain and then proceeds inward as an advancing front along which the reaction occurs between two solid phases (Kracek, 1951). However, the smaller size and uniformity of the less-than-2 micron material would not require as much time for complete particle inversion; thus, when the necessary temperature is reached, there should be a simultaneous and essentially complete transformation of all particles. Any intensity decrease of the (101) peak during this transition would be immediate and thus difficult to record, because following structural inversion the intensity of this reflection is virtually the same as that preceding structural transformation.

The gradual increase of the (101) lattice dimension of quartz is certainly a function of temperature. Jay (1933) reported a progressive increase in the dimensions of quartz as it was heated to the transition temperature, but he also observed a slight contraction parallel to c , above 600°C . Our data show a similar change in lattice dimension, but also indicate an additional progressive increase at higher temperatures until complete transformation to cristobalite is accomplished. After prolonged heating at 650°C ., the (101) dimension is 3.38 \AA —a value reported to be characteristic of β -quartz at that temperature. This gradual increase in d -spacing cannot be correlated with any increases or decreases in the (101) peak intensity measurements (Fig. 2), but it does follow closely the expansion measurements that Jay recorded up to 700°C . Even after some of the material has been converted to cristobalite at 1250°C . the (101) lattice dimension of the remaining quartz continues to increase.

In the literature there is a lack of agreement as to the unit cell dimensions for β -quartz. Bragg and Gibbs (1925) determined their measurements from quartz held at 700°C . for several hours and list dimensions of $c = 5.446\text{ \AA}$ and $a = 4.989\text{ \AA}$. Wyckoff (1926) gives unit cell dimensions of $c = 5.47\text{ \AA}$ and $a = 5.01\text{ \AA}$; whereas, the most recent A.S.T.M. data, based on quartz derived by firing to 1000°C ., but measured at room temperature (Bradley and Grim, 1951), indicates dimensions of $c = 5.37\text{ \AA}$ and $a = 5.11\text{ \AA}$. It is important to emphasize that the dimensions obtained are always dependent on the temperature at which the material is measured.

Wright and Larsen (1909) studied quartz optically as it was heated. They reported gradual changes in birefringence on heating to 1400°C . The fact that birefringence changes occur gradually, taking place over the entire temperature range, and are not restricted to the 570° – 575°C . inversion temperature interval is significant. These continuous optical changes and the gradual d -spacing changes which we recorded both indicate a continuous gradual change in the internal atomic arrangement of

quartz as it is heated. The continual change in dimension through the temperature interval where an abrupt energy reaction occurs, and where optical characteristics change, is in accord with structural considerations brought out by Bragg (1925) and others.

Structural rearrangement begins with heating; however, not until approximately 570° C. is there an abrupt change in the Si-O-Si bonding arrangement of α -quartz to that of β -quartz. This is indicated by the sharp endothermic reaction on the thermal curve. With additional temperature increases, however, there is a continued preferential rearrangement of the silica tetrahedra within the newly developed structural framework to attain a more desired arrangement. The degree of tetrahedral organization is a direct function of temperature and as the temperature is increased, and the rearrangement accomplished, there is once again a progressive change in the lattice dimensions of the material. This additional change in dimension is slow between 600° and 1000° C., but increases more rapidly as the cristobalite crystallization temperature is reached (Fig. 2). This increase in dimension is of the same magnitude as that observed preceding the α - β quartz inversion. It is a predecessor of cristobalite density and depicts the beginning of a tetrahedral rearrangement which ultimately results in the cristobalite structure.

The inversion of the α -quartz structure requires more time in aggregates containing larger particles; whereas, in the smaller less-than-2 micron particles the breakdown is simultaneous. The tetrahedral reorganization which occurs above 600° C. takes place at the same rate regardless of particle size and is only a function of temperature. The ultimate degree of perfection that can be attained is contingent on the structural perfection of the α -quartz before inversion. Rock crystal quartz produces β -quartz with a (101) d -value of 3.42 Å; whereas, chert and chalcedony give β -quartz structures with maximum (101) values of approximately 3.39 Å. This is probably the consequence of larger crystals withstanding higher temperatures before their transformation to cristobalite.

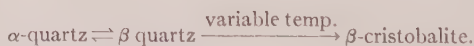
The curves of quartz, chert, and chalcedony all show a gradual intensity increase of the (101) reflection prior to the breakdown of the β -quartz structure to form β -cristobalite. The magnitude of this increase, however, is different for each material (Figs. 3, 4, and 5), and appears to be directly related to the crystallization temperature of β -cristobalite and to the initial structural perfection of the type of silica. Such an intensity increase is again an indication of improved atomic arrangement within the β -quartz framework.

The actual temperatures at which β -cristobalite forms from each of the materials appears to be a consequence of the structural perfection of the starting material. Silicic acid and silica gel, which are mostly amorphous,

both crystallize to form β -cristobalite at 900° C. without any prior quartz phase; whereas, chalcedony, chert, and rock crystal quartz, which develop β -cristobalite at 950°, 1050°, and 1200° C. respectively, represent higher degrees of crystallinity and structural perfection in that order. The heating curves of the latter three materials also show a comparable reduction in the increase in the intensity of the quartz reflection prior to the cristobalite transition, *i.e.*, quartz, which has the highest β -cristobalite crystallization temperature, also has the smallest increase in quartz intensity. This comparable reduction of any increase in the (101) peak intensity preceding transformation, when coupled with the higher temperature at which the structural transition occurs, would indicate that the crystallization temperature for β -cristobalite as it forms from any such siliceous material is a consequence of the initial structural perfection of that material. The better the initial structure, the smaller the (101) peak intensity increase which precedes the β -cristobalite formation, and also the higher the temperature of this transformation.

Because of this apparent relationship between the crystallization temperature of β -cristobalite and the initial perfection of the atomic arrangement or structure of the material, it is suggested that temperature alone be minimized as a major factor controlling this transformation. It is suggested that in the one-component SiO_2 system the formation temperature of β -cristobalite should not be considered as a fixed value, but rather that it be expressed as a function of the crystallinity and structural perfection of the material from which it develops. The formation of cristobalite at 900° C. from amorphous silicic acid and silica gel adds credence to this proposal.

The absence of tridymite when the different SiO_2 materials are heated is noteworthy. More than forty different heating trials were made during the course of our study and not once was any indication of the presence or formation of any tridymite observed. The normal transformation sequence was



The absence of the tridymite "phase" is not unusual in studies of the one-component SiO_2 system; in fact, this modification has never been synthesized in the laboratory without the use of "mineralizers" which introduce foreign ions into the system and thereby result in "complex-stuffed" derivatives (Flörke, 1955).

Hill and Roy (1957) reportedly prepared pure tridymite hydrothermally at a pressure of several hundred atmospheres from all forms of silica; however, Holmquist (1958) states that under hydrothermal conditions the hydronium ion, H_3O^+ , has the same effect as the mineralizing ion

potassium which, according to Flörke (1956) is the best promoter of the formation of tridymite.

Flörke (1955) questions the fact that tridymite can exist as a thermodynamically stable phase of pure silica at one atmosphere pressure. Holmquist (1958) re-examined, thermodynamically, the possible transformations of this system. He concludes that "... the mineral tridymite is not a stable phase of pure silica at one atmosphere but belongs in binary and multicomponent systems."

If tridymite is removed from the SiO_2 system, where should the inversion temperature between the stability fields of quartz and cristobalite be placed? Mosesman and Pitzer (1941) concluded such a hypothetical inversion point at about 1050°C . at ordinary pressures. Our data would support such a direct transformation; however, we would propose that the exact temperature at which this inversion takes place is a consequence of initial structural perfection when dealing with already crystallized materials.

SUMMARY

Phase transformations of various forms of silica on heating to 1400°C . were studied by continuous x-ray diffraction. Curves representing peak intensity of the silica phases versus temperature are presented for the different forms of silica.

On heating silica gel and silicic acid, β -cristobalite forms directly at 900°C . from both materials without any pure quartz phase. On heating chalcedony, chert, and quartz there is a gradual change in the (101) quartz spacing as the temperature increases from 60° to 1370°C . However, only in the case of rock crystal quartz was a 3.42 \AA value attained. In the case of quartz in fairly coarse particles, the intensity of the (101) reflection sharply drops at the initiation of the α - β transition but increases again as the spacing of the β -form develops. This phenomenon is an indirect consequence of particle size, for integrated peak area intensity measurements show no such abrupt change.

The relatively abrupt change in structure at 570°C . is followed by a gradual preferential reorganization of the silica tetrahedra with additional temperature increases. This is suggested by gradual changes in crystal dimension that also accompany heating to higher temperatures. These dimensional changes, however, cannot be attributed solely to thermal expansion for they are often accompanied by a gradual increase in the intensity of the (101) quartz reflection prior to conversion to β -cristobalite. This increase is particularly pronounced for chalcedony and very scant for quartz, and could indicate a better arrangement of silicon and oxygen atoms within the β -quartz structure just prior to structural transformation. There is a more rapid change in dimension above

1000° C. as the cristobalite density is approached. This progressive change resembles that which precedes the α - β quartz inversion.

Variations in the crystallization temperatures of β -cristobalite as formed from different varieties of silica show that the better the crystallinity and structural perfection of the silica, the higher the β -cristobalite crystallization temperature. Rock crystal quartz forms β -cristobalite at 1200° C., but silica gel produces this modification at 900° C.

A direct inversion from β -quartz to β -cristobalite is supported; however, the exact temperature of this transformation is believed to be a function of the crystallinity of the starting material.

At no time was tridymite identified; thus, the authors support those who would eliminate tridymite as a stable phase mineral in the one-component silica system.

REFERENCES

- BRADLEY, W. F., AND GRIM, R. E., High temperature thermal effects of clay and related minerals: *Am. Mineral.*, **36**, 182-201 (1951).
- BRAGG, W. H., AND GIBBS, R. E., The structure of α and β quartz: *Proc. Roy. Soc.*, **A109**, 405-427 (1925).
- BUERGER, M. J., The stuffed derivatives of the silica structures: *Am. Mineral.*, **39**, 600-614 (1954).
- EITEL, W., The silica system: The Physical Chemistry of the Silicates, Univ. of Chicago Press, 616-629 (1954).
- FENNER, C. N., The stability relations of the silica minerals: *Am. Jour. Sci.*, **36**, 331-384 (1913).
- FLÖRKE, O. W., Structural anomalies in tridymite and cristobalite: *Berichte der Deutschen Keramischen Gesellschaft*, **32**, 369-381 (1955): Translation by Eitel, W., *Bull. Am. Cer. Soc.*, **36**, 142-148 (1957).
- FLÖRKE, O. W., Über das einstoffsystem SiO_2 : *Naturwissenschaften*, **43**, 419-420 (1956).
- GRIM, R. E., AND KULBICKI, G., Etude aux rayons X des reactions des mineraux argileux a haute temperature: *Bull. de la Societe Francaise de Ceramique*, 21-27 (1957).
- HILL, V. J., AND ROY, R., New data on the tridymite problem: *Acta Crystallogr.*, **10**, 835 (1957).
- HOLMQUIST, S. B., A note on the sluggish silica transformations: *Zeit. für Krist.*, **111**, 71-76 (1958).
- JAY, A. H., Thermal expansion of quartz: *Proc. Roy. Soc.*, **142**, 237-247 (1933).
- KEITH, M. L., AND TUTTLE, O. F., Significance of variations in the high-low inversion of quartz: *Am. Jour. Sci.* (Bowen Vol.), 203-280 (1952).
- KRACEK, F. C., Phase transformations in one-component silicate systems: Phase Transformations in Solids, Ch. 9, (1951).
- MOSESAN, M. A., AND PITZER, K. S., Thermodynamic properties of the crystalline forms of silica: *Jour. Am. Chem. Soc.*, **63**, 2348-2356 (1941).
- SOSMAN, R. B., The properties of silica: *Am. Chem. Soc. Monograph* **37** (1927).
- WRIGHT, F. E., AND LARSEN, E. S., Quartz as a geologic thermometer: *Am. Jour. Sci.*, **27**, 421-447 (1909).
- WYCKOFF, R. W. G., The crystal structure of the high temperature (β) modification of quartz: *Am. Jour. Sci.*, **11**, 101-112 (1926).

THE MINERALOGY OF THE BAUXITE DEPOSITS NEAR WEIPA, QUEENSLAND

F. C. LOUGHNAN AND P. BAYLISS, *University of New
South Wales, Kensington, N.S.W., Australia.*

ABSTRACT

Chemical and mineralogical data for three bauxite profiles from the Weipa area, Queensland, indicate that the deposits have resulted from the intensive leaching of kaolinitic sandstones. Three zones, each characterized by the mineralogy, are demarcated within the profiles. It is considered that the bauxitization processes probably commenced in the lower to middle Tertiary and are continuing at present under a tropical, monsoonal climate.

INTRODUCTION

The Weipa lateritic bauxites are located on the almost uninhabited west coast of Cape York Peninsula (Fig. 1) where they extend discontinuously over a flat, low-lying and relatively close-timbered terrain from Vrilya Point to Archer Bay, a distance of 150 miles and up to 30 miles inland (Evans 1959). The deposits are underlain by arenaceous sediments which David (1950) considered Cretaceous (Tambo Group) but more recently Evans (1959) has suggested that these may be Tertiary in age.

The climate is hot and monsoonal (Fig. 2) with a mean temperature of 82° F. and an average rainfall of 60 inches per annum concentrated in the period from December to March.

Previous mineralogical investigations (Baker 1958, Edwards 1957, 1958 and Edwards and McAndrew 1956) were non-systematic while proposed mechanisms of genesis, in general, have been speculative.

It is the purpose of the present investigation to demonstrate that in a suitably "aggressive" environment, a parent material containing 90% silica and as little as 4% alumina, may give rise to bauxites relatively deficient in silica. To this end, channel samples from Andoom (maximum depth 19 feet), Weipa (36 feet) and Pera Head (42 feet) and bore cones from Weipa and Pera Head were obtained by courtesy of the Commonwealth Aluminium Corp. Pty. Ltd. Detailed work was carried out on the channel samples only since the bore cones yielded similar results. The channel samples at Weipa and Pera Head extended to sea level.

MINERALOGY

The quantitative determination of the mineralogy was made by x-ray diffraction, differential thermal and chemical analyses, and thermogravimetric methods employing a specially designed program controller which permitted hourly soaking at specific temperatures coincident with the dehydroxylation of gibbsite, boehmite and kaolinite. It is estimated

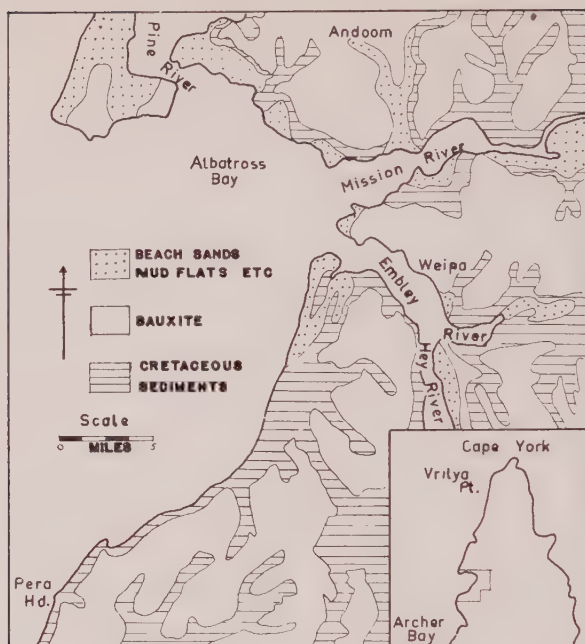


FIG. 1. Geological sketch map of the Weipa Area, Queensland.

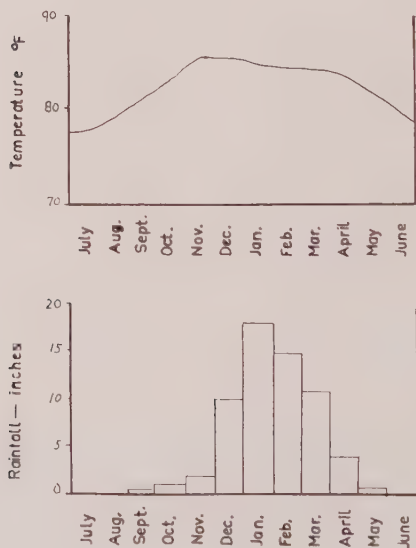


FIG. 2. Rainfall and temperature distribution at Weipa, Queensland.

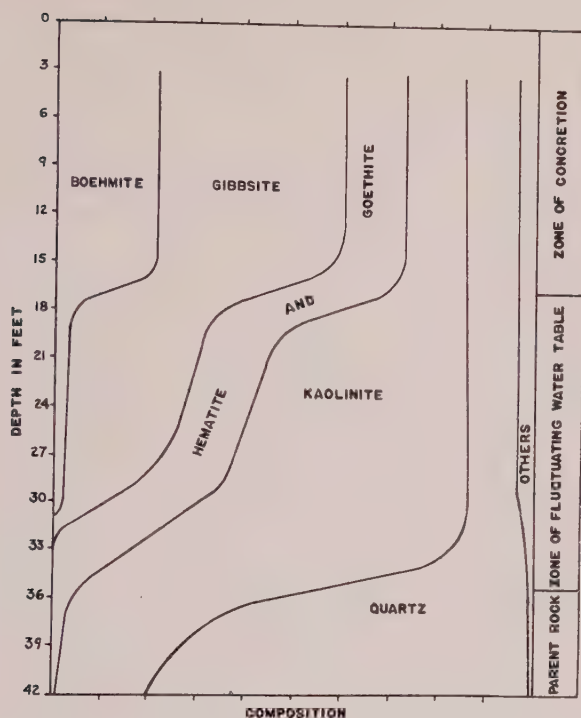


FIG. 3. Mineralogy in relation to depth at Pera Head.

from the combination of these techniques, that the mineralogy given in Table 1 and on which Figs. 3 and 4 are based, has a probable accuracy of plus or minus 2%. Chemical data are given in Table 2.

Three zones, each characterized by the mineralogy, are recognisable in the profiles from Weipa and Pera Head (see Figs. 3 and 4). The sampling program at Andoom did not penetrate to the parent material.

- (a) *The Parent material* is a loosely consolidated, light-colored sandstone with coarse, angular, though well graded quartz which in the Weipa profile approaches 90% of the rock while kaolinite forms the matrix. Edwards (1957) suggested that this sandstone may be arkosic but in the present survey, feldspar was not detected nor did the chemical analyses reveal sufficient alkalis to render the rock arkosic. The boundary with the overlying zone is gradational.
- (b) *The zone of fluctuating water table* approximates 18 feet thick in both the Weipa and Pera Head profiles. The material is dark red but varies in coherence from relatively friable at Weipa to dense and compacted at Pera Head.

The variation in the mineralogy is gradational from the almost permanently saturated lower few feet of the zone where quartz and kaolinite are the dominant constituents to the relatively more arid upper regions where gibbsite predominates. The coarse, angular characteristics of the quartz prevail throughout while etched

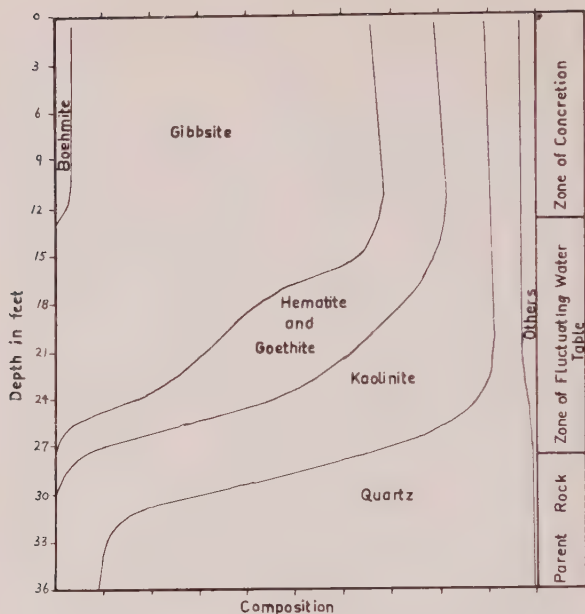


FIG. 4. Mineralogy in relation to depth at Weipa.

and pitted surfaces may be noted on some of the grains. Hematite and/or goethite, principally in the form of irregular concretions, together with kaolinite, reach their maximum development a few feet from the base of the zone, but at higher levels kaolinite gives way to gibbsite. These features are less apparent in the Pera Head profile since marine erosion has modified the water table level in the area, increasing drainage and permitting the development of a little boehmite.

- (c) *The concretionary zone* which is clearly defined from the underlying material, varies in thickness up to 15 feet. Gibbsite, hematite, and/or goethite, in the form of roughly spherical pisolites, frequently bonded together, predominate, though interstitial aluminum hydrates and kaolinite are common. A small but constant amount of quartz with features similar to that in the underlying zone, is present throughout. The pisolites vary from one to twenty mm. in diameter while the concentric bands range up to 0.4 mm. in width. The quartz grains occur in the interstices between small pisolites, in the outer shells and occasionally as the nuclei. Boehmite reaches its maximum development in this zone presumably through the partial dehydroxylation of gibbsite. A few feet of dark colored soil generally overlies the lateritic bauxite.

There is a progressive increase in the pH from approximately 5.5 in the concretionary zone to near neutrality below the water table.

Excluding the ferruginous minerals, the recoverable "heavy fraction" rarely exceeds a few tenths of a per cent of the whole. The variety is limited, with titania minerals (rutile, anatase and leucosene) predominating, though fine zircon euhedra and anhedra are common and ilmenite and a few grains of monazite, were noted in the parent sandstone.

TABLE 1. MINERALOGY OF BAUXITE DEPOSITS

Sample No.	Depth in Feet	Boehmite %	Gibbsite %	Hematite %	Goethite %	Kaolinite %	Quartz %	Others %
Andoom								
A1	0- 3	8	50	4	14	12	7	5
A2	3- 6	5	42	5	14	20	11	3
A3	6- 7	5	6	18	15	41	13	2
A4	9-10	5	6	14	18	42	13	2
A5	12-13	2	6	12	21	43	14	2
A6	15-16	—	4	4	18	58	14	2
A7	18-19	—	—	7	18	59	14	2
Pera Head								
P1	3- 6	21	33	17	—	10	15	4
P2	6- 9	18	49	12	—	10	8	3
P3	9-12	23	37	18	—	9	8	5
P4	12-15	21	37	15	—	12	10	5
P5	15-18	21	35	17	—	10	12	5
P6	18-19	2	30	14	—	38	12	4
P7	21-22	3	27	10	5	40	12	3
P8	24-25	1	19	5	7	54	11	3
P9	27-28	1	22	5	10	50	9	3
P10	29-30	2	18	10	5	53	9	3
P11	32-33	—	—	6	10	70	12	2
P12	35-36	—	—	—	4	41	53	2
P13	38-39	—	—	—	2	25	73	—
P14	41-42	—	—	—	1	20	79	—
Weipa								
W1	1- 4	4	61	4	10	12	5	4
W2	4- 7	4	61	4	10	12	5	4
W3	7-10	4	63	7	5	12	5	4
W4	10-13	4	65	3	7	12	5	4
W5	13-16	—	70	1	10	10	5	4
W6	16-19	—	40	11	16	26	5	2
W7	19-22	—	33	22	6	32	5	2
W8	22-25	—	20	21	6	46	5	2
W9	25-28	—	6	22	5	60	5	2
W10	28-29	—	—	3	—	42	54	1
W11	31-32	—	—	—	—	10	89	1
W12	33-34	—	—	—	—	13	86	1
W13	35-36	—	—	—	—	10	89	1

TABLE 2. CHEMICAL DATA

Sample No.	SiO ₂	Al ₂ O ₃	Fe ₂ O ₃	TiO ₂	K ₂ O	Na ₂ O	H ₂ O+	H ₂ O-	Total
Andoom									
A1	11.0	44.1	16.7	2.6	—	—	23.4	2.2	100.0
A2	20.4	36.1	18.5	2.2	—	—	20.6	1.6	99.4
A3	29.5	25.9	31.1	1.4	—	—	11.1	1.2	100.2
A4	32.5	24.4	30.6	1.4	—	—	10.6	1.0	100.5
A5	33.6	22.5	30.4	1.4	—	—	10.6	1.0	99.5
A6	40.4	24.9	19.7	1.6	0.2	0.7	11.5	0.8	99.8
A7	40.6	23.1	22.4	1.4	0.2	0.2	10.8	0.8	99.5
Pera Head									
P1	18.9	44.5	16.9	2.0	—	—	15.5	2.2	100.0
P2	12.1	49.0	13.6	2.0	—	—	21.3	1.2	99.2
P3	12.0	48.4	17.4	2.0	—	—	17.5	2.4	99.7
P4	15.6	46.4	15.1	1.8	—	—	17.4	2.6	98.9
P5	17.1	44.6	17.0	1.8	—	—	16.5	2.8	99.8
P6	29.4	36.3	14.6	1.6	—	—	16.0	1.0	98.9
P7	30.4	35.7	14.4	1.6	—	—	15.9	0.8	98.8
P8	34.3	36.0	11.7	1.4	—	—	15.5	0.9	99.8
P9	31.6	35.6	14.5	1.4	—	—	16.2	1.0	100.3
P10	32.5	35.4	14.5	1.4	—	—	15.1	1.0	99.9
P11	41.8	30.9	14.0	1.2	—	—	11.0	0.8	99.7
P12	70.6	18.4	3.2	0.6	—	—	6.5	0.4	99.7
P13	82.5	10.1	1.8	0.5	0.1	0.8	3.6	0.2	99.6
P14	88.1	7.9	1.0	0.4	0.1	0.1	2.8	0.0	100.4
Weipa									
W1	9.9	47.1	13.1	2.1	—	—	24.6	2.2	99.0
W2	10.0	46.9	12.9	2.1	—	—	24.5	2.2	98.6
W3	10.6	48.8	11.5	2.2	—	—	24.5	2.2	99.8
W4	10.5	49.4	9.6	2.2	—	—	25.3	2.3	99.3
W5	9.6	50.0	9.2	2.2	—	—	26.6	2.1	99.7
W6	16.9	36.1	25.4	1.2	—	—	19.1	1.4	100.1
W7	19.4	34.3	26.3	1.2	—	—	16.6	1.2	99.0
W8	26.5	31.5	26.1	0.9	—	—	13.4	1.2	99.6
W9	31.5	28.6	25.8	0.9	—	—	11.4	1.0	99.2
W10	73.1	17.9	2.8	0.7	—	—	5.6	0.6	100.7
W11	92.9	4.1	0.5	0.2	—	—	1.0	0.0	98.7
W12	91.1	5.2	0.5	0.3	0.2	0.7	1.8	0.0	99.8
W13	93.2	3.9	0.2	0.2	0.1	0.8	1.4	0.0	99.8

DISCUSSION

The development of an assemblage of bauxite and laterite minerals from a kaolinitic sandstone of low alumina and iron content requires a particularly "aggressive" environment with sufficient rainfall and internal drainage to promote the leaching of silica, in the early stages from quartz but later from the breakdown of kaolinite, with the subsequent concentration of residual hydrates and oxides of aluminum and iron. It would be anticipated that, in such an environment, other stable ions (hydrolzate ions of Goldschmidt, 1937) would have concentration factors

TABLE 3. OXIDE RATIOS ($\times 10^3$) FOR WEIPA AND PERA HEAD PROFILES

Sample	TiO ₂	ZrO ₂	Cr ₂ O ₃	V ₂ O ₅	Sample	TiO ₂	ZrO ₂	Cr ₂ O ₃	V ₂ O ₅
	Al ₂ O ₃	Al ₂ O ₃	Al ₂ O ₃	Fe ₂ O ₃		Al ₂ O ₃	Al ₂ O ₃	Al ₂ O ₃	Fe ₂ O ₃
P1	45	3.9	1.8	2.3	W1	45	0.6	1.5	2.3
P2	41	3.1	1.5	3.0	W2	45	0.6	1.5	2.3
P3	41	3.1	2.1	2.8	W3	45	0.6	1.5	1.8
P4	39	3.0	1.7	2.6	W4	44	0.4	1.0	2.1
P5	40	3.2	2.2	2.3	W5	44	0.4	0.8	2.1
P6	44	3.8	1.7	3.4	W6	33	0.8	1.9	2.3
P7	45	2.6	1.4	4.5	W7	35	0.8	1.2	2.6
P8	39	2.0	1.1	3.5	W8	29	0.9	1.3	3.7
P9	39	2.0	1.4	4.1	W9	32	0.7	1.7	2.3
P10	39	2.5	1.4	3.4	W10	39	0.3	1.6	1.1
P11	39	2.9	1.0	2.9	W11	49	0.5	2.5	3.0
P12	33	4.2	0.9	4.7	W12	58	0.4	2.0	3.0
P13	50	3.0	1.0	4.4	W13	51	0.5	2.5	7.5
P14	50	3.7	1.0	6.0					

similar to alumina. In Table 3 the ratios of three of the stable oxides *viz.* titania, zirconia and chromic oxide, to alumina are given. The constancy of these ratios is remarkable considering the possible heterogeneity of the parent material and inaccuracies due to sampling and the determination of components often in trace amounts. The titania/alumina ratios showed the least deviation and it is significant that these components were determined by "wet" chemical means whereas analyses for zirconia and chromic oxide were made spectrographically.

The persistence of small quantities of quartz throughout the intensively leached zones could be attributed to the particularly coarse grain-size that this mineral attains in the parent rock and the protective coatings of aluminum and iron minerals. Baker (1958) considered that the etched and pitted nature of some of these residual quartz grains indicated chemical attack.

The ferruginous minerals reach their greatest development in the zone of fluctuating water table where the concentration of iron relative to the parent material exceeds that of alumina, indicating that processes in addition to the removal of material have contributed to their concentration. Factors considered pertinent to the greater relative concentration of hematite and/or goethite in this zone are (*a*) the annual fluctuations of the water table (*b*) the persistence of iron in the soluble ferrous state in the anaerobic environment below the water table (*c*) the rapid oxidation to the insoluble ferric state when exposed periodically to warm oxidizing conditions and (*d*) the high atmospheric temperatures which prevent accumulations of leaf mold and other organic matter at the surface thus rendering ineffective the reducing capacity of the infiltrating ground waters. The net result of these factors has been the upward migration and stabilization of the iron at levels where oxidation occurs.

It is interesting to note that vanadium which in the fully oxidized state has an ionic radius similar to iron, maintains a relatively constant ratio with the latter in the oxidized parts of the profile. (See Table 3).

A further correlation exists with the concentration factor on an alumina basis, and the surface topography. Weipa which has the least surface relief with a maximum gradient of two feet to the mile, displays the greatest alumina concentration, whereas at Andoon the surface gradients exceed 20 feet to the mile and the concentration of alumina is least.

In order to gain an indication of the time required for the development of the bauxite profile at Weipa, calculations based on the quantity of silica removed from the profile, were made. These calculations involved certain assumptions (*a*) that the area suffered no geologic disturbance throughout the period (*b*) that there has been no surface erosion (*c*) that the climate has remained static (*d*) that 20% of the rainfall has penetrated the profile (*e*) that the infiltrating waters assumed a pH less than 9 and reached 10% saturation with respect to silica. According to Krauskopf (1959), for a given temperature the solubility of silica is "little affected by changes of pH in the range 0-9."

The value obtained from these calculations was 50 million years placing the commencement of bauxitization at lower to middle Tertiary. However, it should be realized that a variation in any of the above assumptions could seriously affect the result.

ACKNOWLEDGMENTS

The authors are indebted to the staffs of Commonwealth Aluminium Corp. Pty. Ltd. and Exploration Enterprise for the collecting of samples

and for the excellent hospitality during the field trip, and to Mr. A. Rannit for the spectrographic analyses.

REFERENCES

- BAKER, G. (1958), Heavy minerals from the Weipa bauxite and associated sands: *C.S.I.R.O., Min. Inv.* **751**.
- DAVID, T. W. E., SIR (1950), *The geology of the commonwealth of Australia*: Ed. Arnold, Lond.
- EDWARDS, A. B. (1957), Quartz and heavy minerals in the Weipa bauxite: *C.S.I.R.O., Min. Inv.* **749**.
- (1958), Quartz and heavy minerals in the Weipa bauxite: *C.S.I.R.O., Min. Inv.* **750**.
- EDWARDS, A. B. AND MCANDREW, J. (1956), Boehmite and gibbsite in Weipa Bauxite, Queensland: *C.S.I.R.O., Min. Inv.* **749**.
- EVANS, H. J. (1959), The geology and exploration of the Cape York Peninsular bauxite deposits in northern Queensland: *Aust. Inst. Min. & Met. Brisbane Symp.*
- FISHER, N. H. (1958), Notes on lateritisation and mineral deposits: *Aust. Inst. Min. & Met., Stillwell Vol.*
- GOLDSCHMIDT, V. M. (1937), Principles and distribution of chemical elements in minerals and rocks: *J. Chem. Soc. (Lond.)*, 655–673.
- HEIM, R. E. (1952), *Clay Mineralogy*: McGraw-Hill, N. Y.
- KRAUSKOPF, K. B. (1959), Silica in sediments: *S.E.P.M. Symp. No. 7*, 4–18.

Manuscript received May 6, 1960.

RADIATION COLORATION OF SILICA MINERALS*

HAROLD W. KOHN AND BEN M. BENJAMIN, *Chemistry*
Division, Oak Ridge National Laboratory,
Oak Ridge, Tennessee.

ABSTRACT

Radiation produced color centers in both natural and synthetic silicas are associated with impurity atoms although, since impure silicas do not always form color centers upon irradiation, these impurities *per se* are not sufficient to cause coloration. For trivalent impurities the extent and type of coloration seems to depend more upon the manner of incorporation rather than the identity of the impurity atom, although the identity will naturally affect the type of center formed. The degree of general disorder may be important, but specific defects, especially hydroxyl ions associated with positive hole traps, should also be considered. The difference in behavior between some natural specimens and those prepared or treated in the laboratory makes it doubtful that some of these natural quartz specimens were originally colored by ionizing radiation.

INTRODUCTION

The possibility that the colors of some minerals might result from the effects of radiation from naturally occurring radioactive associates was first suggested over half a century ago (1) and has been the subject of several extensive investigations (2). Amethyst and smoky quartz in particular have received the greatest amount of attention. It is now well established that high-energy irradiation of most quartz specimens will produce a smoky discoloration, and that the rate of formation and depth of this color are dependent upon the pre-existence of certain defects in the solid.

We have recently observed that silica gel containing certain impurities, if well degassed, develops a color upon irradiation with cobalt-60 gamma rays or with x-rays (3, 4). The color depends on the kind of impurities present; aluminum gives rise to an amethyst color while iron produces a smoky appearance. At room temperature the color is bleached by the action of various gases (hydrogen, water, and ethylene, for example) and by ultra violet light. It seemed possible that the gross characteristics of the radiation-produced colors in silicate minerals were identical with those produced in these gels, particularly since silica gel might be the progenitor of many hydrothermal silicate minerals, and that the chemical characteristics of these color centers, which are more easily studied on the gels because of their high surface area, might aid in characterizing and identifying the color centers in minerals and synthetic silicates.

* This paper is based upon work performed at Oak Ridge National Laboratory, which is operated for the Atomic Energy Commission by Union Carbide Corporation.

EXPERIMENTAL

All irradiations were done in a 750-curie Co^{60} gamma source (5). The dose rate for water* in the center, measured by ferrous sulfate dosimetry (6), was about 6×10^{17} e.v.g.⁻¹, or about 10,000 R, min⁻¹. Most of the specimens were obtained through commercial channels, hence their sources could not always be accurately defined. The ultra violet light used for bleaching was supplied by a Hanovia 125-watt germicidal lamp, which emits the 2537 Å wave-length almost exclusively. In order to detect slight color changes on ultra violet irradiation, specimens were partially screened with aluminum foil before bleaching. Changes or irradiation were observed visually, comparison with a control being used where necessary.

RESULTS

In general many minerals when irradiated seem to follow the pattern similar to that observed with silica gel. Brazilian agates and "Pecos River Diamonds" (ferruginous quartz) both known to contain iron impurity, turn smoky to black during overnight irradiation. Fused silica, prepared by fusing the previously described gels in an oxygen-gas flame, show the same color patterns as those evidenced by the gels, *i.e.*, smoky for iron impurity and amethyst for aluminum impurity. Certain Mexican or Brazilian banded agates are very resistant to coloration; several days in the radiation source was required to obtain a noticeable effect. The banding is accentuated inasmuch as the opaque portions remained white and the transparent sections turned smoky. Feldspars (North Carolina sunstone, Indian moonstone, and Amelia Court House amazonite) acquire a smoky cast, although this is difficult to see in an opaque material. We have confirmed that opals cannot be colored at all (7), even those high in iron (Mexican cherry opal, for example) probably due to their comparatively high water content. Olivine peridotes and natural obsidian glass ("Apache tears") are also unaffected.

The widest variety of radiation sensitivity occurs among specimens of crystalline quartz. Most samples of natural hydrothermal quartz are easily turned smoky by an overnight irradiation. However, two samples of Brazilian oscillator-grade quartz remained clear during one week in the radiation source while two others became only faintly citrine. Some light amethysts (South Carolina) were also unaffected by a week's irradiation. Darker amethysts (Mexican and Brazilian varieties) and smoky quartz (Brazil, Maine, and North Carolina) after decoloration by heat regain their natural color on irradiation. Rose quartz from several localities (Georgia, Brazil and Maine) and citrine quartz (Maine and Brazil) are easily blackened in a few hours.

* The dose rate for silica would not be greatly different.

All of the previously described materials when colored by γ radiation are bleached by long exposure (65 hours) to ultra violet light unless, of course, they are opaque. It is interesting to compare this behavior with that of the naturally occurring colored minerals. Natural amethysts (those which are fairly dark and which will recolor upon irradiation) can be only partially bleached by ultra violet light. Very long (1 week) exposures are required.

Sections of many specimens of smoky quartz will show patterns of light and dark areas. Three smoky quartz specimens were examined to see how these patterns were affected by gamma irradiation and by ultra violet light. A sliced section of Brazilian smoky quartz was partially screened and exposed to ultra violet light for sixty-five hours. No bleaching or darkening was noted (Fig. 1-A). The sample was then γ irradiated



FIG. 1. Drawings showing effect of gamma irradiation and ultraviolet bleaching on a smoky quartz section.

for three hours, which caused considerable darkening and a reversal of the pattern (Fig. 1-B). The light parts became darker than the (originally) dark sections. The sample was then partially screened and bleached with ultra violet light for 16 hours (Fig. 1-C). The extra darkening produced by the irradiation is made less intense, but the reversed pattern is still the one obtained. Finally the sample was completely bleached by heating to 300°C ., re-darkened by irradiation and again bleached with ultra violet light. The sample was examined at intervals to ascertain if the original dark-light pattern of the natural crystal is reobtained. This is never the case, the pattern is always the "reversed pattern" of the irradiated crystal. Hence it is difficult to reason that this crystal could have derived its original color from a sequence of events involving natural radioactivity and excitations similar to those obtained from ultra violet light. Contact photographs are shown in Fig. 2.

The same series of experiments was performed on a piece of smoky quartz from Maine with somewhat different results. Again a pattern of light and dark areas was noted, but an overnight exposure to ultra violet

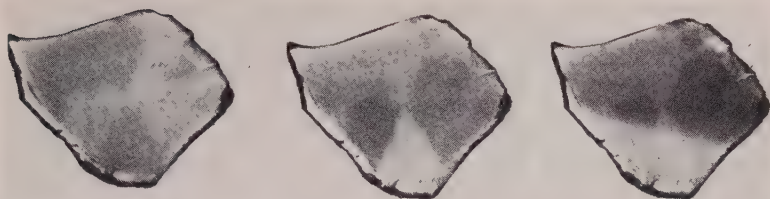


FIG. 2. Contact prints corresponding to Fig. 1.

light bleached the whole crystal section completely. Re-irradiation produced a general darkening but failed to reproduce the pattern. During bleaching with ultra violet light the pattern never reappears. Again it is difficult to imagine a sequence of naturally occurring events involving radioactivity as a coloring agent which would cause this type of behavior.

Finally we performed the same experiments on some smoky quartz, which is obviously colored naturally by irradiation, in order to determine if the effects of geological aging could result in this sort of behavior. The specimens of smoky quartz were collected by one of us (BMB) from the Pine Mountain Mine near Spruce Pine, North Carolina, where the quartz in the pegmatite occurs in association with torbernite (a copper uranium phosphate) as well as with the usual feldspar. The quartz in the undisturbed condition is darkest nearest the veins and crevices bearing the radioactive mineral, and gradually fades to white at a distance of one to three feet from the vein. Lightly colored and heat-decolorized pieces of Pine Mountain smoky quartz are easily darkened in the gamma source in three to five hours ($1.8-3.0 \times 10^6$ R). The radiation level at uranium-bearing formations is generally from 1-5 R per year, and the local dosage immediately adjacent to a pocket or crystal of torbernite might be expected to be several times this value.* Hence, any piece of Pine Mountain quartz associated with torbernite for about one million years should have had the opportunity to become darkened. The granular condition of the original specimens and the presence of dark inclusions of biotite make the bleaching and patterning phenomena previously described difficult to observe and nearly impossible to photograph. The sample is bleached by ultra violet light, however, and the dark-light patterns existing before heat bleaching are reproduced by irradiation.

DISCUSSION

It is generally accepted (8, 9, 10) that irradiation-produced color in quartz and silica is due to the presence of defects associated with one or

* Measurements here of the beta-gamma radiation from a sample of torbernite-bearing rock about $1\frac{1}{2}$ " across gave 12 m.r., hr^{-1} , equal to about 100 R yr^{-1} .

more trivalent impurities, present to the extent of a few tenths of a per cent at most, incorporated substitutionally as replacements for silicon in the silicon-oxygen network. Iron and aluminum are the most common trivalent impurities mentioned. The tendency has been to associate the amethyst color with radiation-produced defects involving the presence of iron (11), and to connect the smoky appearance similarly with the presence of aluminum (9, 10). This evidence is based largely on spectrographic or chemical analysis of the specimens studied. Such evidence is not completely conclusive however, for the only silicas so studied which do not contain both iron and aluminum are fused silicas which contain either aluminum alone, and which then become amethystine upon irradiation, or which contain neither, in which case they remain colorless upon irradiation. Specimens have also been found or prepared which contain iron, aluminum, or both, and which fail to color upon irradiation (9, 12). Some of the experiments previously cited are also at odds with the results of this study, *i.e.* that ferruginous silicas (agate, fused silica gel, and quartz) become smoky upon irradiation, whereas silicas containing only aluminum (gel and fused silica at least) become amethystine.

Previous investigators have reported the effect of various pretreatments on the irradiation coloration of fused silica. Yokota (8) states that fused silica of an unspecified purity after being heated in an atmosphere of silicon at 1400° C., develops a purple color* upon irradiation. Kats (9a) finds that such an experiment gives no coloration if Corning Fused silica, in which Al and presumably Fe are absent, is used as a source material. He also finds that Heraeus fused silica containing Al develops more coloration upon irradiation if first heated at 1250° C. in an oxygen atmosphere. One would normally expect heating in silicon to increase the number of oxygen vacancies, and heating in oxygen to decrease their number.

We have observed that in silica gels the amethyst color is bleached by electron donors, but not by acceptors (3). More recent experiments have shown that if the gels are preheated in oxygen or hydrogen at 400–600° C., allowed to cool, and then freed of excess gas, their tendency to color and to adsorb hydrogen with decoloration is unaffected. Irradiated gels will also adsorb oxygen without decoloration. One would normally expect such oxygen adsorption to annihilate oxygen vacancies. Since this seems to leave the coloration unaffected, one may tentatively assume that the oxygen vacancy is not important to the irradiation-produced purple color center.

There are several ways in which a trivalent atom may be incorporated

* Specifically optical absorption at 5400 Å. Where the exact spectrum is not measured the terms "amethyst" and "amethystine" are used.

into a silica lattice. Trivalent impurities cannot be substituted for silicon without concomitant changes which preserve electrical neutrality. Although these impurity configurations have been described by others (9, 10), we will list the four principal types here for the convenience of the reader. Each trivalent impurity atom may have associated with it (1) a monovalent cationic impurity atom, (2) a monovalent anion, (3) half an oxygen vacancy or (4) a positive hole, as in a semiconductor. The type of color center which forms upon irradiation depends upon the type of defect pre-existing in the solid. Hence the color may be determined more by the manner in which the impurity atom is incorporated into the lattice than by the chemical identity of the atom. Of course the manner of incorporation is partially affected by the chemical identity of the impurity atom, but it is also affected by other variables such as direction of crystal growth (12) and availability of other impurity atoms. For example variations in direction of crystal growth are probably responsible for the patterns in Fig. 1.

Confining our attention to the first two types of impurity configurations, one would expect the relative concentration of each type to be determined by conditions which exist when the material is formed in nature or prepared in the laboratory. The availability of monovalent cations such as Na^+ , the availability of monovalent anions (principally OH^-), the tendency of the trivalent impurity atom (Al^{+++} or Fe^{+++}) to bind either the monovalent anion or cation, and the ease with which the trivalent impurity can be incorporated substitutionally into the lattice will be the principal factors determining the number of different types of centers formed. Studies of silica alumina cracking catalysts have shown that they lose their last traces of water only with great difficulty (13), and that the hydroxyl groups in these catalysts are associated essentially with the aluminum atom (14). One may therefore assume that the gels with an aluminum impurity prepared in this laboratory contain predominantly defects of the second type. Iron, on the other hand, has comparatively little tendency to bind water, or more correctly hydroxyl groups chemically, (15) hence one would expect iron-containing gels to possess more defects of other types. Although iron is not as easily incorporated substitutionally into a silica lattice as aluminum is, the incorporation of a few per cent of iron as a simple substitute for silicon should pose no problem. However, the tendency for iron to form local iron silicate structures is more marked than for aluminum to form similar aluminum silicate structures.

Another noticeable trend is that, in general, highly ordered (crystalline) silicas tend to turn smoky upon irradiation, whereas disordered or highly defective structures tend to turn amethystine. The only crystalline

silicas which turn purple on irradiation are decolorized natural amethysts (which, incidentally, are highly d-l twinned). All attempts to produce amethyst in the laboratory have failed so far. On the other hand, non-crystalline silicas generally turn purple when irradiated, the only exceptions being the smoky silica gel described herein, the fused material obtained from it, and a few agates. Heating to a high temperature (8, 10) which would tend to create more general disorder seems to enhance the possibility of producing amethyst coloration by irradiation in impure fused silicas.* (16) Hence, general disorder as well as specific defect-impurity structures may well be responsible for the amethyst radiation coloration.

Concerning the coloration of natural minerals, it has already been pointed out (17) that the absorption spectra and fading characteristics of natural smoky quartz are different from these properties of smoky quartz prepared in the laboratory. This agrees with our findings concerning the patterning of some samples of natural smoky quartz, and their response to ultra violet light and to gamma irradiation. Although it is possible that the effects of aging for geological periods of time might alter these characteristics somewhat, or that other means of excitation and ionization may produce superficially similar color centers, it would certainly appear that the color centers in many naturally occurring smoky quartz and amethyst specimens are not similar to those produced by ionizing radiations. Concerning amethyst, one need only note that different amethyst samples also respond differently to irradiation and to ultraviolet light, in addition to the fact that many amethysts (particularly those deposited hydrothermally in geodes and vugs) have never been associated with natural radioactivity.

SUMMARY

Color centers in both natural and synthetic silicas are associated with impurity atoms although, since impure silicas do not always form color centers upon irradiation, these impurities per se are not sufficient to cause coloration. For trivalent impurities the extent and type of coloration seems to depend more upon the manner of incorporation rather than the identity of the impurity atom, although the identity will naturally affect the type of center formed. The degree of general disorder may be

* An interesting exception to this is reactor irradiated quartz, which at first darkens, but then becomes bleached at an exposure of $\sim 10^{10}$ n.v.t. Observable disorder does not begin until exposures of $\sim 3 \times 10^{19}$ n.v.t. The effects of neutron irradiation however would be expected to differ from the effects of heating in as much as the former would disrupt individual atoms, and the latter would disorder the relationship between SiO_4 tetrahedra.

important, but specific defects, especially hydroxyl ions associated with positive hole traps, should also be considered. The difference in behavior between some natural specimens and those prepared or treated in the laboratory makes it doubtful that some of these natural quartz specimens were originally colored by ionizing radiation.

ACKNOWLEDGMENTS

The authors would like to thank Dr. Ellison Hall Taylor and Dr. Samuel Colville Lind of this Laboratory for stimulating discussions. We should also like to thank Dr. Robert A. Weeks of the Solid State Division for permission to discuss his unpublished experimental findings.

REFERENCES

1. J. JOLY, *Phil. Mag.*, Series 6, 13 (1907); C. DOELTER, "Das Radium und die Farben," Steinkopff, Dresden, 1910.
2. A recent bibliography has been compiled by R. BECHMANN, *Nucleonics*, **16**, No. 3, 122, 1958.
3. H. W. KOHN, *Nature*, **184**, 630, 1959.
4. H. W. KOHN AND E. H. TAYLOR, International Conference on Catalysis, Paris, 1960.
5. J. A. GHORMLEY AND C. J. HOCHANADEL, *Rev. Sci. Inst.*, **22**, 473 (1951).
6. C. J. HOCHANADEL AND J. A. GHORMLEY, *J. Chem. Phys.*, **21**, 880 (1953).
7. F. H. POUGH AND T. H. ROGER, *Am. Mineral.*, **32**, 31 (1947).
8. R. YOKOTA, *J. Phys. Soc., Japan*, **7**, 222, 316 (1952).
9. A. J. COHEN, *J. Chem. Phys.*, **25**, 908 (1956); *Am. Mineral.*, **41**, 874 (1956); A. J. COHEN AND C. G. SUMMER, *Am. Mineral.*, **43**, 58 (1958).
10. A. KATS, Fourth International Congress on Glass, Paris, 1956, 400; A. KATS AND J. M. STEVELS, *Phillips Res. Repts.*, **11**, 115 (1956); J. M. STEVELS AND A. KATS, *ibid.*, **11**, 103 (1956).
11. E. F. HOLDEN, *Am. Mineral.*, **10**, 203 (1925).
12. F. AUGUSTINE AND D. R. HALE, *J. Chem. Phys.*, **29**, 685 (1959).
13. R. G. HALDEMAN AND P. H. EMMETT, *J. Am. Chem. Soc.*, **78**, 2917 (1956).
14. H. G. WEISS, J. A. KNIGHT AND J. SHAPIRO, *ibid.*, **81**, 1823 (1959).
15. P. W. SELWOOD, M. ELLIS AND C. F. DAVIS, JR., *ibid.*, **72**, 3549 (1950); P. W. SELWOOD, M. ELLIS AND K. WETHINGTON, *ibid.*, **71**, 2181 (1949).
16. R. A. WEEKS AND C. M. NELSON, private communication.
17. N. E. VEDENEVA AND E. S. RUDNETSKAYA, *Doklady Akad. Nauk., S.S.S.R.*, **87**, 361 (1952), *C.A.* **47**, 6259 (1953); L. G. CHENTSOVA AND N. E. VEDENEVA, *Doklady Akad. Nauk., S.S.S.R.*, **60**, 649 (1948); *C.A.* **43**, 8785 (1949).

Manuscript received May 8, 1960.

OPTICAL CRYSTALLOGRAPHY OF ORIENTITE FROM ORIENTE PROVINCE, CUBA

CHARLES B. SCLAR, *Battelle Memorial Institute,
Columbus, Ohio.*

ABSTRACT

The optic orientation, optic angle, optic sign, and pleochroic formula of orientite $[\text{Ca}_4\text{Mn}_4^{+3}(\text{SiO}_4)_5 \cdot 4\text{H}_2\text{O}]$ recorded in the literature are incorrect, and a revision of the optical crystallography of orientite is presented.

Orientite is orthorhombic,

$$\frac{2}{m} \frac{2}{m} \frac{2}{m},$$

dominant forms $\{110\}$, $\{001\}$, and $\{010\}$, prismatic to tabular parallel to $\{010\}$, $(110) \wedge (1\bar{1}0) = 67^\circ 48'$, $a:b:c = 0.6720:1:0.3958$, imperfect basal $\{001\}$ and brachyprismatic $\{120\}$ cleavage, sp. gr. = 3.05. The Barker classification angles are $cr = 30^\circ 30'$, $am = 33^\circ 54'$, and $bq = 68^\circ 24'$.

The optic orientation of orientite is $X=b$, $Y=c$, $Z=a$ with $\alpha = 1.756$, $\beta = 1.777$, $\gamma = 1.794$ (all ± 0.002). The optic plane is transverse to the elongation, and the optic angle is large, negative, and variable ($2V_X = 68-83^\circ$). It has very strong dispersion ($r < v$) of the optic axes which are essentially normal to the brachyprismatic $\{120\}$ cleavage. Orientite is deep red brown in color and strongly pleochroic in section with $X = \text{yellow}$, $Y = \text{yellow-brown}$, $Z = \text{red-brown}$, and $Z > Y > X$.

X-ray powder diffraction data for orientite are given for reference.

INTRODUCTION

During a mineralogical study of several manganese ores from Oriente Province, Cuba, the writer obtained for comparative purposes a specimen of the type orientite from Oriente, Cuba, originally described by Hewett and Shannon (1)*. It was found that several of the optical properties of this sample of orientite were not in agreement with those recorded for orientite in the standard reference works by Larsen and Ber-
man (2) and Winchell and Winchell (3). A check of the paper by Hewett and Shannon (1) revealed that a typographical error in their reported optical orientation of orientite has been propagated in the subsequent literature. Other optical properties of orientite, such as the optic sign and the optic angle, are in error in the original description. A revision of the optical crystallography of orientite is presented in this paper, and x-ray powder diffraction data for the type orientite are included for reference.

OCCURRENCE

Orientite $[\text{Ca}_4\text{Mn}_4^{+3}(\text{SiO}_4)_5 \cdot 4\text{H}_2\text{O}]$ or $4\text{CaO} \cdot 2\text{Mn}_2\text{O}_3 \cdot 5\text{SiO}_2 \cdot 4\text{H}_2\text{O}$ is known only from Oriente Province, Cuba, where it occurs as a minor

* References at end of text.

constituent of oxide manganese ores. The mineral was discovered by Hewett (1) in ores of the Costa, Manuel, and Vicente denouncements, 6 miles south of Bueycito, southwestern Oriente. He later found orientite in ore from the Santa Rosa prospect near Banes, north of Antilla, north central Oriente. The largest known crystals of orientite do not exceed 1 mm. in length.

The regional geology of Oriente Province is discussed by Park (4), Woodring and Daviess (5), and Lewis and Straczek (6), and detailed descriptions of the geology of the manganese deposits in the Bueycito district are given by Burchard (7), Park and Cox (8), and Simons and Straczek (9). In brief, the manganese ores of this district consist of those parts of beds of volcanic tuff which contain a sufficiently high proportion of grains, nodules, pods, and veinlets of manganese-oxide minerals to constitute ore. These bedded tuff ores are intercalated with water-laid basaltic, andesitic, and latitic agglomerates and tuffs and limestone beds which constitute the upper part of the Cobre formation of upper Eocene age. The Bueycito bedded tuff ores are considered to be hypogene and syngenetic, and the manganese oxide minerals are believed to have been deposited by penecontemporaneous replacement of the altered tuff matrix (9). The source of the mineralizing solutions is thought to have been submarine hot springs (4, 9).

According to Hewett and Shannon (1), orientite from the Bueycito district occurs as (1) high-purity drusy aggregates which contain variable amounts of finely disseminated inclusions of a psilomelane-type oxide, (2) drusy cavity linings in psilomelane-type oxide, (3) finely disseminated grains in altered tuff, (4) granular aggregates which selectively replace the glassy portion of rock fragments embedded in the altered tuff, and (4) pseudomorphs after foraminifera (calcite) embedded in psilomelane-type oxide. The principal associated minerals are a psilomelane-type oxide, manganite, pyrolusite, neotocite, ferruginous chalcedony ("bay-ate"), barite, low quartz, calcite, and zeolites (analcite, stilbite, chabazite, and laumontite). Based on cross-cutting relationships of veinlets and successive cavity fillings, Hewett and Shannon tentatively concluded that the sequence of mineral deposition was (1) ferruginous chalcedony, (2) psilomelane-type manganese oxide and plumose manganite, (3) orientite and barite, (4) prismatic manganite, (5) quartz, (6) zeolites, (7) calcite. The pyrolusite was probably formed by surficial supergene oxidation of the psilomelane-type oxide.

OPTICAL CRYSTALLOGRAPHY

Hewett and Shannon (1, p. 501) state that orientite is biaxial positive with the optic plane parallel to (001) and, in outline form, give the optic

orientation as $X=a$, $Y=c$, and $Z=b$. The succeeding text of their paper, however, states that the obtuse bisectrix is normal to (010) which indicates that the correct optic orientation of orientite is $X=b$, $Y=c$, and $Z=a$, provided the optic sign of the mineral was correctly determined. The orientation given in outline form is probably a typographical error which, with one exception, has been repeated in the subsequent literature (2, 3, 10, 11, 12). The exception is an abstract of the original paper by Spencer (13) who correctly recorded the optical orientation of orientite as optic plane parallel to (001) and acute bisectrix (Z) normal to (100). Strangely, Larsen (14) gave the optic orientation as $X=a$, $Z=c$. The present study showed that the optic orientation of orientite is $X=b$, $Y=c$, and $Z=a$, as determined on well-formed crystals.

According to Hewett and Shannon (1) the optic angle of orientite is 67° . This conclusion was based on (1) their observation that crystals that lie on (110) yield a perfectly centered optic axis figure and (2) goniometric measurements that gave $\phi = 56^\circ 06'$ as the angle for the prism or $(110) \wedge (1\bar{1}0) = 67^\circ 48'$. The optic angle as calculated from the indices of refraction reported by Hewett and Shannon ($\alpha = 1.758$, $\beta = 1.776$, $\gamma = 1.795$; all ± 0.005), is, however, $(+)$ $2V = 89^\circ 22'$, although within the stated limits of precision for these indices a calculated $2V_Z$ of 67° is possible.

Both Hewett and Shannon and the writer noted that the axial bars of centered optic axis figures are practically straight. Hewett and Shannon attributed the lack of curvature of the optic axial bars to the high value of β and a resultant $2E$ of 156° for a $2V$ of 67° . The writer, however, questioned whether, for the optical system used in this study, the axial bar of a centered optic axis figure of a substance with $2V = 67^\circ$ and $\beta = 1.776$ would be straight. In addition, it was observed that (1) a greater rotation of the microscope stage was required to make the isogyres leave the field for a B_{xx} figure as compared with a B_{xz} figure, and that (2) the apparent dispersion of the optic axes was $r < v$ for centered B_{xx} figures and $r > v$ for centered B_{xz} figures, whereas the true dispersion determined on slightly off-center optic axis figures in which the curvature of the axial bar was recognizable was $r < v$ which is in accord with the dispersion formula given by Hewett and Shannon. Consequently, the indices of refraction were redetermined with results as follows: $\alpha = 1.756$, $\beta = 1.777$, $\gamma = 1.794$ (all ± 0.002). The calculated optic angle is $(-)$ $2V = 83^\circ 02'$, which is in accord with the indications of the qualitative optical tests, but within the stated accuracy limits for these indices of refraction, the calculated optic angle could range from $(-)$ $2V = 70^\circ 44'$ to $(+)$ $2V = 85^\circ 10'$. A subsequent independent determination of the optic angle and sign of orientite with the universal stage showed that the optic angle is negative and

variable with $2V=68^{\circ}$ – 83° . Grains with the larger optic angles (77° – 83°) appear to be more common.

Hewett and Shannon reported that orientite has a poor prismatic $\{110\}$ cleavage which is normal to the optic axes. The present writer also observed the traces of cleavage planes in the prism $[001]$ zone and noted the frequent occurrence of centered optic axis figures on crushed fragments. If the optic axes of orientite are normal to an imperfect prismatic $\{hk0\}$ cleavage and the optic angle ranges from 68° to 83° , however, this cleavage cannot be parallel to $\{110\}$ inasmuch as $(110) \wedge (\bar{1}\bar{1}0)$ was determined by goniometric measurement of crystal faces to be $67^{\circ} 48'$. For an optic angle which ranges from 68° to 83° , the angle between an optic axis and the pole of (110) would range from about 22° to 14° , respectively, and, as a result, (110) cleavage fragments would not yield a centered optic axis figure. The Mallard formula (16, p. 48) shows that for (110) cleavage fragments, the point of emergence of the optic axis in the conoscopic figure would be displaced from the center of the field a distance of two-fifths to four-fifths the radius of the conoscopic field depending on the optic angle and on the Mallard constant of the optical system employed. Alternatively, if the $\{hk0\}$ cleavage is $\{120\}$, the angle between an optic axis and the pole of (120) would range from $4^{\circ} 51'$ in the direction of the a axis to $2^{\circ} 39'$ in the direction of the b axis for a corresponding range in the optic angle from 83° to 68° . Cleavage fragments parallel to $\{120\}$ would always yield a centered optic axis figure regardless of the magnitude of the optic angle within the stated limits. Coincidence of the optic axes with the poles of $\{120\}$ would occur for a $2V$ of $73^{\circ} 18'$. It is concluded that the imperfect prismatic cleavage of orientite is probably $\{120\}$.

Orientite is strongly pleochroic. In the original paper (1) and all the subsequent literature (2, 3, 10, 11, 12, 13, 14), the pleochroism and absorption is given incorrectly as X =red-brown, Y =yellow, Z =brownish-yellow with $X>Z>Y$. This study shows that X =yellow, Y =yellow-brown, and Z =red-brown with $Z>Y>X$.

Tables 1 and 2 are a summary of the revised optical and crystallographic data for orientite. Shannon's original orientation of the crystallographic axes has been retained for simplicity and because it seems pointless to introduce another arbitrary setting of the orthorhombic axes in the absence of x -ray structural data. For determinative purposes, however, it may be useful to transform the crystallographic data for orientite in terms of the Barker (15) classification angles for the orthorhombic system.

With rare exception, all the known crystals of orientite have only one prism zone and two pinacoids. In the absence of well-developed pyra-

TABLE 1. MORPHOLOGICAL CRYSTALLOGRAPHY AND PHYSICAL PROPERTIES OF ORIENTITE, ORIENTE PROVINCE, CUBA

Symmetry: orthorhombic system; rhombic-dipyramidal (barite) class,

Forms:	common	rare
	basal pinacoid {001}	brachydome {021}
	brachypinacoid {010}	macrodome {101}
	unit prism {110}	unit pyramid {111}
	$(110) \wedge (1\bar{1}0) = 67^\circ 48'.$ *	

Barker classification angles†: $cr = 30^\circ 30'$, $am = 33^\circ 54'$, $bq = 68^\circ 24'$ Axial ratio: $(0.6720:1:0.3958)$ ‡

Habit: dominantly prismatic and pseudo-hexagonal; subordinately tabular parallel to {010}

Cleavage: imperfect parallel to the basal pinacoid {001} and the brachyprism {120};
 $(110) \wedge (120) = 19^\circ 27'$ §

Color: deep red-brown to almost black; brown when powdered

Luster: resinous to sub-vitreous

Specific gravity: 3.05

Hardness: $4\frac{1}{2}$ –5Note: soluble in hot HCl with evolution of chlorine, and separation of residual insoluble silica; insoluble in HNO₃.

* Measured goniometrically by Shannon (1); checked with microscope on basal sections in present study.

† For crystals with complete development of forms.

‡ c/b is an approximation based on measurement with the microscope by Shannon of $(101) \wedge (\bar{1}01) = 61^\circ 00'$ on one crystal (1).

§ Calculated angle.

midal faces and the occurrence of only one prism zone, Barker auxiliary setting rule (v) is applicable. The forms {110}, {010}, and {001} become {101}, {100}, and {010}, respectively, and $cr (001 \wedge 101) = 33^\circ 54'$.

For the orientite crystal with additional forms described by Shannon, the Barker setting of the parametral plane differs from that given by Shannon, but the orientation of the crystallographic axes remains the same. The preferred setting based on the Barker rules is the one which gives the maximum number of simple planes (indices with no numbers except 0, 1, and $\bar{1}$). As a result, {011}, {102}, and {112} of Shannon become {021}, {101}, and {111}, respectively, and $c:b$ of Shannon (0.7916) becomes $c:b/2$ (0.3958). The Barker classification angles are $cr (001 \wedge 101) = 30^\circ 30'$, $am (100 \wedge 110) = 33^\circ 54'$, and $bq (010 \wedge 011) = 68^\circ 24'$.

TABLE 2. OPTICAL PROPERTIES OF ORIENTITE, ORIENTE PROVINCE, CUBA

Indices of Refraction		Optic Angle and Sign
$\alpha = 1.756 \pm 0.002$		(-) $2V = 83^\circ 02'$ (calculated from indices of refraction)
$\beta = 1.777 \pm 0.002$		
$\gamma = 1.794 \pm 0.002$		(-) $2V = 68^\circ - 83^\circ$ (measured with universal stage)
$\gamma - \alpha = 0.038$		
Orientation		Pleochroism and Absorption
$X = b$		$X = \text{yellow}$
$Y = c$		$Y = \text{yellow-brown}; Z > Y > X$
$Z = a$		$Z = \text{red-brown}$
<i>Dispersion of optic axes</i>		
$r < v$ very strong		
<i>Remarks</i>		
Optic plane parallel to {001} and transverse to elongation of prismatic crystals		
Optic axes essentially normal to the brachyprismatic {120} cleavage		

TABLE 3. X-RAY POWDER DIFFRACTION DATA FOR ORIENTITE, ORIENTE PROVINCE, CUBA (Fe radiation, MnO filter)

$d, \text{\AA}$	I	$d, \text{\AA}$	I	$d, \text{\AA}$	I
9.42	50	2.10	25	1.29	5
5.89	25	2.05	20	1.26	5
5.05	50	1.96	10	1.24	15
4.77	10	1.94	5	1.20	10
4.40	60	1.87	10	1.17	15
4.07	30	1.84	15	1.15	5
3.93	10	1.81	5	1.13	15
3.69	10	1.77	10	1.12	5
3.42	10	1.73	5	1.11	5
3.26	50	1.69	50	1.10	20
3.05	75	1.64	35	1.09	5
2.90	40	1.61	10	1.05	5
2.78	10	1.59	15	1.04	5
2.68	100	1.52	50	1.03	5
2.58	50	1.51	10	1.02	5
2.51		1.44	10	1.01	5
2.44	20	1.38	5	1.00	5
2.34	50	1.34	5	0.996	10
2.23	30	1.32	35	0.978	5
2.19	10	1.30	10	0.974	5

X-RAY POWDER DATA

X-ray powder diffraction data for orientite are given in Table 3.

ACKNOWLEDGMENTS

The specimen of the type orientite used in this study was obtained from the U. S. National Museum through the courtesy of Dr. George Switzer of that institution and Dr. Charles Milton of the U. S. Geological Survey.

The writer is indebted to Dr. E. G. Ehlers for many helpful suggestions and for his critical review of the manuscript.

REFERENCES

1. HEWETT, D. F., AND SHANNON, E. V. (1921), Orientite, A New Hydrous Silicate of Manganese and Calcium from Cuba: *Amer. Jour. Sci., 5th Series*, **I**, 491-506.
2. LARSEN, E. S., AND BERMAN, H. (1934), The Microscopic Determination of the Non-opaque Minerals: *U. S. Geol. Survey, Bull.* **848**.
3. WINCHELL, A. N., AND WINCHELL, H. (1951), *Elements of Optical Mineralogy, Part II, Descriptions of Minerals*: Fourth Edition, John Wiley, New York.
4. PARK, C. F. (1942), Manganese Deposits of Cuba; *U. S. Geol. Survey, Bull.* **935-B**.
5. WOODRING, W. P., AND DAVIESS, S. N. (1944), Geology and Manganese Deposits of Guisa-Los Negros Area, Oriente Province, Cuba: *U. S. Geol. Survey, Bull.* **935-G**.
6. LEWIS, G. E., AND STRACZEK, J. A. (1955), Geology of South-Central Oriente, Cuba: *U. S. Geol. Survey, Bull.* **975-D**.
7. BURCHARD, E. F. (1920), Manganese Ore Deposits in Cuba: *Amer. Inst. Min. Met. Eng. Trans.*, **63**, 51-104.
8. PARK, C. F., AND COX, M. W. (1944), Manganese Deposits in Part of the Sierra Maestra, Cuba: *U. S. Geol. Survey, Bull.* **935-F**.
9. SIMONS, F. S., AND STRACZEK, J. A. (1958), Geology of the Manganese Deposits of Cuba: *U. S. Geol. Survey, Bull.* **1057**, 73, 146.
10. FOSHAG, W. F. (1921), New Minerals, Family 6, Silicates, Orientite: *Am. Mineral.*, **6**, 132.
11. WINCHELL, A. N. (1939), *Elements of Optical Mineralogy, Part III. Determinative Tables*: Second Edition, John Wiley, New York.
12. FORD, W. E. (1932), *Dana's Textbook of Mineralogy*: Fourth Edition, John Wiley, New York.
13. SPENCER, L. J. (1921), New Minerals: *Mineral. Abstracts*, **1**, 201-202.
14. LARSEN, E. S. (1921), The Microscopic Determination of the Nonopaque Minerals: *U. S. Geol. Survey, Bull.* **679**.
15. PORTER, N. W., AND SPILLER, R. C. (1951), *The Barker Index of Crystals, Vol. I. Crystals of the Tetragonal, Hexagonal, Trigonal, and Orthorhombic Systems, Part I. Introduction and Tables*: Heffer and Sons, Cambridge.
16. WINCHELL, H. (1946), A Chart for Measurement of Interference Figures: *Am. Mineral.*, **31**, 43-50.

NOTES AND NEWS

INTERNATIONAL MINERALOGICAL ASSOCIATION

The second general meeting of the International Mineralogical Association took place August 22-25, 1960 at the Royal Technical Institute in Copenhagen in conjunction with the International Geological Congress; in addition there were meetings of the Commissions on August 19-21.

The first business meeting in the afternoon of August 22 was attended by 36 voting delegates of the member societies, as well as by about 100 other mineralogists. President Parker presented a thoughtful report summarizing the present state of the Association, together with his suggestions for the future. Highlights of this included his urging that the individual member societies as such take a greater interest in the Association, the suggestion that the mechanism for the election of councilors as given in the constitution adopted at Zürich might need some modification, the hope that future meetings would be apart from those of other bodies, and the problems of financing the travel costs of those attending the meetings. Secretary Amorós in his report stated that there are now 22 member societies (including New Zealand in addition to the 21 listed in his report in the Zürich symposia). He noted that the Zürich symposia are now available in printed form (see *Am. Mineral.*, 45, 1129, September-October, 1960) together with the current constitution and minutes of the meeting; he also mentioned the Zürich field trips (see *GeoTimes*, 4, 29, January-February, 1960, published by the American Geological Institute). Treasurer Fisher's report showed a cash balance on hand July 1, 1960 of \$1,269.44. It was voted to organize a new Commission on the Teaching of Mineralogy. The Association accepted with thanks the offer of the Mineralogical Society of America to serve as host for its next meeting in Washington in April, 1962.

At the second business meeting on the morning of August 24 the chairmen of the four Commissions of the Association reported on their accomplishments; it is hoped that at least some of these will be available in printed form before long. This was followed by the election of a new Council, as well as Commission and Committee officers, to serve until 1964, as follows:

Council

President: D. J. Fisher
1st Vice-President: C. E. Tilley
2nd Vice-President: G. P. Barsanov
Secretary: J. L. Amorós
Treasurer: L. G. Berry
Councilors: P. R. J. Naidu
Th. G. Sahama
H. G. F. Winkler
Past President: R. L. Parker

Commission Officers

<i>Abstracts.</i>	Chairman: M. Fornaseri
	Secretary: R. van Tassel
<i>Mineral Data.</i>	Chairman: H. Strunz
	Secretary: G. T. Faust
<i>Museums.</i>	Chairman: C. Frondel
	Secretary: F. Leutwein
<i>New minerals and</i>	Chairman: M. Fleischer
<i>Mineral names.</i>	Secretary: C. Guillemin
<i>Teaching.</i>	Chairman: J. Orcel
	Secretary: H. J. deWijis

Chairmen of Committees to effect liaison between the Association and other international organizations are: F. Laves (International Crystallographic Union), E. W. Heinrich (Geochemical Society), and (with Commissions of the International Geological Congress), C. Burri (Petrographic Nomenclature) and D. P. Grigoriev (Meteorites).

The first symposium on Mineral Synthesis met the morning and afternoon of August 23 under the chairmanship of J. R. Goldsmith. The second on Feldspars had F. Laves as its chairman and met the afternoon of August 24 and all day on August 25. Abstracts of the talks presented were printed in the program; the complete papers with discussions of the

Feldspar symposium are in the course of being published by the Instituto Lucas Mallada of Madrid. The titles of the papers given are as follows:

Mineral Synthesis

- F. R. Boyd and J. L. England: Synthesis of pyrope, diamond, and other high-pressure phases.
 W. S. Fyfe: Nucleation patterns and mineral synthesis.
 D. L. Hamilton and W. S. MacKenzie: Nephelines as crystallization temperature indicators.
 S. Matthes: Synthesis of pyrope-garnets at relatively low pressures.
 H. S. Yoder, D. B. Stewart and J. R. Smith: Ab-Or-An-H₂O at 5000 bars.
 H. H. Lohse, H. Burzlaff, and E. Hellner: Some remarks on the koenite problem.
 A. E. Ringwood: Prediction and confirmation of the olivine-spinel transformation in Ni₂SiO₄.
 A. Rittmann and E. El-Hinnawi: Quantitative conoscopy for rapid determination of synthetic minerals.

Feldspars

- T. F. W. Barth: Some temperature-dependent crystallo-chemical properties of the feldspar lattices.
 H. C. F. Winkler: On coexisting feldspars (experimental observations).
 D. B. Stewart and E. H. Roseboom: Lower temperature terminations of the three-phase region plagioclase-alkali feldspar-liquid.
 K. S. Heier: The amphibolite-granulite facies transition reflected in the mineralogy of potassium feldspars.
 F. J. Kuellmer: Alkali feldspars from some intrusive porphyries of southwestern United States.
 G. A. Deicha: Les cavités des feldspaths.
 J. B. Jones and W. H. Taylor: The structure of orthoclase.
 J. V. Smith and W. S. MacKenzie: Atomic, chemical and physical factors that control the stability of alkali feldspars.
 W. S. MacKenzie and J. V. Smith: Structural variations in alkali feldspars.
 J. R. Goldsmith and F. Laves: Polymorphism, order, disorder, diffusion and confusion in the feldspars.
 A. S. Marfunin: The relation between structure and optical orientation in potash soda feldspars.
 J. Wyart: L'échange des cations dans les feldspaths et l'action de l'eau.
 H. Curien: Échanges isotopiques des atomes d'oxygène dans les silicates.
 C. J. E. Kempster, H. D. Megaw and E. W. Radoslovich: The structure of anorthite.
 S. Chandrasekhar, S. G. Fleet and H. D. Megaw: Structure of "body-centered anorthite."
 H. D. Megaw: The structure of the intermediate plagioclase feldspars.
 C. Burri, R. L. Parker and E. Wenk: Project of a new general catalogue of data for the determination of plagioclases by the universal stage method.
 P. Gay: Some recent work on the plagioclase feldspars.
 H. D. Megaw: Effects of temperature and composition in the plagioclases and other feldspars.
 E. El Hinnawi: The application of the zonal method for the distinction between high and low temperature plagioclase feldspars.
 St. Karamata: Einfluss des geologischen Alters und des tektonischen Druckes auf die Art der Alkalifeldspäte.

BOOK REVIEWS

GEOLOGY OF THE INDUSTRIAL ROCKS AND MINERALS, by ROBERT L. BATES, 424 pages, Harper and Brothers, 1960, \$10.00.

The author is professor of geology at Ohio State University and a columnist ("Geology in the Public Eye") for *GeoTimes*. This book is a Lindgren-type approach to rocks and minerals of industrial value; in other words, its motivation is geologic rather than economic. It is, therefore, an innovation among books concerned with the non-metallics.

After a brief introduction the author devotes four chapters to the industrial rocks and five to the industrial minerals. The industrial rocks are igneous (granite, basalt, pumice, *et al.*), metamorphic (slate and marble), and sedimentary (two chapters, one covering sand and gravel, sandstone and clay, and the other the carbonate rocks, phosphate, rock gypsum, and salt). The industrial minerals are divided into the igneous, vein and replacement, metamorphic, sedimentary and sulfur, and minor industrial. This reviewer believes that the "minor industrial minerals," of which there are eight, covering nine pages, should either be distributed back through the preceding chapters where they belong or omitted entirely. In all, thirteen rocks and twenty minerals are described.

Within the discussion of a particular rock or mineral the general uses, properties, and origin are covered first, and then the principal occurrences (mostly in the United States) are described, some in considerable detail and with extensive bibliographies. This is the author's main contribution, in my opinion. I know of nowhere else where one can get, in one volume, an adequate modern review of the *geological occurrence* of the principal domestic deposits of these industrial rocks and minerals.

An entirely satisfactory classification of the non-metallics is impossible, as the author implies in his introduction. He has attempted to put together the best possible classification for a strictly geological approach. The teacher, if using this book for a text, will either have to accept this classification or jump around like a flea on a hot skillet if he follows the traditional approach. For example, if the subject under consideration is dimension stone, the particular rocks involved will be found in all four chapters on industrial rocks. The same chapters would be involved in a study of raw materials for concrete aggregate, or roadstone. If refractories are taken up as a unit, parts of two rock and three mineral chapters would have to be covered. But other classifications present other problems, so one has to adapt in any case.

The book is both readable and authoritative. It, no doubt, will have wide use as a text, and in addition should be in the personal library of everyone interested in industrial geology.

KENNETH K. LANDES
The University of Michigan

TECHNICAL PETROGRAPHY OF PRODUCTS OF REFRACTORIES, WHITE-WARE-CERAMICS AND HYDRAULIC BINDERS (Technische Petrographie von Erzeugnissen der Feuerfest-, Feinkeramik- und Bindemittelindustrie), by D. S. BELJANKIN, B. W. IWANOW, AND W. W. LAPIN; German Edition by JOHANNES WINKLER (Institute of Glass Technology, Coswig).—Bauverlag G.m.b.H., and VEB Verlag Technik, Berlin, xvi+455 pp., 216 text figures.

It is with a feeling of deep respect that the reviewer wants to give his impression of the present book in the memory of his late friend, with whom the best tradition of Russian petrography of the great school of Loewinson-Lessing and E. Fedorow has ended. The book is by no means a common text book; it does not give any instructions for the use

of the petrographic microscope or of the techniques of the examination of minerals in polished sections. It is, however, the summary of a rich life of research and experience, a mine of wealth for all investigators who wish to compare their observations in applied mineral microscopy with the data collected by a master in this art. Beyond that, the book is an indispensable source of information on the not always easily available Russian literature of the last four decades in the fields of microscopic investigation of the constitution of ceramic products. The bibliographic collection of this literature extending over the last 40 pages of the book is practically unique, and therefore most important for more detailed studies. The book is a first-class reference collection supplementing similar works in English and German languages, chiefly the books of F. H. Norton and K. Konopocky on Refractories or that of H. Salmang on Ceramics in General, but also comparable to the well-known work of H. Insley and V. D. Frechette on the microscopy of ceramics, cements, slags, and glasses. It is a truly Russian book, entirely based on experience with Russian raw materials and Russian industrial products, but for just this reason of utmost interest. The reviewer is of the opinion that it is indispensable for the American investigator to learn from the rich data offered; it manifests in a particular degree the tremendous advance which industry (not only in the countries of the U.S.S.R.!) owes to the microscopist by the careful study of their materials. On the other hand, it is much to be regretted that the book does not contain much information beyond the year 1950 (the book appeared first in Moscow, 1952).

The first Section of the book treats the Refractories, classified as silica: alumina-silica; highly aluminous and corundum products; magnesia refractories, chrome magnesia refractories; magnesium silicate materials; dolomite products; spinels. A very interesting supplementary chapter is concerned with the reaction products between silica and fireclay, or magnesia brick. The second large Section concerns the porcelains of the classical type, and the modified steatite porcelains, cordierite materials, etc. A special chapter is dedicated to the sintered alumina products and to special porcelains on the basis of zirconia, alkaline earth titanates, and of beryllia. The third large Section is that on hydraulic Binders, Portland cement, alumina cement, and their hydration products. A supplement considers gypsum plasters.

Especially in the first two sections the full mastership of Beljankin and his school is evident. With a nearly infinite carefulness the microscopic constitution of ceramic products of all kinds are described, analyzed in their mineral ingredients, and their chemical-petrographic reactions discussed with the surroundings. The practitioner will learn many details from this rich experience even if he never comes in contact with the Russian raw materials from which the products described by Beljankin have derived. These chapters have many parallelisms with what we observe in American raw materials and industrial products. There is a wealth of mostly excellent micrographs, valuable tabulations of chemical bulk analyses and graphs. In everything, the exact petrographic identification of the mineral constituents is in the foreground of discussion and the final conclusions are based on the accurate determination of the optical constants. Over 90 per cent of the methods used are of the classical ones with the polarization microscope; only occasionally is reflected light examination added if opaque minerals participate in the constitution of a given sample. In this point the American reader will be perhaps somewhat disappointed. Especially in the third Section on hydraulic binders the microscopy of Portland cement clinkers and the special methods in use of production control are still somewhat "underdeveloped." The nature of the hydration products of Portland cement was not yet a well known field when Beljankin finished his book, and even the excellent methods of B. Tavasci on the differentiation of the constituents of the Portland cement clinkers by etching methods are not sufficiently appreciated in their importance for modern clinker microscopy. Never-

theless, Beljankin spent much work on studies of the constitution of aluminate cements, and in his book tabulations of the powder diagram data of x -ray diffraction are found side-by-side with the fundamental optical data for all the important minerals of hydraulic binders. Beljankin was a sincere investigator zealous in having all his data accurate and reliable. He defended also with fervor clear definitions and precise wording, and he is a sharp critic of "liberties" which occurred in the International literature by arbitrary definitions. He really hated confusion arising if authors abused mineral names for industrial products or in physical-chemical conditions inadequate to the petrographic units in which they are found in nature. Equally sharply he criticizes the tremendous confusion which unfortunately exists in the literature of the Western hemisphere in the definition of polymorphous modifications. The uniformity of definitions of modifications as it is evident not only in Beljankin's book but all over the Russian literature, contrasts impressively with the confusion in our common textbooks and reference books. Beljankin is right when he assures that it is most unfortunate when authors forget every rule established on thermodynamic principles and define modifications they discovered rather à son gré. The reviewer must sympathize with Beljankin, because it is alarming how the confusion in this important field has grown in the last decade; and there is in our Western literature no sign of any improvement. Videant Consules! It is of minor importance that even such an accurate mineralogist as Beljankin occasionally slipped into errors of phase identification, *e.g.* he defined a typical iron-alumina spinel as gahnite (in the place of hercynite), or that he does not believe in the reality of protoenstatite, and some other slight misconceptions which are easily forgivable. The general tenor of the present book is so excellent that one also cannot object too much against some broadness in the text. One must regret to a higher degree that the sections on metallurgical slags, inclusions in steel, or of stones in glass have been omitted in the German translation which are an important part in the Russian original.

The printing of the book was done with great care, especially in the beautiful micrographs and well-readable graphs; the publishers may be congratulated for the very good make-up of the book and the valuable indexes added to the text. A particular appreciation must be given to the translator who mastered the difficult original text and has given in the German-written edition a most helpful tool to Western investigators to get fully acquainted with the rich results of Beljankin and his school.

W. EITEL

*Institute for Silicate Research
University of Toledo.*

OPTISCHE DATEN ZUR BESTIMMUNG ANORGANISCHER SUBSTANZEN MIT DEN POLARISATIONS-MIKROSKOP, by ERNST KORDES. 192 pp., 8 charts (in rear pocket), 8 figures, 2 color plates. Verlag Chemie, G.M.B.H., Bergstrasse, Weinheim, Germany. 1960. DM 43.00 (\$10.75).

Professor Kordes, who is Professor of Crystal Chemistry at the University of Bonn, has performed an outstanding service to chemists, crystallographers and mineralogists in compiling data for the optical identification of 1771 inorganic compounds. The introduction and a list of the abbreviations and symbols used are followed by the general section of the book, divided into chapters dealing successively with (1) Determinative methods for inorganic substances by means of the polarizing microscope in transmitted light. (This includes the two color plates depicting chiefly interference figures.) (2) A one-page diagram indicating the sequence of determining the optical characteristics with the polarizing microscope in transmitted light, (3) A list of liquids for the immersion method. (This is completely out of date and should be disregarded.) (4) A brief list of heavy liquids for

mineral separation. (This also requires modernization and expansion.† (5) A one-page list of major references. The only work cited from the relatively extensive modern literature on ceramic compounds is the *Glastechnische Tabellen* of Eitel *et al.* which was published in 1932.

The second part of the work begins with a description of the tables and charts. The main section which follows, consists of two sets of tables: (1) a descriptive set Table 0 (isotropic substances), Tables 1+, 1- (uniaxial positive and negative), Tables 2+, 2- (biaxial positive and negative), and Table 2± (biaxial with unknown sign); and (2) a determinative set. In the latter the arrangements are by increasing indices with separate tables for both ϵ and ω for (+) and (-) uniaxial crystals and for both γ and α for (+) and (-) biaxial crystals. Each substance in the descriptive tables receives a number (Table number plus a decimal species designation) to which reference is made in the determinative tables and in the following table which lists the mineral name equivalents of those substances that occur naturally. An alphabetical list (alphabetically by chemical symbol) closes the book. Charts 1-3 plot index versus birefringence, charts 4-8 plot specific gravity versus indices.

E. WM. HEINRICH
University of Michigan

ULTRAVIOLET GUIDE TO MINERALS, by CHARLES M. RILEY, Van Nostrand Co., Inc., Princeton, New Jersey, x plus 244 pages, 16 color and 8 black-and-white photos, price \$6.95.

This is a welcome, practical handbook on fluorescent minerals. It is written clearly and is well illustrated. The text serves the needs of both the technical and popular reader. The author's treatment of the subject matter is more applied than theoretical; however, many modern and new applied techniques are discussed or suggested.

In addition to the applied concepts, Mr. Riley amiably contributes a long-needed collection of knowledge pertaining to fluorescent minerals in the form of seven tables, one for each color. The tables enable the investigator to compare the fluorescent color of his specimen with the chart for that color, thus narrowing down his search to a few possibilities. Then, with the aid of the accompanying data the searcher can readily determine the mineral species.

This handbook is recommended for collectors, lapidaries, prospectors, and technical investigators.

WILLIAM A. KNELLER
Eastern Michigan University
Ipsilanti, Michigan

SYSTEMATIC MINERALOGY OF URANIUM AND THORIUM, by CLIFFORD FRONDEL. U. S. Geological Survey, Bulletin 1064. 400 pp., 1 plate, 24 figures, 8 tables, 1958. Supt. of Documents, Gov't Printing Office, Washington 25, D. C. \$1.50.

Unfortunately not reviewed in *The American Mineralogist* at the time of its publication two years ago, this monograph deserves widespread recognition as an authoritative reference on the properties and characteristics of many uranium and thorium minerals. It includes not only a critical selection of data from the older descriptions, but also represents the summation of much original research by Frondel, his associates and his students, the results of many of which have previously appeared in the last several years in *The American Mineralogist* as contributions from the Department of Mineralogy and Petrography of Harvard University.

Already, of course, a large number of new uranium and thorium minerals have been described since the manuscript went to press and a supplement is clearly in order.

The general section of the bulletin presents a brief review of the history of the study of radioactive species followed by statements on radioactivity, on its use in age determination, on autoradiography and on radiation damage in crystals. These short sections, in their present form, are actually of but minor service to the main purpose of the work and should either be expanded or omitted.

Nearly 90 species are described according to synonymy, composition, crystallography, habit, physical and optical properties, synthesis, identification and formation and occurrence in nature. One of the most valuable features is the incorporation of x-ray powder spacing data obtained on authenticated material. The descriptive section is followed by identification tables in which the species are arranged to their d-spacings, composition, optical properties, color, specific gravity and fluorescence. More than 800 references document the monograph.

Only two regrets trouble this reviewer: one, that the work was so long delayed in press (no fault of the authors), and two, that Professor Frondel failed to include descriptions of many other species that contain significant amounts of uranium, thorium or both. The choice under the multiple oxides seems particularly arbitrary, and this section surely remains incomplete without the inclusion of such species as euxenite, fergusonite, samarskite, etc., as well as a discussion of the identification problems of the various phases that appear, attendant upon recrystallization in air and neutral atmospheres. Likewise should such silicates as gadolinite, chevkinite and allanite be overlooked? The last is a particularly widespread radioactive mineral, and its content of radioactive elements varies much as does that of monazite in which Th is also essentially a "vicarious element," but which is described. These are but minor disappointments in an otherwise outstanding and extraordinarily useful piece of work which can only be improved in any major manner by a much-to-be-hoped-for supplement.

E. WM. HEINRICH
University of Michigan
Ann Arbor, Mich.

SEAMAN'S MINERAL TABLES, by KIRIL SPIROFF. The Michigan College of Mining and Technology Press, Houghton, Michigan, 1959. 82 pages (ring binder 11×8½). \$2.50.

This book is essentially a revision of *Mineral Classification According to Cleavage and Crystal Habit*, fourth edition, by W. A. Seaman. The latter, which has been out of print for a number of years, found long usage in courses in mineralogy at the Michigan College of Mining and Technology.

The present tables are arranged essentially as in the previous work. The major portion of the tables is based upon cleavage, desirable from the point of view of constancy among individual specimens of minerals. The first minerals listed are those with one cleavage (pinacoidal) or one cleavage much better than the others, followed by minerals with two cleavage directions, alike (prismatic) or different (two pinacoidal directions) and with specified angular relations. The complexity of the cleavage increases progressively and systematically through the tabulation. The last section of the cleavage tables is six directions, all alike, with angles of 60° and 90° (dodecahedral). Cleavage perfection is divided into seven categories. Within the basic framework of cleavage geometry, the minerals are listed according to luster, cleavage perfection, and angular values.

In addition to the tables based upon cleavage, other tables based upon crystal morphology, luster (arranged by color), streak (if diagnostic), and taste, are included. Also given are tables of fibrous minerals with no streak and nodular or earthy minerals. A chart of

the classification of the igneous rocks is particularly noteworthy. Also a chart of sedimentary rocks and their metamorphic equivalents is given.

Drawings of several crystals are shown. An error of projection appears in the clinographic projection of the orthorhombic crystal.

The introductory remarks are rather chatty and seem to be directed to the amateur mineralogist. For example, "Someone once said, 'To be a mineralogist you have to be a queer duck with pockets and car full of odd trash called "minerals." ' But we know there is more to it than that." A sort of history of mineralogy is included in the introduction. Various physical properties of minerals are discussed. Within the text, several pages are devoted to the calculation of the empirical chemical formulas of minerals, with worked-out examples. The tables are intended to be used in conjunction with *Dana's Textbook of Mineralogy*, 4th edition, Wiley, 1932. Page references are given and the letters referring to crystal forms follow the Dana usage.

The book is a valuable compilation, in that it includes a rather large tabulation of the macroscopically observable cleavage of minerals, appropriate to the long tradition at the Michigan College of Mining and Technology of the use of cleavage as a major determinative property of minerals. The reviewer detected no errors in the tabulation, although he does not pretend to be familiar with all of the minerals listed. The large number of rare minerals may tend to confuse the beginning student, unless the primary object of his course of study is a systematic approach to the methodology of mineral identification by cleavage and crystal form. It is hoped that a future edition will employ various sizes of type and style of listing to indicate the approximate relative importance of the minerals tabulated. The chemical compositions of the minerals would add to the usefulness of the book, as would an index of species.

While *Seaman's Mineral Tables* is not in itself suitable for most elementary or intermediate courses in mineralogy as generally taught today, the reviewer considers it a very useful reference.

R. M. DENNING
University of Michigan
Ann Arbor, Michigan

OPTICAL CRYSTALLOGRAPHY, by ERNEST E. WAHLSTROM. 3rd Edition (1960). John Wiley and Sons, Inc., vii+356 pp.

The first and second editions of *Optical Crystallography* (2nd Edition reviewed, *Am. Mineralogist*, **36**, p. 924) have enjoyed wide acceptance for use as standard textbooks in beginning crystal optics courses. The third edition, which has been expanded and revised, should continue to be of value, not only to the mineralogist and geologist, but to workers in other fields as well.

The general format of the textbook remains essentially unchanged from that of the previous editions. As in the previous editions, the author has avoided a purely mathematical approach to the subject in favor of a practical, graphical presentation suitable for the beginning student's use with the polarizing microscope. The many new figures added to the third edition continue to maintain the high quality of illustration exemplified by its predecessors. Several sections have been rewritten and reorganized and the expanded chapter dealing with crystal rotation methods, especially the detailed instructions on the use of the universal stage, will be of special value to the student.

JOEL SHAPPIRIO
University of Michigan
Ann Arbor, Michigan

NEW MINERAL NAMES

Beryllsodalite, Beryllium Sodalite Unnamed Be mineral

E. I. SEMENOV AND A. V. BYKOVA. Beryllsodalite. *Doklady Akad. Nauk S.S.S.R.*, **133**, 1191-1193 (1960) (in Russian).

HENNING SPØRENSEN. Beryllium minerals in a pegmatite in the nepheline syenites of Ilimaussaq, South West Greenland. *Internatl. Geol. Congress, Rept. 21st Session, Norden, 1960, Pt. 17*, 31-35.

These two papers describe what is apparently the same mineral. It occurs as a hydrothermal alteration product of chkalovite in pegmatites of Mt. Sengischorr and Mt. Punkaruaiv, Lovozero massif, Kola Peninsula, U.S.S.R., and as veins cutting chkalovite in an albite-analcime vein in nepheline syenite pegmatite, Tugtup agtakôrfa, Ilimaussaq, Greenland. Analysis by A. V. Bykova of the Kola mineral gave SiO_2 50.45, Al_2O_3 12.56, Ga_2O_3 0.043, BeO (given as Be_2O_3) 5.30, CaO 0.50, Na_2O 23.26, K_2O 0.40, H_2O^+ 1.50, H_2O^- 1.51, Cl 6.04, sum 101.56, $-(\text{O}=\text{Cl}_2)$ 1.40 (should be 1.37 M.F.), sum 100.26% (should be 100.19% M.F.). Spectrographic analysis by N. V. Lizunov showed also weak lines of Fe, Cu, and Mg. The analysis gives $\text{Na}_4\text{BeAlSi}_4\text{O}_{12}\text{Cl}$, i.e., sodalite with BeSi replacing Al_2 . The slightly low Na_2O and the presence of water may be due to alteration. The Greenland mineral has not been analyzed; spectrographic analysis showed the mineral to have main components Al, Ca, Na, Si, Mg, to be fairly rich in Be and Ga. The Ga/Al ratio of the Kola mineral is unusually high. The Kola mineral fuses easily B. B.; in ultraviolet light luminesces strongly rose-colored.

The Kola mineral is rose-colored, bluish, greenish; the Greenland mineral is white, changing to light pink in strong sunlight. The Kola mineral is translucent, luster vitreous, fracture conchoidal, H. about 4, G 2.28.

The Kola mineral is cryptocrystalline, weakly anisotropic, n about 1.495. The Greenland mineral is uniaxial positive, $ns \omega$ 1.496 ± 0.001 , ϵ 1.502 ± 0.002 , apparently tetragonal with a distinct bipyramidal cleavage.

The x-ray powder diagrams of both minerals are stated to resemble that of sodalite, but to show splitting of reflections. The Greenland mineral (x-ray powder data not given) is tetragonal, a 8.583, c 8.817 Å. The Kola mineral is not cubic, but approximates a 8.72 Å. The strongest lines are 3.95 (10), 2.53 (8), 2.05 (broad) (8), 6.15 (7), 2.35 (7).

Associated with the Kola mineral is a weathering product of chkalovite, unnamed, which is white, fine-foliated, with pearly luster, anisotropic, n 1.492. Spectrographic analysis gave Be, Si very strong, Mg, Al, Ca, Na medium. The x-ray powder pattern is given; the strongest lines are 4.11 (10), 2.96 (10), 2.50 (10), 1.806 (8).

MICHAEL FLEISCHER

Zincsilite

N. N. SMOL'YANINOVA, V. A. MOLEVA AND N. I. ORGANOVA. A new aluminum-free member of the montmorillonite-sauconite series. *Acad. Sci. U.R.S.S., Comm. for Study of Clays, Repts. to Meeting of Internatl. Comm. for Study of Clays, 1960*, 45-52 (in Russian).

The mineral occurs in the zone of oxidation of the skarn galena-sphalerite-chalcopryrite deposits of Batystau, central Kazakhstan. It forms as a homo axial pseudomorph after diopside and is associated with chrysocolla, supergene fluorite, opal, and manganese oxides.

The mineral is white to bluish, occurring as fine foliae or lamellae up to $2 \times 1.5 \times 0.5$ mm. Cleavage (001) perfect, luster pearly on cleavage face. G. 2.67-2.71 (by suspension),

H. $1\frac{1}{2}$ –2. Optically biaxial, negative, n_s , α 1.514 ± 0.002 , β 1.559 ± 0.033 (misprint for 0.003 ? M.F.), γ 1.562 ± 0.002 , 2V variable 0 – 22° . $c:Z = 3^\circ$, X nearly perpendicular to (001), plane of optic axes parallel to (010). After being heated to 400° , the mineral becomes greenish-brown and distinctly pleochroic, X pale green, Z dark brownish-green, n_s , α 1.512 ± 0.002 , γ 1.570 ± 0.003 .

Analyses were made by V.A.M. of white and bluish varieties, both containing fine-grained diopside, garnet, chrysocolla, opal and quartz. These gave, respectively: ZnO 26.64, 35.00; CuO 0.60, 3.07; MgO 4.62, 1.08; MnO 0.40, —; CaO 6.40, 2.00; Al₂O₃ 0.84, 0.70; Fe₂O₃ 2.16, 1.55; SiO₂ 47.60, 42.75; H₂O⁻ 6.35, 8.50; H₂O⁺ 4.35, 6.00; sum 99.96, 100.65%. The analyses were recalculated by subtracting total Al₂O₃ and Fe₂O₃ and corresponding CaO and SiO₂ as garnet, the remaining CaO and MgO and corresponding SiO₂ as diopside, and the CuO with SiO₂ and H₂O as chrysocolla. This gives formulas $3\text{ZnO} \cdot 5.01\text{SiO}_2 \cdot 5.37 \text{H}_2\text{O}$ and $3\text{ZnO} \cdot 4.17\text{SiO}_2 \cdot 5.31 \text{H}_2\text{O}$. If it is assumed that some opal and quartz were present, the formula might be written $\text{Zn}_x \text{Si}_4 \text{O}_{10}(\text{OH})_2 \cdot n\text{H}_2\text{O}$, with n about 4.

The mineral is decomposed by acids and partly decomposed by treatment with 5% Na₂CO₃ solution. Ion exchange experiments with 10% NH₄Cl solution gave in solution for the first sample SiO₂ 0.40, CaO 0.70, MgO+ZnO 0.20%; for the second SiO₂ 0.32, CaO 0.46%. Because SiO₂ was found, it is not clear whether there was ion exchange or partial decomposition. The mineral treated with benzidine hydrochloride is colored pale greenish blue, which turns to intense blue.

A D.T.A. curve and loss of weight curve by E. P. Val'yashikhina are similar to those of saucnite, with a large endothermal break at about 200° and small exothermal breaks at about 765° and 920° . Willemite was found at 765° .

X-ray powder data are given (for sample No. 2). The strongest lines are 15.3 (10), 4.09 (7), 1.528 (6). After treatment with glycerol, the strongest line is at 17.6; after heating at 400° , this (001) line is at 10.0 Å. The (060) reflection gives $b_0 = 9.17$ Å.

The authors consider the mineral to be the end-member of the series montmorillonite-sauconite-zincsilite, all analyzed saucnites containing 6% or more Al₂O₃, corresponding to the Mg series montmorillonite saponite-beta kerolite (most mineralogists would replace the ill-defined beta-kerolite by stevensite M.F.).

The name is for the composition.

DISCUSSION.—The formula derived is somewhat uncertain, because 15–30% impurities had to be deducted. The authors point out that the optics indicate some variation in composition and that Fe is probably present in the mineral, judging from the behavior when heated. Nevertheless, the formula deduced must be nearly correct. An exact analogy to stevensite must remain questionable because of the uncertainty of the ion-exchange data.

I would have preferred to extend the definition of saucnite to cover this composition, without the introduction of a new term, but the authors have followed the present practice as applied to Mg minerals.

M. F.

Rozenite

J. KUBISZ. Rozenite, FeSO₄·4H₂O, a new mineral. *Bull. acad. polonaise sci., Ser. sci. geol. geogr.*, **8**, 107–113 (1960) (in English).

The mineral was found on the slopes of Ornak, Western High Tatra, as efflorescences on weathered gneisses containing pyrite, and in an old gallery of the "Staszic" pyrite mine at Rudki, Poland, where air temperatures were close to 30° C. At both places it was probably formed by the dehydration of melanterite. The mineral is colorless. Optically negative, 2V about 90° , n_s (Na)—Ornak α' 1.529, γ' 1.543, "Staszic" α' 1.527, γ' 1.5428. G. 2.195 ("Staszic"). Analysis from "Staszic" mine gave FeO 31.13, MgO 0.97, MnO

0.06, SO_3 36.29, H_2O 32.98, sum 100.43%, corresponding to $\text{FeSO}_4 \cdot 4\text{H}_2\text{O}$. X-ray powder data are given; the mineral is isomorphous with ilersite and starkeyite (leonhardtite). D.T.A. and thermogravimetric curves are given. Synthetic $\text{FeSO}_4 \cdot 4\text{H}_2\text{O}$ is stated by Groth to be monoclinic.

DISCUSSION.—This is identical with siderotil, see Dana's System, 7th Ed., v. II, pp. 491–492, and is therefore an unnecessary name. Dana gives it as " $\text{FeSO}_4 \cdot 5\text{H}_2\text{O}$ (?). The water content is uncertain and the natural mineral may be the tetrahydrate." The optical data given by Kubisz agree perfectly with those given for siderotil.

M. F.

Magnesium szomolnokite

J. KUBISZ. Magnesium szomolnokite, $(\text{Fe}, \text{Mg})\text{SO}_4 \cdot \text{H}_2\text{O}$. *Bull. acad. polonaise sci., Ser. sci. geol. geogr.*, **8**, 101–105 (1960) (in English).

An analysis, optics —ms (Na) α 1.558, γ 1.629), and x-ray powder data are given for $(\text{Fe}_{0.59}\text{Mg}_{0.41})\text{SO}_4 \cdot \text{H}_2\text{O}$ from the "Staszic Mine," Rudki, Poland. The name magnesium szomolnokite is suggested.

DISCUSSION.—This should be called simply *magnesian* szomolnokite to avoid the difficulty that magnesium szomolnokite might be construed as meaning kieserite and to avoid separating it in indexes from szomolnokite.

M. F.

Hydronium jarosite

J. KUBISZ. Hydronium jarosite— $(\text{H}_3\text{O})\text{Fe}_3(\text{SO}_4)_2(\text{OH})_6$. *Bull. acad. polonaise sci., Ser. sci. geol. geogr.*, **8**, 95–99 (1960) (in English).

Kubisz gives a new analysis of a jarosite mineral from "Staszic Mine," Holy Cross Mt., which gives the formula $[\text{K}_{0.10}\text{Na}_{0.11}(\text{H}_2\text{O})_{0.79}]\text{Fe}_3(\text{SO}_4)_2(\text{OH})_6$, and reviews earlier analyses. Material like this has been called carphosiderite (see Dana's System, 7th Ed., **1**, 566–567), with the ascribed formula $(\text{H}_2\text{O})\text{Fe}_3(\text{SO}_4)_2(\text{OH})_5 \cdot \text{H}_2\text{O}$. Since Moss (see *Am. Mineral.*, **42**, 586 (1957)) has shown that carphosiderite is an alkali-containing jarosite, it is suggested that this name be dropped in favor of hydronium jarosite.

M. F.

Sokolovite

A. K. SHAROVA AND A. K. GLADOVSKII. Mineral composition, genesis, and alteration of the Lower Cretaceous bauxites of the eastern slope of the Urals and the Turgaisk Plain. Bauxites, their mineralogy and genesis. *Akad. Nauk S.S.S.R., Otdel geol.-geogr. Nauk*, **1958**, 70–79 (in Russian).

The mineral occurs in cavities between bauxite pebbles in the Sokolov deposits, eastern slope of the Middle Urals. It is snow-white, finely crystalline, weakly birefringent with birefringence 0.008, mean n 1.623 ± 0.002 , H . 2.5, G . 2.94. A D.T.A. curve shows a weak endothermal effect at 425° and a strong one at 575° . A heating curve shows losses of weight 4.46% at 325° , 10.68% at 500° , 16.92% at 650° , 19.54% at 900° , 20.58% at 1000° and 1200°; the n decreases steadily to 1.534 at 800° , then increases to 1.550 at 900° , 1.568 at 1000° , 1.630 at 1200° .

Analysis gave Al_2O_3 47.18, Fe_2O_3 trace, CaO 6.23, SrO 10.77, MgO trace, P_2O_5 14.01, H_2O 21.80, SiO_2 , TiO_2 , CO_2 traces, sum "99.90%." After subtracting 5.6% gibbsite, this corresponds to $2(\text{Ca}, \text{Sr})\text{O} \cdot 4\text{Al}_2\text{O}_3 \cdot \text{P}_2\text{O}_5 \cdot 11\text{H}_2\text{O}$, with Ca slightly in excess of Sr.

X-ray powder data are given. The strongest lines are 2.20 (s), 1.80 (s), 3.5 (m), 3.3 (m), 2.43 (m), 1.45 (m), 1.28 (m), 1.195 (m).

The name is for the deposit.

DISCUSSION.—Inadequate data. The mineral is similar in composition to goyazite.

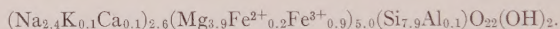
($2\text{SrO} \cdot 3\text{Al}_2\text{O}_3 \cdot 2\text{P}_2\text{O}_5 \cdot 6\text{H}_2\text{O}$) and the analogous calcium mineral crandallite, but the x-ray pattern differs noticeably from the published data for these minerals. The x-ray pattern agrees rather closely with data published for *svanbergite* ($2\text{SrO} \cdot 3\text{Al}_2\text{O}_3 \cdot \text{P}_2\text{O}_5 \cdot 2\text{SO}_3 \cdot 6\text{H}_2\text{O}$) and its calcium analogue, *woodhouseite*. It is not stated whether *sokolovite* was tested for sulfate. Material close to *svanbergite* in composition has been described from a bauxite deposit (see *tikhvinite*, Dana's System, 7th Ed., vol. 2, p. 1006).

M. F.

Rezhikite

M. V. SOBOLEVA AND N. D. SOBOLEV. Genesis and prospecting criteria of deposits of azure-blue *rezhikite* asbestos. *Sovetskaya Geol.*, 1959, No. 9, 94-104 (in Russian)

The name *rezhikite* is given to a deep blue amphibole asbestos, of which many deposits are known. Complete analyses are given of 13 samples; these show SiO_2 54.36-57.97, Al_2O_3 0.30-1.29, Fe_2O_3 8.38-11.90, FeO 0.72-3.66, MgO 14.41-19.75, CaO (partly from calcite) 0.21-1.79, Na_2O 7.80-10.24. The general formula is given as



Despite the variation in composition, the indices of refraction are stated to fall into the narrow range, $n_s \alpha$ 1.635-1.637, γ 1.640-1.644, birefringence 0.005-0.007, $c:Z = 4-6^\circ$, 2V small. The mineral is in composition near *magnesioriebeckite* and *magnesioarfvedsonite* (see *Am. Mineral.*, 43, 797-798 (1958)), but differs somewhat in optics.

The source of the name is not stated.

DISCUSSION.—Inadequate data, especially none on pleochroism. New names should not be given without a thorough comparison of all the data on this complex group.

M. F.

Wöhlerite

G. P. VDOVYKIN. Preliminary results of luminescence-bituminological studies of four carbonaceous chondrites. *Akad. Nauk S.S.S.R., Meteoritika*, 18, 78-82 (1960) (in Russian).

The name *wöhlerite* is proposed for the organic matter found in carbonaceous chondrites. If this must be named, and I see no reason why it should be, it should have been possible to find a name not already pre-empted for a well-known mineral. The sodium-calcium-zirconium-niobium silicate *wöhlerite* was named by Scheerer in 1843.

M. F.

NEW DATA

Hsiangkualite

A. A. BEUS. Geochemistry of beryllium and the genetic types of beryllium deposits. *Akad. Nauk SSSR, Inst. mineral., geokhim., i kristallogchim redkikh elementov* 1960, 1-329 (in Russian)

On pp. 60-61 is given a description of a mineral, described under the name *Hsiang-hua-shih* (shih = stone) in *Am. Mineral.*, 44, 1327 (1959). The Russian transliteration of the name is *Syankhualite* (or *syanhualite*). The data given differ somewhat from those in the previous description.

Formula $\text{Li}_2\text{Ca}_3\text{Be}_3(\text{SiO}_4)_5\text{F}_2$. Analyses SiO_2 35.66, 36.64; CaO 34.60, 35.18; BeO 15.78, 16.30; Li_2O 5.85, 5.60; Na_2O 0.13; 0.03; K_2O 0.06, 0.03; Al_2O_3 0.50, —; Fe_2O_3 0.22, 0.06; MgO 0.18, 0.17; F 7.81, 7.27; loss on ignition 1.28, —; sum 102.07, 101.28—($\text{O}=\text{F}_2$) 3.2, 3.06=98.87, 98.22%. Cubic, a_0 12.897, H $6\frac{1}{2}$, G . 2.97-3.00, n 1.613, no cleavage. Beus points out that n and G . are very high for this composition; the structure is not yet known.

M. F.

The Name Is Appropriate . . .

MINERALS UNLIMITED

can supply most of your classroom mineral and rock needs at competitive prices. Poundage, lots of 1 × 1" specimens, larger specimens—all are available in quality material. Sorry, no school catalog available, but why not give us the opportunity of bidding on the minerals you need? We have more than 500 species in stock.

Some examples of what is available, and at what prices:

25¢ per lb.

Chromite—Phillipine "leopard ore"

Epidote—solid green massive (California)

Actinolite—coarse green crystallized masses (California)

35¢ per lb.

Anorthite—cleavages in hornblende norite (California)

Oolitic hematite—reddish pisolitic masses (New York)

Magnetite—black massive, no polarity (California)

50¢ per lb.

Psilomelane—black massive, some reniform (New Mexico)

Burkeite—buff crystalline masses (California)

Glauconite—dark green cementing sandstone (Texas)

55¢ per lb.

Knotted schist—shows incipient porphyroblasts (California)

Bishop tuff—an unwelded tuff (California)

Campito sandstone—magnetite-rich arkosic sandstone (California)

Peridotite—"Kimberlite" (Arkansas)

Olivine peridotite—"Dunite" (No. Carolina)

75¢ per lb.

Galena—good quality cleavable and cleavages (Tri-State)

Tremolite—coarse radiating silky masses, some rock (Utah)

Oligoclase—white to brown-stained, striated. Ratio $AB_{85} : AN_{15}$ (New York)

\$1.00 per lb.

Clinozoisite—yellow-green granular, with quartz, mica (Oregon)

Nephrite—grey-green crystalline masses (California)

\$2.00 per lb.

Cinnabar—blood-red cleavages scattered on quartzite (Nevada)

Turquoise—blue masses in rock (Arizona)

\$2.25 per lb.

Smaltite—tin white metallic, very rich, with other arsenides (Canada)

Tyuyamunite—bright yellow encrustations on limestone (New Mexico)

\$5.00 per lb.

Jamesonite—grey metallic in quartz, with scheelite. (Idaho)

\$7.50 per lb.

Bismuthinite—rich grey metallic (Ariozna-Colorado)

Melanocerite—brown to black masses in calcite, etc. (Canada)

All of the "usual" minerals in good quality—Azurite, Arsenopyrite, Hornblende, Beryl, Gypsum (many forms), Almandine, Biotite, etc.

MINERALS UNLIMITED

724 University Avenue

Berkeley 3, California

WARD'S BIG GEOLOGY CATALOG

Our largest and finest geology catalog offers you the widest choice of the best:

1. Mineral, rock and fossil teaching, study and reference collections.
2. Mineral, rock and soil specimens; individually and in bulk.
3. Special series of reference clay minerals.
4. Individual fossil specimens.
5. Paleontology and animal kingdom charts.
6. Light weight plastic relief maps.
7. Aids for crystallography (models, goniometers, protractors).
8. Geomorphological models.
9. Color slides for geology, mineralogy, paleontology; black and white transparencies on glaciers, astronomy.
10. Field and laboratory equipment—the largest listing ever.
11. Superb selection of the finest storage and display equipment.
12. Petrographic supplies; refractive index media.
13. Thin section and lapidary equipment.
14. A full line of weather instrument.
15. Fluorescence and radiation equipment.

Ward's big geology catalog, #603, is the answer to every geologist's needs. We are just as anxious to send you this new catalog as we think you will be to receive it. If you are affiliated with a teaching, industrial or research institution, your copy is absolutely free. Just write on your school or business letterhead. Ask for Ward's Geology Catalog #603.

WARD'S NATURAL SCIENCE ESTABLISHMENT, INC.
P.O. BOX 1712 ROCHESTER 3, N.Y.